EARLY LIFE HISTORY DYNAMICS OF RAINBOW TROUT IN A LARGE REGULATED RIVER

by

Josh Korman

B.Sc., McGill University, 1984
M.Sc., University of British Columbia, 1989

A THESIS SUBMITTTED IN PARTIAL FULFILLMENT OF
THE REQUIREMENTS FOR THE DEGREE OF

DOCTOR OF PHILOSOPHY

in

THE FACULTY OF GRADUATE STUDIES

(Zoology)

THE UNIVERSITY OF BRITISH COLUMBIA

(Vancouver)

February 2009

Abstract

The central objective of this thesis is to better understand early life history dynamics of salmonids in large regulated rivers. I studied spawning, incubating, and age-0 life stages of rainbow trout in the Lee's Ferry reach of the Colorado River below Glen Canyon Dam, AZ. My first objective was to evaluate the effects of hourly fluctuations in flow on nearshore habitat use and growth of age-0 trout. Catch rates in nearshore areas were at least 2- to 4-fold higher at the daily minimum flow compared to the daily maximum and indicated that most age-0 trout do not maintain their position within immediate shoreline areas during the day when flows are high. Otolith growth increased by 25% on Sundays in one year of study, because it was the only day of the week when flows did not fluctuate. My second objective was to evaluate the effects of flow fluctuations on survival from fertilization to a few months from emergence (early survival). Fluctuations were predicted to result in incubation mortality rates of 24% in 2003 and 50% in 2004, when flow was experimentally manipulated to reduce trout abundance, compared to 5% in 2006 and 11% in 2007 under normal operations. Early survival increased by over 6-fold in 2006 when egg deposition decreased by at least 10-fold. Because of this strong compensatory dynamic, flow-dependent incubation mortality in experimental years was likely not large enough to reduce the abundance of age-0 trout. My final objective was to determine how flow, fish size and density effects habitat use, growth, and survival of age-0 trout. Apparent survival rates from July to November were 0.18 (2004), 0.19 (2006), and 0.32 (2007). A stock synthesis model was developed to jointly estimate parameters describing early life history dynamics, and indicated that early survival was lower for cohorts fertilized during the first half of the spawning period and was negatively correlated with egg deposition, that movement of age-0 trout from low- to high-angle shorelines increased with fish size, and that survival varied by habitat type and over time in response to flow changes from Glen Canyon Dam.

Table of Contents

List of Tables

List of Figures

Acknowledgements

.

Dedication

I dedicate this dissertation to my parents, Hinda and Sonny Roseman, and to Carl Walters. The enduring support from my parents gave me the confidence to follow my interests and pursue a career in fisheries science. I am forever indebted to Carl Walters for mentoring my scientific development over the last two decades, and for inspiring my interest in the fields of applied ecology and natural resource management.

Co-Authorship Statement

I designed the research summarized in this thesis, but acknowledge substantive inputs from C. Walters and S. Martell on some aspects of the field design and research focus. I directed and conducted the research of this thesis, but acknowledge considerable help in the field and laboratory from biologists, surveyors, technicians, and boatmen mentioned in the acknowledgement section. I conducted all the data analyses in this thesis, but received some direction from S. Martell, C. Walters, M. Bradford, and E. Parkinson. I prepared all the manuscripts in this thesis, but acknowledge helpful editorial comments and suggestions on content from C. Walters, E. Parkinson, M. Bradford, S. Martell, and E. Taylor.

1.0   General Introduction

1.1   Introduction

Recruitment variability is one of the least understood processes in fisheries science (Houde 1987). It is generally accepted that recruitment strength is established early in life history by a combination of density-dependent (Vandenbos et al. 2006) and – independent (Savoy and Crecco 1988) factors. Ontogenetic habitat shifts (Biro et al. 2003), body size (Werner and Gilliam 1984), density (Elliot 1994), and growth rate (e.g., Post et al. 1999, Biro et al. 2006) can be important determinants of the survival rate of young fish. Flow regulation is a widespread anthropogenic disturbance in stream environments that potentially influences both the abiotic conditions in egg, larval, and juvenile habitats, as well as the intensity of biotic interactions such as competition and predation (Heggenes and Dokk 2001, Shea and Peterson 2007). The foraging arena theory of Walters and Juanes (1993) provides a useful framework for conceptualizing the complex interrelationship between these factors. Juvenile fish living in rivers need to grow as quickly as possible because survival is often size-dependent. However, growing quicker requires spending more time foraging, which likely results in higher predation risk or increased interference competition with larger conspecifics (e.g., Post et al. 1999). Thus, juvenile fish will generally forage in highly restricted spatial 'arenas' in close proximity to refuges from predation and interference competition, and adjust the time they spend foraging and hiding to optimize their survival rate or to achieve a threshold size. Changes in abiotic factors caused by flow regulation potentially alter both the energetics (metabolic costs, food delivery rates) and intensity of competition and predation in these arenas.

Attempts to improve the status of fish populations in regulated rivers by manipulating flows are limited by a poor understanding of recruitment dynamics of young fish. Current methodologies for determining instream flow requirements for juvenile fish can be classified into application of highly uncertain physical habitat models and long-term Adaptive Management (AM) experiments (Castleberry et al. 1996). Physical habitat models such as PHABSIM (Milhous et al. 1989) are used to predict how

'useable area' changes as a function of minimum flow. These assessments have been widely criticized on many fronts, most notably on their assumption that there is a strong correlation between useable habitat area and the survival and growth of juvenile fish (Mathur et al. 1985, Castleberry et al. 1996). AM experiments require definition of a series of flow treatments that are typically assessed through changes in abundance of key species or other resources. Initiating such experiments, let alone maintaining consistent treatments if they are implemented, has proven to be very difficult because of longer-term variation in basin hydrology, competing demands for water, and changes in political and management regimes (Walters 1997). Limitations of habitat models and Adaptive Management have to some extent motivated the development of the natural flow paradigm (Poff et al. 1997). Proponents of this approach argue that the natural flow regime of most rivers is inherently variable, that this variability is critical to ecosystem function, and that flow prescriptions used for long-term management or AM experiments be developed by reconstructing certain elements of the natural regime. This natural system model has intuitive appeal, but usually provides little guidance on what aspects of the natural regime should be restored to meet specific objectives.

In the few cases when an Adaptive Management experiment is actually carried out, the usual lack of temporal or spatial controls (Walters 1997) will result in considerable uncertainty about the mechanism behind the treatment effect, and in some cases, uncertainty about whether the treatment actually caused the effect. This uncertainty limits the development of more precise flow prescriptions or refined management experiments. Poor understanding of critical mechanisms regulating population size and recovery rates make it very difficult to provide a reasonably substantiated argument in support of a particular flow experiment in the first place. This in turn results in an experimental design that is dominated by political, legal, and economic reasoning. In such cases, potential inferences from the AM experiment will be weakened because of limited contrasts and duration of treatments, or confounding due to implementation of simultaneous treatments. Implementation of uninformative experiments limits the rate at which we learn about the effects of management on key resources, and makes it hard to justify conducting more informative experiments in the future (Failing et al. 2004). I term this situation the "catch-22" of Adaptive Management.

One way out of the catch-22 dilemma is to improve our understanding of recruitment processes in larger, managed systems by using more resolute field, laboratory, and analytical methods to learn as much as possible within an available set of 'experimental' contrasts. Three types of events provide these contrasts: 1) accidental changes in physical and biological conditions driven by hydrology or unforeseen biological events; 2) regular changes in physical or biological conditions that occur under normal management actions; and 3) by so-called 'mini-experiments'. I define mini-experiments as small-scale Adaptive Management experiments whose designs are substantially constrained by a variety of competing management objectives, and the costs and risks that society, as embodied by multi-stakeholder management groups, are willing to incur. These three types of contrasts do not provide the scientifically ideal set of treatments or adequate replication, and should not be considered a replacement for a well-designed long-term experiment. Nevertheless, they are often what applied scientists have to work with, and we should attempt to learn as much as possible within this constrained setting. Gains in knowledge that can be achieved by adopting this philosophy can be used to build stronger cases for more rigorous experimentation in the future, and therefore help break-out of the catch-22 dilemma. This argument is the main motivation for the field and modeling approaches developed in this thesis.

The history of the rainbow trout population in the Lee's Ferry reach of the Colorado River provides a good illustration of the catch-22 Adaptive Management dilemma, and is necessary background for understanding the context of this thesis. The construction of Glen Canyon Dam on the Colorado River in 1962 created a clear and cold tailwater reach in the first 15 miles downstream of the dam. This section of river is known as the Lee's Ferry reach, and is all that remains of Glen Canyon since impoundment. Approximately 100,000 fingerling trout were planted annually in the Lee's Ferry reach, and by the 1970's the population supported a nationally recognized trophy trout fishery. Reductions in stocking rates in the early 1980's and possible changes in food availability resulted in a collapse of the fishery, and subsequent studies showed that only 27% of the fish caught in the Lee's Ferry reach were the result of natural reproduction (Maddux 1987). Current and historical estimates of the absolute size of the adult population of rainbow trout in the Lee's Ferry reach are uncertain. Estimates based

3

on snorkel surveys ranged 50,000-100,000 adult trout between 2002 and 2003 (Korman et al. 2006). Maintenance of the trout fishery in the Lee's Ferry reach is among the goals of the Glen Canyon Dam Adaptive Management Program. The explicit goal is to "maintain a naturally reproducing population of rainbow trout above the Paria River, to the extent practicable and consistent with the maintenance of viable populations of native fish". The fishery is managed for a "blue ribbon" fishing experience by the Arizona Game and Fish Department. The intent is to support a fishery where anglers can catch larger than average trout at a relatively high catch rate in a unique recreational setting. Current regulations required that fish over 26 cm must be immediately released alive and anglers can retain 4 smaller trout per day (http://www.gcdamp.gov/keyresc/tf.html).

High hourly fluctuations in flow resulting from power load following at Glen Canyon Dam (daily flow range up to 850 $m^3 \cdot sec^{-1}$) from the 1960's to the early 1990's were hypothesized to have reduced survival rates of eggs, alevins, and young fish which in turn limited natural recruitment rates of juveniles to the adult population (McKinney et al. 1999). In the early 1990's, daily variation in flow was restricted to reduce the rate of erosion of fine sediment in Grand Canyon. Serendipitously, the natural reproductive rate of the rainbow trout population in Lee's Ferry reach was enhanced, and within a decade adult abundance had increased by 3-fold (Fig. 1.1). Rainbow trout abundance in the Colorado River in the vicinity of the Lower Colorado River (LCR), located 60 miles downstream of the Lee's Ferry reach, increased over 6-fold between 1995 and 2000, likely in response to reduced flow fluctuations (S. Rogers, Arizona Game and Fish Department, unpublished data). Concerns about potential negative effects of high trout abundance on the largest aggregation of humpback chub (Gila cypha) in Grand Canyon (ESA-listed in 1973) led to a large-scale mechanical removal program of rainbow trout in the mainstem Colorado River in the vicinity of the LCR between 2002 and 2006 (Coggins 2008).
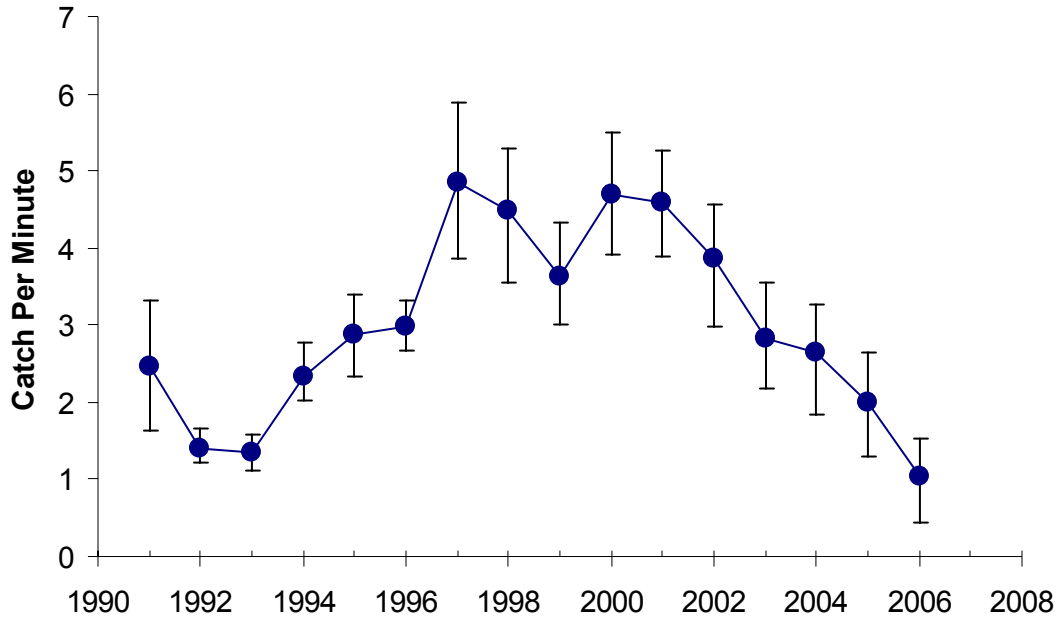
Figure 1.1. Trend in the annual abundance of rainbow trout > 150 mm in the Lee's Ferry reach of the Colorado River as indexed by boat electrofishing catch rates. Error bars denote 2 standard errors around the mean. Data reproduced with permission from Ward and Rogers (2006).

In addition, operations at Glen Canyon Dam were experimentally altered to evaluate whether changes in flow could be used to reduce trout abundance. This 'non-native reduction flow experiment', which is a good example of a mini-experiment, was conducted from 2003-2005, and consisted of increasing the extent of within-day flow variation from the normal Record-of-Decision range of 200-340 $m^3 \cdot sec^{-1}$ during most winter months, to an experimental range of 140-570 $m^3 \cdot sec^{-1}$ between January and March. The accidental AM experiment that occurred over the 1990's demonstrated that some aspect of flow stabilization increased natural reproduction of rainbow trout. However, the mechanism behind the increase was unknown because only the adult population had been monitored. Thus, when designing the non-native reduction flow experiment, there was considerable uncertainty about when, how much, and what flow component to adjust to limit trout reproduction (e.g., ramping rates, minimum or maximum daily flows, or the extent of daily variation flow). The flow range and time period of the experimental 2003-

2005 trout-limiting experimental flows was determined based on available water supply, economic interests, legal concerns, limitations imposed by perceived effects of flows on other ecosystem components, and a correlation between the extent of daily fluctuations during the winter and estimated recruitment rates of trout in the Lee's Ferry reach (C.J. Walters and D. Speas, University of British Columbia, unpublished data). It is likely that a more informative experiment would have been supported if a better understanding of the early life history dynamics for rainbow trout populations in the Colorado River were available. At the least, better scientific understanding would have made the trade-off between objectives targeted at reducing trout and other resources much more apparent, making it easier to separate science- and value-based components of the flow decision.

This history provides the context for the primary of objective of this thesis, which is to increase understanding of the early life history dynamics for salmonids in large regulated rivers. The majority of informative field studies on early life history of freshwater fish have been conducted in relatively small and stable environments such as small lakes and artificial ponds (e.g., Post et al. 1999, Biro et al. 2003, Vandenbos et al. 2006) or streams (e.g. Hartman and Scrivener 1990, Elliot 1994, Nislow et al. 1998, Imre et al. 2005). There has been very little work to determine which aspects of the results from these studies apply in a large river setting. This uncertainty is particularly acute in regulated rivers where abiotic conditions may shift suddenly and have very unnatural dynamics (Poff et al. 1997). In this thesis, I develop a variety of hypotheses about early life history dynamics for the rainbow trout population in the Lee's Ferry reach, focusing on the following three questions:

1. What are the effects of hourly fluctuations in flow on the nearshore habitat use and growth of age-0 trout?
2. What are the effects of flow and spawner density on spawning habitat use, incubation mortality, and recruitment to the age-0 trout population? and
3. What are the effects of flow, fish size, and density on habitat use, ontogenetic habitat shifts, growth, and mortality of age-0 trout?

Specific hypotheses related to these questions are developed within individual chapters of this thesis, and are evaluated using data on physical conditions, redd counts, and the

growth and abundance of age-0 trout in the Lee's Ferry reach collected in 2003, 2004, 2006 and 2007.

This thesis is divided into five main chapters and a final summary chapter that provides a synthesis of the main findings. Much of the analysis is based on catch rates of age-0 trout. Catch rate data have a variety of uses in the study of fish populations, but all require an understanding of the dynamics of capture probability, which is the proportion of a population that is captured per sampling event. Chapter 2 examines how the capture probability of age-0 trout in the Lee's Ferry reach is affected by flow, fish size, and density. Results from Chapter 2 are critical to various assumptions and functional relationships use in subsequent chapters. Chapter 3 examines the effects of hourly variation in flow on nearshore habitat use and potential growth of age-0 trout (question 1 above). Chapter 4 examines how flow and habitat structure effect somatic growth, habitat use, ontogenetic movement, and mortality of age-0 trout (question 3). Observations of behavioral and growth responses to hourly fluctuations in flow (Chapter 3) contribute to the development of flow-habitat hypotheses introduced in Chapter 4. Effects of flow fluctuations and spawner density on spawning habitat use, incubation mortality, and overall survival from fertilization to a few months from emergence (question 2) are addressed in Chapter 5. This chapter focuses on evaluating the effects of the non-native reduction flow experiment. Relatively simple analytical methods, such as comparisons of population trends through time, and hatch date and stock-recruitment analysis, are used in Chapters 4 and 5. Simple approaches have the advantage of being more familiar, more transparent, and easier to follow for a wider audience. However, simple analyses are usually based on relatively restrictive assumptions, and do not make full use of all data sources. In Chapter 6, I therefore develop and apply a stock synthesis model, that integrates data on spawn timing and magnitude and incubation mortality (Chapter 5), and on the growth and abundance (Chapter 4), and capture probability (Chapter 2) of age-0 trout, to re-examine some of the criticaql hypothesis initially evaluated in Chapters 4 and 5.

This thesis provides an example of what can be learned by adopting a more resolute approach to monitoring and assessment within a context of limited experimental contrasts. The findings will be useful in the design and study of future experiments

targeted at understanding the effects of flow from Glen Canyon Dam on fish populations in the Colorado River. More generally, this thesis contributes to the understanding of early life history dynamics for trout, and perhaps other salmonids, in large rivers. Some of the field methodologies and modeling approaches that were developed are relatively unique, and can potentially be applied to a wide range of fish species and environments.

1.2   References

Biro, P.A., Post, J.R., and M.V. Abrahams. 2006. Ontogeny of energy allocation reveals selective pressure promoting risk-taking behaviour in young fish cohorts. Proc. R. Soc. B. **272:** 1443-1448.

Biro, P.A., Post, J.R., and Parkinson, E.A. 2003. Population consequences of a predator-induced habitat shift by trout in whole-lake experiments. Ecology **84:** 691-700.

Castleberry, D.T., J.J. Cech Jr., D.C. Erman, D. Hankin, M. Healey, G.M. Kondolf, M. Mangel, M. Mohr, P. Moyle, J. Nielsen, T.P. Speed and J.G. Williams. 1996. Uncertainty and Instream Flow Standards. Fisheries **21:** 20-21.

Coggins, L.G. Jr. 2008. Active Adaptive Management for native fish conservation in the Grand Canyon: Implementation and Evaluation. Ph.D. thesis, Department of Fisheries and Aquatic Sciences, University of Florida. 170 pp.

Elliott, J.M. 1994. Quantitative ecology and the brown trout. Oxford University Press, Oxford.

Failing, L., Horn, G., and P. Higgins. 2004. Using expert judgment and stakeholder values to evaluate adaptive management options. Ecol. Soc. 9(1): 13 ([Online] URL:httyp://www.ecologyandsociety.org/vol9/iss1/art13).

Hartman, G.F., and J.C. Scrivener. 1990. Impacts of forestry practices on a coastal stream ecosystem, Carnation Creek, British Columbia. Can. Bull. Fish. Aquat. Sci. **223:** 148 p.

Heggenes, J., and J.G. Dokk. 2001. Contrasting temperatures, waterflows, and light: Seasonal habitat selection by young Atlantic salmon and brown trout in a boreonemoral river. Regul. Rivers: Res. Mgmt. **17**: 623-635.

Imre, I., Grant, J.W.A., and R.A. Cunjak. 2005. Density-dependent growth of young-of-year Atlantic salmon *Salmo salar* in Catamaran Brook, New Brunswick. J. An. Ecol. **74:** 508-516.

Korman, J., Yard, M., and D. Speas. 2006 An evaluation of the utility of snorkel surveys for estimating population size and tracking trends in relative abundance of rainbow trout in the Lee's Ferry reach of the Colorado River. Report prepared for Arizona Game and Fish Department, Phoenix, AZ.

Houde, E.D. 1987. Fish early life dynamics and recruitment variability. Am. Fish. Soc. Symp 2:17-29.

Maddux, H.R., D.M. Kubly, J.C. deVos, W.R. Persons, R. Staedicke, and R.L. Wright. 1987. Evaluation of varied flow regimes on aquatic resources of Glen and Grand Canyon, final report. [Prepared for Glen Canyon Environmental Studies, Bureau of Reclamation, Flagstaff, Arizona.] Contract # 4-AG-40-01810. Arizona Game and Fish Department, Phoenix.

Mathur, D., W.H. Bason, E.J. Purdy Jr. and C.J. Silver. 1985. A Critique of the Instream Flow Incremental Methodology. Can J. Fish. Aquat. Sci. **42:** 825-831.

McKinney, T., Speas, D.W., Rogers, R.S., and W.R. Persons. 1999. Rainbow trout in a regulated river below Glen Canyon Dam, Arizona, following increased minimum flows and reduced discharge variability. Nor. Am. J. Fish. Mgmt. **21:**216-222.

Milhous, R.T., Updike, M.A., and D.M. Schneider. 1989. Physical habitat simulation system reference manual, version 2. Instream flow information paper 26. U.S. Fish and Wildlife Service Biological Report 89 (16).

Nislow, K.H., Folt, C., and M. Seandel. 1998. Food and foraging behaviour in relation to microhabitat use and survival of age-0 Atlantic salmon. Can. J. Fish. Aquat. Sci. **55:**116-127.

Poff, N.L., Allan, J.D., Bain, M.B., Karr, J.R., Prestegaard, K.L., Richter, B.D., Sparks, R.E., and J.C. Stromberg. 1997. The natural flow regime. Bioscience **47:** 769-784.

Post, J.R., Parkinson, E.A., and N. T. Johnston. 1999. Density dependent processes in structured fish populations: interaction strengths in whole-lake experiments. Eco. Mono. **69:** 155-175.

Savoy, T.F., and V.A. Crecco. 1988. The timing and significance of density-dependent and density-independent mortality of American Shad, *Alosa sapidissima*. Fish. Bull **86:** 467-481.

Shea, C.P., and J. T. Peterson. 2007. An evaluation of the relative influence of habitat complexity and habitat stability on fish assemblage structure in unregulated and regulated reaches of a large Southeastern warmwater stream. Trans. Am. Fish. Soc. **136:** 943-958.

Vandenbos. R.E., Tonn, W.M., and S. M. Boss. 2006. Cascading life-history interactions: alternative density-dependent pathways drive recruitment dynamics in a freshwater fish. Oecologia **148**:573-582.

Walters, C.J. 1997. Challenges in adaptive management of riparian and coastal ecosystems. Cons. Ecol. [online] **1**(2): 1. http://www.ecologyandsociety.org/vol1/iss2/art1/

Walters, C.J. and F. Juanes. 1993. Recruitment limitation as a consequence of natural selection for use of restricted feeding habitats and predation risk taking by juvenile fishes. Can. J. Fish. Aquat. Sci. **50:** 2058-2070.

Ward, D., and S. Rogers. 2006. Lee's Ferry, Long-term rainbow trout monitoring. 2006 Trip Report. Report submitted to Grand Canyon Monitoring and Research Center, Flagstaff, AZ.

Werner, E.E., and Gilliam, J.F. 1984. The ontogenetic niche and species interactions in size-structured populations. Annu. Rev. Ecol. Syst. **15:** 393-425.

2.0 Effects of Fish Size, Habitat, Flow, and Density on Capture Probabilities of Age-0 Rainbow Trout Estimated from Electrofishing at Discrete Sites in a Large River[1]

2.1 Introduction

Catch information has a variety of uses in the study of animal populations, but all require an understanding of the dynamics of capture probability, which is the proportion of a population that is captured per sampling event (Williams et al. 2002). For example, in commercial or recreational fisheries, changes in catch-per-effort over time can be used to assess trends in abundance under the assumption that capture probability has remained stable, or alternately, that temporal changes in capture probability can be estimated (Hilborn and Walters 1992). In scientific surveys of stream-dwelling fishes, differences in catch rates among habitat types can be used to evaluate their relative importance, but only if capture probabilities in these habitats are known. Studies conducted over a period where fish are growing and undergoing ontogenetic habitat shifts must account for the effects of both changes in fish size and habitat use on capture probability. Efforts targeted at improving the status of freshwater fish populations, such as increasing minimum stream flows in regulated rivers, are sometimes assessed by comparing catch rates before and after flow changes. In this situation, it is important to understand how persistent environmental changes, such as flow, potentially alter capture probability. A common assumption required in all such studies is that catch rates are proportional to abundance, in other words, that capture probability is independent of density.

Electrofishing is a commonly used means of sampling stream-dwelling juvenile salmonids and other fishes. A variety of studies have investigated the effects of electrofishing on movement (Dunham et al. 2002, Young and Schmetterling 2004), and behaviour (Cross and Stott 1975, Mesa and Schreck 1989, Ainslie et al. 1998), and how

---

[1] A version of this chapter has been accepted for publication. Korman, J., Yard, M., Walters, C., and L.G. Coggins. 2009. Effects of Fish Size, Habitat, Flow, and Density on Capture Probabilities of Age-0 Rainbow Trout Estimated from Electrofishing at Discrete Sites in a Large River. Transactions of the American Fisheries Society: 138 (1):xx-xx.

capture probability is influenced by habitat and environmental variables (Bayley and Austen 2002, Peterson et al. 2004, Rosenberger and Dunham 2005), fish size (Borgstrom and Skaala 1993, Anderson 1995), and density (Bayley and Austen 2002). The vast majority of studies have been conducted in small streams and lakes or in very small artificial systems. Very few have been undertaken in medium- to large-sized rivers. Speas et al. (2004) found that capture probability for adult rainbow (Oncorhynchus mykiss) and brown trout (Salmo trutta) in the Colorado River (Mean Annual Discharge, MAD = 385 $m^3 \cdot sec^{-1}$) varied with turbidity, and was density-independent and –dependent for rainbow trout and brown trout, respectively. Mitro and Zale (2002) used mark-recapture to estimate capture probability for age-0 rainbow trout in a tributary of the Snake River (MAD=24 $m^3 \cdot sec^{-1}$). They found that capture probabilities at discrete sites tended to be low (average 0.17), and that sites could be treated as effectively closed because emigration rates of marked fish were relatively low (16%). To our knowledge, there have been no attempts to estimate capture probabilities at discrete sites for juvenile fish in large rivers using depletion or mark-recapture experiments or other methods. This represents a significant limitation in our ability to estimate the abundance, distribution, growth and survival of juvenile fish in these environments, which is critical for understanding effects of habitat enhancement and other management efforts.

The objective of this paper is to evaluate the feasibility of estimating capture probabilities for juvenile fish populations in larger rivers. We define capture probability as the proportion of a population within a discrete shoreline site that is removed by a single-pass of electrofishing effort. The assumption that populations within sites can be treated as closed is evaluated based on recovery rates of marked fish outside of mark-recapture sites, and by 24-hour holding experiments to determine the potential mortality of fish between release and recovery periods. We compare capture probabilities estimated by depletion and mark-recapture experiments, and examine how capture probabilities vary with fish size, habitat, flow, recovery period, and density. Results from this investigation should be of interest to researchers wishing to study the population dynamics of small or juvenile fish in large river environments.

2.2 Methods

Study Area

This study was conducted in the Lee's Ferry reach of the Colorado River, AZ, which begins at Glen Canyon Dam below Lake Powell and extends 26 km downstream to the confluence of the Paria River (Lat:36.86638, Long:-111.58638). The average flow during months when the study was conducted in 2006 (July-November) and 2007 (June-November) was 325 and 339 $m^3 \cdot sec^{-1}$, respectively (USGS gauge 09380000). Although located in a canyon, the reach is broad, shallow, and low gradient. The average wetted width, depth, and gradient at 325 $m^3 \cdot sec^{-1}$ is 144 m, 5.2 m, and 0.25 $m \cdot km^{-1}$, respectively (Randle and Pemberton 1987). There are no significant tributary inputs to the reach and water quality is determined by the hypolimnetic release from Glen Canyon Dam. The annual range of mainstem water temperatures recorded at the downstream end of the reach since 2003 has ranged from 9-15 ^{o}C (Voichick and Wright 2007) and secchi depths have consistently ranged from 6-7 m (Vernieu et al. 2005). The fish fauna in the Lee's Ferry reach is almost exclusively comprised of a large self-sustaining population of nonnative rainbow trout (McKinney et al. 2001).

Flow from Glen Canyon Dam normally fluctuates on a diel cycle that is driven by power demand but controlled through regulations on the maximum daily flow range (141-227 $m^3 \cdot sec^{-1}$), minimum (141 $m^3 \cdot sec^{-1}$) and maximum (708 $m^3 \cdot sec^{-1}$) flows, and maximum downramp (42 $m^3 \cdot sec^{-1} \cdot hr^{-1}$) and upramp (113 $m^3 \cdot sec^{-1} \cdot hr^{-1}$) rates. There is little variation in flow during low and high flow periods within a day. Flow was very similar within months across years during the study period (Table 2.1), being relatively high with large daily flow variation during summer months (June-August), and low with less daily variation during fall (September-November).

Field Methods

Depletion and mark-recapture methods were used to estimate capture probability and population size for age-0 rainbow trout at discrete sites within the Lee's Ferry reach. Both these methods rely on the assumption that a population within a site can be treated as effectively closed. In other words, that the number of fish that migrate from or into the site, or that die over the period when the site is sampled, is negligible. Shoreline habitat in the reach has been classified into the five following strata based on low-level aerial

photographs: cobble bars; vegetated sand bars; debris fans; talus (large angular boulders); and cliffs (Mietz 2003). In total there are 96 shoreline habitat units summing to 56.5 km. The total shoreline length is slightly greater than twice the total length of the river because it includes both banks and the shorelines are more sinuous than centerline of the channel. We reclassified the 5 original habitat strata into low- (cobble and vegetated sand bars and debris fans summing to 27.8 km of shore length) and high-angle (talus slopes summing to 21.5 km of shore length) shoreline habitat types that could be sampled by backpack and boat electrofishing, respectively. Cliff habitat was excluded because it comprises only 12% of the total shoreline length, and because pilot sampling showed it was very rarely utilized by age-0 trout. Sites where depletion or mark-recapture experiments were conducted were randomly selected units from low- and high-angle habitat strata.

All sampling was conducted after dark between midnight and 6:00 a.m. when sampling at the daily minimum flow, and between 21:00-23:00 when sampling at the daily maximum flow. Electrofishing sites extended 3-4 m from shore, were not enclosed by block-nets, and were fished very methodically in upstream (backpack electrofishing) or downstream (boat electrofishing) directions. The effects of daylight and flow on the distribution of age-0 trout within the immediate shoreline areas that were electrofished are explored in Chapter 3. Backpack and boat electrofishing were conducted using a two-person crew operating Smith-Root Type 12b and Coffelt CPS electrofishers, respectively. A single pass of electrofishing required an average of 10 seconds of electrofishing effort per meter of shoreline sampled. Boat electrofishing was conducted from a shallow-draw 5.3 m aluminum boat with 50 Hp outboard motor with power trim. The combination of boat design, highly experienced operators, and slow shoreline water velocities, allowed fine control of anode position and very thorough coverage of the immediate shoreline area relative to typical boat electrofishing operations. After electrofishing, fish were anesthetized using clove oil and fork lengths were measured to the nearest mm.

In 2006, 66 depletion experiments (n=19 in low-angle and 47 in high-angle habitats) were conducted over 4 sampling trips between July and November (Table 2.2a). Experiments were conducted at either the daily minimum (n=42) or maximum (n=24) flow. Each depletion experiment consisted of repeatedly removing fish from a single site

over 3 (n=62) or 4 (n=4) passes and holding them until the experiment was complete. We allowed a 1-2 hour period between passes, and ensured that fishing effort (seconds shocked per meter of shoreline) was approximately constant among passes (± 15%). Site lengths varied and depended on the number of fish captured on the first pass. At a minimum, sites were 30 m and 50 m long in low-angle and high-angle shorelines, respectively, but were extended up to approximately twice these distances if time permitted or if catches were low. In rare cases where 10 fish were not captured over the maximum distance, the site was abandoned and another random site was selected. Average site lengths in low- and high-angle habitats were 37 (range 30-61 m) and 57 (range 50-116 m) m, respectively.

In 2007, we conducted 42 mark-recapture experiments over five sampling trips between June and November (n=7 and 35 in low- and high-angle habitats, respectively, Table 2.2b). On the first pass (marking pass), fish were captured by electrofishing and measured to the nearest millimeter. Live fish were put in an aerated bucket with neutral red biological stain (2 g per 15 l, Sigma-Aldrich Ltd.) for 20 minutes and then transferred to aerated buckets of clear water to recover (Gaines and Martin 2004). The fork lengths of dead fish and those that were not actively swimming after processing were recorded so they could be excluded from the count of marked fish released into the site. The remaining marked fish were released one or two at a time near the shore throughout most of the length of the sample site. No fish were released within 5 m of the upstream or downstream borders of the sites. Sites were resampled by electrofishing either one hour (n=11) or 24 hours (n=31) after fish were released. All sites were resampled at the same flow that they were initially sampled at, and sites re-sampled after 24 hours experienced a complete diel flow cycle. Effort (seconds electrofished per meter of shoreline) during the second pass (recapture pass) was consistent with effort during the initial marking pass and during depletion experiments in 2006. The number and fork length of marked and unmarked fish that were captured on the second pass were recorded. Average site lengths in low- and high-angle habitat were 112 (range 95-273 m) and 88 m (range 50-247 m), respectively. Twenty-five m long shoreline sections located immediately upstream and downstream of each of the mark-recaptures sites were sampled at the end of the recapture pass. The number of marks captured in these areas was expanded by the estimated site-

specific capture probabilities to determine the total number of marked fish that had emigrated between marking and recapture events.

To determine whether electrofishing, handling, and staining resulted in post-release mortality of marked fish, we conducted two holding experiments in September 2007. A large sample of fish were captured by backpack and boat electrofishing and measured to the nearest millimeter. One-half of all fish with fork lengths > 60 mm had a small portion of the upper lobe of their caudal fin removed and were held for 20 minutes in clear water. The other half of fish > 60 mm, and all fish ≤ 60 mm, were placed in neutral red stain for 20 minutes. This design allowed us to determine whether use of the neutral red stain resulted in additional mortality relative to the more traditional method of marking juvenile fish using fin clips. Fish were then put in mesh baskets (1 x 0.5 x 0.4 m) that were placed on the stream bottom in calm water. We returned to the baskets after 24 hours and counted and measured the number of stained and clipped live and dead fish.

Model Structure and Estimation

Capture probability (p) and population size were estimated from depletion and mark-recapture experiments using the generalized mark-recapture and depletion models of Otis et al. (1978). Capture probability may change across passes due to changes in effort, or because of the effects of past fishing effort on physical habitat (i.e., increasing turbidity) or fish behaviour (Mesa and Shreck 1989, Peterson et al. 2004). We therefore evaluated two alternate depletion models: 1) a simpler model where capture probability was constant across passes (Model D_1, where D refers to a depletion experiment and subscript 1 refers to the number of capture probabilities that are estimated) and; 2) a more complex model where capture probability on the first and subsequent passes are separate parameters and can therefore differ (D_2). We evaluated simple and complex mark-recapture models where capture probability was assumed constant across passes (MR_1) or could vary (MR_2), respectively. Parameters for depletion and mark-recapture models were estimated by maximizing the log of the multinomial probability that depends on differences between the observed and predicted number of fish with different capture histories. This approach exactly follows Otis et al. (1978). Computations were implemented using the AD model-builder (ADMB) software (Otter Research 2004). Population density per 100 meters of shoreline (*N*) was calculated by dividing the most

likely estimate (MLE) of population size by the site length and multiplying by 100. The approximate asymptotic estimate of the standard error for the MLE of capture probability was computed from the inverse of the Hessian matrix returned by the ADMB software. The coefficient of variation (CV) for capture probability estimates, computed as the ratio of the standard error of the MLE to the MLE, was used to provide a standardized measure of uncertainty.

The influence of fish size on capture probability was modeled using mark-recapture data where the size distribution of marked fish present at the start of the recapture event is known. Data from each mark-recapture experiment were aggregated into 10 mm fork length classes. Capture probability for each length class was predicted using the following model,

$$(1) \qquad pL_j = \frac{\beta}{1 + e^{\frac{-(\overline{L}_j - \mu)}{\sigma}}}$$

where, pL_j is the predicted capture probability for the 10 mm size class j (e.g., $j=4$ for size class 30-40 mm) and a mid-point fork length $\overline{L}_j$ (in mm), β is the base capture probability, that is the capture probability where size is not limiting (i.e., when the denominator = 1), and μ and σ are the mean and standard deviation of the logistic fork length-vulnerability function that determine the length where capture probability is 50% of the maximum, and the inverse of the slope of the relationship, respectively. We fit equation 1 to data stratified by habitat type as well as aggregated across habitats. Parameters were estimated by maximizing the sum of the log likelihood of the binomial probability of the number of recaptures across all length classes,

$$(2) \qquad r_{i,j} \sim Binomial(M_{i,j}, pL_j)$$

where, pL_j is the size-specific capture probability estimate from equation 1, and $r_{i,j}$ and $M_{i,j}$ are the number of recaptures on pass 2 and marks applied on pass 1 in size class j at site i, respectively. Note this is equivalent to using the multinomial likelihood from Otis et al. (1978), but without estimation of N or consideration of the unmarked component of the population. We refer to the size-based capture probability model as L_3 (L for length, 3 for the number of parameters that determine capture probability for each size class). This

model collapses to a null model (L_1) where capture probability is assumed to be constant across size classes by removing the denominator in equation 1 and only estimating β.

We attempted to fit the size-based capture probability model (equation 1) to depletion data by aggregating catches across sites within 10 mm size classes as for the mark-recapture data. However, parameter estimates for this model were very uncertain because, in the case of depletion data, it is necessary to jointly estimate the size of the aggregate population for each size class as well as capture probability parameters. To avoid this problem yet still evaluate effects of size on capture probability, we first independently estimated capture probability and abundance for each size class using the standard depletion model of Otis et al. (1978). We then fitted linear capture probability-fork length models to the estimates of capture probability, and tested whether the slopes of these models were significantly different than zero. It was not necessary to transform capture probability estimates using logit or arcsine transformations prior to conducting regression analyses. Quantile-quantile plots showed that capture probability estimates were normally distributed, and only 5 of 108 estimates were <0.2 or > 0.8 where the effects of transformation would be substantive (Gelman et al. 2004).

Evaluating Effects of Flow, Habitat, and Recovery Period on Capture Probability

We defined a series of candidate models that encompassed our hypotheses about the effects of sampling, habitat type, flow, and fish size on capture probability, and then compared these models using an information theoretic approach. We used the Akaikie Information Criteria corrected for small sample size (AIC_c), for the comparisons. The AIC_c statistic is used to measure the amount of information lost among competing models by formally recognizing the tradeoff between bias and variance (Burnham and Anderson 2002). A more complex model with more parameters will almost always fit the data better than a simpler model with fewer parameters, however parameter estimates from the more complex model will be more uncertain. When comparing a range of candidate models, the model with the lowest AIC_c value is considered to have the best out-of-sample predictive power. Models with similar AIC_c values relative to the best model (ΔAIC_c 0-2) are considered to have strong support, while those with larger AIC_c values are considered to have moderate (ΔAIC_c 4-7) or essentially no (ΔAIC_c >10) support.

To evaluate evidence for changes in capture probability across passes, we compared model D_1 with D_2 for depletion data, and model MR_1 with MR_2 for mark-recapture data. As we compute the parameters for each experiment individually, we refer to these models as $D_{1,i}$, $D_{2,i}$, $MR_{1,i}$, and $MR_{2,i}$, respectively (the 'i' subscript denotes individual estimates for each experiment). AIC_c was computed for each experiment and compared across models, and the sum of experiment-specific AIC_c values was also compared. Note that AIC support criteria apply to all model comparisons, whether comparing two models for a single experiment, or two models applied to a group of experiments. The AIC_c for the size-based capture probability model (L_3) was compared to the AIC_c from the model where capture probability was assumed constant across size classes (model L_1). The effects of the combination of habitat and gear type on capture probability was evaluated by comparing models with common capture probabilities across all experiments and habitat types ($D_{1,c}$ or $MR_{2,c}$, where 'c' denotes a common habitat type) with more complex models that allowed capture probabilities to vary by habitat type ($D_{1,h}$ or $MR_{2,h}$, where 'h' denotes habitat-specific stratification). We refer to habitat-gear effects as habitat effects throughout the remainder of this paper, and provide a rationale for this nomenclature in the discussion. Note that these models estimate common capture probabilities across groups of experiments, but experiment-specific population sizes. In the case of mark-recapture experiments, it was also possible to evaluate effects of habitat on size-dependent capture probability, by comparing the sum of AIC_c values from habitat-specific relationships (model $L_{3,h}$) with the AIC_c from a model that was common to both habitat types (model $L_{3,c}$). As the asymptotic capture probability (β from equation 1) was similar across habitat types, we also compared $L_{3,c}$ and $L_{c,h}$ with a size-dependent model with habitat-specific means (μ) and standard deviations (σ) but a common asymptote (model $L_{2+,c}$).

The effects of flow on capture probability was evaluated by comparing models where capture probability could vary across habitat types and across low- (September and November) and high-flow (June-August) months ($D_{1,h\text{-}mf}$ or $MR_{2,h\text{-}mf}$, where 'mf' refers to stratification by monthly flow level), with simpler models where capture probability could only vary by habitat type ($D_{1,h}$ or $MR_{2,h}$). In the case of depletion data, we were also able to compare models where capture probability could vary across experiments

conducted during the daily minimum and maximum discharges ($D_{1,h-df}$, where 'df' refers to stratification by the daily flow level), with models where capture probability was constant across these strata ($D_{1,h}$). Finally, for mark-recapture data, we evaluated the effect of the period between marking and recovery by comparing models where capture probabilities could vary between one-hour and 24-hour experiments ($MR_{2,h-rp}$, where 'rp' refers to stratification by recovery period), with the simpler model where capture probability was constant across these recovery periods ($MR_{2,h}$).

Evaluating the Effects of Density on Capture Probability

We examined the relationship between estimates of capture probability (p) and population density (N) to determine whether capture probability was density dependent. These parameter estimates can be negatively correlated due to sampling error alone, because larger estimates of N require smaller estimates of p (Schnute 1983). We therefore used a bootstrap procedure to test for density dependence in p following some of the methods of Speas et al. (2004). We simulated both 3-pass depletion and 2-pass mark-recapture data assuming binomial sampling error. The population sizes and capture probabilities used in the simulations were randomly selected from ranges that bounded the estimates from our data (simulated p=0.2-0.8, N=10-200 fish·100m^{-1}, site length= 50 m for depletion data from 2006, simulated p=0.05-0.8, N=50-1500 fish·100m^{-1}, site length=100 m for mark-recapture data from 2007). Most likely estimates of p and N for each set of simulated data were computed using a non-linear iterative search procedure to minimize the log multinomial likelihood as described above. The number of estimation failures was also determined. For depletion data, a failure was designated whenever the slope of the relationship between catch on each pass and the cumulative catch from previous passes was positive, or when the total catch across three passes was less than or equal to one. For mark-recapture simulations, a failure was designated whenever the number of fish caught on the first pass, or the number of marked fish recaptured on the second pass, was zero. The simulation-estimation procedure was repeated and linear-log p-N models ($p = a + b \cdot log(N)$) were fit to the p-N estimates for each level of simulated capture probability. Bias in capture probability estimates was computed by comparing the estimated values to the true simulated values (% bias=100*(estimated p-simulated p)/simulated p).

Comparisons of simulated and observed p-N slopes were made using graphical and probabilistic approaches. For the graphical comparison, the observed p-N slopes were compared to slopes based on simulated data, where the latter slopes were computed from a fixed range of simulated capture probabilities (0.2, 0.4, 0.6, and 0.8) and random population densities within the ranges specified above. 250 trials were completed for each simulated capture probability. For the probabilistic comparison, cumulative frequency distributions (CFDs) of p-N slopes were generated based on 100 trials of either 19 or 47 sets of simulated depletion data, and 7 or 35 sets of simulated mark-recapture data. These sample sizes reflect those available to estimate the p-N slopes from our depletion or mark-recapture data in low- and high-angle habitats, respectively. Capture probability and density values used in the simulations were random draws from the ranges specified above. The value of the observed p-N slope for each habitat type was then overlaid on the corresponding simulation-based CFD to determine the probability that the observed slope, or a steeper slope, could have arisen due to chance alone. This probability is equivalent to a Type I error rate, that is, the probability of incorrectly rejecting the null hypothesis of no density dependence in capture probability.

2.3   Results

Population Closure and Capture Probability Estimates

There were very few captures of marked fish in 25 m shorelines bordering the downstream and upstream boundaries of mark-recapture sites. Capture of one or more marked fish in these areas occurred in 2 of 7 experiments in low-angle habitat, and in 10 of 35 experiments in high-angle habitat. Incidences of marked fish being captured outside of the original sites were limited to the 24-hour recovery experiments. Of 1,060 and 1,906 marks released in low- and high-angle habitats, respectively, only 0.47% (n=5) and 0.68% (n=13) were recaptured in adjacent areas. The total emigration rates in low- and high-angle habitats, estimated by expanding the number of marked fish captured in adjacent areas for each experiment by the estimated capture probabilities on the second pass (Fig. 2.1), were 2.6% and 2.2%, respectively. Averaged across all mark-recapture experiments, there was an initial mortality due to electrofishing and capture of 8%

22

(CV=0.37) and 20% (CV=0.57) in low- (backpack) and high-angle (boat electrofishing) habitats, respectively. Based on 24-hour holding experiments, survival was 100% for all 194 fish captured by backpack electrofishing (96 stained fish and 98 clipped fish, fork lengths ranging from 30-74 mm), and for all 157 fish caught by boat electrofishing (85 stained fish and 72 clipped fish, fork lengths ranging from 40-110 mm).

There was essentially no support for the more complex depletion model that estimated different capture probabilities for the first and subsequent passes (D2). Out of 66 experiments, there were only 3 cases where the AIC_c from $D_{2,i}$ was lower than values from $D_{1,i}$ by more than 2 units. Summed across all experiments within habitat types, there was essentially no support for $D_{2,i}$ relative to $D_{1,i}$ in both low- and high-angle habitats (Table 2.3a). In contrast, the AIC_c for $MR_{2,i}$ was lower than the AIC_c for $MR_{1,i}$ by more than 2 units in 21 out of 42 experiments and there was strong support for $MR_{2,i}$ relative to $MR_{1,i}$ when AIC_c values were summed across experiments (Table 2.3b). The mean difference between capture probability estimates on the 1st pass and second passes across the 42 experiments was 0.03. This suggests that while there was strong evidence for variation in capture probabilities between the marking and recapture passes for individual experiments, there was no general tendency for either higher or lower capture probabilities on the second pass. Based on these results, we used models D_1 and MR_2 for subsequent analyses of depletion and mark-recapture data, respectively.

Average capture probability across 66 depletion experiments based on model $D_{1,i}$ was 0.54 with 80% of the estimates between 0.27 and 0.75 (Fig. 2.1). Average capture probability on the first and second passes across 42 mark-recapture experiments based on model $MR_{2,i}$ were 0.31 and 0.28, with 80% of the estimates between 0.17-0.48 and 0.16-0.43, respectively (Fig. 2.1). Sampling error of capture probability, indexed by the average of CVs from individual estimates, was 0.26 for both depletion and mark-recapture experiments.

Effects of Fish Size on Capture Probability

Size-dependent capture probability models based on mark-recapture data in low- and high-angle habitats (models $L_{3,h}$) had strong support relative to models where capture probability was assumed to be independent of size (models $L_{1,h}$, Table 2.4). The logistic size-dependent capture probability models (equation 1) fit the length-stratified mark-

recapture data well, explaining 90% of the variability in the MLEs of length-stratified recapture rates (Fig. 2.2a). Fork length also explained 94% and 71% of the variation in capture probabilities from depletion experiments that were independently estimated for each size class in low- and high-angle habitat, respectively (Fig. 2.2b). The slopes of the relationships were significantly different than zero (p=0.006 and 0.002, respectively).

Effects of Habitat on Capture Probability

The effect of habitat type on capture probability depended on the estimation method and whether effects of fish size were accounted for. Based on depletion experiments, there was strong support for both habitat-dependent (sum of AIC_c values for $D_{1,h}$ models across habitat types: 281.7+730.9=1012.6) and -independent models ($D_{1,c}$=1010.5), and the most likely estimates of the capture probabilities across habitat types were very similar (Table 2.3a, Fig. 2.3a). In contrast, there was strong support for habitat-specific capture probability models ($MR_{2,h}$) relative to the habitat-aggregated model ($MR_{2,c}$) based on mark-recapture experiments (Table 2.3b). In this case, capture probability in low-angle habitat tended to be greater than in high-angle habitat (Fig. 2.3b), especially on the 1st pass (Table 2.3b). A similar result was obtained from the size-stratified analysis (Table 2.4). There was strong support for the habitat-dependent models ($L_{3,h}$) relative to the habitat-aggregated one ($L_{3,c}$). The major difference between models in this case was the higher capture probability of small fish (lower μ) in the low-angle habitat type. Asymptotic capture probabilities (β) were similar among habitat types. As a result, the model which assumed that the β was constant across habitat types ($L_{2+,c}$) had slightly better predictive power than the model that allowed all 3 parameters to vary (Table 2.4).

Effects of Flow on Capture Probability

There was little evidence to suggest that flow influenced capture probability based on differences across flows within a day, but flow effects were confounded with the effects of fish size in the case of the across-month flow comparison. Most likely estimates of capture probabilities based on depletion experiments at the daily minimum and maximum flows, and in high- and low-flow months based on both depletion and mark-recapture data, differed by no more than .08 (Table 2.3, Fig. 2.3a). Depletion models applied to data from low-angle habitat, which accounted for daily ($D1_{h-df}$) or

monthly ($D1_{,h\text{-mf}}$) effects of flow changes, had very similar AIC_c values to those from models that did not ($D_{1,h}$, Table 2.3a, Fig. 2.3a). The addition of a flow effect resulted in a negligible improvement in fit as evidenced by almost equivalent log likelihood values. In this case the more complex flow-dependent models is not supported by the data even though the AIC_c values are close (see p. 131 of Burnham and Anderson 2002). Small differences in the magnitude of the flow effect reinforce this result (Fig. 2.3a). A similar result was obtained for the daily flow change model in high-angle habitat ($D_{1,h\text{-df}}$). In contrast, there was moderate support for the monthly flow effect model in high-angle habitat ($D_{1,h\text{-mf}}$). However in this case, fork length was lower in high-flow months (July-August) compared to low-flow months (September and November, Table 2.2a), making it difficult to separate the effects of fork length and flow on capture probability. A similar result occurred for the monthly flow comparison in high-angle habitat from mark-recapture data (Tables 2.2b and 2.3b, $MR_{2,h\text{-mf}}$ vs. $MR_{2,h}$), mainly due to higher capture probabilities during low-flow months on the first pass. The fish size-monthly flow effect confounding was also seen in the size-stratified analysis for high-angle habitat (Table 2.4), where the increase in the number of parameters in the flow-stratified model ($L_{3,h\text{-mf}}$) relative to the model that did not account for flow ($L_{3,h}$) was almost identical to the increase in the log-likelihood across models. As a result, the AIC_c values for both models were the same.

Effects of Recovery Period on Capture Probability

Capture probabilities based on one-hour recovery experiments tended to be higher than those from 24-hour experiments but the magnitude of differences depended on habitat type. The most likely estimate of capture probability on the second pass of mark-recapture experiments with a one-hour recovery period in low-angle habitat was over twice the value based on experiments with a 24-hour recovery period (Table 2.3b, Fig. 2.3b). The model that accounted for recovery time was strongly supported relative to the model that did not. Capture probabilities for one-hour and 24-hour recovery period experiments in high-angle habitat were very similar and the difference in AIC_c between models was negligible. However, in high-angle habitat, the distribution of one-hour recovery experiments was concentrated in early months when fish were smaller relative to the 24-hour experiments (Table 2.2b). Thus, the effect of recovery period was

25

confounded with the effect of fish size. When the effect of size was accounted for by repeating the analysis using the size-dependent model, there was moderate support for the model that accounted for recovery period ($L_{3,h\text{-rp}}$) relative to the model that did not ($L_{3,h}$, Table 2.4). There was strong support for the size-stratified recovery period model in low-angle habitat.

Density-Dependence and Bias in Capture Probability

The effect of density on capture probability estimates depended on both habitat type and the method used to estimate capture probability. Based on depletion data, there was little evidence for density dependence in capture probability estimates in low-angle habitat, but strong evidence in high-angle habitat. Capture probability estimates were negatively correlated with estimates of log population density (Fig. 2.4a and b, Table 2.5) and the slopes were significantly different than zero in both low- (n=19, slope= -0.136, p<0.001) and high-angle habitats (n=47, slope=-0.175, p<0.001). However, simulations revealed that the expected slope of p-N relationships due to sampling error increased as capture probability was reduced (Fig 4a and b, dashed lines). Based on the bootstrap analysis of expected p-N slopes, the probability that the observed slope of the p-N relationship could be due to chance alone, was 23% in low-angle habitat, but only 1% in high-angle habitats (Fig. 2.5a). The difference in probabilities of density-dependent effects among habitat types was due both to the lower observed p-N slope in low-angle habitat, as well as the greater variance in the distribution of expected slopes because of smaller sample size.

For mark-recapture experiments, there was strong evidence for density dependence in capture probability estimates in low-angle habitat, but little evidence for this dynamic in high-angle habitat. The strength of the negative correlation between capture probability and log density varied by habitat type (Fig. 2.4c and d, Table 2.5). In low-angle habitat, the slope was steep and significant (n=7, slope=-0.249, p=0.011), while in high-angle habitat it was not (n=35, slope=-0.020, p=0.42). Simulations showed that when a large number of mark-recapture experiments are conducted (n=250), there is little correlation between p and N (Fig. 2.4c and d). This occurs because, unlike the case for depletion experiments, estimates of capture probability on the second pass are not dependent on population size because they are based on the recovery rate of a known

number of marked fish. This difference also results in lower variance of the distributions of expected p-N slopes based on mark-recapture relative to depletion experiments (Fig. 2.5). The observed slope in low-angle habitat was relatively steep and comparison with the CDF suggests there was <1% probability that it could have arisen due to chance alone. In contrast, the probability that the observed slope in high-angle habitat could be due to sampling error was 32%.

The correlation between density and fork length confounded the evaluation of the effects of density on capture probability. The log of density was significantly negatively correlated with fork length based on data from both depletion and mark-recapture experiments in both habitat types (Table 2.5). This occurred because fish densities declined and fish grew over the sample period from early summer through late fall, and because within sampling periods, populations at sites with higher fish densities tended to be comprised of smaller fish (Fig. 2.4). The bootstrap analysis implied strong support for density dependence in capture probabilities based on depletion experiments in high-angle habitat, and based on mark-recapture experiments in low-angle habitat (Fig.'s 2.4, 2.5). However, these were also the only cases where the relationships between capture probability and fork length were both positive and significant (Table 2.5), and where the confounding between size, density, and capture probability was apparent in the size-stratified capture probability-density relationships (Fig. 2.4b and c).

Simulations demonstrated that capture probability is substantially overestimated from depletion experiments when the true capture probability is low and population size at discrete sites is small. Depletion estimation failure rates were 25% and capture probability was overestimated by 54% at a simulated capture probability of 0.2 across the range of densities we simulated. Bias in capture probability (% bias=100*(estimated-simulated)/simulated) increased with decreasing population size when capture probability was ≤0.4 (Fig. 2.4a or b, dashed lines). At a simulated capture probability of 0.3, which is close to the observed mean from mark-recapture experiments, capture probability was overestimated by 23% and the estimation failure rate was 15% across the range of densities we simulated. Failure rate and bias in depletion estimates were minor or negligible at capture probabilities ≥ 0.6, regardless of density. In contrast, there were

virtually no estimation failures or bias (<0.4%) in capture probabilities from simulated mark-recapture experiments.

2.4   Discussion

This study has demonstrated that it is feasible to estimate capture probabilities for juvenile fish in a range of large river habitat types using a combination of backpack and boat electrofishing. Capture probabilities based on both depletion and mark-recapture experiments were reasonably precise (CV=0.26). While estimates from depletion experiments (mean p = 0.54) were higher than those from mark-recapture experiments (mean p=0.31 and 0.28 on 1st and 2nd passes, respectively), both were sufficiently large to allow reasonably precise estimation of population sizes at discrete sites. Capture probability increased with fish size in both mark-recapture and depletion experiments, and field data supported the assumption that populations within discrete sites can be treated as effectively closed.

Given that capture probability has been shown to decline with increasing stream size (Peterson et al. 2004, Rosenberger and Dunham 2005), one might expect capture probability to be lower in larger river systems like the Colorado River. Our data suggest this is not the case as capture probability estimates were within ranges reported for smaller streams. Eighty percent of depletion-based estimates were between 0.28 and 0.75, similar to ranges reported for juvenile brown trout (0.4-0.6, Wyatt 2002), bull trout (Salvelinus confluentus) and cutthroat trout (Oncorhynchus clarki, 0.2-0.6, Peterson et al. 2004), and rainbow trout (0.5-0.65, Rosenberger and Dunham 2005). Eighty percent of mark recapture-based estimates of capture probability fell between 0.17 and 0.45, a range similar to those reported for bull trout and cutthroat (0.1-0.3, Peterson et al. 2004), and rainbow trout (0.3-0.5, Rosenberger and Dunham 2005). The range in our capture probability estimates was larger than the ranges reported in other studies, perhaps because we sampled age-0 trout over the growing season, where fish size, and therefore vulnerability to capture, changed substantially.

Data from holding and mark-recapture experiments supported the fundamental assumption that populations at discrete sites are effectively closed. Holding experiments showed that there is very likely negligible mortality of marked fish after release for at

least 24 hours. In large rivers, it is not logistically feasible to enclose mark-recapture or depletion sites with stop-nets as is commonly done in small streams. However, capture of marked fish in 25 m sections adjacent to mark-recapture sites was extremely rare, indicating that populations within sites can be treated as effectively closed for the 24-hour period between release and recapture. This conclusion is supported by studies that show limited effects of electrofishing (Dunham et al. 2002) and electrofishing-based capture and marking (Mitro and Zale 2002, Young and Schmetterling 2004) on salmonid movement, as well as those that show salmonids tend to have very restricted movements over short and sometimes extended time periods (e.g., Edmundson et al. 1968, Roni and Fayram 2000, Rodriquez 2002). It is certainly possible that some marked fish moved beyond the 25 m lengths of shoreline that was sampled upstream and downstream of mark-recapture sites, and that we therefore underestimated the extent of emigration and capture probability. However, the proportion of a population that is displaced over increasing large distances is well described by a steep negative slope (see meta-analysis of Rodriquez 2002). Considering that there were few individuals found within the 25 m shoreline areas bordering the mark-recapture sites, the number of fish that migrated further then this distance must be very small, and would therefore have a minor effect on capture probability estimates. In addition, had emigration out of depletion and mark-recapture sites been a significant problem in our study, capture probability estimates should have been lower than those reported for smaller streams where sites were enclosed with stop-nets, which was not the case

There was strong evidence from mark-recapture and depletion experiments that capture probability increased with fish size. A positive relationship between fish length and electrofishing capture probability, such as the ones estimated in this study from mark-recapture data, is consistent with many other investigations (Borgstrom and Skaala 1993, Anderson 1995, Bayley and Austen 2002, Peterson et al. 2004) and is not surprising considering larger fish have a greater head-to-tail voltage potential in an electric field, are easier to see and net, and make less use of interstitial spaces relative to smaller fish and are therefore easier to capture. However, the relationship between size and capture probability should be estimated for each specific study as the functional form can be variable, ranging from linear (e.g. Borgtrom and Skaala 1993), to logistic

29

(Peterson et al. 2004, this study), to dome-shaped (Bayley and Austen 2002). The form and parameters will likely depend on the range of fish sizes available for capture, gear type, habitat, environmental variables, and fish behaviour.

We found significant differences in capture probability across habitat types from mark-recapture experiments. Capture probability tended to be higher in low-angle habitat sampled by backpack eletrofishing. The mean of the size-capture probability function in high-angle habitat sampled by boat electrofishing (μ=39.9 mm) was greater than in low-angle (μ=26.6 mm) habitat sampled by backpack electrofishing, which implies lower vulnerability of smaller fish in high-angle habitat, a result consistent with depletion data. This was likely caused by the larger interstitial spaces between talus blocks in high-angle shorelines, making it more difficult to see and retrieve very small fish that were stunned, and because the very immediate shoreline areas utilized by smaller fish could be more effectively sampled using a backpack electrofisher than a boat electrofisher. Our evaluation of 'habitat' effects on capture probability could perhaps be more accurately described as a comparison of 'habitat-and-gear type' effects. We argue that such a distinction is irrelevant; what matters is that capture probability be quantified by habitat type, regardless of whether different gears, or ways of using the same gear, are employed. Or stated more broadly, it is not necessary to use the same gear to quantify relative habitat use, as long as differences in capture probability between specific combinations of habitat and gear are accounted for.

There was no affect of flow on capture probability estimates based on depletion experiments conducted at the daily minimum and maximum flows during the summer, but the effect of flow based on monthly changes was difficult to discern because of confounding between fish size and monthly flow levels. Physical conditions within immediate nearshore habitats in the Lee's Ferry reach are not very sensitive to flow, at least over the range experienced in this study. Measurements of nearshore (1.5 m from shore) average water-column velocities across 24 sites in 2004, taken at discharges of 260 (daily minimum flow) and 500 (daily maximum flow) $m^{3 \cdot} sec^{-1}$, very close to the range in this study (Table 2.1), differed by no more than 3-6 $cm^{\cdot}sec^{-1}$ (see Table 3.1 from Chapter 3). In large rivers, velocities in the immediate nearshore environment that can be sampled by electrofishing are less influenced by discharge than in smaller rivers because the ratio

of nearshore sample width to the total wetted width is much lower. We suspect this is why our capture probability estimates were relatively insensitive to the effects of flow, and perhaps why capture probability has been shown to be sensitive to indices of flow, such as cross-sectional area, in smaller systems (e.g., Rosenberger and Dunham 2005).

The effects of fish density on capture probability were challenging to discern, variable among habitat types and estimation methodologies, and confounded with the effect of fish size. Using bootstrap simulation, we concluded there was a significant relationship in high-angle habitat based on depletion experiments, and in low-angle habitat based on mark-recapture experiments. However, these were also the cases where a negative correlation between fish size and density was most apparent. Density-dependent growth in stream-dwelling populations of age-0 salmon and trout has been well documented (e.g., Armstrong 1997, Jenkins et al. 1999, Imre et al. 2005), and will result in a negative correlation between density and fish size among sites sampled within a short time interval, and among sites sampled through time. Cumulative growth and mortality over the growing season will also result in a negative correlation between density and fish size based on samples collected through time even in the absence of density-dependent growth (e.g., Elliott 1994). Effects of density and fish size on capture probability are separable by manipulations of size and density in artificial ponds or streams (e.g. Bayley and Austen 2002). In field studies of juvenile fish such as the one presented here, it will likely be very difficult to empirically separate the effects of fish density and size on capture probability. However, this difficulty is not necessarily a problem in assessments of juvenile abundance if the size-density relationship is stationary and the relationship between size and capture probability is accounted for in the estimation of capture probabilities.

Capture probabilities determined from depletion experiments were on average 80% higher than those based on mark-recapture. Results from the simulation study and previous investigations strongly suggest that the latter estimates are more realistic. Positive bias in capture probabilities estimated from the depletion method occurs because of both model misspecification and the nature of the likelihood function. There was not enough information in the depletion data to select a removal model that allowed capture probability to decline with successive passes, or even between the first pass and later

31

ones. However, it is well recognized that the power of such tests is generally very low (Otis et al. 1978, Rosenberger and Dunham 2005). Failure to account for declining capture probability across successive passes of electrofishing has been shown to result in overestimates in capture probability of 39% for bull trout and cutthroat trout (Peterson et al. 2004), and 30-50% for rainbow trout (Rosenberger and Dunham 2005), with the extent of bias being greater for smaller fish which generally have lower capture probability. Our simulations showed that even if capture probability is constant over passes, it can still be substantially overestimated if population size and capture probability are low. For example, at a true capture probability of 0.3, capture probability will be overestimated by 25% at densities of 100 fish$\cdot$100 m^{-1} (or 50 fish in a typical 50 m site). This bias occurs because the multinomial likelihood function used in Otis et al. (1978) is derived from probabilities associated with finite samples, and these probabilities depend on sample size (Schnute 1983). For example, the probability of obtaining five heads of a perfectly balanced coin flipped 10 times will be higher than the probability of obtaining 50 heads if it is flipped 100 times. Thus, when jointly estimating capture probability and population size in the depletion method by maximizing the likelihood function, slightly higher probabilities occur at lower population sizes, resulting in the tendency to overestimate capture probability. The combined bias associated with model-misspecification reported from previous studies, and from the likelihood function estimated in this study, implies our depletion-based estimates of capture probability are approximately 50-75% too high. The 80th percentile range of capture probability estimates from depletion experiments (0.28-0.75), adjusted for biases of 50% and 75%, were 0.19-0.50 and 0.16-0.43, respectively. These ranges are much closer to the range from our mark-recapture experiments of 0.18-0.37.

We recommend that mark-recapture experiments, rather than depletion experiments, be used to estimate capture probabilities for juvenile fish in large rivers in all cases where it is possible to mark fish. Our recommendation is similar to those from recent studies conducted in smaller systems (Peterson et al. 2004, Rosenberger and Dunham 2005, Sweka et al. 2006). Over the range of capture probabilities and population densities experienced in this study, simulation results showed that values determined from depletion experiments were likely substantially overestimated due to the likelihood

function. Differences between mark-recapture and depletion estimates suggest there was additional bias due to changing capture probability over passes, a dynamic that could not be detected from the depletion data alone. Direct estimation of size-dependent capture probabilities should be a fundamental component in the evaluation of juvenile populations if fish size has the potential to vary substantially over the study period or among study sites. Mark-recapture experiments have a distinct advantage over depletion methods in this respect because they do not require the estimation of abundance by size class, reducing the number of parameters that need to be estimated. Finally, mark-recapture experiments allow for field-based validation of key closure assumptions. These assumptions must be evaluated when electrofishing at discrete sites due to the potential for latent mortality and emigration after release. In this study, we did not test whether marked fish had the same capture probability as unmarked fish. We are currently evaluating this assumption by using different gear types for capture (dip netting via snorkeling) and recapture (e.g., electrofishing) passes, an approach that cannot be used in depletion studies unless capture probability is allowed to vary among passes. Although our study was based only on juvenile rainbow trout, it is likely that the general approach and recommendations are applicable to a wide range of fish species.

The dynamics of capture probability for juvenile fish are complex because they depend in large part on patterns of behaviour and habitat use that occur over a wide range of temporal and spatial scales. For example, in this study we showed that daily changes in flow do not influence capture probability within immediate nearshore zones that were sampled. However, in Chapter 3, I show that most age-0 trout in the Lee's Ferry reach do not migrate with the waters edge as it rises and falls over a 24-hour period with changing discharge. At the daily maximum flow, most fish remain further offshore closer to or within the portion of the channel that is continuously wetted over 24 hours. As a result, fish densities within the immediate nearshore zones that are sampled at the daily maximum flow were 50-80% lower then when sampled at the daily minimum. Thus, if we define capture probability as the proportion of fish that are caught over a cross-section of the river, or on a reach-wide basis, rather than within the immediate shoreline zone of sampling areas (as in this study), flow can have an effect on capture probability because of its influence on fine-scale patterns of habitat use. In the longer-term study of

recruitment dynamics in the Lee's Ferry reach (Chapters 4-6), we have controlled for this effect by sampling only at the daily minimum flow, which is why most of the depletion and mark-recapture experiments in this study were conducted at the minimum flow. The longer-term study has also clearly documented an ontogenetic habitat shift from low- to high-angle shorelines, which occurs over a period of a few months. Had we only used backpack electrofishing to sample age-0 trout, a tactic common to many juvenile fish assessments in rivers, the sampling universe would have been restricted to low-angle shorelines. Estimates of capture probability in this habitat type over the growing season, which would increase with fish size, would not detect the reach-wide decline in capture probability that results from an increasing proportion of the population moving to habitats outside of the sampling universe. Thus, to make valid reach- or system-wide assessments of juvenile fish populations, it is not sufficient to simply estimate capture probability at discrete sites that are easy to sample. Rather, sampling and capture probability estimation should be conducted over the full range of habitats that are used over the period of interest, which in many cases will likely require use of more than one gear type and considerably more effort than is commonly applied.

Table 2.1. Average monthly discharge, and average daily minimum and maximum flow in the Lee's Ferry reach during study months in 2006 and 2007 ($m^3 \cdot sec^{-1}$). The daily range is the variation in flow within a day, and is the difference between the daily minimum and maximum.

Year	Month	Average	Daily Min.	Daily Max.	Daily Range
2006	June	381	253	476	223
	July	381	269	491	223
	August	381	269	493	224
	September	253	173	312	138
	November	285	197	368	171
2007	June	381	253	475	222
	July	370	255	475	220
	August	370	255	478	223
	September	287	182	351	169
	November	288	202	368	167

Table 2.2. Summary statistics of data collected from depletion and mark-recapture experiments. For depletion experiments (a), the 'Daily Flow' column denotes whether sampling was conducted at the daily minimum or maximum flow. The Total Catch and Avg. FL columns denote the total number of fish caught over 3 passes across sites and the average fork length of fish caught on the first pass, respectively. For mark-recapture experiments (b), the 'M', 'r', 'r/M' and 'FL' columns denote the total number of marks applied, recaptured, the ratio of marks recaptured to applied, and the average fork length of fish caught on the 1st pass.

a) Depletion Experiments

Habitat Type	Daily Flow	Sampling Month	Sites Sampled	Meters Sampled	Total Catch	Avg. FL (mm)
Low-Angle	Min.	Jul.	5	150	217	41
		Aug.	6	204	188	45
	Max.	Aug.	5	221	113	51
		Sep.	3	120	55	63
High-Angle	Min.	Jul.	8	400	384	54
		Aug.	8	400	463	59
		Sep.	7	377	214	67
		Nov.	8	589	272	79
	Max.	Aug.	8	486	195	59
		Sep.	6	323	132	71
		Nov.	2	125	29	78

Table 2.2. Con't.

b) Mark-Recapture Experiments

Habitat Type	Recovery Period	Sampling Month	Sites Sampled	Meters Sampled	M	Total r	r/M	Avg. FL (mm)
Low-Angle	1-Hr.	Aug.	2	280	424	239	0.56	43
	24-Hr.	Jul.	3	218	271	31	0.11	36
		Aug.	2	283	365	97	0.27	44
High-Angle	1-Hr.	Jul.	4	272	203	46	0.23	55
		Aug.	4	247	264	94	0.36	57
		Sep.	1	57	46	13	0.28	61
	24-Hr.	Jun.	5	279	58	16	0.28	90
		Jul.	4	271	196	46	0.23	60
		Aug.	4	265	214	63	0.29	62
		Sep.	4	360	192	38	0.20	62
		Nov.	9	1,324	723	227	0.31	84

Table 2.3. Summary of AIC results comparing alternate models applied to depletion (a) and mark-recapture data (b). Column headings k, LL, AICc, and p, denote the number of parameters, log-likelihoods, AIC_c values, and the most likely capture probability estimates, respectively. Subscripts for model names denote the number of capture probabilities (1=common across passes, 2= different probabilities between 1st and subsequent passes) and stratification (i=by experiment, h= by habitat type, df = by daily flow, mf = by monthly flow, c=combined across habitat types). Most-likely estimates for p for the experiment-stratified models are not shown for brevity, but values for $D_{1,i}$ and $MR_{2,i}$ are shown in Fig. 2.1. N denotes population size. See text for more details about specific models.

a) Depletion Experiments

Habitat	Model	Strata	p	k	LL	AIC_c
Model Type (N and p estimated for each exp't)						
Low-Angle	$D_{1,i}$			38	-106.4	294.3
	$D_{2,i}$			57	-96.9	320.7
High-Angle	$D_{1,i}$			94	-253.1	705.4
	$D_{2,i}$			141	-234.4	776.8
Flow and Habitat Effects (N estimated for each exp't but p is common)						
Low-Angle	$D_{1,h}$		0.50	20	-120.1	281.7
	$D_{1,h\text{-}df}$	Daily Min.	0.48	21	-119.6	282.8
		Daily Max.	0.54			
	$D_{1,h\text{-}mf}$	High Flow	0.50	21	-119.9	283.4
		Low Flow	0.55			
High-Angle	$D_{1,h}$		0.51	48	-316.0	730.9
	$D_{1,h\text{-}df}$	Daily Min.	0.50	49	-314.1	729.1
		Daily Max.	0.57			
	$D_{1,h\text{-}mf}$	High Flow	0.48	49	-311.5	724.0
		Low Flow	0.57			
Combined	$D_{1,c}$		0.51	67	-436.2	1,010.5

Table 2.3. Con't.

b) Mark-Recapture Experiments

Habitat	Model	Strata	p_1	p_2	k	LL	AIC$_c$
Model Type (N and p's estimated for each exp't)							
Low-Angle	MR$_{1,i}$				14	-129.3	286.8
	MR$_{2,i}$				21	-93.3	229.1
High-Angle	MR$_{1,i}$				70	-372.4	887.2
	MR$_{2,i}$				105	-257.2	730.1
Flow and Habitat Effects (N estimated for each exp't but p's are common)							
Low-Angle	MR$_{2,h}$		0.43	0.35	9	-195.5	409.1
High-Angle	MR$_{2,h}$		0.29	0.29	37	-419.3	913.2
	MR$_{2,h\text{-}mf}$	High Flow	0.26	0.29	39	-401.3	881.4
		Low Flow	0.34	0.29			
Combined	MR$_{2,c}$		0.34	0.31	44	-644.4	1,377.5
Recovery Period (N estimated for each exp't but p's are common)							
Low-Angle	MR$_{2,h\text{-}rp}$	1 Hr.	0.55	0.47	11	-131.7	285.6
		24 Hrs.	0.27	0.20			
High-Angle	MR$_{2,h\text{-}rp}$	1Hr.	0.28	0.30	39	-417.5	913.7
		24 Hrs.	0.30	0.29			

Table 2.4. Summary of AIC results comparing alternate models applied to mark-recapture data stratified by 10 mm forklengh classes. Column headings k, LL, AICc, denote the number of parameters, log-likelihoods, and AIC_c values, respectively. β, μ, and σ show the maximum likelihood estimates for the maximum, mean, and standard deviation of the size-capture probability function (equation 1). Subscripts for model names denote the number of estimated parameters (1=size-independent capture probabilities, 3= equation 1, 2+ = equation 1 by habitat type with a common β across habitat types) and stratification (h= by habitat type, c=combined across habitat types, mf = by monthly flow, rp = recovery period). See text for more details about specific models.

Habitat	Model	Strata	β	μ	σ	k	LL	AICc
Habitat and Flow Effects								
Low-Angle	$L_{1,h}$		0.31			1	-139.9	281.9
	$L_{3,h}$		0.34	26.61	2.60	3	-128.4	262.8
High-Angle	$L_{1,h}$		0.29			1	-364.8	731.7
	$L_{3,h}$		0.31	39.89	4.57	3	-348.5	703.0
Combined	$L_{3,c}$		0.31	27.21	3.49	3	-492.5	990.9
	$L_{2+,c}$	Low-Angle	0.32	25.25	0.46	5	-477.4	964.8
		High-Angle	0.32	40.23	4.85			
High-Angle	$L_{3,h\text{-}mf}$	High Flow	0.33	39.95	4.57	6	-345.5	703.0
		Low Flow	0.30	45.00	0.00			
Recovery Period Effect								
Low-Angle	$L_{3,h\text{-}rp}$	1 Hr.	0.52	25.02	0.40	6	-82.4	176.9
		24 Hrs.	0.24	29.52	4.39			
High-Angle	$L_{3,h\text{-}rp}$	1Hr.	0.33	35.42	4.33	6	-341.5	695.0
		24 Hrs.	0.31	45.00	0.01			

Table 2.5. Pearson correlation coefficients for relationships between log population density (Log(N)), capture probability (p), and fork length on the 1st pass (FL) based on depletion and mark-recapture data in low- and high-angle habitats.

Method	Habitat	Sample Size	Log(N)-p	Log(N)-FL	p-FL
Depletion	Low-Angle	19	-.59**	-0.48*	0.20
	High-Angle	47	-.70***	-0.35*	.29[1]
Mark-Recapture	Low-Angle	7	-0.87*	-0.87*	0.77*
	High-Angle	35	-0.14	-0.48**	-0.10

*$0.01 < p \leq 0.05$; ** $0.001 < p \leq 0.01$; *** $p \leq 0.001$.

[1] p=0.052 for this correlation
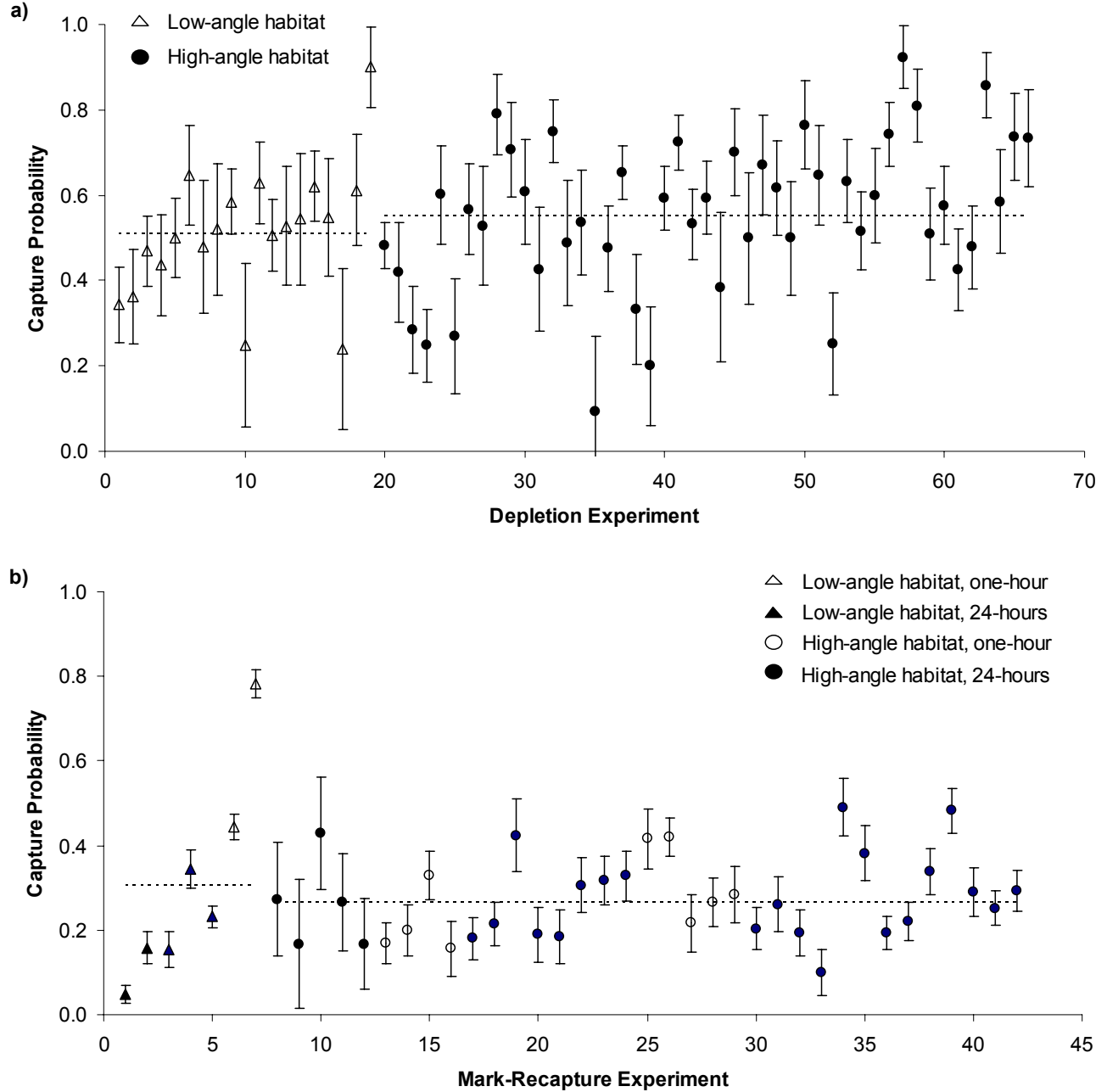
Figure 2.1. Most likely estimates (MLEs) of capture probabilities from depletion (a) and mark-recapture (b) experiments based on models $D_{1,i}$ and $MR_{2,i}$, respectively. Error bars denote the standard error of the MLEs. b) shows capture probability estimates for the second pass of mark-recapture experiments. Triangles and circles represent estimates from low- and high-angle habitats, respectively. Open and filled triangles and circles in b) denote one-hour and 24-hour recovery periods, respectively. Dashed lines represent the average capture probabilities in low- and high-angle habitats. Experiments are presented in chronological order within habitat types.

42

Low	Marks:	102	339	375	209	30	4	1					(1,060)
	Recaps:	12	110	155	74	13	1	1					(366)
High	Marks:	12	70	272	373	328	268	238	161	64	40	24	(1,850)
	Recaps:	0	6	62	115	99	92	79	45	21	9	7	(535)
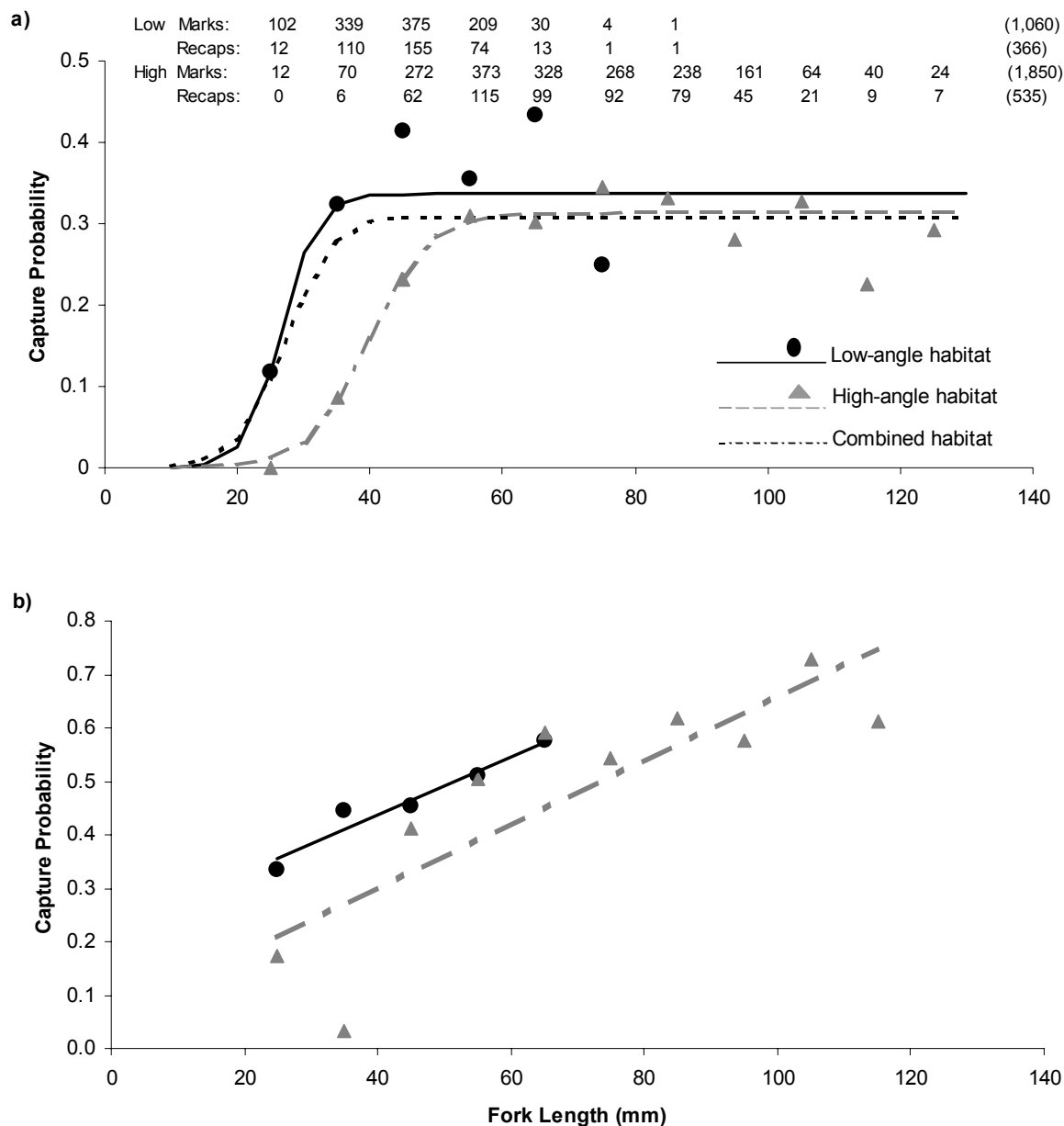
Figure 2.2. Relationships between capture probability and fork length in low- (solid black line) and high-angle (gray dashed line) habitat types based on mark-recapture (a) and depletion (b) data. a) shows the best-fit logistic relationships (equation 1) to habitat specific data as well as data combined across habitat types (black dashed line). Data points in a) represent the ratio of the sum of recaptured marks across experiments to the sum of marks applied, by 10 mm size class and habitat type (i.e., independent Peterson estimates). Text at top of a) denotes the number of marks and recaptures in each length class, with the totals across length classes shown in parentheses. Note that the data point for the 85 mm length class in low-angle habitat is not shown (capture probability = 1) as it exceeds the maximum of the y-axis scale. In b), data points are the best-fit capture probabilities independently estimated for each size class, and lines show best-fit linear relationships.

43
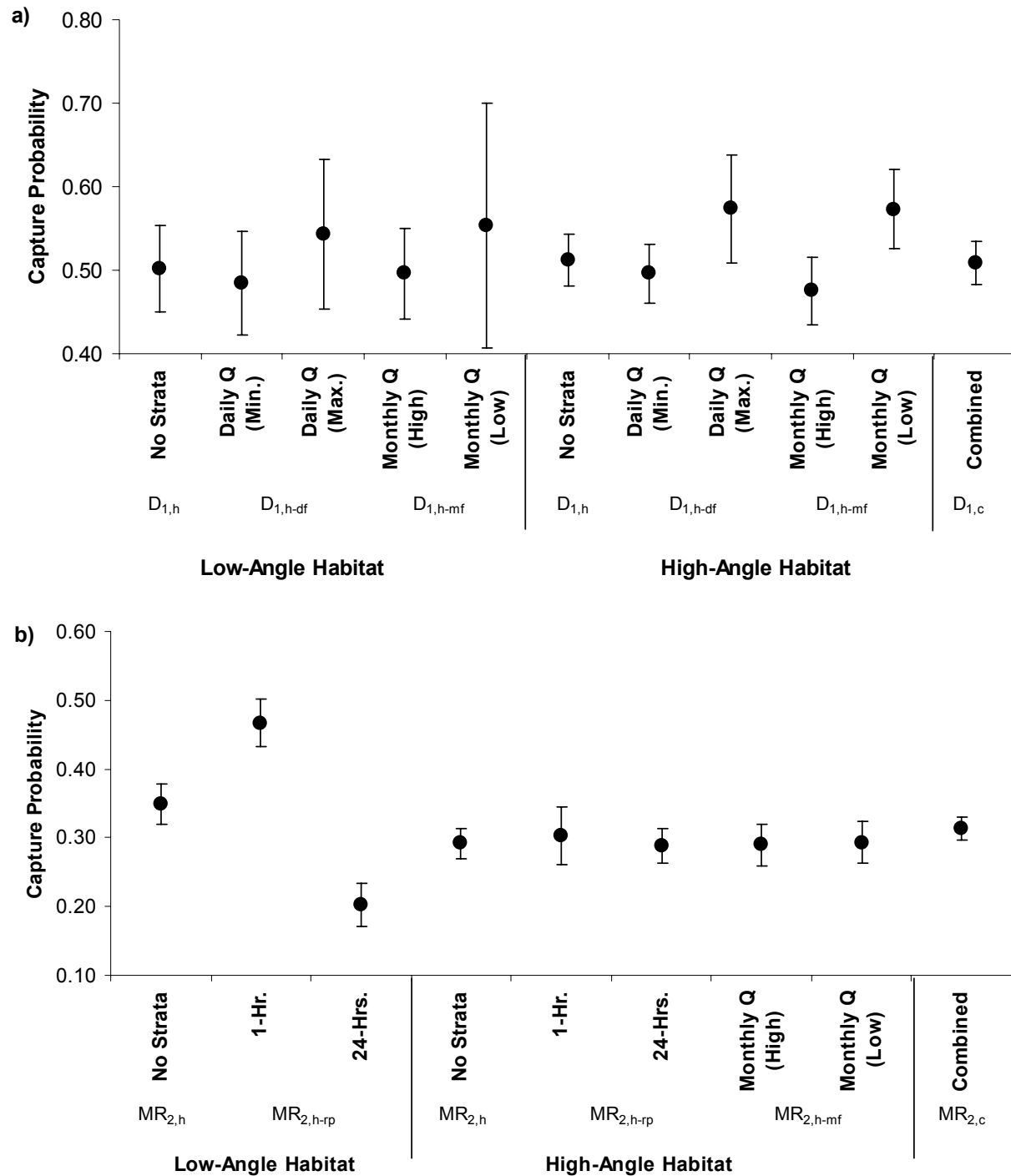
Figure 2.3. Most likely estimates of capture probability from depletion (a) and mark-recapture experiments (b) in low- and high-angle habitat based on different models. Error bars denote 95% confidence limits. Capture probabilities in a) are based on the depletion model that assumes equal capture probability across passes. Capture probabilities in b) are based on the mark-recapture model that allows capture probabilities to differ across passes, and values for the second pass are shown. See Table 2.3 for definition of models.
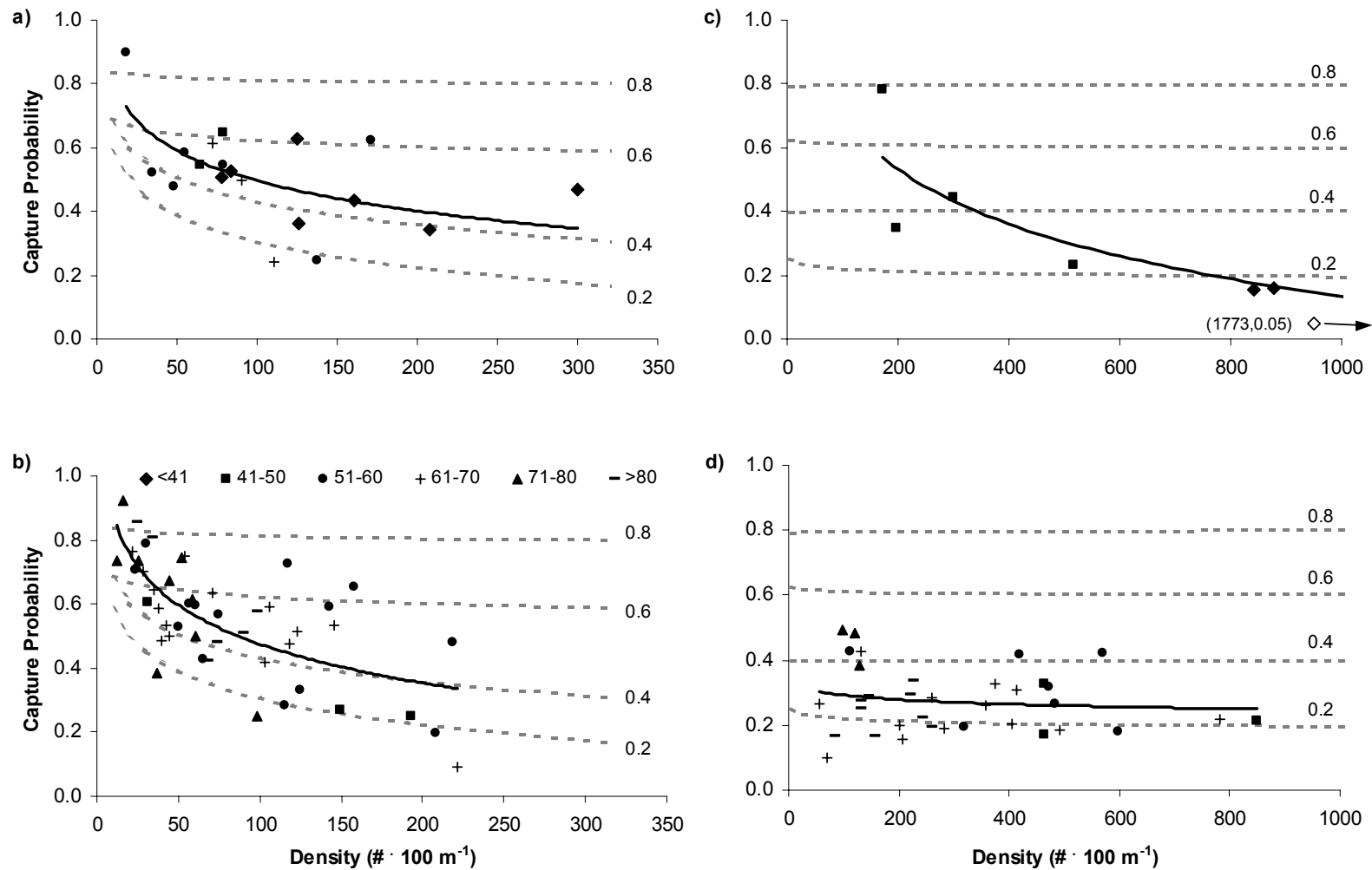
Figure 2.4. Relationships between estimated capture probability (p) and population density (N) in low- and high-angle habitats from depletion (a and b, respectively) and mark-recapture (c and d, respectively) experiments. Symbols shown in the legend of b) denote the average fork length on the first pass in 10 mm increments. The best-fit linear-log relationships to the estimates are shown by solid lines. The expected relationships due to sampling error under a range of simulated capture probabilities (0.2-0.8) and random densities are shown by the dashed lines. The open diamond in c) denotes a point that is off the graph scale, with the true coordinate shown in parentheses.
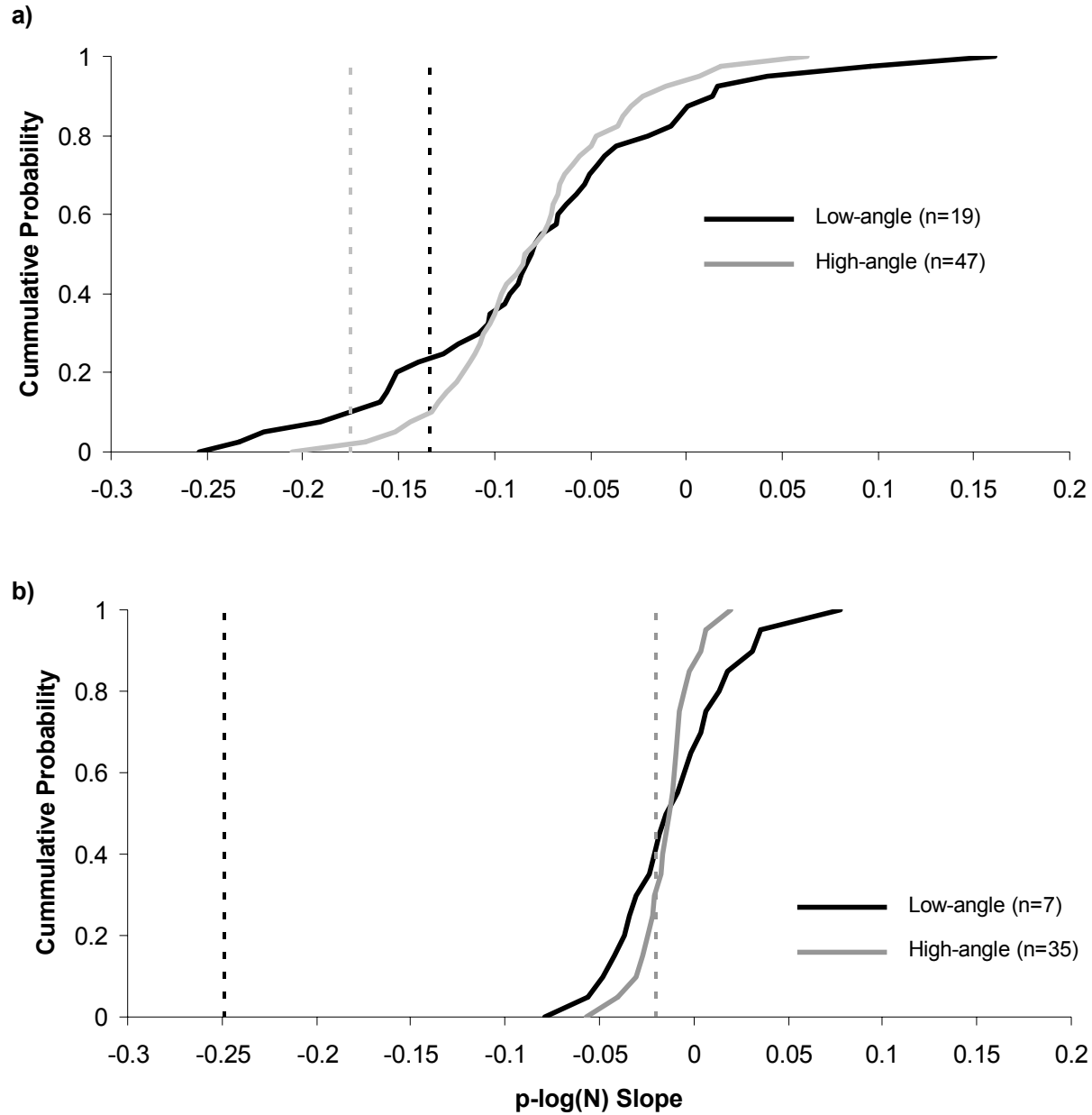
Figure 2.5. Cumulative frequency distributions (CFD's) of the expected slopes of the capture probability-log population density relationship ($p = a + b \cdot log(N)$) generated from simulated data (solid lines), compared to slopes fit to the data (vertical dashed lines, slope of solid lines in Fig. 2.4) based on depletion (a) and mark-recapture (b) data. The CFD's were computed by estimating p-log(N) slopes from 100 sets of simulated data based on the actual sample sizes of 19 (low-angle, black lines) and 47 (high-angle, gray lines) to represent depletion experiments, and 7 (low-angle) and 35 (high-angle) to represent mark-recapture experiments.

2.5 References

Ainslie, B.J., Post, J.R., and A.J. Paul. 1998. Effects of pulsed and continuous CD electrofishing on juvenile rainbow trout. North American Journal of Fisheries Management 18:905-918.

Anderson, C.S. 1995. Measuring and correcting for size selection in electrofishing mark-recapture experiments. Transactions of the American Fisheries Society 124:663-676.

Armstrong, J.D. 1997. Self-thinning in juvenile sea trout and other salmonid fishes revisited. Journal of Animal Ecology 66:519-526.

Bayley, P.B. and D.J. Austen. 2002. Capture efficiency of a boat electrofisher. Transactions of the American Fisheries Society 131:435-451.

Borgstrom, R., and O. Skaala. 1993. Size-dependent catchability of brown trout and Atlantic salmon parr by electrofishing in a low conductivity stream. Nordic Journal of Freshwater Research 68:14-21.

Burnham, K.P., and D.R. Anderson. 2002. Model Selection and Multimodel Inference, 2nd edition. Springer-Verlag, NY.

Cross, D.G. and B. Stott. 1975. The effect of electric fishing on the subsequent capture of fish. Journal of Fish Biology 7:349-357.

Dunham, K.A., Stone, J., and J.R. Moring. 2002. Does electric fishing influence movements of fishes in streams? Experiments with brook trout, *Salvelinus fontinalis*. Fisheries Management and Ecology 9:249-251.

Edmundson, E., F. E. Everest, and D. W. Chapman. 1968. Permanence of station in juvenile chinook salmon and steelhead trout. Journal of the Fisheries Research Board of Canada 25:1453-1464.

Elliott, J.M. 1994. Quantitative ecology and the brown trout. Oxford University Press, Oxford. 287 pp.

Gaines, P.C., and C.D. Martin. 2004. Feasibility of dual-marking age-0 Chinook salmon for mark-recapture studies. North American Journal of Fisheries Management 24: 1456-1459.

Gelman, A., Carlin, J.B. Stern, H.S., and D.B. Rubin. 2004. Bayesian data analysis. Chapman and Hall/CRC. 668 pp.

Hilborn, R., and C.J. Walters. 1992. Quantitative fisheries stock assessment. Chapman and Hall, New York. 570 pp.

Imre, I., Grant, J.W.A., and R.A. Cunjak. 2005. Density-dependent growth of young-of-year Atlantic salmon *Salmo salar* in Catamaran Brook, New Brunswick. Journal of Animal Ecology 74:508-516.

Jenkins, T.M. Jr., Diehl, S., Kratz, K.W., and S.D. Cooper. 1999. Effects of population density on individual growth of brown trout in streams. Ecology 80:941-956.

McKinney, T., Speas, D.W., Rogers, R.S., and W.R. Persons. 2001. Rainbow trout in a regulated river below Glen Canyon Dam, Arizona, following increased minimum flows and reduced discharge variability. North American Journal of Fisheries Management 21:216-222.

Mesa, M.G., and C.B. Schreck. 1989. Electrofishing mark-recapture and depletion methodologies evoke behavioural and physiological changes in Cutthroat trout. Transactions of the American Fisheries Society 118:644-658.

Mietz, S.W. 2003. Evaluating historical electrofishing distribution in the Colorado River, Arizona, based on shoreline substrate. M.Sc. thesis, Department of Biology, Northern Arizona University, Flagstaff, AZ.

Mitro, M.G., and A.V. Zale. 2002. Estimating abundances of age-0 rainbow trout by mark-recapture in a medium-sized river. North American Journal of Fisheries Management 22:188-203.

Otis, D.L. Burnham, K.P., White, G.C., and D.R. Anderson. 1978. Statistical inference from capture data on closed populations. Wildlife Monographs 62. 135 pp.

Otter Research Ltd. 2004. An introduction to AD Model Builder version 7.1.1. for use in nonlinear modeling and statistics. 194 pp. Report available from otter-rsch.com.

Peterson, J.T., Thurow, R.F., and J.W. Guzevich. 2004. An evaluation of multipass electrofishing for estimating the abundance of stream-dwelling salmonids. Transactions of the American Fisheries Society 133:462-475.

Randle, T.J., and E.L. Pemberton. 1987. Results and analysis of STARS modeling efforts of the Colorado River in Grand Canyon. U.S. Department of Interior, Bureau of Reclamation. NTIS No. PB88-183421/AS.

Rodriquez, M.A. 2002. Restricted movement in stream fish: The paradigm is incomplete, not lost. Ecology 83:1-13.

Roni, P., and A. Fayram. 2000. Estimating winter salmonid abundance in small western Washington streams: a comparison of three techniques. North American Journal of Fisheries Management 20:683-692.

Rosenberger, A.E., and J.B. Dunham. 2005. Validation of abundance estimates from mark-recapture and removal techniques for rainbow trout captured by electrofishing in small streams. North American Journal of Fisheries Management 25:1395-1410.

Schnute, J. 1983. A new approach to estimating populations by the removal method. Canadian Journal of Fisheries and Aquatic Sciences 40:2153-2169.

Speas, D.W., Walters, C.J., Ward, D.L, and R.S. Rogers. 2004. Effects of intraspecific density and environmental variables on electrofishing catchability of brown and rainbow trout in the Colorado River. North American Journal of Fisheries Management 24:586-596.

Sweka, J.A., Legault, C.M., Beland, K.F., Trial, J., and M.J. Millard. 2006. Evaluation of removal sampling for basinwide assessment of Atlantic salmon. North American Journal of Fisheries Management 26:995-1002.

Vernieu, W.S, Hueftle, S.J., and S.P. Gloss. 2005. Water quality in Lake Powell and the Colorado River. *In* The state of the Colorado River ecosystems in Grand Canyon. Edited by S.P. Gloss, J.E. Lovitch, and T.S. Melis. U.S. Geological Survey Circular 1282. Available from http://www.gcmrc.gov/products/score/2005/score.htm.

Voichick, N., and S.A. Wright. 2007. Water temperature data for the Colorado River and tributaries between Glen Canyon Dam and Spencer Canyon, Northern Arizona, 1988-2005. USGS Data Series Report. U.S. Geological Survey.

Williams, B. K., J. D. Nichols, and M. J. Conroy. 2002. Analysis and management of animal populations. Academic Press, London, UK.

Wyatt, R.J. 2002. Estimating riverine fish population size from single- and multiple-pass removal sampling using a hierarchical model. Canadian Journal of Fisheries and Aquatic Sciences 59:695-706.

Young, M.K. and D.A. Schmetterling. 2004. Electrofishing and salmonid movement: reciprocal effects in two small montane streams. Journal of Fish Biology 64:750-761.

3.0 Effects of Hydropeaking on Nearshore Habitat Use and Growth of Age-0 Rainbow Trout in a Large Regulated River[2]

3.1 Introduction

Hydroelectric dams alter the magnitude and frequency of flows and can have negative impacts on downstream fish communities (Cushman 1985). In some regulated rivers, power load following operations, often referred to as hydropeaking, result in considerable hourly and diel variation in flow, depth, and water velocity, creating a very unnatural and potentially harsh physical environment. This impact is of special concern for juvenile fish, which in large rivers, rear almost exclusively in shallow shoreline habitats (Gaudin 2001) that are destabilized by hydropeaking operations (Freeman et al. 2001). Diel variation in flow has been shown to result in stranding and mortality of juvenile fish (Bradford 1997, Saltveit et al. 2001, Halleraker et al. 2003), and is hypothesized to limit survival rates via indirect effects from displacement out of preferred habitats, food depletion, and increases in stress, energetic costs, and predation risk (Scruton et al. 2003).

Most studies of indirect effects of short-term flow fluctuations have focused on the behavioural and energetic responses of juvenile salmonids. Short-term variation in flow has been shown to result in both negligible (Robertson et al. 2004) and extensive (Berland et al. 2004) movement in Atlantic salmon (Salmo salar) parr. Flow-dependent movement responses can be highly variable among individuals, with some parr showing strong site fidelity across a wide range of flows (Kemp et al. 2003, Scruton et al. 2003). Juvenile salmonids have been shown to use higher nose velocities with increasing water flow and to not fully compensate for increased velocity by changing microposition (Vehanan et al. 2000, Girard et al. 2004). Shirvell (1994) reported juvenile salmonids initially responded to increased flow by moving closer to the streambed and then, if necessary, by moving laterally to seek out appropriate velocity conditions. Surprisingly,

there is little evidence that such responses increase stress levels or have negative bioenergetic consequences. Cardiac activity for adult brook trout and walleye (Sander vitreus vitreus, Murchie and Smokorowksi 2004), and oxygen consumption for juvenile white sturgeon (Geist et al. 2005), did not increase under fluctuating flows. Stress response in juvenile brown trout caused by moderate flow fluctuations in experimental flumes subsided within a few days after the fish became habituated to the flow regime (Flodmark et al. 2002). Hourly variation in flow in experimental channels had no negative effects on the growth or survival of rainbow trout fry (Irvine 1987).

On the whole, experimental studies document relatively little impact of hourly variation in flows on juvenile fish, yet stabilization of regulated flows has been shown to increase the abundance of fish populations (Travnichek et al. 1995, McKinney et al. 2001, Connor and Pflug 2004). However in all these cases, flow was stabilized by increasing the minimum flow and by reducing the extent of within-day variation, so the effects of the two changes are confounded. Further, the stabilized flow regimes may have benefited spawning and incubation life stages as well as juvenile fish survival. Reduction in the extent of hourly variation in flow is commonly recommended as a way to improve the status of fish populations (Dejalon and Sanchez 1994, Poff et al. 1997), but empirical support for such recommendations is limited. This discrepancy leads to considerable debate, especially in large river settings, where lost hydropower revenues resulting from flow stabilization can be substantial.

In this paper, we evaluate the effects of hourly variation in flow caused by hydropeaking at Glen Canyon Dam on the nearshore habitat use and growth of age-0 rainbow trout in the Lee's Ferry reach of the Colorado River, Arizona. Maximum flows over a 24-Hour (diel) cycle at Glen Canyon Dam occur during the day and early evening when power demand is high, and are reduced at night when demand subsides (Fig. 3.1a). We propose two alternate hypotheses of how age-0 fish will respond to this diel regime (Fig. 3.2). The shoreline-tracking hypothesis assumes that trout move freely in response to hourly changes in flow so that they remain in shallow and low velocity habitat typically used by young of year (Chapman and Bjornn 1969, Everest and Chapman 1972). If this hypothesis holds in the Lee's Ferry reach, age-0 trout will need to make two lateral movements per day with the rise and fall in flow so as to remain within immediate

nearshore areas where these depth and velocity conditions occur. The restricted-movement hypothesis assumes that age-0 trout restrict the extent to which they move in response to hourly flow variation. If this hypothesis holds in the Lee's Ferry reach, only a limited proportion of trout will be found within immediate nearshore areas at the daily maximum flow. The remainder will be found further from the bank in deeper and faster water, with some perhaps remaining in the permanently submerged zone. During the day in the Lee's Ferry reach in summer months, when daily maximum air temperatures on the surface of exposed gravel and sand bars can reach 50-60 $^{\circ}$C, a horizontal gradient in water temperature is created where temperatures in the immediate shoreline areas within 1-2 m from the waters edge are 3-5 $^{\circ}$C warmer than in the main flow further offshore (Fig. 3.2, Korman et al. 2006). Under the shoreline-tracking hypothesis, age-0 trout will experience warmer water temperatures during the day because they maintain their position in immediate nearshore areas. In contrast, trout that behave according to the restricted-movement hypothesis would mostly be located further offshore during the day, and therefore in colder water.

The shoreline-tracking hypothesis assumes that habitat use for age-0 fish in regulated rivers follows the pattern observed in natural systems (e.g., Chapman and Bjornn 1969, Everest and Chapman 1972, Bustard and Narver 1975, Sheppard and Johnson 1985), where fish limit themselves to immediate shoreline areas where water depths and velocities are optimal for feeding (Nislow et al. 2000, 2004), resting, and avoiding piscivorous predators (Schlosser 1987, Walters and Juanes 1993, Rosenfeld and Boss 2001). The restricted-movement hypothesis assumes that the benefits of tracking optimal depths and velocities on an hourly basis by remaining in immediate nearshore areas do not outweigh the costs associated with moving, such as increased exposure to predation while moving (Biro et al. 2003), or the competitive disadvantage of abandoning territories (Elliott 1986, Ward et al. 2007). Density of benthic invertebrates in the Lee's Ferry reach in shoreline areas that are exposed to air due to hourly variation in flow, sometimes referred to as varial zones, are considerably lower than in permanently submerged zones (Blinn et al. 1995, Benenati et al. 1998). Thus, reduced food density within the varial zone could also limit the use of these areas at the daily maximum flow and therefore contribute to restricted movement.

We evaluate shoreline-tracking and restricted-movement hypotheses by comparing catch rates of age-0 rainbow trout in immediate shoreline areas sampled at daily minimum and maximum flows. If the shoreline-tracking hypothesis is correct, catch rates should be similar under both flows (Fig. 3.2). If the restricted-movement hypothesis is correct, catch rates should be much lower at the daily maximum flow because fish will be more dispersed, with the majority residing outside of the immediate shorelines areas that are sampled. Both shoreline-tracking and restricted-movement hypotheses predict potential negative bioenergetic consequences associated with hourly fluctuations in flow, and that growth should improve under a more stable regime. Under the shoreline-tracking hypothesis, food availability in the varial zone that is occupied by fish during the day would be lower, and there would be higher energetic costs associated with the additional movement required to always remain within immediate nearshore areas as flows fluctuate. Under the restricted-movement hypothesis, fish would occupy areas further offshore during the day, where water velocity is higher and water temperature is colder. This would lead to higher energetic costs and reduced feeding efficiency associated with holding position at higher velocities, and reduced growth due to lower water temperature. In one year of our study (2003), flow remained low and steady over a 24-hour period on Sundays during summer months (Fig. 3.1). We evaluate whether growth improved under this situation by comparing otolith microstructure from samples taken in 2003, with microstructure from 2004, when flows on Sunday underwent normal hourly fluctuations. Results from the habitat use and growth analysis are interpreted in relation to existing information and current hypotheses on the effects of hourly variation in flow on the behaviour and growth of juvenile fish.

3.2   Methods

Study Area

The Lee's Ferry reach of the Colorado River, AZ, begins at Glen Canyon Dam below Lake Powell and extends 26 km downstream to the confluence of the Paria River. The average flow in 2003 and 2004, when the study was conducted, was 328 $m^3 \cdot sec^{-1}$ (USGS gage 09380000). The reach is wide and shallow, with an average wetted width

and depth at this flow of 144 m and 5.2 m, respectively (Randle and Pemberton 1987). Mainstem water temperatures recorded at the downstream end of the reach since 2003 have ranged from 9-15 $^{\circ}$C, but typically range from 9-11 $^{\circ}$C (Voichick and Wright 2007). The fish fauna in the Lee's Ferry reach is almost exclusively comprised of nonnative rainbow trout that reproduce naturally (McKinney et al. 2001). Flow from Glen Canyon Dam normally fluctuates on a diel cycle that is driven by power demand but controlled through regulations on the maximum daily flow range, minimum and maximum flows, and maximum downramp and upramp rates. There is little variation in flow during low and high flow periods within a day (e.g., Fig. 3.1a), and because upramp and downramp periods are relatively short (total of 6 hours per day), high flows occur over the majority (13 hours) of the day. Hourly variation in flow during weekdays was very similar in 2003 and 2004, but variation in flow on Sundays during the summer was much lower in 2003 (Fig. 3.1).

Effects of Hourly Flow Variation on Nearshore Habitat Use

Catch rates of age-0 rainbow trout at 24 shoreline locations sampled by electrofishing at both daily minimum and maximum flows between June 30th and July 6th, 2004, were compared to evaluate the effects of diel variation in flow on nearshore habitat use. Shoreline habitat was stratified into low- (cobble and vegetated sand bars and debris fans) and high-angle (talus slopes) types that could be sampled by backpack and boat electrofishing, respectively. Twelve units were randomly selected for sampling from both low- and high-angle habitat strata, and in the field, divided into four non-contiguous 30 and 50 m sections, respectively. Each section was then electrofished under one of the four following light and flow conditions: 1) light (daytime)-daily maximum flow; 2) light-daily minimum flow; 3) dark (nighttime)-daily maximum flow; and 4) dark-daily minimum flow. Thus, 12 replicate samples for each habitat type (low- or high-angle) were obtained for each of the four alternate light level-daily flow combinations. Electrofishing sites were 3-4 m wide, were not enclosed by block-nets, and were fished very methodically in upstream (backpack electrofishing) or downstream (boat electrofishing) directions. After collection, fish were anesthetized and fork lengths were measured to the nearest mm (see Chapter 4 for additional details on sampling). We assume that catch in nearshore zones (C) always represents a constant proportion of the

total abundance in these areas (N) because capture probability (p) does not vary with abundance or flow (i.e., C=pN). This assumption is supported by a large number of depletion (n=66) and mark-recapture (n=42) experiments conducted in the Lee's Ferry reach in 2006 and 2007, respectively (Chapter 2).

The statistical significance of differences in log-transformed catch rates measured at daily minimum and maximum flows and during the day and night were determined using a two-way nested Analysis of Variance (ANOVA), where the effects of flow and light were nested within sites. Log-transformed catch data met ANOVA assumptions of normality based on the Kolmogorov-Smirnov test (p-values=0.397 and 0.950 for low- and high-angle habitat, respectively), and homoscedastic variance among treatments based on Bartlett's test (p-values= 0.617 and 0.315 for low- and high-angle habitat, respectively).

Physical characteristics at diel sampling sites were measured to evaluate the change in habitat conditions in nearshore areas at daily minimum and maximum flows. Depth and average water column velocity were measured at 10 equally spaced locations 1.5 m from shore along an axis parallel to the direction of flow at each site using a Swoffer current meter with topset wading rod (Model 2100). Measurements were taken at both the daily minimum and maximum flows. Measurements at the daily maximum flow were also taken further offshore at the edge of the permanently submerged zone (Fig. 3.2). The cross-sectional slope at each site was measured using a laser level and survey rod to estimate the vertical and horizontal distances between elevations inundated by the daily minimum and maximum flows. Statistical differences in depth and velocity at daily maximum and minimum flows within sites were evaluated using paired t-tests.

Effects of Hourly Flow Variation on Growth

Otoliths were extracted from a subsample of fish captured by electrofishing during multiple surveys conducted in 2003 and 2004 as part of a longer-term study on early life history dynamics of rainbow trout in the Lee's Ferry reach (Chapters 4-6). Following the random-stratified design described above, 20 units were selected from both low- and high-angle habitat strata to sample by backpack and boat electrofishing, respectively. On each sampling trip, we returned to these same 40 units, but randomly selected different 30 m and 50 m sections to sample in low- and high-angle habitat,

respectively. In 2003, six sampling trips were conducted between April and October, and only low-angle shorelines were sampled (934 age-0 trout fish captured). In 2004, both shoreline types were sampled and 8 trips were conducted between April and December (4459 age-0 trout captured). On each trip, 2.5% of low-angle shorelines (600 m) were sampled in 2003 and 2004, and 4.5% of high-angle shorelines (1000 m) were sampled in 2004. Electrofishing protocols were identical to those described for the nearshore habitat study component with two exceptions: 1) sampling was only conducted during darkness between midnight and dawn at the daily minimum flow; and 2) on each trip, a subsample of 5 fish from each habitat type within 10 mm length categories between 20 and 100 mm were sacrificed and preserved in 95% ethanol for later analysis of otolith microstructure.

Both sagittal otoliths were removed from a sample of preserved fish to determine the daily age from hatch and otolith growth using methods described in Stevenson and Campana (1992) and Campana (1992). A total of 259 and 334 otoliths were successfully extracted and aged from fish collected in 2003 and 2004, respectively. A striped pattern in daily increments was observed on the otoliths of many individuals (see results). This visual pattern was identified by atypical increments (different appearance, usually light in color under transmitted light) formed at regular intervals. The number of otoliths where the striping pattern was present, absent, or ambiguous, was recorded. To determine if the striping pattern was associated with periodic growth, a random sample of otoliths (n = 15) with a clear striping pattern were examined and the width of individual daily increments was measured. The significance of differences in the width of atypical and typical increments was determined using a two-level nested analysis of variance (ANOVA), where the effect of increment type on width was nested within fish.

To determine if the presence of otolith striping was related to somatic growth, we compared length-at-age relationships based on data from fish with and without otolith striping. The constant, slope, and standard deviation of linear length-at-age models were estimated assuming observation error was log-normally distributed from,

(1) $$L_{x,i} = (\alpha_x + \beta_x A_{x,i})e^{v_{x,i}}$$

where, L is fork length (mm), A is age (days from hatch), α and β are the constant (size-at-hatch) and slope (growth rate in mm·day^{-1}), respectively, v is a random deviate from a normal distribution with a mean of 0 and a standard deviation σ_x, x is a classification term

that denotes whether the data and parameters are based on fish where striping was present (x=p) or absent (x=a), and i denotes the index number for individual fish. Although length-at-age is commonly described using non-linear models because growth rates typically decline in older fish, there was no indication of this pattern in our data (see results).

Parameters for length-at-age models were estimated by maximizing the log-normal likelihood using a non-linear iterative search procedure. Four models were evaluated: 1) Pooled ($\alpha_p = \alpha_a$, $\beta_p = \beta_a$, $\sigma_p = \sigma_a$); 2) Individual (α_p, α_a, β_p, β_a, σ_p, σ_a); 3) Individual Slopes ($\alpha_p = \alpha_a$, $\sigma_p = \sigma_a$, β_p, β_a); and 4) Expected Striping Slope ($\alpha_p = \alpha_a$, $\sigma_p = \sigma_a$, β_a, $\beta_p = \beta_a z$, where $z = og * f$). The last model assumes that the proportional increase in somatic growth rate of fish with otoliths where striping was present (z) can be computed based on the measured average proportional increase in the width of atypical increments (og), and the expected frequency at which such increments form (f). We evaluate the hypothesis that short-term increases in growth rate occurred only on Sundays when flows were low and steady, by setting f=1/7. Models were compared using the Akaike information criterion (AIC), where the model with the smallest AIC value is considered to have the best out-of-sample predicted power if the difference in AIC values is ≥ 2 (Burnham and Anderson 2002). Models were also compared using likelihood ratio tests to determine the probability that the improved fit of more complex models that accounted for the effects of otolith striping (models 2-4), relative to the simplest model that did not (model 1), could be due to chance alone.

3.3   Results

Effects of Hourly Flow Variation on Nearshore Habitat Use

The difference between the daily minimum and maximum flow during summer months of approximately 225 $m^3 \cdot sec^{-1}$ (Fig. 3.1) resulted in an average horizontal shift in the waters edge of 6.5 m and 2.2 m in low- and high-angle shorelines, respectively. At a typical cross-section, the increase in stage from the daily minimum to maximum flow was 0.75 m. In low-angle habitat at the daily maximum flow, average water velocity was over 5-fold higher at the edge of the permanently submerged zone (6.5 m from shore)

compared to 1.5 m from shore (Table 3.1). In high-angle habitat, the difference in the distance 1.5 m from shore and the edge of the permanently submerged zone (2.2 m from shore) was very small due to the higher gradient of the shoreline. As a result, average velocities at these two locations were very similar (Table 3.1). Although daily variation in flow during the summer was substantial (Fig. 3.1b), there were relatively minor absolute changes in depth and velocity within the immediate shoreline habitats that were sampled (Table 3.1). Average depth 1.5 m from shore was 10-15 cm greater at the daily maximum flow compared to at the daily minimum, but the difference was only statistically significant ($p < 0.05$) in high-angle habitat (paired t-test, p=0.028). Average velocity was marginally higher at the daily minimum flow compared to the daily maximum in low-angle habitats and marginally lower in high-angle habitats, but neither difference was significantly different (paired t-test, p=0.100 and 0.107, respectively).

There was a very strong effect of flow on catch rates. In low-angle habitats, catches at the daily minimum flow were higher than at the daily maximum at 11 of 12 sites sampled at night, and 9 of 11 sites sampled during the day (Table 3.2). In high-angle shorelines, catches at the daily minimum flow were higher than at the daily maximum in 9 of 10 and 10 of 11 sites sampled during night and day, respectively. On average, catch rates in low-angle habitat at the daily minimum flow were 4.5- and 5.1-fold higher than at the daily maximum flow during day and night, respectively (Table 3.2). At high-angle sites, catch rates at minimum flows were 3.5- and 2.2-fold higher than at maximum flows during day and night respectively. The increase in catch rates at the daily minimum flow compared to the maximum flow within sites was statistically significant in both low-($F_{12,12}$=4.09, p=0.011) and high-($F_{11,12}$=6.41, p=0.003) angle habitats (Fig. 3.3).

Effects of Hourly Flow Variation on Otolith and Somatic Growth

A striping pattern was evident in many of the otoliths sampled in 2003 but in only a fraction of those sampled in 2004. The visual pattern was identified by the presence of atypical daily increments formed at a frequency of exactly 7 days (Fig. 3.4). The weekly pattern was evident in at least 51% (131) of the 259 otoliths examined in 2003, but in only 6% (20) of the 334 otoliths examined in 2004 (Table 3.3). In general, striping was most evident in the middle and outer sections of the otolith, and in larger individuals. The dates on which atypical increments were formed were determined for 12 randomly

selected otoliths where striping was present and where the edge of the otolith was clearly defined. In all cases, atypical increments were formed on Sundays, the only day of the week in 2003 when flows were low and steady during the day (Fig. 3.1a). The frequency of otolith striping varied over time (Table 3.3). In 2003, striping was common in samples from all months except April, while in 2004, striping was only common in April and May and declined steadily in later months. Atypical increments tended to be 25% wider (3.12 microns) compared to the other increments (2.51 microns) when averaged across all striping cycles from 15 fish. Within fish, the average increment width of the atypical bands was larger than the average width of the other increments in between the atypical bands in 14 of 15 cases. Atypical increment widths were significantly wider than typical ones based on the nested ANOVA ($F_{15,235}=19.2$, $p<0.0001$).

Length-at-age comparisons indicated that somatic growth was similar in fish with and without otolith striping. There was a strong linear relationship between age from hatch and fork length (Fig. 3.5), with age from hatch explaining 85% (n=123), 92% (n=76), and 88% (n=199) of the variation in fork lengths measured in 2003 based on otoliths where striping was present, absent, and when both datasets were combined, respectively. Growth rates estimated from separate regressions for fish without striping and with striping were 0.360 (β_a) and 0.375 (β_p) mm·day^{-1}, respectively (Table 3.4). The expected growth rate for fish with striping present, computed based on the average increase in otolith increment widths formed on Sundays (1.25-fold wider) and the expected flow-dependent frequency of such improved growth events (1 out of 7 days per week), was 0.374 mm·day^{-1} ($\beta_p = \beta_a * z$, where $z = 1.25 * \frac{1}{7}$). The expected growth rate was almost identical to the estimates from the Individual ($\beta_p=0.375$) and Individual Slopes models ($\beta_p=0.373$) for fish with otolith striping present.

AIC and likelihood ratio tests both indicated that differences in length-at-age between age-0 trout with and without otolith-striping were not statistically discernable. The Expected Striping Slope model had the best out-of-sample predictive power (lowest AIC) of all length-at-age models considered. However, there was substantial support (*sensu* Burnham and Anderson 2002) for the Pooled and Individual Slope models as well, indicating that there was no evidence that growth rates of fish with and without otolith

striping were different. Likelihood ratio tests indicated that there was a high probability that the improved fit of the Individual (p=0.409), Individual Slopes (p=0.175), and Expected Striping Slope (p=0.177) models relative to the Pooled model could be due to chance alone.

3.4   Discussion

Our catch data provide support for the restricted-movement hypothesis of juvenile salmonid response to hourly variation in flow. Catch rates of age-0 trout at the daily minimum flow were at least 4- and 2-fold higher compared to catch rates at the daily maximum flow in low- and high-angle habitats, respectively. Differences in catch rates reflect true differences in density in nearshore areas, and hence habitat use, since capture probabilities at the daily minimum and maximum flows were similar (Chapter 2). Limited use of immediate shoreline areas by age-0 trout may seem unusual, however, short-term variation in flow is a very unnatural characteristic, and observations made under more stable conditions (e.g., Chapman and Bjornn 1968, Everest and Chapman 1972) are likely not applicable under all conditions. Our results are consistent with findings from experimental manipulations, which show that juvenile fish are reluctant to shift their lateral position in response to sudden increases in flow (Shirvell 1994, Vehenan et al. 2000, Kemp et al 2003, Vilizzi and Copp 2005)

The incidence of weekly striping pattern varied with the frequency of steady flows from Glen Canyon Dam. In 2003, when striping was common in samples collected after April, flow on Sunday during the summer (Fig. 3.1) was very stable (daily flow range of 24-73 $m^3 \cdot sec^{-1}$) compared to operations on weekdays and on Saturday (daily flow range of 167-262 $m^3 \cdot sec^{-1}$). In 2004, when there was little evidence for weekly striping, hourly variation in flow on Sunday during the summer was similar to the variation on other days of the week and to weekday operations in 2003. Eighty-five percent of the 20 fish with a striping pattern in 2004 were caught in April and May, while in 2003, the incidence of striping was evenly distributed among monthly samples collected after April. Fish with striping in April and May 2004, were on average, 95 and 128 days old from hatch, respectively. These fish therefore came from the cohort that

hatched in January, which would have been exposed to Sunday flows in February, March, and April that were relatively stable compared to the higher variation seen on other days in these months. Thus, the conditions that created a weekly striping pattern in 2004, only affected the cohort that hatched in January, and the frequency of striping for fish captured after May declined progressively as the abundance of this cohort declined over the growing season due to mortality.

There was strong evidence of increased otolith growth on Sundays in 2003, the only day of the week when flows were low and stable. Many authors have speculated that there may be an energetic cost associated with short-term variation in flows due to hydropeaking (e.g., Scruton et al. 2003 and 2005, Geist et al. 2005), and the weekly otolith striping pattern that we documented supports this hypothesis. In the introduction, we proposed that patterns of nearshore habitat use driven by flow fluctuations could influence growth. The catch data showed that most age-0 trout in the Lee's Ferry reach do not use the immediate nearshore areas during the day at the daily maximum flow, and must therefore be holding further offshore. In this situation, age-0 trout may spend more time concealed in the substrate to avoid piscivorous predators and higher velocities. This strategy would likely minimize the energetic cost of holding position in faster water, but ration would decline. Alternatively, if age-0 trout do not increase the amount of time they are concealed and do not change their foraging behaviour, energetic costs would likely increase and may not be offset if feeding efficiency is reduced because of higher velocities (Nislow et al. 2000 and 2004). Either way, there is likely an energetic cost associated with a restricted-movement response to fluctuating flows. We speculate that the formation of atypical increments and the increase in otolith growth on Sundays in 2003, occurred because this was the only day of the week when flows were low and stable and this cost was not incurred.

The formation of atypical increment and higher otolith growth may also have been driven by differences in temperatures that age-0 trout were exposed to on Sundays relative to other days of the week. During the day on Sundays in 2003, age-0 trout would be holding in immediate nearshore areas and would therefore have experienced daytime water temperatures that were 3-5 $^{\circ}$C warmer and near optimal for growth (Fig. 3.2). Given the support for the restricted-movement hypothesis, during other days of the week,

age-0 trout would be located further offshore in colder water. This temperature dynamic alone could have caused the increased otolith growth on Sundays in 2003. Our data are not sufficient to determine the dominant factor or combination of factors leading to increased otolith growth on Sundays. However, both energetic and temperature hypotheses describing the mechanism behind the increased otolith growth are consistent with results from Neilsen and Geen (1985), who showed that mean otolith increment width and somatic growth of Chinook salmon fry increased with higher ration and warmer temperature, and was reduced when fry were forced to become more active.

Differences in somatic growth rates in 2003 for age-0 trout with and without atypical increments, based on a comparison of length-at-age relationships, were not statistically discernable in this study. Effects of hourly flow fluctuation on somatic growth must therefore be inferred from the observed otolith growth response and results from other studies that describe the relationship between otolith and somatic growth. Over time frames of multiple weeks to months, otolith growth is very strongly correlated with somatic growth (Bradford and Geen 1987). For example, in this study, the length of the longitudinal axis of otoliths from age-0 rainbow trout predicted 90% and 83% of the variation in fork length in 2003 (n=235) and 2004 (n=310), respectively. However, Bradford and Geen (1987), who measured somatic growth of Chinook salmon fry based on changes in length and weight, showed that otolith and somatic growth decouple over time scales of days to a few weeks. In contrast, Mugiya and Oka (1991), who used more sensitive methods to measure both otolith (calcium uptake rates) and somatic (RNA-DNA ratios) growth in rainbow trout, showed that growth was coupled at a daily time-scale. We conclude that the wider otolith increments of age-0 trout that were associated with low and steady flows on Sundays in 2003, was indicative of a short-term increase in somatic growth, but that this increase was not detectable because our measure of somatic growth (length-at-age) was not sensitive enough.

This study has shown that hourly variation in flow caused by hydropeaking alters patterns of nearshore habitat use for young of year, and that reducing hourly variation in flow can lead to increased otolith growth. In the introduction, we proposed that restricted-movement of age-0 trout under fluctuating flows could be caused by factors that select for strong site attachment (e.g., increased predation risk while moving or competitive

63

disadvantages from abandoning feeding territories) or by reduced food availability in the varial zone, which limits the energetic profitability of immediate nearhore areas during the daily maximum flow. Data from this study are not sufficient to determine which of these mechanisms, or combination of mechanisms, caused the habitat use pattern that was observed, and this would be a useful focus for future research. The effects of limited use of nearshore habitats during the day under fluctuating flows on juvenile somatic growth and survival rate remain to be determined, and will require field experiments where contrasting levels of flow stability are maintained for long intervals (e.g. months). Although the costs of such an experiment would be high due to lost power revenues, there is no substitute for large-scale field experiments that provide contrasting conditions at the broad temporal and spatial scales that determine population-level responses.

Table 3.1. Average depth (cm) and velocity (cm·sec^{-1} at 0.6 total depth) at 12 sites in both low- and high-angle shoreline habitats based on 10 measurements per site taken 1.5 m from shore (immediate nearshore zone) sampled at the daily minimum (Min.) and maximum (Max.) flow, June 30th - July 6th, 2004. Also shown are the average gradients between the elevations inundated by the daily minimum and maximum flows, and the average depths and velocities taken at the edge of the permanently submerged zone at the daily maximum flow, which occurred 6.5 and 2.2 m from shore in low- and high-angle habitat, respectively (see Fig. 3.1). Standard errors are shown in parentheses and show the variation in mean conditions across sample sites.

	Low-Angle		High-Angle	
	Min. Flow	**Max. Flow**	**Min. Flow**	**Max. Flow**
Gradient (%)	12		37	
Immediate nearshore zone				
Depth	29 (7)	39 (13)	60 (19)	75 (16)
Velocity	7 (6)	3 (6)	6 (7)	12 (13)
Edge of permanently submerged zone				
Depth		63 (8)		85 (14)
Velocity		17 (16)		12 (17)

Table 3.2. Catch of age-0 rainbow trout in low- and high-angle shoreline sites sampled at night and day at the daily minimum (Min.) and maximum (Max.) flow. Site lengths in low- and high-angle shorelines were 30 and 50 m, respectively. Cells with missing values denote cases where no sampling was conducted. The average catch across sites (Avg.), average catch per 100 m (Avg. (100 m^{-1})), and the ratio of the average catch at the daily minimum to maximum flows (Min./Max.) are shown at the bottom of the table.

| Site | Low-Angle | | | | High-Angle | | | |
| | Night | | Day | | Night | | Day | |
	Min.	Max	Min.	Max	Min.	Max	Min.	Max
1	123	23	70	25	9	11	9	2
2	55	27	12	2	64	45	56	25
3	25	0	30	1	74	33	22	4
4	21	1		5		22	31	9
5	20	2	19	2	44	14	15	13
6	5	3	6	0	47	6	65	9
7	15	0	17	0	32	14	22	8
8	7	0	4	0		15		2
9	2	0	0	1	4	0	48	5
10	29	1	11	2	18	7	10	5
11	15	3	11	2	31	10	18	19
12	3	3	5	5	9	7	49	7
Avg.	27	5	17	4	33	15	31	9
Avg. (100 m^{-1})	89	18	56	13	66	31	63	18
Min./Max.	5.1		4.5		2.2		3.5	

Table 3.3. The number of otoliths sampled and percentage with a weekly striping pattern by sampling month in 2003 and 2004. The last row shows the total number of otoliths sampled across all months and the average percentage that were striped.

	2003		2004	
	# Sampled	% Striped	# Sampled	% Striped
April	15	13	23	17
May	37	59	58	22
June	58	48	66	3
July	56	63	68	1
August			41	0
September	60	43	37	0
October	33	55		
November			20	0
December			21	0
Total/Average	259	51	334	6

Table 3.4. Comparison of model fit and predictive power of four alternate linear models fit to the 2003 length-at-age data. β_a and β_p are the slopes of the regressions, or daily growth rates, based on otoliths where striping was absent and present, respectively. In the case of the Expected Striping Slope model, β_p was not estimated but computed as a function of β_a and the expected increase in somatic growth based on the increase in otolith growth seen on Sundays. The model with the lowest AIC (Akaike Information Criteria) has the best predictive power. ΔAIC is the difference between each models AIC value and the lowest AIC values among models.

| | | **Growth Rate** | | | | |
| | | **(Slope in mm·day^{-1})** | | | | |
Model	**# Parameters**	**β_a**	**β_p**	**Log Likelihood**	**AIC**	**ΔAIC**
Pooled	3	0.370		143.42	-280.83	1.82
Individual	6	0.360	0.375	144.86	-277.73	4.93
Individual Slopes	4	0.361	0.373	144.34	-280.67	1.99
Expected Striping Slope	3	0.360	0.374	144.33	-282.66	
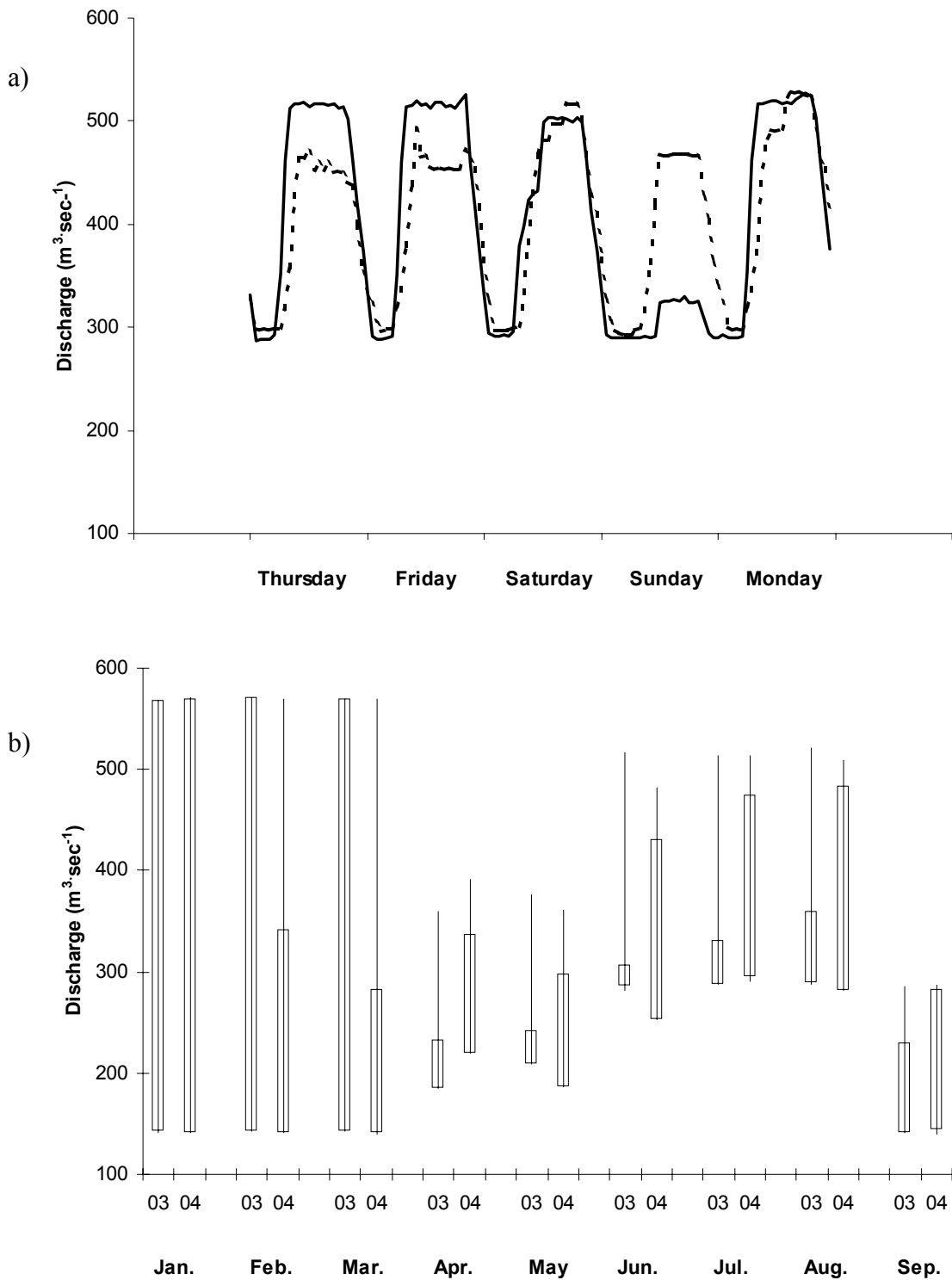
Figure 3.1. Release hydrograph from Glen Canyon Dam during a typical 5-day period (a) in 2003 (July 10th-14th, solid line) and 2004 (July 8th-12th, dashed line), and the average daily minimum and maximum flows during the week (lines) and on Sundays (open bars) from January through September (b). Monthly averages of the daily minimum and maximum flows are based on 15-minute automated flow measurements taken at Glen Canyon Dam.
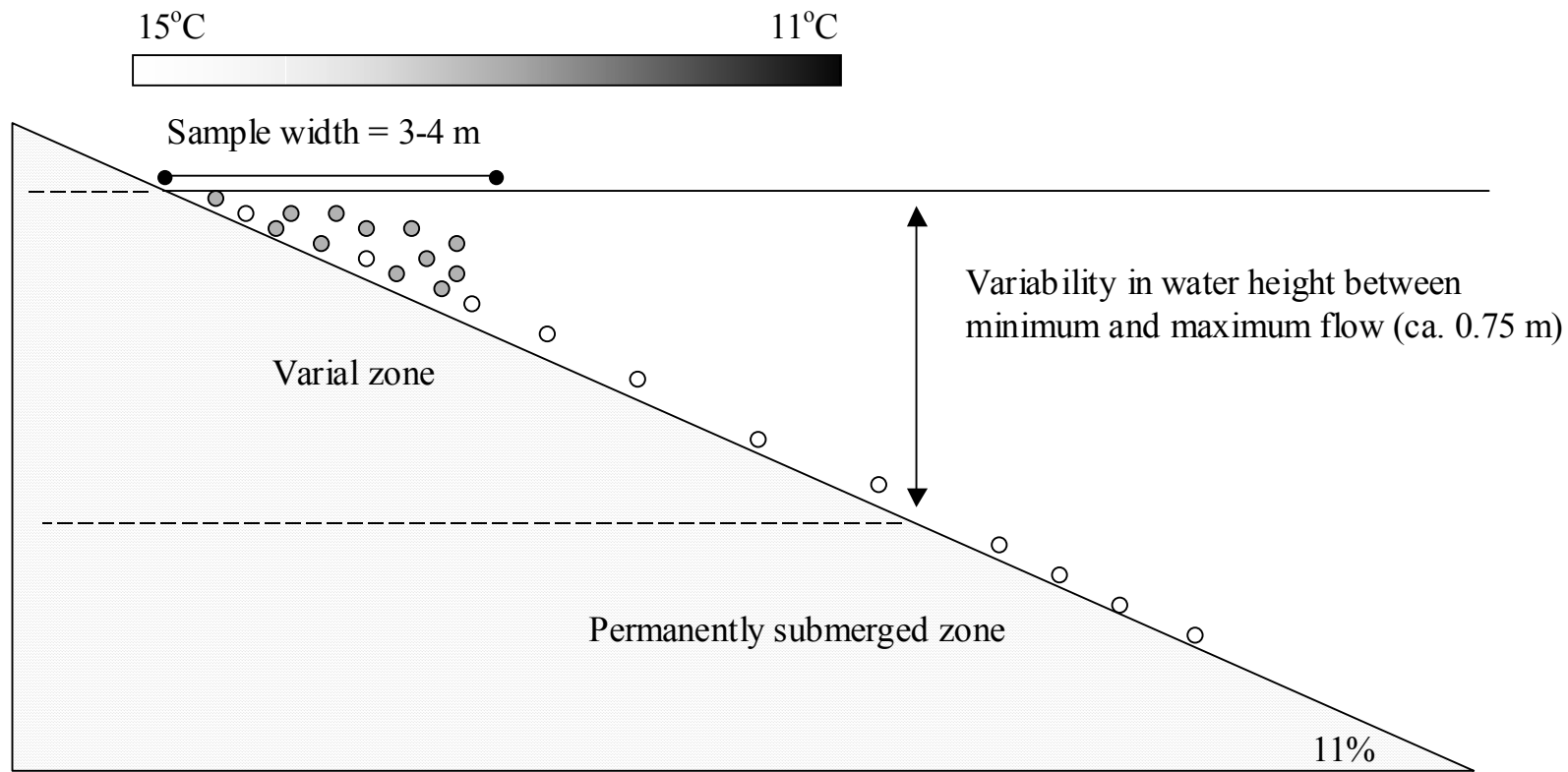
Figure 3.2. Depiction of a cross-section of low-angle shoreline habitat at the maximum daily discharge showing the daytime horizontal water temperature gradient and the daily variation in water surface elevation during summer months. Shaded circles represent the hypothesized distribution of age-0 fish during the daily maximum flow on weekdays under the shoreline-tracking hypothesis. Open circles represent the distribution under the restricted-movement hypothesis, where only a small proportion of individuals remain in the immediate nearshore area close to the waters edge. The width of shoreline habitat sampled by electrofishing, referred to in the text as the immediate nearshore area, is also shown. Note that the same sample width is applied when sampling at the minimum flow, and that the same water temperature gradient occurs at the minimum flow elevation when flows remain low during the day (Sunday 2003, see Fig. 3.1).
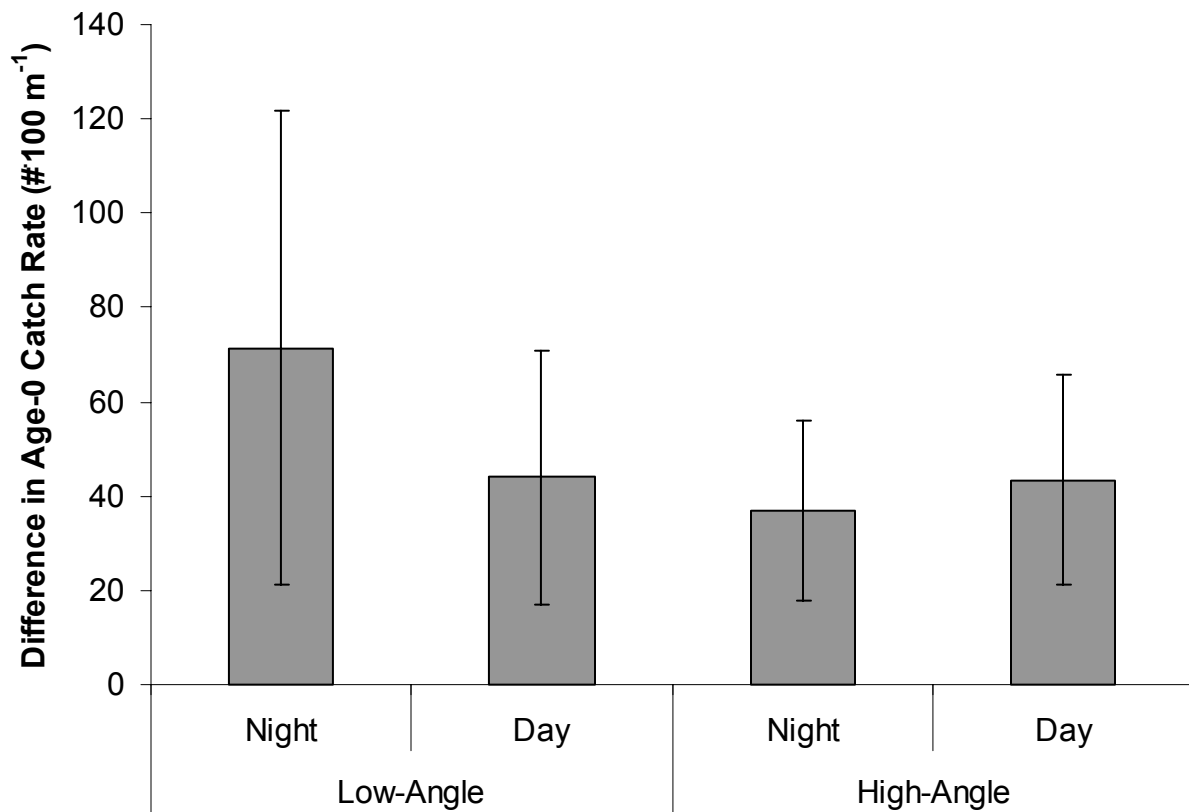
Figure 3.3. The average differences in catch rates of age-0 rainbow trout based on sampling at the daily minimum (Min.) and maximum (Max.) flow between June 30th and July 6th, 2004 (Δ=Min.-Max.) by time of day and habitat. Error bars denote 95% confidence intervals of the mean difference. Raw data to compute differences are presented in Table 3.2.
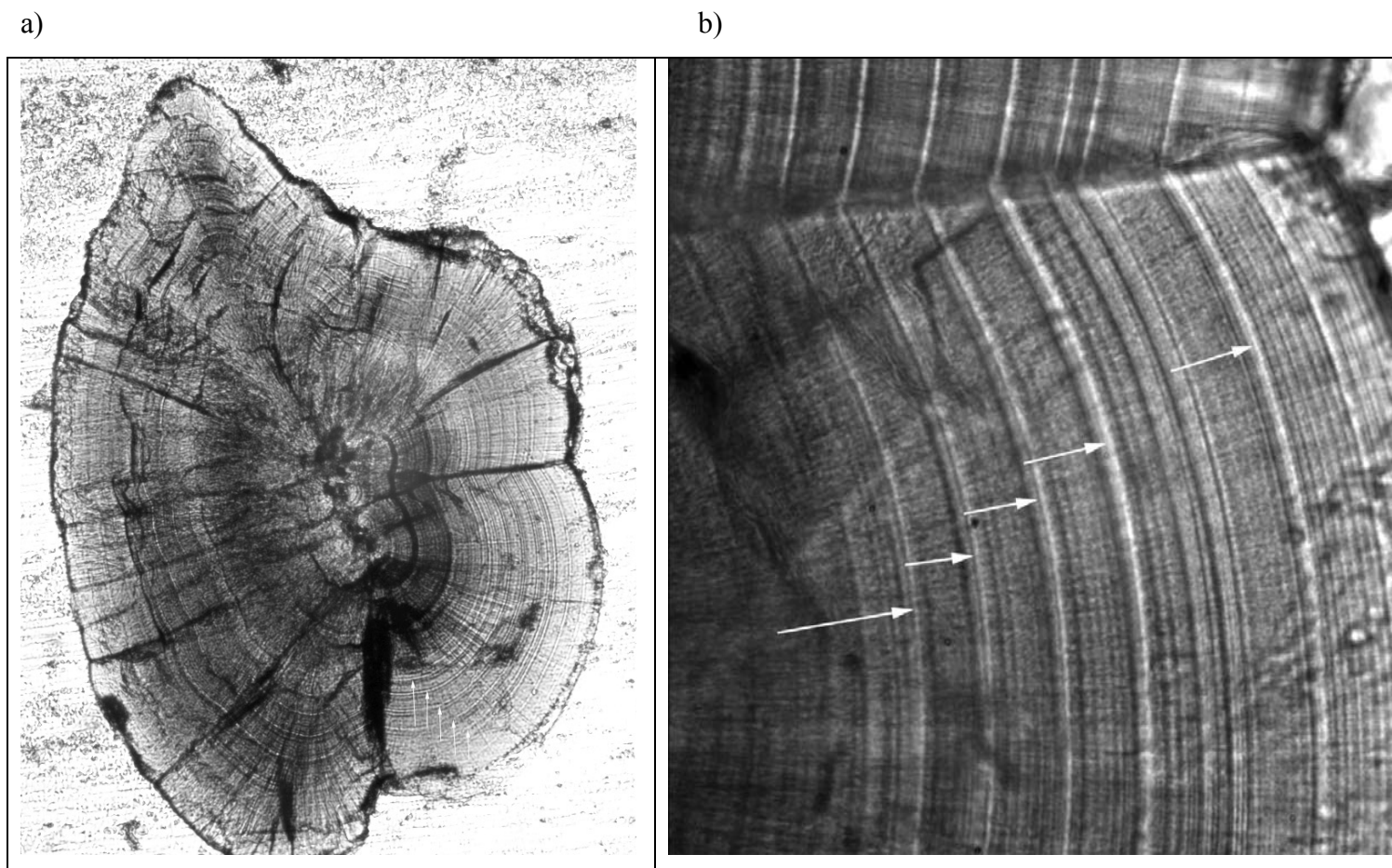
Figure 3.4. Photomicrograph of an otolith cross-section from a 43 mm age-0 rainbow trout that was 81 days old (from hatch) when sampled on July 30th, 2003. The images show the weekly striping pattern, identified by white arrows, at magnifications of 16x (a) and 400x (b). Stripes are indicative of increased otolith growth on Sundays in 2003, when flow was low and steady relative to normal weekday operations (see Fig. 3.1).
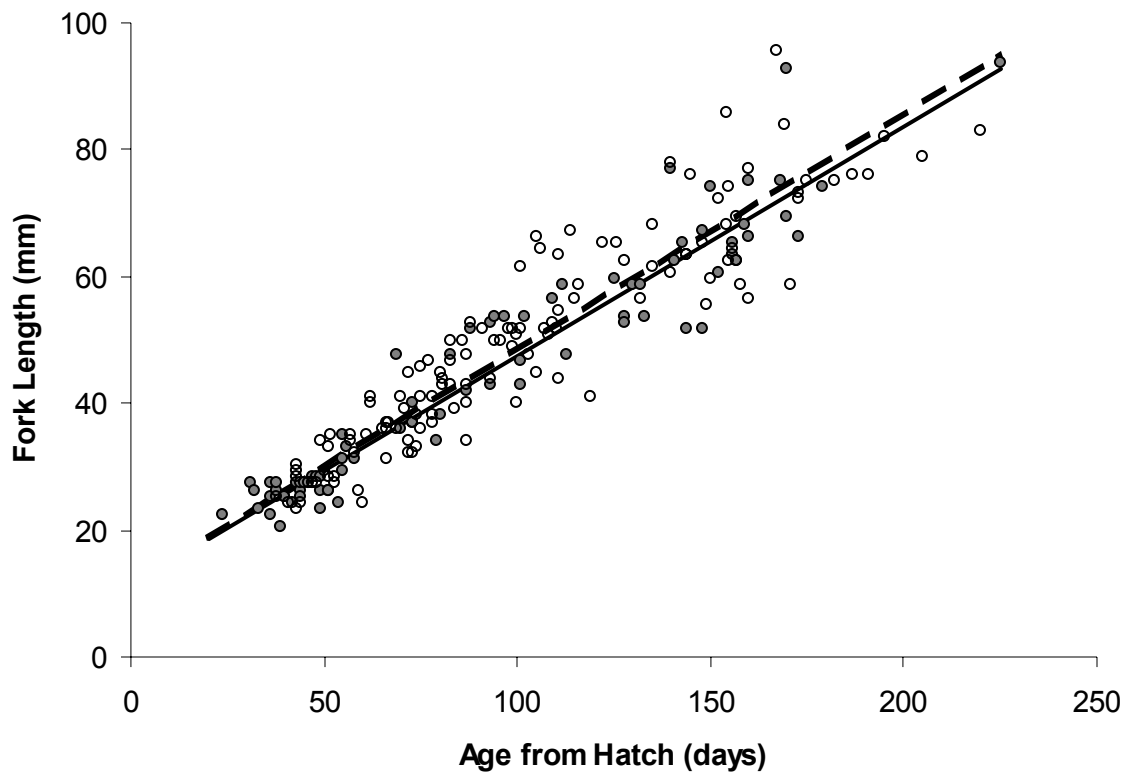
Figure 3.5. Relationships between age from hatch and fork length in 2003 based on otoliths where a weekly striping pattern was present (open circles, dashed line) and absent (shaded circles, solid line).). Predictions are based on the Individual Slope model (Table 3.4) where growth rate estimates differ for fish with and without striping but the intercept and variance estimates are common to both data sets.

3.5 References

Benenati, P.L, Shannon, J.P., and D.W. Blinn. 1998. Desiccation and recolonziation of phytobenthos in a regulated desert river; Colorado River at Lee's Ferry, Arizona, USA. Regulated Rivers 14: 519-532.

Berland, G., Nickelsen, T., Heggenes, J., Okland, F., Thorstad, E.B., and J. Halleraker. 2004. Movements of wild Atlantic salmon parr in relation to peaking flows below a hydropower station. River Research and Applications 20: 957-966.

Blinn, D.W., Shannon, J.P., Stevens, L.E., and J.P. Carder. 1995. Consequences of fluctuating discharge for lotic communities. Journal of the American Benthological Society 108: 215-228.

Biro, P.A., Post, J.R., and E.A. Parkinson. 2003. Population consequences of a predation-induced habitat shift by trout in whole-lake experiments. Ecology 84:691-700.

Bradford, M.J. 1997. An experimental study of stranding of juvenile salmonids on gravel bars and in sidechannels during rapid flow decreases. Regulated Rivers 13: 395-401.

Bradford, M.J., and G.H. Geen. 1987. Size and growth of juvenile Chinook salmon back-calculated from otolith growth increments, p. 453-461. *In* The Age and Growth of Fish. *Edited by* R.C. Summerfelt and G.E. Hall. The Iowa State University Press.

Burnham, K.P., and D.R. Anderson. 2002. Model Selection and Multimodel Inference, 2nd edition. Springer-Verlag, NY.

Bustard, D.R., and D.W. Narver. 1975. Aspects of the winter ecology of juvenile coho salmon (Oncorhynchus kisutch) and steelhead trout (Salmo gairdneri). Journal of the Fisheries Research Board of Canada 32: 667-680.

Campana, S.E. 1992. Measurement and interpretation of the microstructure of fish otoliths. P. 59-71. *In* Otolith microstructure examination and analysis. *Edited by* D.K. Stevenson and S.E. Campana. Canadian Special Publication of Fisheries and Aquatic Sciences 117.

Chapman, D.W., and T.C. Bjornn. 1969. Distribution of salmonids in streams, with special reference to effects of food and feeding, p. 153-156. *In* Symposium on salmon and trout in streams. *Edited* by T.G. Northcote. H.R. MacMillan Lectures in Fisheries, University of British Columbia. Vancouver, BC.

Connor, E.J., and D.E. Pflug. 2004. Changes in the distribution and density of pink, chum, and Chinook salmon spawning in the Upper Skagit River in response to flow management measures. North American Journal of Fisheries Management 24: 835-852.

Cushman, R.M. 1985. Review of ecological effects of rapidly varying flows downstream from hydroelectric facilities. North American Journal of Fisheries Management 5: 330-339.

Dejalon, G.G., and P. Sanchez. 1994. Downstream effects of a new hydropower impoundment on macrophyte, macroinvertebrate and fish communities. Regulated Rivers 9: 253-261.

Elliott, J.M. 1986. Spatial distribution and behavioural movements of migratory trout Salmo Trutta in a Lake District stream. Journal of Animal Ecology. 55: 907-922.

Everest, F.H., and D.W. Chapman. 1972. Habitat selection and spatial interaction by juvenile Chinook salmon and steelhead trout in two Idaho streams. Journal of the Fisheries Research Board of Canada 29: 91-100.

Flodmark, L.E.W., Urke, H.A., Halleraker, J.H., Arnekleiv, J.V., Vøllestad, L.A. & Poléo, A.B.S. 2002. Cortisol and glucose response in juvenile brown trout subjected to a fluctuating flow regime in an artificial stream. Journal of Fish Biology 60: 238-248.

Freeman, M.C., Bowen, Z.H., Bovee, K.D., and E.R. Irwin. 2001. Flow and habitat effects on juvenile fish abundance in natural and altered flow regimes. Ecological Applications 11: 179-180.

Gaudin, P. (*Editor*). 2001. Habitat shifts in juvenile riverine fishes. Hydrobiologia (supplement) 135/2-4. 393 p.

Geist, D.R., Brown, R.S., Cullina, V., Brink, S.R., Lepla, K. Bates, P., and J.A. Chandler. 2005. Movement, swimming speed, and oxygen consumption of juvenile white sturgeon in response to changing flow, water temperature, and light level in the Snake River, Idaho. Transactions of the American Fisheries Society 134: 803-816.

Girard, I.L., Grand, J.W.A., and S.O. Steingrimsson. 2004. Foraging, growth, and loss rate of young-of-the-year Atlantic salmon (*Salmo salar*) in relation to habitat use

in Catamaran Brook, New Brunswick. Canadian Journal of Fisheries and Aquatic Sciences 61: 2339-2349.

Halleraker, J.H., Saltveit, J.J., Harby, A., Arnekleiv, J.V., Fjesdstad, H.P., and B. Kohler. 2003. Factors influencing stranding of wild juvenile brown trout (*Salmo trutta*) during rapid and frequent flow decreases in artificial stream. River Research and Applications 19: 589-603.

Irvine, J.R. 1987. Effects of varying flows in man-made streams on rainbow trout (Salmo Gairneri Richardson) fry. In Regulated Streams. *Edited by* J.F. Craig and J.B. Kemper.

Kemp, P.S., Gilvear, D.J., and J.D. Armstrong. 2003. Do juvenile Atlantic salmon parr track local changes in water velocity? River Research and Applications 19: 569-575.

Korman, J., Kaplinski, M., and J. Buszowski. 2006. Effects of air and mainstem water temperatures, hydraulic isolation, and fluctuating flows from Glen Canyon Dam on water temperatures in shoreline environments of the Colorado River in Grand Canyon. Report prepared for Grand Canyon Monitoring and Research Center, Flagstaff, AZ.

McKinney, T., Speas, D.W., Rogers, R.S., and W.R. Persons. 2001. Rainbow trout in a regulated river below Glen Canyon Dam, Arizona, following increased minimum flows and reduced discharge variability. North American Journal of Fisheries Management 21: 216-222.

Neilsen, J.D., and D.H. Geen. 1985. Effects of feeding regime and diel temperature cycles on otolith increment formation in juvenile Chinook salmon (Oncorhynchus tshawytscha). Fisheries Bulletin 83: 91-101,

Nislow, K.H., Folt, C.L., and D.L. Parrish. 2000. Spatially explicit bioenergetic analysis of habitat quality for age-0 Atlantic salmon. Transactions of the American Fisheries Society 129: 1067-1081.

Nislow, K.H., Sepulveda, A.J., and C.L. Folt. 2004. Mechanistic linkage of hydrologic regime to summer growth of age-0 Atlantic salmon. Transactions of the Amercian Fisheries Society 133: 79-88.

Mugiya, Y. and H. Oka. 1991. Biochemical relationship between otolith and somatic growth in the rainbow trout *Oncorhynchus mykiss*: Consequence of starvation, resumed feeding, and diel variations. Fisheries Bulletin 89: 239-245.

Murchie, J.J. and K.E. Smokorowski. 2004. Relative activity of brook trout and walleyes in response to flow in a regulated river. North American Journal of Fisheries Management 24: 1050-1057.

Poff, N.L., Allan, J.D., Bain, M.B., Karr, J.R., Prestegaard, K.L., Richter, B.D., Sparks, R.E., and J.C. Stromberg. 1997. The natural flow regime. Bioscience 47: 769-784.

Randle, T.J., and E.L. Pemberton. 1987. Results and analysis of STARS modeling efforts of the Colorado River in Grand Canyon. U.S. Department of Interior, Bureau of Reclamation. NTIS No. PB88-183421/AS.

Robertson, M.J., Pennell, C.J., Scruton, D.A., Robertson, G.J., and J.A. Brown. 2004. Effect of increased flow on the behaviour of Atlantic salmon parr in winter. Journal of Fish Biology 65: 1070-1079.

Rosenfeld, J.S., and S. Boss. 2001. Fitness consequences of habitat use for juvenile cutthroat trout: energetic costs and benefits in pools and riffles. Canadian Journal of Fisheries and Aquatic Sciences 58: 585-593.

Saltveit, S.J., Halleraker, J.H., Arnekleiv, J.V., and A. Harby. 2001. Field experiments on stranding in juvenile Atlantic Salmon (*Salmo Salar*) and Brown Trout (*Salmo Trutta*) during rapid flow decreases caused by hydropeaking. Regulated Rivers 17: 609-622.

Schlosser, I.J. 1987. The role of predation in age- and size-related habitat use by stream fishes. Ecology 68: 651-659.

Scruton, D.A., Ollerhead, L.M.N, Clarke, K.D., Pennel, C., Alfredsen, K. Harby, A., and D. Kelley. 2003. The behavioural response of juvenile Atlantic salmon (*Salmo Salar*) and brook trout (*Salvelinus fontinalis*) to experimental hydropeaking on a Newfoundland (Canada) River. River Research and Applications 19: 577-587.

Scruton, D.A., Pennell, C.J., Robertson, M.J., Ollerhead, L.M.N., Clarke, K.D., Alfredsen, K., Harby, A., and McKinley, R.S. 2005. Seasonal response of juvenile atlantic salmon to experimental hydropeaking power generation in

Newfoundland, Canada. North American Journal of Fisheries Management 25: 964-974.

Sheppard, J.D. and J.H. Johnson. 1985. Probability-of-use for depth, velocity, and substrate by subyearling coho salmon and steelhead in Lake Ontario tributary streams. North American Journal of Fisheries Management 5: 277-282.

Shirvell, C.S. 1994. Effect of changes in streamflow on the microhabitat use and movements of sympatric juvenile coho salmon and chinook salmon in a natural stream. Canadian Journal of Fisheries and Aquatic Sciences 51: 1644-1652.

Stevenson, D.K. and Campana, S.E. (*Editors*). 1992. Otolith microstructure examination and analysis. Canadian Special Publication of Fisheries and Aquatic Sciences 117.

Travnichek, V.H., Bain, M.B., and M.J. Maceina. 1995. Recovery of a warmwater fish assemblage after the initiation of a minimum-flow release downstream from a hydroelectric dam. Transactions of the American Fisheries Society 124: 836-844.

Vehanen, T., Bjerke, P.P. Heggenes, J., Huusko, A., and A. Maki-Petays. 2000. Effect of fluctuating flow and temperature on cover type selection and behaviour by juvenile brown trout in artificial flumes. Journal of Fish Biology 56: 923-937.

Vilizzi, L., and G.H. Copp. 2005. An analysis of 0+ barbell (Barbus barbus) response to discharge fluctuations in a flume. River Research and Applications 21: 421-438.

Voichick, N., and S.A. Wright. 2007. Water temperature data for the Colorado River and tributaries between Glen Canyon Dam and Spencer Canyon, Northern Arizona, 1988-2005. USGS Data Series Report. U.S. Geological Survey.

Walters, C.J., and F. Juanes. 1993. Recruitment limitation as a consequence of natural selection for use of restricted feeding habitats and predation risk taking by juvenile fishes. Canadian Journal of Fisheries and Aquatic Sciences 50: 2058-2070.

Ward, D.M. Nislow, K.H., Armstrong. J.D., Einum, S., and C.L. Folt. 2007. Is the shape of the density-growth relationship for stream salmonids evidence for exploitative rather than interference competition? Journal of Animal Resource Ecology 76:135-138.

4.0 Habitat Use, Growth, and Survival of age-0 Rainbow Trout in a Large Regulated River[3]

4.1 Introduction

Growth and survival of early life stages plays a central role in controlling the abundance of fish populations. Improving the status of fish populations in regulated rivers requires an understanding of how the hydrograph and other factors affect growth and survival. Patterns of habitat use (Biro et al. 2003, 2004), body size (Nislow 2001, Imre et al. 2005), food availability (Nislow et al. 1998), growth rate (Post et al. 1999, Biro et al. 2006), and density (Elliott 1994, Vandenbos et al. 2006) have all been shown to be important factors effecting juvenile survival rates. Flow regimes and other environmental variation will influence the quantity and quality of habitat through changes in abiotic factors like depth and velocity, as well as through changes in biotic factors like rates of food delivery, the intensity of competition, and the risk of predation, which are often density-dependent (Rosenfeld and Boss 2001). The sensitivity of particular early life stages to flow will likely vary and depend on their specific habitat requirements, the extent of flow-driven physical changes in those habitat types, and the ability of individuals to tolerate environmental variation (Bain et al. 1988, Shea and Peterson 2007). The effects of flow-dependent mortality are potentially mitigated through compensatory (density-dependent) growth and survival responses (Fletcher and Deriso 1988, Rose et al. 2001), which may vary considerably by life stage (Elliot 1989, Ratikainen et al. 2007). Our understanding of these important early life history dynamics is poor in large river environments, which limits the progress of very substantive restoration efforts occurring in these systems.

The majority of informative field studies on the dynamics of early life history of freshwater fish have been conducted in relatively small and stable environments such as small lakes and artificial ponds (e.g., Post et al. 1999, Biro et al. 2003, Vandenbos et al. 2006) or streams (e.g. Chapman and Bjornn 1969, Everest and Chapman 1972, Hartman

---

[3] A version of this chapter may be submitted for publication. Korman, J. Habitat use, growth, and survival of age-0 rainbow trout in a large regulated river.

and Scrivener 1990, Elliot 1994, Nislow et al. 1998, Imre et al. 2005,). There has been very little work to determine which aspects of the early life history dynamics developed from these smaller and intensively studied systems apply in a large river setting. This uncertainty is particularly acute in regulated rivers where abiotic conditions may shift suddenly and have very unnatural dynamics (Poff et al. 1997). Investigations of effects of abiotic factors on small fish in regulated rivers have been restricted to assessing direct mortality effects due to stranding of redds or juveniles caused by sudden reductions in flow (e.g., Becker et al. 1982, Bradford et al. 1995, Saltveit et al. 2001, Halleraker et al. 2003, McMichael et al. 2005) or displacement and mortality due to sudden increases (e.g., Heggenes and Traaen 1988). Many of these studies are based on laboratory experiments with unknown applicability to natural settings, or are field assessments that only provide estimates of numbers of fish killed without any measure of population-level consequences. Methodologies and results from system-wide and more holistic investigations of early life history dynamics in large regulated rivers are lacking.

In this analysis, I describe how critical early life history characteristics of the age-0 rainbow trout population in the Lee's Ferry reach of the Colorado River, Arizona, are affected by flow and fish size and density. The relative abundance of the adult component of the Lee's Ferry population increased by 3-fold in the 1990's in response to a reduction in the extent of hourly flow fluctuations and an increase in the minimum flow from Glen Canyon Dam (McKinney et al. 1999). This is one of only a few cases where a positive population response to flow stabilization has been well documented (see also Bain et al. 1988, Connor and Pflug 2004). However, because basic elements of the early life history of the Lee's Ferry trout population are poorly understood, the causal mechanism behind its response to flow stabilization remains highly uncertain. My objective is to reduce this uncertainty by determining the extent to which incubation success, and the habitat use, ontogenetic movement, and growth and mortality of age-0 trout is controlled by the flow regime from Glen Canyon Dam, as well as by important biotic factors like fish density. The analysis is presented in three companion papers. In this paper, I describe patterns of habitat use and ontogenetic habitat shifts, and how growth and survival varies across habitat types, and with changes in flow and fish density. I combine estimates of reach-wide age-0 abundance over the summer and fall, with annual estimates of spawning

activity, to identify life stages that show strong compensation in survival rates. In a second paper (Chapter 5), the effects of flow and spawner density on spawning habitat use, incubation mortality and the abundance of the age-0 population are described. In a third paper (Chapter 6), this information is integrated in a stock synthesis model to estimate parameters describing early life history dynamics from spawning to approximately one year from fertilization. Hypotheses related to early life history dynamics are developed and examined using relatively simple methods with somewhat restrictive assumptions in the first two papers, before being incorporated in the more sophisticated quantitative framework of the stock synthesis model in the final paper.

4.2   Methods

Study Area

The Lee's Ferry reach of the Colorado River, AZ, begins at Glen Canyon Dam below Lake Powell and extends 26 km downstream to the confluence of the Paria River (Lat:36.86638, Long:-111.58638). The average flow across study years (2003, 2004, 2006, and 2007) was 334 $m^3 \cdot sec^{-1}$ (USGS gage 09380000). The reach is wide and shallow, with an average wetted width and depth at this flow of 144 m and 5.2 m, respectively (Randle and Pemberton 1987). There are no significant tributary inputs to the reach and water quality is determined by the hypolimnetic release from Glen Canyon Dam. The annual range of mainstem water temperatures recorded at the downstream end of the reach since 2003 has ranged from 9-15 ^{o}C (Voichick and Wright 2007) and secchi depths have consistently ranged from 6-7 m (Vernieu et al. 2005). The fish fauna in the Lee's Ferry reach is almost exclusively comprised of nonnative rainbow trout that reproduce naturally (McKinney et al. 2001). Spawning occurs over an extended period from November through May, with a pronounced peak between mid-March and mid-April (see Chapter 5). Flow from Glen Canyon Dam normally fluctuates on a diel cycle that is driven by power demand but controlled through regulations on the maximum daily flow range (141-227 $m^3 \cdot sec^{-1}$, depending on monthly release volume), minimum (141 $m^3 \cdot sec^{-1}$) and maximum (708 $m^3 \cdot sec^{-1}$) flows, and maximum downramp (42 $m^3 \cdot sec^{-1} \cdot hr^{-1}$) and upramp (113 $m^3 \cdot sec^{-1} \cdot hr^{-1}$) rates (Fig. 4.1).

Age-0 Abundance and Length Frequency Distributions in Shoreline Areas

The abundance of age-0 rainbow trout in the Lee's Ferry reach was determined based on catch rates from backpack and boat electrofishing in shoreline areas. Abundance was estimated using a two-stage habitat-stratified design where single-pass electrofishing was used as a low-effort method to index population density at a large number of shoreline sites over the four years of study. These catch rates were then converted to population estimates based on capture probabilities determined from mark-recapture experiments conducted at a smaller number of sites in 2007. Sample sites were selected randomly from two habitat types based on shoreline angle. Shorelines in the Lee's Ferry reach have been classified into cobble bars, vegetated sand bars, debris fans, talus (large angular boulders), and cliff types from low-level aerial photographs (Mietz 2003). In total there are 96 shoreline habitat units averaging 588 m in length. I reclassified the five original habitat strata into low- (cobble and vegetated sand bars and debris fans) and high-angle (talus slopes) shoreline habitat types that could be sampled by backpack and boat electrofishing, respectively. There are a total of 48 and 32 units of low- and high-angle habitat types, summing to 27.8 (49%) and 21.5 (38%) km of shoreline habitat, respectively, out of a total of 56 km in the Lee's Ferry reach. Cliff habitat units were excluded from the classification and sampling because no fry were caught in these habitats during initial pilot sampling efforts, and the cliff shorelines comprise only 12% of the total shoreline length.

For the first stage of the sampling program, twenty units were randomly selected from both low- and high-angle habitat strata. On each sampling trip, which occurred on a near-monthly basis over the summer and fall, I returned to these same 40 units, but randomly selected different sections to sample using single-pass electrofishing in low- and high-angle habitat, respectively. Based on sampling twenty 30 m sites in low-angle habitat, and twenty 50 m sites in high-angle habitat, I sampled 2.5% and 4.5% of the total shoreline length of each habitat type per survey, respectively. Five to eight sampling trips were conducted each year, typically between June and November (Table 4.1).

Habitat characteristics of low- and high-angle shorelines are described in Chapter 3 but are briefly summarized here. Talus shorelines are comprised exclusively of large and angular sandstone boulders with large interstitial spaces. Substrate in low-angle

habitat is dominantly cobble or sand. In a minor proportion of low-angle habitat gravel is present, and sand may be covered by submerged aquatic vegetation. Between the daily minimum (282 $m^{-3}.sec^{-1}$) and maximum (510 $m^{-3}.sec^{-1}$) flow during summer months, average shoreline gradients (perpendicular to direction of flow) are 12% and 37% in low- and high-angle habitat, respectively (Table 4.2). As a result of the diurnal cycle in flow, there is an average horizontal shift in the waters edge of 6.5 m and 2.2 m in low- and high-angle shorelines, respectively. At a typical cross-section, the increase in stage from the daily minimum to maximum flow is 0.75 m. Velocity in both habitat types is generally low due to the low gradient of the reach, but varies over the day as a function of discharge, and with distance from shore.

Electrofishing was conducted after dark between midnight and 6:00 at the daily minimum flow. Electrofishing sites extended 3-4 m from shore, were not enclosed by stop-nets, and were fished very methodically in upstream (backpack electrofishing) or downstream (boat electrofishing) directions. Backpack and boat electrofishing were conducted using a two-person crew operating Smith-Root Type 12b and Coffelt CPS electrofishers, respectively. A single pass of electrofishing required an average of 10 seconds of electrofishing effort per meter of shoreline sampled. Boat electrofishing was conducted from a shallow-draw 5.3 m aluminum boat with 50 Hp outboard motor with power trim. The combination of boat design, highly experienced operators, and relatively slow shoreline water velocities, allowed fine control of anode position and very thorough and slow coverage of the immediate shoreline area relative to typical boat electrofishing operations. After electrofishing, fish were anesthetized using clove oil and fork lengths were measured to the nearest mm. A subsample of fish were weighed to the nearest gram. To determine growth rate, a random sample of five fish from each habitat type within 10 mm length categories between 20 and 100 mm were sacrificed on each trip and preserved in 95% ethanol for later analysis of otolith microstructure (Table 4.1).

To characterize capture probability for the second stage of the sampling program, 42 mark-recapture experiments were conducted in randomly selected habitat units in 2007. Flows during mark-recapture experiments were very similar to those in other sampling years. The methods and results of this effort are reported in Chapter 2 and are briefly summarized here. There was no mortality of 351 fish that were captured by

electrofishing, marked, and held for 24 hours. Of a total of 2966 fish that were marked and released, only 0.61% was captured outside of mark-recapture sites. Total emigration from mark-recapture sites was estimated at 2.2-2.6%. These data strongly suggest that populations within discrete sites can be treated as effectively closed. Eighty percent of capture probability estimates from mark-recapture experiments were between 0.17 and 0.45 and the average CV of estimates was 0.25. There was strong support for a fish size-capture probability relationship that accounted for differences in vulnerability across habitat types. Smaller fish were less vulnerable in high-angle shorelines that were sampled by boat electrofishing compared to those in low-angle shorelines sampled by backpack electrofishing. There was little support for capture probability models that accounted for almost two-fold variation in flow within a day. The effect of population density on capture probability was confounded with effects of fish size, but the weight of evidence suggested that fish size was the key determinant. Thus, capture probability used to determine population estimates in this analysis is assumed to depend on fish size and to be independent of fish density and flow.

I used the following logistic relationship to predict length-dependent capture probability (Chapter 2),

$$(1) \qquad p_{h,j} = \frac{\pi_h}{1 + e^{\frac{-(\overline{L}_j - \psi_h)}{\tau_h}}}$$

where, $p_{h,j}$ is the predicted capture probability for a 5 mm size class with an index of j and a mid-point fork length $\overline{L}_j$ (in mm) in habitat type h (low- or high-angle), π_h is the base capture probability, that is the capture probability where size is not limiting (i.e., when the denominator = 1) for that habitat type, and ψ_h and τ_h are the mean and standard deviation of the logistic fork length-vulnerability function that determine the length where capture probability is 50% of the maximum, and the inverse of the slope of the relationship, respectively. Parameter values for π_h, ψ_h, and τ_h were determined by maximum likelihood and were 0.34, 26.61, and 2.60 in low-angle habitat, and 0.31, 39.89, and 4.57 in high-angle habitat, respectively (see Table 2.4 from Chapter 2).

The population size at each single-pass electrofishing site sampled in the first stage was determined from,

$$(2) \qquad n_{t,h,i} = \sum_{j=1}^{31} \frac{c_{t,h,i,j}}{p_{h,j}}$$

where, $n_{t,h,i}$ is the population estimate for site i in habitat type h on sampling trip t, $c_{t,h,i,j}$, is the catch at the site for fish in size category j (20-170 mm in 5 mm increments), and $p_{h,j}$ is the size-dependent capture probability defined in equation 1. The total population size in each habitat type for the entire Lee's Ferry reach was determined from,

$$(3) \qquad N_{t,h} = \frac{\sum_i n_{t,h,i}}{\dfrac{\sum_i SL_{t,h,i}}{SL_h}}$$

where, $N_{t,h}$ is the total population size in habitat type h on sampling trip t, $SL_{t,h,i}$ is the shoreline length of each sample site (in meters), and SL_h is the total length of shoreline of that habitat type in the reach. The denominator represents the total proportion of shoreline of each habitat type that is sampled on trip t, which was typically 0.022 (=20 sites·30 m·site^{-1}·27800 m^{-1}) and 0.047 (=20 sites·50 m·site^{-1}·21500 m^{-1}) in low- and high-angle habitat respectively. To construct length-frequency distributions for a given habitat type and sampling trip, corrected for size-dependent capture probability, I compute $n_{t,h,i,j}$ as an intermediate step in equation 2, summed estimates across sites to determine $n_{t,h,j}$, and then computed the proportions in each size class as the ratio of $n_{t,h,j}$ to the sum of the population estimates across size classes ($n_{t,h}$).

Uncertainty in population size estimates was determined using a non-parametric bootstrap procedure. For each trial, catch data from single-pass sites within a year, sample period, and habitat type strata, were randomly selected with replacement. Size-specific catches from the selected sites were expanded to population estimates for each site using equation 2, and then to a reach-wide estimate using equation 3. The procedure was repeated 200 times for each strata and the standard deviation in population estimates across trials was computed. Population biomass by habitat and survey was computed by multiplying the size- and site-specific population estimates ($n_{t,h,i,j}$) by the predicted weight for each length class, and then expanding those estimates by the proportion of habitat sampled according to equation 3. Weight was predicted from the best-fit regression between weight and fork length using data aggregated across all sampling trips and habitat types (W=5.0·10^{-6}·L$^{3.1927}$, r^2=0.97, n=1765).

Apparent survival rates for age-0 trout were computed based on the ratio of reach-wide population estimates from different sampling periods. I use the term 'apparent survival' because the calculation is based solely on differences in abundance over time across and within habitat types, and does not account for recruitment to the age-0 population over time, nor losses or gains from individual habitat types due to ontogenetic movement. Apparent survival rates (S) were converted to weekly instantaneous rates ($M = -\log(S)/t$, where t is the number of weeks for the period of interest) so they could be easily compared with estimates determined from the stock synthesis model (Chapter 6). High-angle habitat was not sampled in 2003. To develop a reach-wide population estimate in this year for July and November sample periods, the average ratio of abundances in low- and high-angle habitats during these periods in other study years was computed and used to predict the abundance in high-angle habitat in 2003.

I estimated the apparent survival rate from egg deposition to about one to two months from emergence based on the ratio of age-0 abundance in July to the reach-wide egg deposition. I refer to this as 'early survival', which depends on survival during incubation and for free-swimming fry up to one- or two-months from emergence when individuals first become vulnerable to the sampling gear (Chapter 2). The annual total egg deposition was calculated as the product of the number of viable redds and the number of eggs/deposited per redd. The total number of redds created each year was determined from repeat redd counts and an estimate of redd survey life (see Chapter 5). The number of viable redds was determined as the product of total redds and the proportion which were not exposed to lethal temperatures due to flow fluctuations. I assumed that each female spawner created one redd over the spawning season, and that 2000 eggs were deposited in each redd. The latter estimate is based on the product of the average female spawner fork length of 35 cm and a fecundity of 58 eggs·cm^{-1} (Allen and Sanger 1960). This analysis focuses on relative differences in early survival rates across years. The absolute value of the number of eggs per redd is simply a scalar, and does not affect the relative comparison. The key assumption is that the number of eggs deposited per redd and the number of redds per female is constant across years.

Age-0 Growth in Shoreline areas

The daily age of trout from hatch and emergence to the date of capture was determined based on otolith microstructure. Both sagittal otoliths were removed from preserved fish and mounted individually on microscope slides in cyanoacrylate glue. Otoliths were polished close to the mid-plane, flipped and re-glued, then polished to the growth plane with 30 μm and 3 μm lapping film, as per established procedures (Stevenson and Campana 1992). All otoliths were examined at a magnification of 400-1250x under a compound microscope. Using the well-defined hatch and emergence checks as a reference points, daily increments between the checks and edge were counted 2-4 times in at least one otolith of each pair (Campana 1992). The average count was recorded as the age from hatch and emergence to capture. For brevity, only estimates of age from hatch are presented here.

I estimated parameters of length-at-age relationships assuming that observation error was log-normally distributed from,

$$(4) \qquad L = (\alpha_{0x} + \alpha_{1x} A)e^{v_{x,i}}$$

where, L is fork length (mm), A is age (days from hatch), α_{0x} and α_{1x} are the intercept (size-at-hatch) and slope (growth rate in mm·day^{-1}), respectively, v is a random deviate from a normal distribution with a mean of 0 and a standard deviation σ_x, and x is a classification term that denotes whether the data and parameters are grouped by year ($x=y$), habitat type ($x=h$) or both ($x=y,h$). Sample sizes to estimate length-at-age relationships are provided in Table 4.1.

Length-at-age models were fit to the data using maximum likelihood and compared using the Akaike Information Criteria (AIC) corrected for small sample size (AIC$_c$). AIC is an information theoretic approach that can be used to identify the most parsimonious model by formally recognizing the tradeoff between bias and variance (Burnham and Anderson 2002). A more complex model with more parameters will almost always fit the data better than a simpler model with fewer parameters (i.e., will have a higher log likelihood), however parameter estimates from the more complex model will be more uncertain. In comparing length-at-age relationship, the simplest model has 3 parameters (α, β, and σ) that are common to all years and habitat types. The most complex model has parameters which are unique for each year-habitat combination

($\alpha_{y,h}$, $\beta_{y,h}$, and $\sigma_{y,h}$). When comparing a range of candidate models, the model with the lowest AIC$_c$ value is considered to have the best predictive capabilities (i.e., best out-of-sample predictive power) based on the bias-variance trade-off incorporated in the AIC statistic. Models with similar AIC$_c$ values relative to the best model (ΔAIC$_c$ 0-2) are considered to have strong support, while those with larger AIC$_c$ values are considered to have moderate (ΔAIC$_c$ 4-7) or essentially no (ΔAIC$_c$ >10) support.

I tested whether emergence timing affected growth rate of age-0 trout by determining whether residuals (predicted-observed) from year-specific length-at-age relationships were related to hatch date. If growth is higher for fry that emerge earlier due to prior residence advantage (Letcher et al. 2004) or better environmental conditions (Nislow et al. 2004), the slope of the residual-hatch date relationship should be positive and significantly different from zero.

4.3   Results

Catch rates of age-0 trout increased from spring to early summer, with peak catch rates in low-angle habitat (Fig. 4.2a) occurring in June or July, approximately one month earlier than in high-angle habitat (Fig. 4.2b). Catch rates in both habitats declined between summer and fall. The general seasonal trend in population estimates (Fig. 4.2c and d) was similar to the trend from raw catch rates but there were noticeable differences on ascending and descending limbs. These differences were caused by the affects of increasing fish size over the summer and fall and size-specific capture probability. Subsequent analyses therefore focus on trends in population size, which account for both these factors.

Low-angle habitats were only extensively utilized during spring and early summer, with peak abundance occurring between June and July (Fig. 4.2c and d). At that time, 38%, 30%, and 42% of the population was found in low-angle habitat in 2004, 2006, and 2007, respectively. In both 2004 and 2007, when sampling was conducted early enough to capture initial habitat colonization by age-0 trout, increases in abundance in high-angle habitat occurred at least one-month later than in low-angle habitat. As the summer progressed, abundance in both habitat types declined, presumably due to

declining recruitment to the age-0 population and the cumulative effects of mortality, but the decline in low-angle habitat was more severe. By early November, the proportion of the reach-wide population in low-angle habitat was 11% in 2004 and 2006, and 27% in 2007. By November, age-0 densities in low-angle habitat in 2004 and 2006 were very low, averaging 10 fish·100 m^{-1}, which was 10-fold lower than densities in high-angle habitat at that time.

The proportion of the reach-wide population utilizing low-angle habitat was lowest in 2006 when the total population size was lowest, and greatest in 2007 when abundance was highest. With the exception of 2007, there was very limited use of low-angle habitats by the September sampling period (Fig. 4.2c). This change coincided with a decline in discharge from an average of 395 m^{-3}·sec^{-1} in July and August during study years, to 250 m^{-3}·sec^{-1} in September (Fig. 4.1). There was over a 3-fold decline in population size between November and December when an experimental flood was conducted (Fig.'s 4.1 and 4.2d). This decline was much greater than changes observed between the September and November sample periods in 2004, or between fall sample periods in other years. In general, age-0 rainbow trout in high-angle habitat were larger (Fig. 4.3). During the July sample period, only very small age-0 trout were found in both low- and high-angle habitats. As the summer progressed, fish grew and length-frequencies in both habitat types shifted upwards. However, within a month, larger fish were much more prevalent in high-angle habitat, and this difference in length-frequency distributions increased over time.

The apparent early survival rate (egg deposition to approximately one to two months from emergence) was much higher when egg deposition was low. Early survival rate was 6-fold greater in 2006 when the number of viable redds was over 10-fold lower relative to other years (Table 4.3a). There was little evidence for density dependence in survival rates of age-0 fish between July and November. Apparent survival in 2006, when the population size in July was approximately 1/3rd of the abundance estimated in 2004 and 2007, was equal to or lower than survival rates in other years (Table 4.3a).

Trends in abundance indicated that apparent survival rates were higher between fall sampling periods (September-November) than between summer periods (June-August) in both habitat types, and that survival between August and September was

89

lower than during other periods (Fig. 4.2c and d). Apparent survival in high-angle habitat was two-fold greater than in low-angle habitat (Table 4.3b). Although population size declined beginning mid-summer due to declining recruitment to the age-0 population and cumulative mortality, biomass increased because the gain in weight of surviving fish exceeded the loss of biomass resulting from mortality (Fig. 4.4). This trend was most apparent in high-angle habitat where fish were bigger.

There were strong linear relationships between age from hatch and fork length in all study years. Age predicted 82-93% of the variation in fork length among individuals within years (Fig. 4.5, Table 4.4a). Growth rate, as inferred by the slope of the length-at-age relationship (α_1, Table 4.4a), was highest in 2006 when age-0 densities were lowest. However, growth rate was also high in 2007 even though age-0 abundance was greatest in this year. The maximum difference in growth rates among years (2004 vs. 2006) lead to relative differences in length-at-age at 40 and 200 days from hatch of 19% and 15%, respectively, equating to relative differences in weight-at-age of 74% and 56%, respectively. Within years, growth rates in low- and high-angle habitats were equivalent in 2006, but were 10% and 5% greater in high-angle habitat in 2004 and 2007, respectively, equating to relative differences in weight-at-age of 31% and 9%, respectively. These habitat-dependent differences were modest in an absolute sense, resulting in a maximum difference in length of 7 mm after 200 days from hatch, equivalent to a weight difference of 2 g.

The AIC analysis (Table 4.4b) indicated that the length-at-age model that had separate slopes for each year and habitat combination, and separate intercepts for each year (Model 6) had the best predictive capability. There was moderate support for the more complex model with separate intercepts and slopes for each year-habitat combination (model 5), as well as for the simpler model with only year-specific effects (model 2). There was virtually no support for the null (model 1) or habitat-specific models (model 4), indicating substantial differences in length-at-age among years, and larger differences among years than among habitats types overall. A comparison of year-specific (model 2) and habitat- and year-specific (model 6) models by year showed little support for the former model in 2004 (2.1 vs. 6.1), indicating substantial difference in

length-at-age among habitat types. In contrast, in 2006 and 2007, there was moderate to near strong support for the model that did not include habitat effects (model 2.2 and 2.3).

There was a negligible effect of hatch date on growth. Hatch date explained almost none of the variation in residuals of the length-at-age models (r^2=0.011, 0.024, 0.002, and 0.017 in 2003, 2004, 2006, and 2007, respectively). The slopes of the relationship between residuals (predicted-observed) from year-specific length-at-age relationships and hatch date were very close to zero (-0.014, -0.020, 0.008, and –0.013 in 2003, 2004, 2006, and 2007, respectively). A significant negative slope would imply that trout that hatch earlier have reduced growth relative to those that hatch later. The slope of the regression lines was not significantly different than zero in 2003, (p=0.13), 2006 (p=0.58) and 2007 (p=0.11), but was in 2004 (p=0.006). Even in this latter case, the effect of hatch date on growth was very minor and was only significant because of the very large sample size (Table 4.1). The 2004 regression model predicted that fish of any age hatching on January 1st would on average be 2.4 mm smaller than fish that hatched on the peak hatch date of April 31st, four months later (Chapter 5).

4.4   Discussion

There was evidence of strong density-dependence in early survival rates between egg deposition and one- to two-months from fry emergence for rainbow trout in the Lee's Ferry reach. The apparent early survival rate increased over 6-fold in 2006 when egg deposition was less than 1/10th the level estimated in other years. Apparent survival rates of age-0 fish from summer through fall were relatively consistent, ranging from 0.18-0.32 in years when both habitat types were sampled (2004, 2006, 2007). There was no indication that these survival rates were density-dependent, as the highest survival rate occurred in the 2007 when abundance was greatest, and survival in 2006 was not higher than other years even though abundance was considerably less. Apparent survival rate in high-angle habitat was on average two-fold greater than in low-angle habitat, however, this difference is very likely overestimated because the survival computation does not account for ontogenetic habitat shifts. This dynamic will be explored using the integrated stock synthesis model in a companion paper (Chapter 6).

More years of data are required to determine whether preliminary conclusions regarding the potential magnitude and timing of compensatory survival responses are robust. The conclusion that that early survival is strongly density dependent is consistent with the Early Critical Period (ECP) concept, which states that high-density dependent mortality during the transition from the alevin stage to independent foraging is the key recruitment bottleneck for some stream salmonid populations, and that there is relatively little density-dependent mortality following this transition period (Elliot 1994, Armstrong 1997, Einum and Nislow 2005, Lobon-Cervia 2006, Coleman and Fausch 2007). Effective densities may be extremely high during the ECP when hundreds of thousands of alevins emerge from redds at discrete locations (Nislow et al. 2004). The resulting strong density-dependent mortality may be magnified in regulated rivers, where hourly fluctuations in flow reduce the availability of stable, shallow, and low-velocity areas (Bain et al. 1988, Shea and Peterson 2007) preferentially utilized by small fish shortly after emergence (Bardonnet et al. 2006). High discharge during the emergence period has been shown to reduce survival rates of Atlantic salmon fry (Jensen and Johnsen 1999, Letcher et al. 2004, Einum and Nislow 2005) and brown trout (Lobon-Cervia 2006).

High-angle shorelines contained greater densities and much higher biomass of age-0 trout than low-angle shorelines in the Lee's Ferry reach. Early in the summer, both habitat types were colonized by newly emerged-trout. As the summer progressed and fish grew, larger age-0 trout were more common in high-angle habitats. The delay in the increase in population size in high-angle habitat relative to low-angle habitat in 2004 and 2007 was indicative of movement from low- to high-angle habitat, and differences in vulnerability-corrected length-frequencies indicated that this habitat shift depended on size. However, an alternative hypothesis consistent with these data is that there is no movement from low- to high-angle habitat, and that differences in abundance and length frequencies among habitats through time are driven by differences in size-dependent mortality rates. These alternative hypotheses will be evaluated using a stock synthesis model in a companion paper (Chapter 6).

Habitat utilization appeared dependent on both age-0 density and flow. In 2006, when age-0 densities were lowest, abundance in high-angle habitat was over 7–fold greater than in low-angle habitat by the fall low-flow period. In contrast, in 2007, when

juvenile densities were highest, abundance in high-angle habitat in the fall was only 3-fold greater than in low-angle habitat. In all years, there appeared to be a greater decline in abundance between August and September when there was a sudden decrease in the minimum flow relative to other months. However, the apparent drop in abundance could be a normal change related to declining recruitment to the age-0 population, and requires more detailed investigation using the integrated stock synthesis model (Chapter 6). There was a 3-fold decline in abundance following the experimental flood in November 2004 that was not confounded with trends in recruitment due to close proximity of samples before and after the flood. Attributing this decline to mortality is uncertain, as high flows could also have displaced fish downstream out of the Lee's Ferry reach.

I speculate that the patterns of habitat use that were observed were driven by differences in predation risk and bioenergetics among habitat types, and that both mechanisms are potentially influenced by flow regime. A shift from low- to high-angle habitats could be considered analogous to a shift from riffles to pools in small streams (e.g., Chapman and Bjornn 1968), or from littoral to pelagic zones within lakes (e.g., Biro et al. 2003). Many authors have suggested that habitat shifts of young fish are dominated by differences in avian and piscivorous predation risk as determined by depth (Gaudin 2001, Werner and Hall 1988). Applying this model to the Lee's Ferry reach, age-0 trout should shift from low (shallow)- to high (deep)-angle habitats as they grow and become more vulnerable to birds and less vulnerable to piscivorous fish. Although I did not quantify predation risk in this study, catches of adult rainbow trout, which consume small fish in the Colorado River (M. Yard, Grand Canyon Monitoring and Research Center, unpublished data), only occurred when sampling high-angle habitat, thus it is very likely that the risk of predation from larger fish is greater in this habitat type. The abundance of older and larger conspecifics in high-angle habitats likely determines the extent of competition and predation risk for smaller age-0 trout in these environments (Kennedy and Strange 1986, Gibson et al. 1993, Post et al. 1999). In 2006, when densities of both adults (Ward and Rogers 2006) and age-0 trout were very low, the abundance of age-0 trout in high-angle habitat relative to low-angle habitat was much greater, especially earlier in the summer, compared to other years when juvenile and adult abundance was greater (Fig. 4.2c and d).

Differences in the energetic profitability among habitat types could also be driving the observed size-dependent variation in habitat use. Rosenfeld and Boss (2001) showed that larger juvenile cutthroat trout (Oncorhynchus clarki) could only achieve positive growth by using deeper pool habitats, and had negative growth in riffles. In contrast, smaller age-0 cutthroat trout could achieve positive growth in both environments, but avoided pool habitat in the presence of larger conspecifics. In the Lee's Ferry reach, the biomass of age-0 trout in high-angle habitat was typically 2 to 8-fold greater than in low-angle habitat (Fig. 4.4). This difference suggests that energetics for larger age-0 trout in high-angle habitat type are considerably better. The almost complete absence of age-0 trout from low-angle habitat in early September in 2003 and 2006 (Fig. 4.2c), shortly after flows were reduced by approximately 50% (Fig. 4.1), further suggests that absolute levels of flow also control the energetics in these environments and have an effect on habitat use.

Hourly variation in discharge has been hypothesized to cause greater destabilization in lower angle shallow shoreline environments relative to steeper shorelines with deeper water (Cushman 1985, Heggenes 1988, Bain et al. 1998, Bowen et al. 1998, McKinney et al. 1999, She and Peterson 2007). Shallow environments, normally more profitable for small fish in stable systems like the littoral areas in small lakes or riffles in streams, may be less so in fluctuating regulated rivers. Bain et al. (1988) suggest that hourly flow fluctuations reduce the capability of low-angle habitats to provide effective refuge from predation. Diurnal variation in stage during the summer averaged 0.75 m over the study period, and resulted in an average horizontal shoreline shift of 6.5 m and 2.2 m in low- and high-angle habitats, respectively. In the Lee's Ferry reach, this physical dynamic has been shown to reduce benthic invertebrate densities (Blinn et al. 1995) and limit use of immediate nearshore areas by age-0 trout (Chapter 3). Although 56% of the useable shoreline length in the Lee's Ferry reach is comprised of low-angle habitat, it supported on average only 36% (July) to 17% (November) of the total age-0 population. I hypothesize that due to differences in morphometry, hourly variation in flow reduces both energetic profitability and cover from predation to a greater extent in low-angle habitat than in high-angle habitat. Thus, the productive capacity of low-angle habitat to support age-0 trout should increase under a more stable flow regime, leading to

a substantive increase in the reach-wide abundance of age-0 trout. Testing this hypothesis, through long-term monitoring of abundance and mortality rates in habitats with differing sensitivities to flow fluctuations, under both fluctuating and more stable flow regimes, is critical to determine how flow controls juvenile recruitment in large regulated rivers.

There were modest differences in age-0 growth rates among years and habitat types. Growth rates were highest in 2006 when age-0 densities were lowest, but were almost as high in 2007 when age-0 densities were greatest. Given this pattern and only four years of data, I cannot determine whether age-0 growth was density-dependent. Fork length of age-0 trout 40 days from hatch was 10-20% greater in 2006 than in all other years, which could be indicative of better growth resulting from considerably lower densities during the emergence period. There was no indication that larger size-at-age in 2006 resulted in higher survival during the summer-fall period. With the exception of 2004, there was little indication that growth rates were substantially different among habitat types. However, as some fish that are captured and sampled for growth in high-angle habitat are potentially recent immigrants from low-angle habitat, average size-at-age in high-angle habitat would only partially reflect its potential for growth. Assessing differences in growth rates among habitats in cases where fish are not permanent residents requires recapture of marked individuals whose affinity to each habitat type can be unambiguously determined. Variation in growth rates among individuals was essentially independent of hatch date. Nislow et al. (2004) attributed faster growth rates of early-emerging Atlantic salmon fry to improved feeding conditions resulting from greater habitat availability during early spring. In laboratory experiments, Letcher et al. (2004) found that early-stocked fry outgrew late-stocked fry when reared together, implying that fish that emerge early can suppress growth of later groups. Neither of these dynamics appears to influence growth rates for age-0 trout in the Lee's Ferry reach.

Long-term monitoring of early life history dynamics is a potentially powerful tool that can be used in Adaptive Management programs to better understand how flow regulates population size of stream fishes. Given the costs and risks of many Adaptive Management experiments, a more sophisticated analysis of early life history data relative to the one provided in this chapter, is warranted. For example, the comparison of

apparent survival rates across years, which was based on a simple ratio of abundances through time, did not account for differences in seasonal variation in recruitment to the age-0 population driven by variation in spawn-timing and temporal variation in incubation mortality (Chapter 5). The comparison of apparent survival rates among habitat types did not account for losses and gains resulting from ontogenetic habitat shifts. Furthermore, determining the significance of differences in mortality rates between habitat types, or between years or sampling periods, requires robust estimates of uncertainty. Uncertainty in mortality rates would be substantially underestimated based on the simplifying assumptions inherent in the abundance ratio method used in this paper, and was therefore not computed. The stock synthesis model addresses all these limitations by estimating parameters defining key early life history processes by jointly maximizing the fit of the model to redd counts, catch rates, length-frequencies, capture probabilities, and length-at-age within a single framework. In a companion paper (Chapter 6), this model is applied to data from the Lee's Ferry reach to readdress a variety of hypotheses about early life history dynamics that were evaluated in this paper based on simpler methods that did not account for the interaction among key parameters.

Table 4.1. Summary of sampling effort for age-0 trout in the Lee's Ferry reach. No sampling in high-angle habitat was conducted in 2003.

			Low-Angle Habitat			High-Angle Habitat		
			Avg. Meters	Avg. Fish		Avg. Meters	Avg. Fish	
	Sampling	Period	Sampled	Caught	Fish	Sampled	Caught	Fish
Year	Trips	Sampled	per Trip	per Trip	Aged	per Trip	per Trip	Aged
2003	4	Jun-Nov	563	147	237			
2004	8	Apr-Dec	656	188	120	1056	369	198
2006	5	Jun-Nov	547	90	59	1070	346	78
2007	5	Jun-Nov	606	355	70	1036	689	82

Table 4.2. Average depth (cm) and velocity (cm·sec^{-1} at 0.6 total depth) at 12 sites in both low- and high-angle shoreline habitats based on 10 measurements per site taken 1.5 m from shore sampled at the daily minimum (Min.) and maximum (Max.) flow, June 30th - July 6th, 2004. Also shown are the average depths and velocities taken at the edge of the permanently submerged zone at the daily maximum flow, which occurred on average 6.5 and 2.2 m from shore in low- and high-angle habitat, respectively. Standard errors shown in parentheses denote the variation in mean conditions across sample sites.

| | Low-Angle | | High-Angle | |
	Min. Flow	Max. Flow	Min. Flow	Max. Flow
Gradient (%)	12		37	
Immediate nearshore zone				
Depth	29 (7)	39 (13)	60 (19)	75 (16)
Velocity	7 (6)	3 (6)	6 (7)	12 (13)
Edge of permanently submerged zone				
Depth		63 (8)		85 (14)
Velocity		17 (16)		12 (17)

Table 4.3. Annual estimates of the number of redds, viable redds, viable eggs (millions) and age-0 rainbow trout, and apparent survival rates, in the Lee's Ferry reach, 2003-2007. Apparent survival rates were computed based on the ratio of age-0 abundance in July to the number of viable eggs, and the ratio of age-0 abundance in July to the abundance in November (a). The latter survival rates were converted to instantaneous weekly mortality rates (Inst. M) for comparisons with estimates in Chapter 6. b) shows apparent survival and instantaneous mortality rates by habitat type. Note age-0 abundance in 2003 was estimated based on data collected from low-angle habitat only.

a)

	Redds		Viable Eggs (x10^6)	Abundance		Apparent Survival Jul. Fry Viable Eggs	Nov. Fry July Fry	Nov.-Jul. Weekly Inst. M
Year	Total	Viable		Jul.	Nov.			
2003	3,264	2,494	4.99	144,873	79,572	0.03	0.55	0.03
2004	2,142	1,076	2.15	177,617	31,421	0.08	0.18	0.10
2006	88	84	0.17	86,976	16,427	0.52	0.19	0.10
2007	1,215	1,078	2.16	193,852	62,786	0.09	0.32	0.07

b)

	Apparent Survival Rate Nov. Fry/July Fry		Instantaneous Weekly Mortality Rate	
Year	Low-Angle	High-Angle	Low-Angle	High-Angle
2003	0.22		0.09	
2004	0.05	0.25	0.17	0.08
2006	0.07	0.24	0.15	0.08
2007	0.21	0.40	0.09	0.05
Average	0.14	0.30	0.11	0.07

Table 4.4. Parameter estimates (a) and comparison of out-of-sample predictive power based on AIC (b) for alternative length-at-age models. Columns α_0, α_1, σ, r^2, and n in a) denote the most likely estimates of the intercept, slope, and standard deviation of the linear length-at-age relationships, the proportion of variation in observed fork length predicted by the models, and the sample size, respectively. Columns K, LL, AIC_c, and ΔAIC_c in b) denote the number of parameters that are estimated, log-likelihood, Akaike information criteria statistic, and the difference in AIC values relative to the model with the lowest AIC_c value, respectively. The effect of habitat on length-at-age is compared by year in the bottom portion of b). In this case, ΔAIC_c is the difference between AIC_c values among habitat-dependent and –independent models within years. For brevity, a) shows statistics for only a subset of models in b).

a)

Model #	Model Name	Strata	α_0	α_1	σ	r^2	n
1	Null (L=α_0+α_1A)		10.09	0.40	0.14	0.84	843
2	Year (L=α_{0y}+α_{1y}A)	2003	11.63	0.37	0.12	0.87	237
		2004	8.00	0.40	0.14	0.82	318
		2006	10.39	0.46	0.12	0.87	136
		2007	9.19	0.43	0.10	0.93	152
4	Habitat (L=α_{0h}+α_{1h}A)	Low	11.00	0.38	0.13	0.84	486
		High	9.79	0.42	0.14	0.82	357
5	Year-Habitat (L=$\alpha_{0y,h}$+$\alpha_{1y,h}$A)	2003-Low	11.63	0.37	0.12	0.87	237
		2004-Low	9.55	0.37	0.12	0.85	120
		2004-High	8.26	0.41	0.15	0.78	198
		2006-Low	10.54	0.46	0.12	0.86	59
		2006-High	10.23	0.46	0.12	0.87	77
		2007-Low	9.81	0.42	0.09	0.93	70
		2007-High	8.91	0.44	0.10	0.93	82

Table 4.4. Con't.

b)

Model #	Model Name	K	LL	AIC_c	ΔAIC_c
1	Null ($L=\alpha_0+\alpha_1 A$)	3	477.2	-948.4	182.9
2	Year ($L=\alpha_{0y}+\alpha_{1y}A$)	12	574.3	-1124.3	7.0
3	Year ($L=\alpha_0+\alpha_{1y}A$)	9	568.6	-1119.0	12.3
4	Habitat ($L=\alpha_{0h}+\alpha_{1h}A$)	6	492.8	-973.5	157.8
5	Year-Habitat ($L=\alpha_{0y,h}+\alpha_{1y,h}A$)	21	584.5	-1125.8	5.5
6	Year-Habitat ($L=\alpha_{0y}+\alpha_{1y,h}A$)	18	584.1	-1131.3	0.0
	Habitat Effect (by year)			$\Delta AIC_c = AIC_{6.x} - AIC_{2.x}$	
2.1	2004 ($L=\alpha_{0y}+\alpha_{1y}A$)	3	169.5	-332.9	
6.1	2004 – Habitat ($L=\alpha_{0y}+\alpha_{1y,h}A$)	5	178.8	-347.3	-14.4
2.2	2006 ($L=\alpha_{0y}+\alpha_{1y}A$)	3	98.0	-189.8	
6.2	2006-Habitat ($L=\alpha_{0y}+\alpha_{1y,h}A$)	5	98.0	-185.5	4.3
2.3	2007 ($L=\alpha_{0y}+\alpha_{1y}A$)	3	141.1	-276.0	
6.3	2007-Habitat ($L=\alpha_{0y}+\alpha_{1y,h}A$)	5	141.6	-272.7	3.3
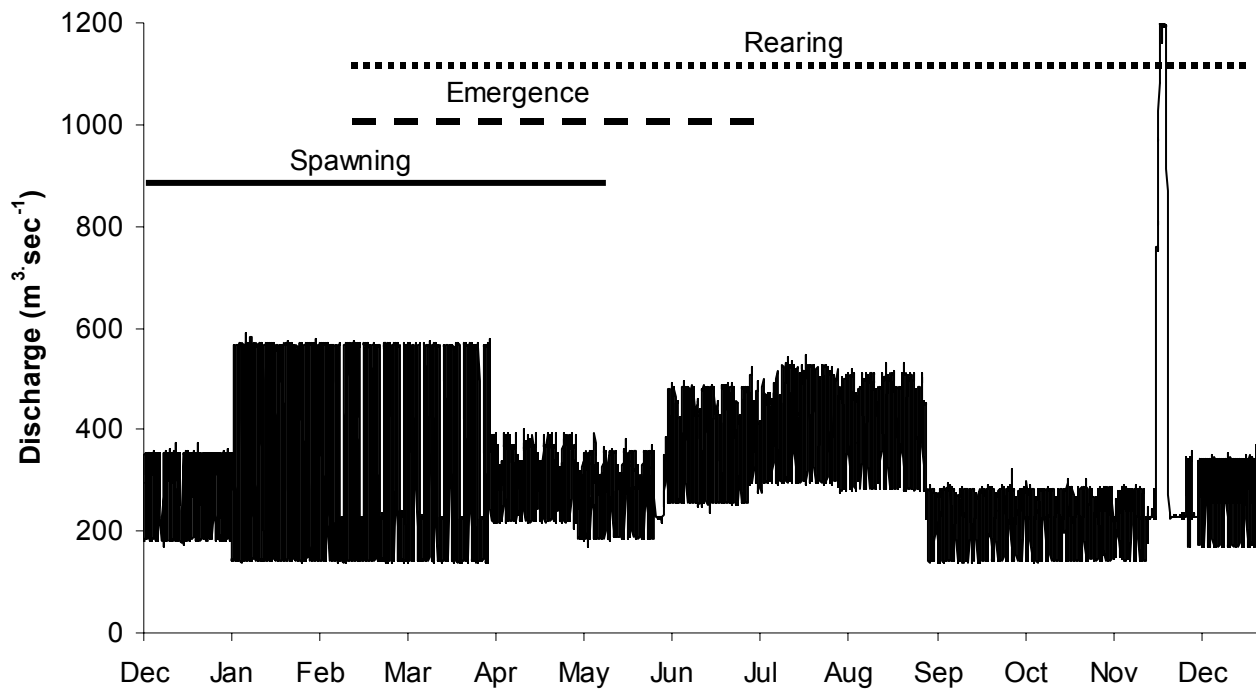
Figure 4.1. Typical hourly hydrograph for a 13-month period (December 1st 2003 – December 31st, 2004) from Glen Canyon Dam in relation to the timing of spawning, emergence, and rearing for age-0 rainbow trout in the Lee's Ferry reach. The width of the discharge band represents the extent of hourly variation in flow with a day. The experimental increase in hourly fluctuations between January 1st and March 31st, the sudden reduction in minimum flow between August and September, and the experimental flood on November 21st-25th, are clearly visible.
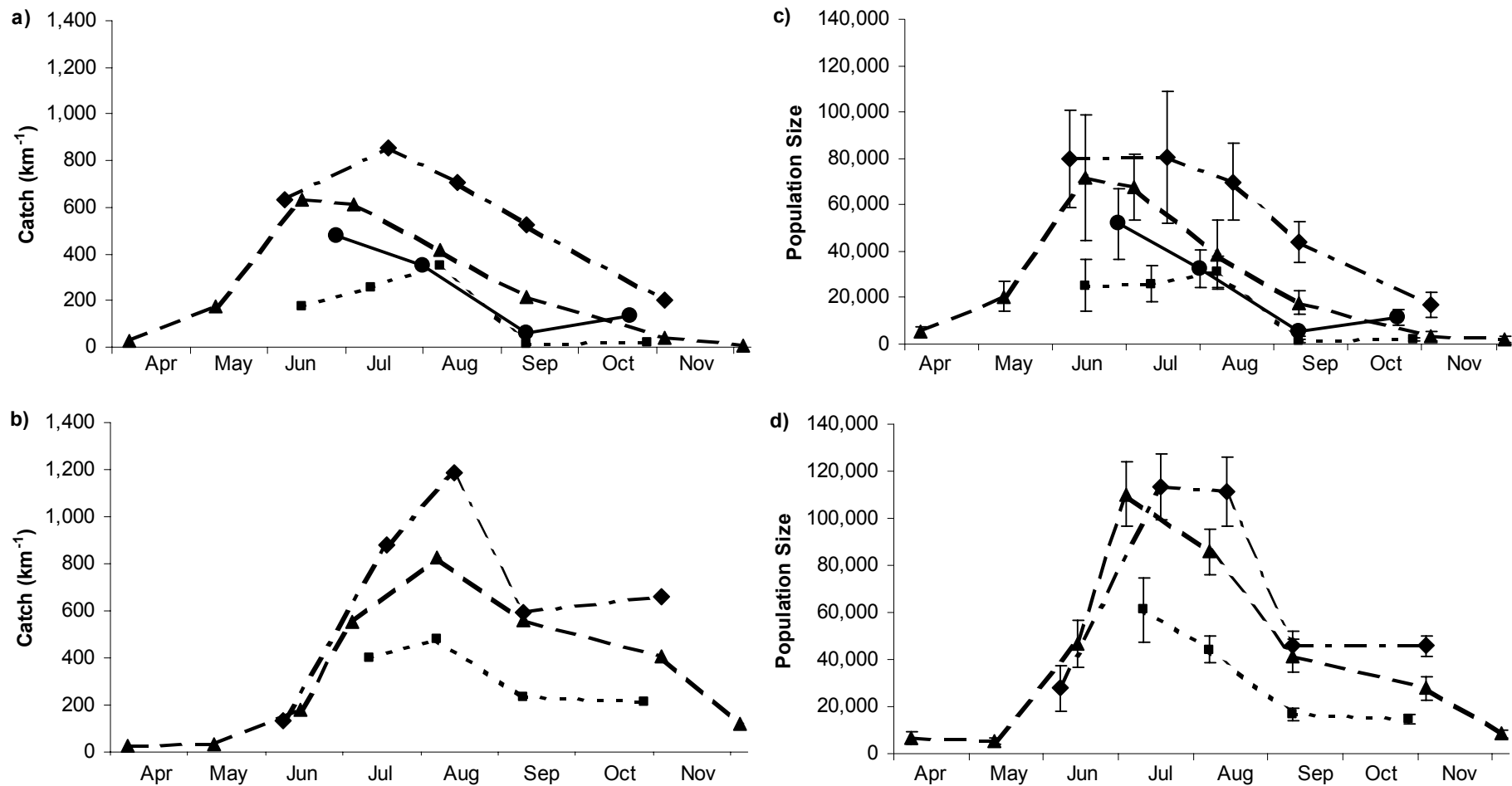
Figure 4.2. Seasonal rends in catch rate (a and b) and reach-wide population estimates (c and d) in low (a, c)- and high (b, d) - angle habitat by year. Confidence intervals for population estimates denote 1 standard deviation of the mean. Lines with circles, triangles, squares, and diamonds denote 2003, 2004, 2006, and 2007, respectively.
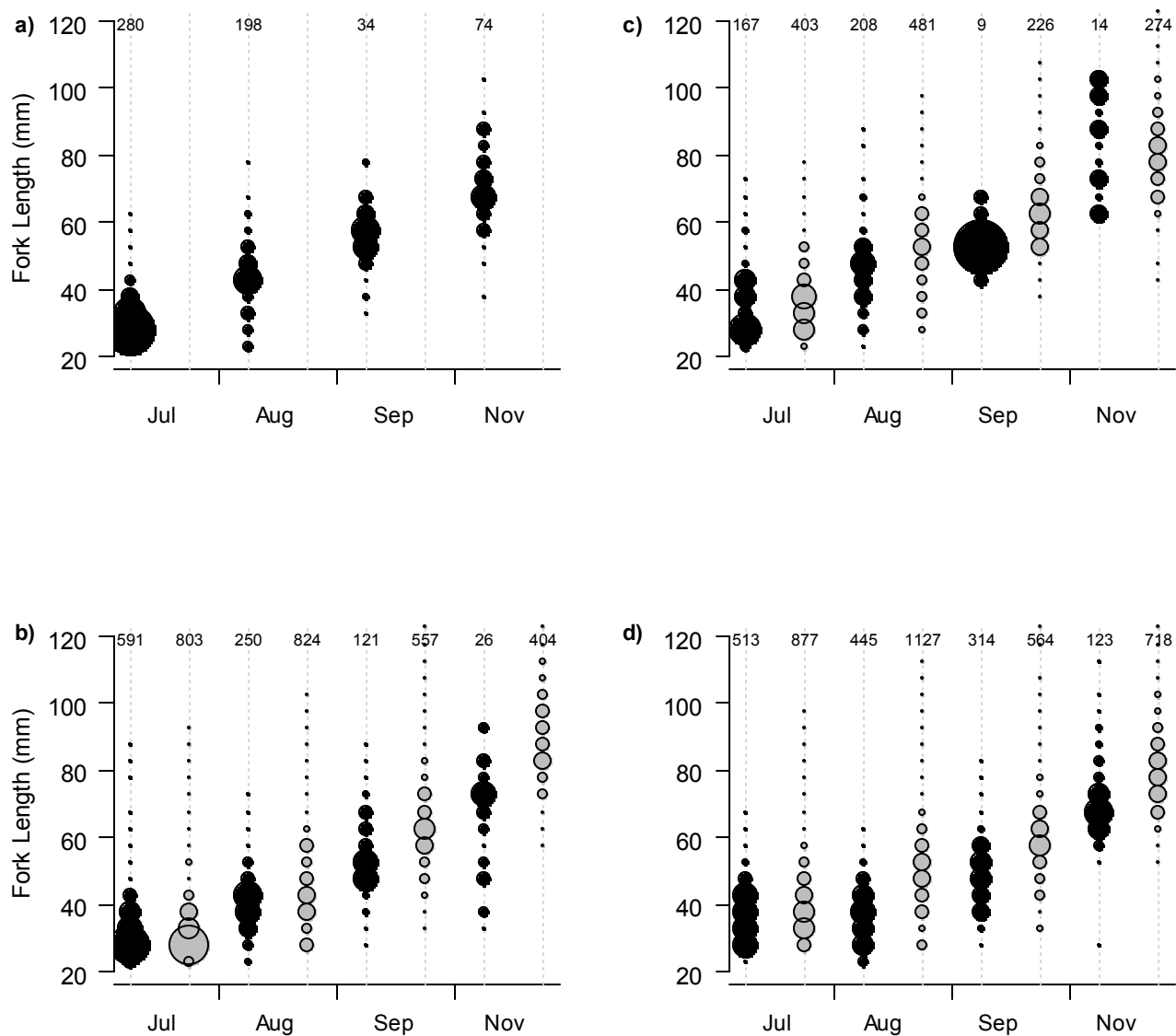
Figure 4.3. Length-frequency distributions of age-0 trout by month and habitat type corrected for size-dependent capture probability in (a) 2003, (b) 2004, (c) 2006, and (d) 2007. Black and gray circles denote low- and high-angle habitat respectively. The size of the circles is proportional to the ratio of fish caught by size class to the total fish caught within each stratum (column). Numbers at the top of each column denote the total catch by stratum. No sampling was conducted in high-angle habitat in 2003.

a)
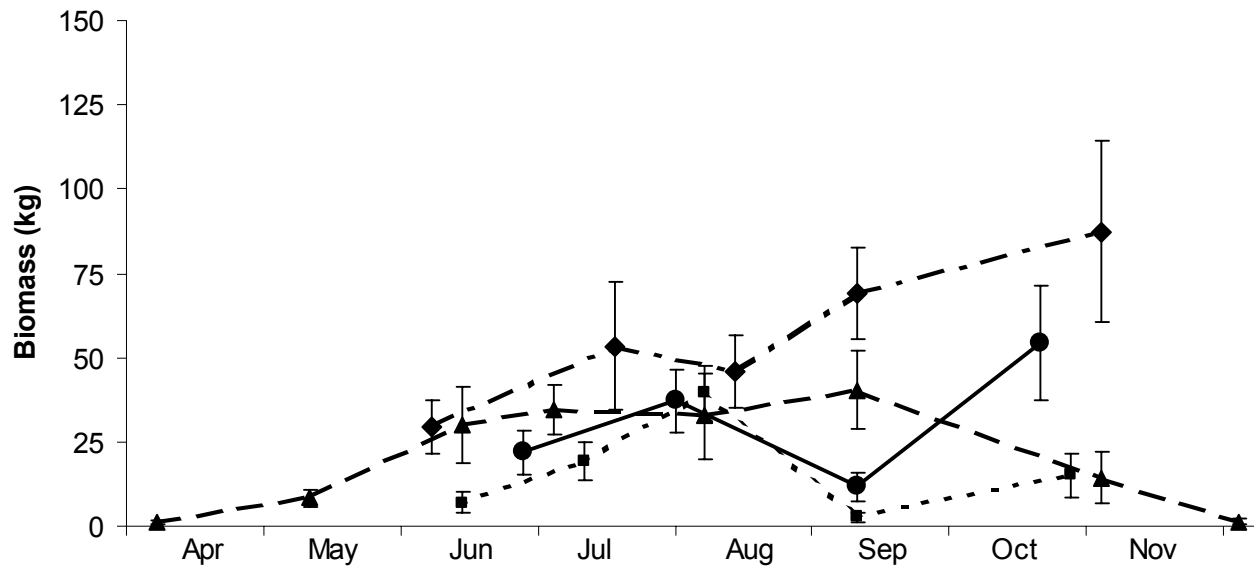
b)
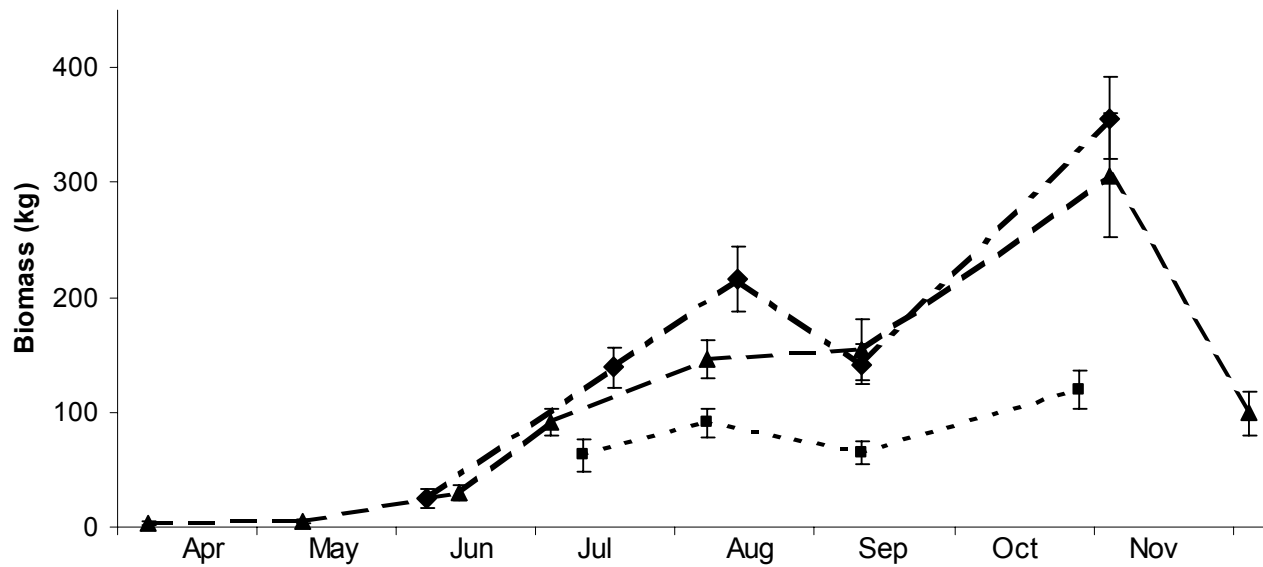
Figure 4.4. Reach-wide total biomass estimates in (a) low- and (b) high-angle habitat by sample period and year. Error bars denote 1 standard deviation of the mean. Lines with circles, triangles, squares, and diamonds denote 2003, 2004, 2006, and 2007, respectively.
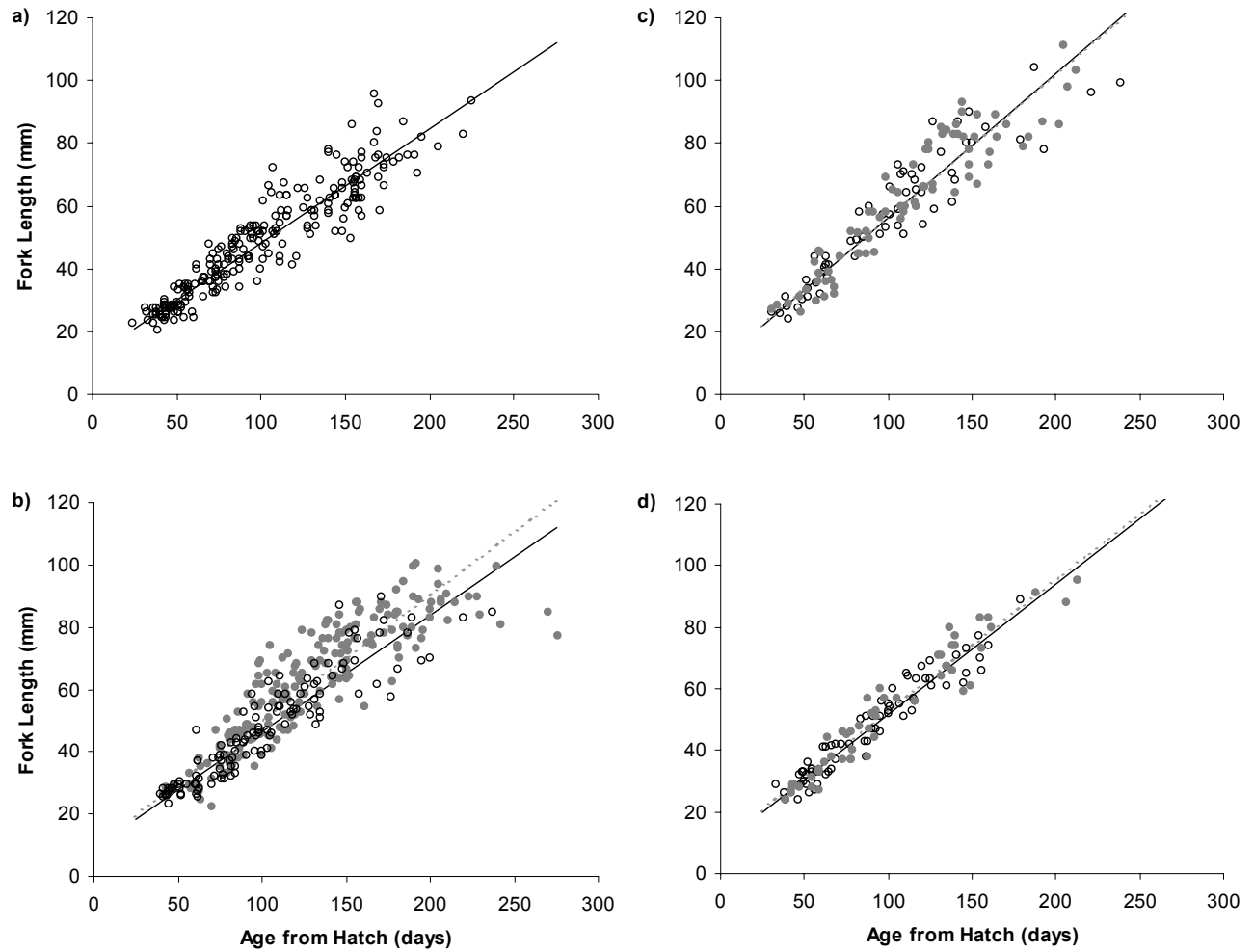
Figure 4.5. Length-at-age in (a) 2003, (b) 2004, (c) 2006, and (d) 2007 stratified by habitat type. Open and filled circles represent fish from low- and high-angle habitat types, respectively. Solid and dashed lines represent the best-fit relationships based on the year-habitat model with common intercepts across habitat types within years for low- and high-angle habitat types, respectively (model 6, $L=\alpha_{0y}+\alpha_{1y,h}A$, Table 4.4).

4.5   References

Armstrong, J.D. 1997. Self-thinning in juvenile sea trout and other salmonid fishes revisited. J. Anim. Ecol. **66:** 519-526.

Bain, M.B., Finn, J.T., and H.E. Booke. 1988. Streamflow regulation and fish community structure. Ecology **69:** 382-292.

Bardonnet, A., Poncin, P., and J.M. Roussel. 2006. Brown trout fry move inshore at night: a choice of water depth or velocity? Ecol. Fresh. Fish. **15:** 309-314.

Becker, C.D., D.A. Neitzel, and D.H. Fickeisen. 1982. Effects of dewatering on Chinook salmon redds: Tolerance of four developmental phases to daily dewaterings. Trans. Am. Fish. Soc. **111:** 624-637.

Biro, P.A., Post, J.R., and Parkinson, E.A. 2003. Population consequences of a predator-induced habitat shift by trout in whole-lake experiments. Ecology **84**: 691-700.

Biro, P.A., Abrahams, M.V., Post, J.R., and E.A. Parkinson. 2004. Predators select against high growth rates and risk-taking behaviour in domestic trout populations. Proc. R. Soc. Lond. B. **271:** 2233-2237.

Blinn, D.W., Shannon, J.P., Stevens, L.E., and J.P. Carder. 1995. Consequences of fluctuating discharge for lotic communities. J. Am. Ben. Soc. **108:** 215-228.

Bowen, Z. .K., Freeman, M.C., and K.D. Bovee. 1998. Evaluation of generalized habitat criteria for assessing impacts of altered flow regimes on warmwater fishes. Trans. Am. Fish. Soc. **127:** 455-468.

Bradford, M.J. Taylor, G.C., Allan, A., and P.S. Higgins. 1995. An experimental study of the stranding of Coho Salmon and Rainbow Trout during rapid flow decreases under winder conditions. Nor. Am. J. Fish. Manag. **15:** 473-479.

Burnham, K.P., and D.R. Anderson. 2002. Model Selection and Multimodel Inference, 2nd edition. Springer-Verlag, NY.

Campana, S.E. 1992. Measurement and interpretation of the microstructure of fish otoliths. *In* Otolith microstructure examination and analysis. Edited by D.K. Stevenson and S.E. Campana. Can. Spec. Publ. Fish. Aquat. Sci. **117**. pp. 59-71.

Chapman, D.W., and T.C. Bjornn. 1969. Distribution of salmonids in streams, with special reference to effects of food and feeding, p. 153-156. *In* Symposium on

salmon and trout in streams. H.R. MacMillan Lectures in Fisheries, Iniv. British Columbia. Vancouver, BC.

Coleman, M.A., and K.D. Fausch. 2007. Cold summer temperature regimes cause a recruitment bottleneck in age-0 Colorado River cutthroat trout reared in laboratory streams. Trans. Am. Fish. Soc. **136:** 639-654.

Connor, E.J., and D.E. Pflug. 2004. Changes in the distribution and density of pink, chum, and Chinook salmon spawning in the Upper Skagit River in response to flow management measures. Nor. Am. J. Fish. Mgmt. **24:** 835-852.

Cushman, R.M. 1985. Review of ecological effects of rapidly varying flows downstream from hydroelectric facilities. Nor. Am. J. Fish. Mgmt. **5:** 330-339.

Einum, S.A. and K.H. Nislow. 2005. Local-scale density-dependent survival of mobile organisms in continuous habitats: an experimental test using Atlantic salmon. Oecologia **143**: 203-210.

Elliott, J.M. 1994. Quantitative ecology and the brown trout. Oxford University Press, Oxford. 287 pp.

Everest, F.H., and D.W. Chapman. 1972. Habitat select and spatial interaction by juvenile Chinook salmon and steelhead strout in two Idaho streams. F. Fish. Res. Bd. Canada **29:** 91-100.

Fletcher, R.I., and R.B. Deriso. 1988. Fishing in dangerous waters: remarks on a controversial appeal to spawner-recruit theory for long-term impact assessment. Pp. 232-244 in Barnthouse, L.W., Klauda, R.J., Vaughn, D.S., and R.L. Kendall [eds.]. Science, law, and Hudson River power plants. American Fisheries Society Monograph No. 4.

Gaudin, P. 2001. Habitat shifts in juvenile riverine fishes. Arch. Hydrobiol. Suppl. **135**/2-4. 393 p.

Gibson, R.J., Stansbury, D.E., Whalen, R.R. and K.G. Hillier. 1993. Relative habitat use, and inter-specific and intra-specific competition of brook trout (Salvelinus fantinalis) and juvenile Atlantic salmon (Salmo salar) in some Newfoundland rivers. In Production of juvenile Atlantic salmon, Salmo salar, in natural waters. R.J. Gibson and R.E. Cutting [eds.]. Can. Sp. Pub. Fish. Aquat. Sci **118.**

Halleraker, J.H., Saltveit, J.J., Harby, A., Arnekleiv, J.V., Fjesdstad, H.P., and B. Kohler. 2003. Factors influencing stranding of wild juvenile brown trout (*Salmo trutta*) during rapid and frequent flow decreases in artificial stream. Riv. Res. Applic. **19:** 589-603.

Hartman, G.F., and J.C. Scrivener. 1990. Impacts of forestry practices on a coastal stream ecosystem, Carnation Creek, British Columbia. Can. Bull. Fish. Aquat. Sci. **223**. 148 pp.

Heggenes, J. 1988. Effects of short-term flow fluctuations on displacement of, and habitat use by, Brown Trout in a small stream. Trans. Am. Fish. Soc. **117:** 336-344.

Heggenes, J. and T. Traaen. 1988 Downstream migration and critical water velocities in stream channels for fry of four salmonid species. J. Fish Biol. **32:** 717-727.

Imre, I., Grant, J.W.A., and R.A. Cunjak. 2005. Density-dependent growth of young-of-year Atlantic salmon *Salmo salar* in Catamaran Brook, New Brunswick. J. Anim. Ecol. **74:** 508-516.

Jensen, A.J., and B.O. Johnsen. 1999. The functional relationship between peak spring floods and survival and growth of juvenile Atlantic salmon (Salmo salar) and brown trout (Salmo trutta). Funct. Ecol. **13:** 778-785.

Kennedy, G.J.A., and C.D. Strange. 1986. The effects of intra- and inter-specific competition on the survival and growth of stocked juvenile Atlantic salmon, Salmo salar L., and resident trout, Salmo trutta L., in an upland stream. J. Fish. Biol. **28:** 479-489.

Lobon-Cervia, J. 2006. Numerical changes in stream-resident brown trout (Salmo trutta): uncovering the roles of density-dependent and density-independent factors across space and time. Can. J. Fish. Aquat. Sci **64:** 1429-1447.

Letcher, B.H., Dubreuil, T., O'Donnell, M.J., Obedzinski, M., Griswold, K., and K.H. Nislow. 2004. Long-term consequences of variation in timing and manner of fry introduction on juvenile Atlantic salmon (Salmo salar) growth, survival, and life-history expression. Can. J. Fish. Aquat. Sci. **61:** 2388-2301.

McKinney, T., Speas, D.W., Rogers, R.S., and W.R. Persons. 1999. Rainbow trout in a regulated river below Glen Canyon Dam, Arizona, following increased minimum flows and reduced discharge variability. Nor. Am. J. Fish. Mgmt. **21**: 216-222.

McMichael, G.A., Rakowski, C.L., James, B.B., and J.A. Lukas. 2005. Estimated fall Chinook salmon survival to emergence in dewatered redds in a shallow side channel of the Columbia River. Nor. Am. J. Fish. Mgmt. **25**: 876-884.

Mietz, S.W. 2003. Evaluating historical electrofishing distribution in the Colorado River, Arizona, based on shoreline substrate. M.Sc. thesis, Department of Biology, Northern Arizona University, Flagstaff, AZ.

Nislow, K.H. Einum, S., and C.L. Folt. 2004. Testing predictions of the critical period for survival concept using experiments with stocked Atlantic salmon. J. Fish Biol. **65** (Supplement A):188-200.

Nislow, K.H. 2001. International symposium on the implications of salmonid growth varitiation. Rev. Fish Biol. and Fisheries. **10:** 521-527.

Nislow, K.H., Folt, C., and M. Seandel. 1998. Food and foraging behaviour in relation to microhabitat use and survival of age-0 Atlantic salmon. Can. J. Fish. Aquat. Sci. **55:** 116-127.

Poff, N.L., Allan, J.D., Bain, M.B., Karr, J.R., Prestegaard, K.L., Richter, B.D., Sparks, R.E., and J.C. Stromberg. 1997. The natural flow regime. Bioscience **47:** 769-784.

Post, J.R., Parkinson, E.A., and N. T. Johnston. 1999. Density dependent processes in structured fish populations: interaction strengths in whole-lake experiments. Eco. Mono. **69:** 155-175.

Randle, T.J., and E.L. Pemberton. 1987. Results and analysis of STARS modeling efforts of the Colorado River in Grand Canyon. U.S. Department of Interior, Bureau of Reclamation. NTIS No. PB88-183421/AS.

Ratikainen, I.I., Gill, J.A., Gunnarsson, T.G., Sutherland, W.J., and H. Kokko. 2008. When density dependence is not instantaneious: theoretical developments and management implications. Ecol. Lett. **22:** 184-198.

Rose, K.A., Cowan, J.H., Winemiller, K.O., Myers, R.A., and R. Hilborn. 2001. Compensatory density dependence in fish populations: Importance, controversy, understanding and prognosis. Fish and Fisheries **2:** 293-327.

Rosenfeld, J.S., and S. Boss. 2001. Fitness consequences of habitat use for juvenile cutthroat trout: energetic costs and benefits in pools and riffles. Can. J. Fish. Aquat. Sci. **58:** 585-593.

Saltveit, S.J., Halleraker, J.H., Arnekleiv, J.V., and A. Harby. 2001. Field experiments on stranding in juvenile Atlantic Salmon (Salmo Salar) and Brown Trout (Salmo Trutta) during rapid flow decreases caused by hydropeaking. Reg. Rivers: Res. Mgmt. **17:** 609-622.

Shea, C.P., and J. T. Peterson. 2007. An evaluation of the relative influence of habitat complexity and habitat stability on fish assemblage structure in unregulated and regulated reaches of a large Southeastern warmwater stream. Trans. Am. Fish. Soc. **136:** 943-958.

Shirvell, C.S. 1994. Effect of changes in streamflow on the microhabitat use and movements of sympatric juvenile coho salmon and chinook salmon in a natural stream. Can. J. Fish. Aquat. Sci**. 51:** 644-1652.

Stevenson, D.K. and S.E. Campana [*Editors*]. 1992. Otolith microstructure examination and analysis. Can. Spec. Publ. Fish. Aquat. Sci. **117**. 130 p.

Vandenbos. R.E., Tonn, W.M., and S. M. Boss. 2006. Cascading life-history interactions: alternative density-dependent pathways drive recruitment dynamics in a freshwater fish. Oecologia **148:** 573-582.

Vernieu, W.S, Hueftle, S.J., and S.P. Gloss. Water quality in Lake Powell and the Colorado River. *In* The state of the Colorado River ecosystems in Grand Canyon. Edited by S.P. Gloss, J.E. Lovitch, and T.S. Melis. U.S. Geological Survey Circular 1282. Available from http://www.gcmrc.gov/products/score/2005/score.htm.

Voichick, N., and S.A. Wright. 2007. Water temperature data for the Colorado River and tributaries between Glen Canyon Dam and Spencer Canyon, Northern Arizona, 1988-2005. USGS Data Series Report. U.S. Geological Survey.

Ward, D., and S. Rogers. 2006. Lee's Ferry, Long-term rainbow trout monitoring. Report prepared by Arizona Game and Fish Department for Grand Canyon Monitoring and Research Centre, Flagstaff AZ.

Werner, E.E., and D.J. Hall. 1988. Ontogenetic habitat shifts in bluegill: the foraging rate – predation risk trade-off. Ecology **69:**1352-1366.

5.0 Effects of Fluctuating Flows on Incubation Mortality, Hatch Timing, and Age-0 Abundance of Rainbow Trout in a Large Regulated River[4]

5.1 Introduction

The impact of the loss of eggs and larvae on fish populations that result from the operation of nuclear powerplants (Barnthouse et al. 1998), hydroelectric dams (McKinney et al. 2001), and natural causes (Method 1983, Crecco and Savoy 1985, Peterman et al. 1988) has been a subject of much interest. The extent of the impact will depend on the proportion of individuals from early life stages that are killed, and the potential for density dependent compensation in survival rates in latter life stages. Although numerous studies have shown that egg and larval densities are a poor predictor of recruitment because of strong density dependence in early life stages (e.g. Houde 1987), legislation designed to protect fish populations and their spawning habitat, such as the Canadian Fisheries Act (http://laws.justice.gc.ca/en/showtdm/cs/F-14), does not explicitly recognize this dynamic. Incorporating the effects of density dependence when assessing or predicting human impacts is controversial (Fletcher and Deriso 1988).

Fluctuations in water levels below hydroelectric dams can result in periodic dewatering of gravels in spawning areas, potentially increasing mortality rates for the egg and alevin incubating life stages of salmonids (Reiser and White 1983). Dewatering of redds is a highly visible impact, and in some systems, such as the Columbia and Skagit rivers, flow regimes have been stabilized over the spawning and incubation period to minimize the number of redds that are exposed (Connor and Pflug 2004, McMichael et al. 2005). Typically, maximum flows during the spawning period are reduced to inhibit spawning on high elevation bars, and minimum flows during the incubation period are increased to limit the extent of dewatering. The efficacy of these flow regimes needs to

---

[4] A version of this chapter may be submitted for publication. Korman, J., and M. Kaplinski. Effects of fluctuating flows on incubation mortality, hatch timing, and age-0 abundance of rainbow trout in a large regulated river.

be assessed because lost revenues from flow stabilization can be substantial, and flow regimes focused on improving survival rates for older life stages may produce greater benefits. We know of only one published example where an increase in salmonid population abundance resulting from flow stabilization was attributed to improvements during the spawning and incubation period (Connor and Pflug 2004). Even in this case, the authors caution that other environmental factors could have caused the observed changes in spawner abundance.

Changes in dam operations targeted at increasing incubation success are generally rationalized based on the belief that the dewatering of spawning habitat results in higher rates of incubation mortality that cannot be compensated by reduced density dependent mortality in latter life stages. Results from laboratory and in-situ studies have shown that the affects of dewatering on incubation mortality rates are not always severe, and depend on a number of factors including exposure period, life stage, sediment composition, and temperature (Becker et al. 1982, Rieser and White 1983). It is difficult to apply results from laboratory and in-situ dewatering studies to predict the effects of flow regimes at a meaningful population-scale. First, transferring results from laboratory studies to the field is problematic because differences in factors like moisture content of the egg pocket and ambient temperatures can have large effects on mortality rates. Second, variation in spawning location and timing will determine the proportion of redds vulnerable to dewatering which will control the overall mortality rate for the population. Finally, even if additional incubation mortality resulting from fluctuating flows is substantial, there may be little reduction in the abundance of the juvenile population due to compensatory density dependent mechanisms.

Recent changes in the flow regime at Glen Canyon Dam on the Colorado River provided a unique opportunity to better understand the effects of flow fluctuations on incubation success at a meaningful population scale. The first 26 km below Glen Canyon Dam is a clear and cold tailwater known as the Lee's Ferry reach, which supports a large self-sustaining population of rainbow trout and a nationally recognized trout fishery. In the early 1990's, daily fluctuations in flow from Glen Canyon Dam were reduced to limit fine sediment erosion in Grand Canyon, which begins at the downstream boundary of the Lee's Ferry reach. The flow change was also intended to improve the survival rate of

humpback chub (Gila cypha) in Grand Canyon, which was listed as endangered under the Endangered Species Act in 1973. Although the humpback chub population continued to decline after the flow regime change, the natural reproductive rate of the rainbow trout population in Lee's Ferry reach was enhanced, and within a decade, adult abundance had increased by 3-fold (McKinney et al. 2001). Rainbow trout in the upper reaches of Grand Canyon increased over 6-fold over a similar time period (S. Rogers, Arizona Game and Fish Department, unpublished data), and concerns about potential negative effects of high trout abundance on humpback chub led to a mechanical removal program of rainbow trout in Grand Canyon between 2002 and 2006. In addition, the flow regime from Glen Canyon Dam was experimentally altered in 2003 to 2005 with the intent of increasing the mortality rates on early life stages of rainbow trout.

The objective of this paper is to evaluate the effects of the experimental flow regime on early survival rates of trout in the Lee's Ferry reach. The study focuses on evaluating two central hypotheses concerning the effects of flow fluctuations on early life stages. First, the extent of flow-dependent incubation mortality will depend on intergravel temperatures that will in turn be determined by the timing and extent of dewatering and ambient air temperatures. We predict that incubation mortality in dewatered redds should be higher for cohorts spawned later in the year when air temperature is higher, and that mortality should be greater at higher spawning site elevations that are dewatered for longer periods. Second, we hypothesize that density dependent reductions in post-emergent mortality rates will not be sufficient to mitigate for flow-dependent incubation losses. As a result, we predict that the effects of increased flow fluctuations during experimental periods will be visible in backcalculated hatch date distributions and also reduce the abundance of the age-0 trout population.

Our study has a few very unique aspects and results are relevant to monitoring and instream flow assessments in other large regulated rivers. The limited number of investigations that have examined the consequences of flow regimes from hydroelectric dams on fish populations have always evaluated regimes targeted at improving population status (Travnichek et al. 1995, McKinney et al. 2001, Connor and Pflug 2004). In contrast, we evaluated a regime targeted specifically at reducing the survival rates of early life stages. This unusual situation provided good experimental contrasts and

113

opportunities for using informative sampling techniques. This study also describes some unique aspects of spawning dynamics of salmonids in a large regulated river, and some insights on the strength and timing of density dependence at early life stages in this environment.

5.2   Methods

We evaluate the effect of the flow regime from Glen Canyon Dam on spawning locations, incubating life stages (eggs and alevins), hatch date distributions, and the abundance of age-0 rainbow trout in the Lee's Ferry reach of the Colorado River, Arizona. We estimate the spatial and seasonal variation in spawning over four years based on frequent redd surveys and track the quality of incubation environments based on dewatering frequency and intergravel temperatures. We integrate these data, and results from previously published laboratory studies that define thermal mortality limits and development times, in a model that predicts flow-dependent incubation mortality for daily spawning cohorts across a range of elevations. Temporal and spatial predictions of mortality are compared to the observed frequency of egg mortality determined by redd excavations. Predictions of seasonal variation in flow-dependent mortality are evaluated using hatch date analysis. The combined effects of flow-dependent incubation mortality and egg deposition on the abundance of age-0 trout are examined using a stock-recruitment analysis.

Study Site and Flow Experiment

The Lee's Ferry reach of the Colorado River begins at Glen Canyon Dam and extends 26 km downstream to the confluence of the Paria River (Lat:36.86638, Long:-111.58638). The average discharge (USGS gage 09380000) in study years (2003, 2004, 2006, and 2007) was 334 $m^3 \cdot sec^{-1}$. The reach is wide and shallow, with an average wetted width and depth at this flow of 142 m and 5.2 m, respectively (Randle and Pemberton 1987). There are no significant tributary inputs to the reach and water quality is determined by the hypolimnetic release from Glen Canyon Dam, which is clear and cold. Water temperatures typically range from 9-12 ^oC with secchi depths of 6-7 m (Vernieu et al. 2005). The fish fauna in the Lee's Ferry reach is almost exclusively comprised of nonnative rainbow trout (McKinney et al. 2001). The majority of spawning activity

114

occurs between February and May. Air temperature is considerably warmer than water temperature during the latter part of the spawning period and incubation period, with normal daytime high temperatures increasing from 16 $^{\circ}$C in March to 32 $^{\circ}$C in June.

Discharge from Glen Canyon Dam fluctuates on a diurnal cycle that is driven by power demand but controlled through regulations on the maximum daily flow range, minimum and maximum flows, and hourly ramping rates. The extent of daily flow variation during winter and early spring was increased from the normal range of 283-510 m^3·sec^{-1} (January) and 198-368 m^3·sec^{-1} (February-March) to 142-566 m^3·sec^{-1} (January-March) in 2003-2005 to reduce the survival rate of the early life stages of rainbow trout (Fig. 5.1). The rationale was that higher flows during the day would promote spawning on high-elevation gravel bars that would subsequently be dewatered when flows were reduced during the night and weekend off-peak power demand periods.

Our evaluation of the effects of flow fluctuations is based on spatial, seasonal, and annual contrasts. We compare the predicted spatial and seasonal trend in incubation mortality from the flow-dependent model with direct observations of egg mortality determined from redd excavations. Assuming the seasonal pattern of flow-dependent incubation mortality is correct, hatch date distributions predicted by the flow-dependent incubation mortality model should provide a better fit to the backcalculated distributions based on catches of age-0 trout, relative to those from the flow-independent model, where hatch timing is solely determined by spawning and incubation timing. This prediction depends on the assumption that density dependence in mortality rate from fertilization to first capture by electrofishing for daily or weekly cohorts of fish is minimal, resulting in a linear relation between the number of fish from each cohort that survive to emerge and the resulting abundance of that cohort in the age-0 population. The flow-dependent prediction of the hatch date distribution should hold in experimental years (2003, 2004) when flow-dependent mortality is expected to be substantial. In the control years (2006, 2007), flow-dependent incubation mortality should be lower and we expect that both models would adequately predict the backcalculated hatch date distributions. Finally, if the overall post-emergent compensatory survival response to increased rates of flow-dependent incubation mortality is minimal, we would expect the abundance of age-0 trout

115

to be negatively correlated with the extent of incubation mortality and positively correlated with egg deposition.

Redd Counts and Intergravel Temperatures

Rainbow trout redds were enumerated at 27 spawning locations in the Lee's Ferry reach approximately every two weeks during the peak spawning period and once per month during non-peak periods. A total of six, 11, 11, and seven surveys were conducted in 2003, 2004, 2006 and 2007, respectively. Redd counts were conducted by traversing exposed and shallow (< 1m depth) cobble bars by foot, by surveying from the deck of a motorized boat over moderate depths (1-2 m), or by towing a clear-bottom kayak or underwater video camera beside a motorized boat over deeper spawning habitats. The combination of relatively shallow depth and clear water in the Lee's Ferry reach provides ideal conditions for conducting redd surveys; the vast majority of the river bottom can be seen from the surface because the secchi depth exceeds the average depth. Criteria used to define active redds included the presence of a pit which was characterized by a coarser grain size relative to sediments in the rest of the redd, a sorted finer deposit, often referred to as a tailspill, located downstream of the pit, appropriate grain sizes (5-50 mm) in the tailspill, and a lack of periphyton and large macro-benthic invertebrates which indicates recent disturbance.

The location and elevation of redds were determined by an electronic total station at three intensively monitored sites that in total, contained 40-50% of redds counted over the entire reach (Four Mile Bar, Powerline Bar, and Pumphouse Bar) in some years. Redd elevations were measured with a laser level and survey rod at the remaining 23 locations, or using a depth sounder at sites where surveys were conducted by boat. When measuring redd elevations, we placed the survey rod in the center of the redd pit, which was within a few cm of the elevation of the egg pocket as determined from redd excavations. Stage-discharge relationships were empirically developed for each site. The typical stage difference at elevations inundated by flows of 142 and 566 $m^3 \cdot sec^{-1}$ was 1.75 m and was relatively linear over this discharge range. Thus, a 100 $m^3 \cdot sec^{-1}$ change in discharge results in a 40 cm change in water surface elevation. The elevation of each redd was translated into the discharge required to inundate it. The proportion of redds created at different elevations, hereafter referred to as redd hypsometry, was summarized by

determining the proportion of redds within the following elevation classes: <142; 142-227; 227-340; 340-425; and 425-566 $m^3 \cdot sec^{-1}$. The discharge record from Glen Canyon Dam (www.gcmrc.gov/products/flow_data/) was used to determine the dewatering frequency for these elevation ranges.

Replicate lines of continuously recording temperature loggers were buried at two gravel bars located 2.5 and 18 km downstream of Glen Canyon Dam (Powerline and Four Mile Bars, respectively) to measure intergravel temperature. Loggers were buried at the observed egg pocket depth of 15 cm at elevations that correspond to the water surface at 113, 198, 283, 368, and 481 $m^3 \cdot sec^{-1}$ to represent intergravel temperatures in the <142, 142-227, 227-340, 340-425, and 425-566 $m^3 \cdot sec^{-1}$ redd hypsometry classes, respectively. Loggers recorded the average temperature over 15 minute intervals. We excavated 120 redds in 2004 between February and May at a range of elevations and examined them for the presence of live and dead eggs. These data were used to quantify seasonal and spatial trends in flow-dependent incubation mortality.

Spawn Timing Model and Estimation of Redd Survey Life

Discharge, redd dewatering frequency and timing, and air temperatures, which will control the extent of flow-dependent incubation mortality, are unlikely to be uniform over the incubation period. Thus, an understanding of spawn timing in relation to the temporal variation in incubation quality is required. The magnitude and timing of spawning was predicted by fitting a spawn timing model to the redd count data using Hilborn et al.'s (1999) maximum likelihood approach. The total number of redds present on each day ($\hat{r}_t$) was predicted from,

(1) $$\hat{r}_t = A_t - F_t \text{,}$$

where, A_t is the cumulative number of redds created up to and including day t, and F_t is the cumulative number of redds that have 'faded', that is, are no longer visible to an observer because they have lost their distinguishing characteristics. The timing and magnitude of spawn timing was modeled using a beta distribution,

(2) $$A_t \propto \chi \int_0^t \theta_t^{(\alpha-1)} (1-\theta_t)^{(\beta-1)} dt \text{,}$$

where, χ is the total number of redds created over the spawning season, α and β are parameters of the beta distribution, and θ_t represents the proportional day over the spawning season. The cumulative number of redds that have faded, that is, have exceeded their survey life is simply,

(3) $$F_t = A_{t-SL},$$

where, *SL* is redd survey life. The total number of redds created over the spawning season (*x*) and arrival model parameters (α, β) were fit to the redd count data (r_t) assuming that observation errors were Poisson distributed ($r_t \sim Poisson(\hat{r}_t)$). Most-likely parameter estimates (MLEs) were computed by minimizing the sum of negative log of probabilities returned by the Poisson model across all surveys in each year of study.

A spatial analysis of the redd survey data from intensive sites was used to estimate redd survey life using an Area-Under-the-Curve (AUC) approach which is commonly used to estimate total escapement from periodic count data. In our application, AUC is the area under a curve that plots the number of redds counted over time. The total number of redds created at a site (χ_i) over a defined period is the ratio of AUC_i to redd survey life. If χ_i is known, it is possible to estimate redd survey life by simply rearranging the AUC equation as follows,

(4) $$SL_i = \frac{AUC_i}{\chi_i}.$$

Assuming the average survey life across intensive sites is representative of the survey life over the entire reach, the average value can be substituted into equation 3 to estimate the parameters of the spawn timing model.

We computed AUC_i at each intensive site from redd count data, and used changes in the spatial locations of redds over time to estimate χ_i. This calculation could only be done at intensively monitored sites where redd locations were accurately determined by total station ($\pm$ 5 cm). Each site was divided into a grid of 1-m^2 cells using a geographic information system and the presence or absence of redds in each cell for each survey period was then computed. The number of cells which gained a redd between surveys was determined to provide a minimum estimate of the actual number of 'new' redds created (χ_i in equation 4). The number of cells which lost a redd between surveys, which

118

would occur because they exceeded their survey life, was used to compute the number of 'faded' redds. The number of cells with a redd present in two consecutive sampling periods was also computed and represents the number 'old' redds, that is, redds that had not yet exceeded their survey life between surveys. The combined total number of cells with 'new' and 'old' redds on any survey is equivalent to the number of that would be counted, and was used to compute the AUC in equation 4.

Flow-Dependent Incubation Mortality Model

We developed a model that integrated the effects of spawn timing, redd hypsometry, and intergravel temperatures to predict the relative incubation mortality caused by fluctuations in flow for daily spawning cohorts. A key assumption of the model is that intergravel temperatures, rather than redd dewatering frequency and duration, determines the impact of flow fluctuations on incubation mortality. This assumption is supported by laboratory and in-situ studies. Eggs dewatered in laboratory channels for up to 12 hours per day for as long as 4 weeks (steelhead trout) and 1-5 weeks (Chinook salmon) showed essentially no effect on hatching success, or on the development and growth rate of alevins and juveniles, provided the sediment moisture content was maintained at 4% or higher (Rieser and White 1983). Montgomery and Tinning (1993) found that periods of exposure of artificial rainbow trout redds in the Lee's Ferry reach to the air for up to 12 hours had no influence on hatching success, but that higher temperatures substantially reduced the exposure period required to cause substantive mortality.

The model consists of five components:

1. *Spawn Timing.* The spawn timing model (eqn. 2) is used to predict the number of redds created by day over a one year period (November 1 – October 31);

2. *Redd Hypsometry.* Redds created on each model day are distributed across five elevation bands (<142, 142-227, 227-340, 340-425, and 425-556 $m^3 \cdot sec^{-1}$) based on the observed redd hypsometry. Redds from each model day-elevation combination have unique intergravel temperature histories which determine incubation time and the extent of temperature-dependent mortality;

3. *Incubation Time.* The number of days from spawning to hatch and from hatch to emergence is determined based on the time required to exceed Accumulated Thermal

Unit (ATU) thresholds for hatching and emergence. ATU thresholds depend on the average daily temperature history at each spawning date-elevation combination. The thresholds are computed using the incubation models summarized by Jensen et al. (1992). At a constant temperature of 10 $^{\circ}$C, they correspond to 329 and 307 degree-days, or 33 and 31 days, respectively.

4. ***Temperature-Dependent Incubation Mortality.*** Daily maximum intergravel temperatures over egg and alevin incubation periods are compared to temperature-mortality thresholds. Redds created for each spawning day-elevation band are recorded as not producing viable young if the daily maximum temperature at any point in the projected incubation period exceeds the assumed lethal threshold.

5. ***Hatch Timing.*** The numbers of both viable and total redds are summed across elevation bands for each spawning day. Predictions are shifted from spawning date to hatch date based on the computed time from spawning to hatch for each model day-elevation strata.

The total flow-dependent mortality per year is computed as the ratio of non-viable to total redds. Note that predictions of mortality do not depend directly on dewatering. Instead, measured intergravel temperatures are used to integrate the combined effects of the duration and timing of dewatering and ambient air temperatures. Lower elevations will be dewatered for shorter periods than higher elevation, and due to the hourly timing of discharge fluctuations in the Lee's Ferry reach (Fig. 5.1a), lower elevations will be inundated earlier in the day when air temperatures are cooler. As a result, the intergravel temperatures at lower elevations will tend to be cooler relative to higher elevations, and incubation mortality resulting from flow fluctuations will therefore be lower. Note that in rare cases, lethal temperature thresholds could be exceeded at elevations that are not dewatered when air temperature is high, if reduced discharge increases warming near the waters edge to the point where intergravel temperatures exceed the threshold. Early in the season, elevations dewatered during periods when air temperatures are cooler may not exceed the temperature threshold.

The model was applied using redd count, hypsometry, and temperature data aggregated over the entire Lee's Ferry reach. The predicted hatch date distribution based on spawn and incubation timing alone (model components 1-3 only), hereafter referred to

120

as flow-independent mortality model, assumes that incubation mortality is constant across all cohorts regardless of spawning date or elevation. This is equivalent to the null model since it does not include the effects of flow fluctuations on incubation mortality rates. The hatch date distribution predicted from the combined spawn and incubation timing and incubation mortality models (model components 1-5), hereafter referred to as the flow-dependent mortality model, represents the distribution that results from temporal and spatial variation in incubation mortality driven by flow fluctuations.

We assume that eggs and alevins are equality sensitive to temperature and use a lethal temperature limit of 16 $^{\circ}$C for both life stages (Piper et al. 1986, Ford et al. 1995, Oliver and Fiddler 2001). Although this value is well established from previous experiments, all were based on constant temperature regimes. The effects of short-duration high temperature events are less certain and may be less severe. Thus, we performed a sensitivity analysis by rerunning the model using higher lethal thresholds for eggs and alevins of 18 and 20 $^{\circ}$C. We assume that alevins have limited mobility in the gravel and cannot adjust their position to maintain suitable temperatures. In the wild, alevins may be able to migrate deeper into the riverbed and may therefore be less sensitive to unsuitable temperatures measured at the egg pocket depth. However, if alevins have limited mobility, experimental studies suggest that they are more sensitive to higher temperatures and dewatering than eggs (Becker et al. 1982, Montgomery and Tinning 1993). We reran the model at a lower alevin mortality threshold of 14 $^{\circ}$C, and by turning off the alevin mortality component, to examine the sensitivity of model predictions to alternate assumptions about their sensitivity to higher temperatures and behavioural response to dewatering.

Backcalculated Hatch Date Distributions and Comparison with Predictions

Age-0 rainbow trout were sampled by backpack and boat electrofishing in low angle (cobble and vegetated sand bars and debris fans), and steep angle (talus) shorelines, respectively. A detailed description of the sampling design and methodology is provided in Chapter 4 and is briefly summarized here. A total of 20 sites in each habitat type of 30-50 m length were randomly selected from a spatial referenced shoreline habitat database for the Lee's Ferry reach (Mietz 2003). On average, 2.5% and 4.5% of all low and steep angle shorelines were sampled on each trip, respectively. Sampling effort was lowest in

2003 (n=4 surveys between June and October), highest in 2004 (n=8 surveys between April and December) and intermediate in 2006 and 2007 (n=5 surveys between June and November). Surveys were always conducted from midnight to dusk to coincide with the daily minimum discharge period to maximize catch rates (see Chapter 3). After electrofishing a site, fish were anesthetized using clove oil and fork lengths were measured to the nearest mm. The majority of fish were released back into the site. A subsample of 3-5 fish within 10 mm length categories between 20 and 100 mm were sacrificed and preserved in 95% ethanol for ageing by examination of otolith microstructure.

Hatch date distributions were determined by length backcalculation. We fit year-specific linear models predicting age from fork length using the otolith data under the assumption that error in age was log-normally distributed,

(5) $$Age = (b_0 + b_1 L)e^v$$

where, b_o and b_1 are the constant and slope of the linear regression predicting the mean age (Age) at fork length L, and v is a random normal deviate with mean 0 and standard deviation σ. Parameters were estimated using an iterative nonlinear search procedure. . The age of each fish in the catch samples for which otoliths were not collected (586, 4815, 1872, and 5311 age-0 trout in 2003, 2004, 2006, and 2007, respectively) was then determined from equation 5, accounting for the uncertainty in age estimates. To do this, 50 age estimates for each fish captured were drawn from a normal distribution defined by b_o, b_1 and the length of the fish, and variance σ^2. The hatch date for each random draw for each fish was then computed by subtracting its predicted age from the date of capture. To account for the cumulative mortality between hatch and date of capture, and length-dependent differences in vulnerability to electrofishing, each observation was multiplied (expanded) by the factor $[e^{-M \cdot Age} \cdot P_{Age}]^{-1}$, where M is the instantaneous daily mortality rate and P is the relative vulnerability of each age to sampling which depends on fish size and habitat type (Fig. 2.2a). Distributions were computed for M = 0, 0.005, 0.01, and 0.02. These values spanned the range of age-0 summer mortality rates estimated in Chapter 4 (0.009-0.014) as well as those reported for Atlantic salmon (Nislow et al. 2004: 0.01-0.02; Einum and Nislow 2005: 0.002-0.027), brown trout (Berg and Joregensen 1991: 0.007; Elliot 1994: 0.012), and rainbow trout (Hume and Parkinson 1988; 0.003-0.005).

Predicted and backcalculated hatch date distributions were aggregated to weekly intervals and compared based on the degree of correlation between weekly proportions, as determined from Pearson product moment correlation coefficients.

Response of Age-0 Abundance to Flow-Dependent Incubation Mortality

We evaluated the consequences of flow-dependent incubation mortality on age-0 abundance using a stock-recruitment approach, where the age-0 abundance in treatment and control years was plotted against the total number of redds created in each year. We fit a Beverton-Holt stock-recruitment model to these data assuming log-normal error in recruitment. We then compared the extent of the reduction in the effective spawning stock, predicted from the difference between the number of total redds and viable redds, in relation to the spawning stock required to achieve the carrying capacity for age-0 trout determined by the stock-recruitment curve. The estimate of the initial slope of the best-fit Beverton-Holt model was converted to a dimensionless Goodyear compensation ratio (Goodyear 1980) to compare with productivity estimates for other freshwater salmonid populations. The Goodyear ratio is computed by dividing the initial slope of the stock recruitment curve by the slope of the replacement line. The latter slope was computed by assuming the average of the total number of redds created in all years, except 2006, when there was very limited spawning, represents an equilibrium condition.

Age-0 trout population estimates for the Lee's Ferry reach during the July sampling period were used to index recruitment for the stock-recruit analysis. Methods for obtaining population estimates are described in Chapter 4 but are briefly summarized here. The catch of fish per meter at each of the 40 sample sites was stratified by 5 mm length intervals and expanded based on habitat-specific capture probabilities for each length-interval determined from mark-recapture experiments (Chapter 2). Size-specific population estimates were then summed to determine the total population density at each site. Finally, these densities were expanded based on the proportion of total shoreline length in the reach that was sampled by habitat type. These expanded estimates were summed across habitat types to determine reach-wide population estimates.

5.3 Results

Flow and Temperature

The extent of daily fluctuations from January to March during experimental years (2003 and 2004) of 142-566 $m^3 \cdot sec^{-1}$ was considerably greater than the daily range under normal operations (2006, 2007). The maximum flow on Sundays, which occurred during the day and early evening (Fig. 5.1a), was low (283 $m^3 \cdot sec^{-1}$) in January in both experimental years (Fig. 5.1b). However, in February and March, the maximum flow on Sunday was high in 2003 and low in 2004, which, as we show later, resulted in a substantive difference in incubation mortality among years. Discharge in non-experimental months (April – July) was generally similar among years with the exception of lower Sunday maximum flows in 2003. Elevations inundated by flows of 227 and 340 $m^3 \cdot sec^{-1}$ were dewatered for 7-9 and 9-11 hours per day between January and March during weekdays in experimental years, respectively (Table 5.1). Lower maximum flows on Sundays in February and March 2004, resulted in much higher dewatering periods compared to other days of the week. Dewatering periods between January and March in 2006 and 2007 were much reduced compared to experimental years at an elevation inundated by 227 $m^3 \cdot sec^{-1}$. Elevations greater than 340 $m^3 \cdot sec^{-1}$ were dewatered for at least 30 consecutive days after March 31st in experimental years.

As expected, intergravel temperatures increased with the extent of dewatering and ambient air temperatures. For brevity we show data collected at Four Mile Bar in 2003 and 2004 only to illustrate critical aspects of temperature dynamics that determine incubation mortality (Fig. 5.2). Intergravel temperatures within elevation bands increased over the spring with the rise in air temperature. Temperatures at elevations above 227 $m^3 \cdot sec^{-1}$ first exceeded the upper lethal limit of 16 ^{o}C within the first two weeks of March (March 10th 2003; March 14th, 2004; March 4th 2006; and March 10th, 2007). Implementation of lower flows during the day on Sunday, and the timing of the flow increase in the morning during the weekdays, had a noticeable influence on intergravel temperatures. A weekly pattern in maximum temperatures in February and March in 2004, at elevations > 142 $m^3 \cdot sec^{-1}$ (Fig. 5.2) occurred because the low daytime Sunday flow (Fig. 5.1) substantially increased dewatering periods during the day relative to weekday operations (Table 5.1). The earliest date that the maximum thermal limit was

124

exceeded in 2004 would have occurred almost a month later had Sunday daytime flows been maintained at the weekday level. The time of the diurnal increase in discharge was an important determinant of the date when the maximum temperature limit was first exceeded in 2003. The increase in discharge at Glen Canyon Dam under normal operations begins between 5:00 and 6:00 a.m. (Fig. 5.1a), but in January through March 2003, discharge was not increased until 9:00 a.m. The 3-hour travel time of the discharge wave between Glen Canyon Dam and Four Mile Bar, located 18 km downstream, delayed the morning stage increase until about noon. As a result, intergravel daily maximum temperatures at elevations > 142 $m^3 \cdot sec^{-1}$ at Four Mile Bar during the week were much warmer in February in 2003 compared to 2004 (Fig. 5.2).

Spawn Timing and Redd Hypsometry

The peak count of redds summed across 27 sites in 2003, 2004, 2006, and 2007 was 757 (March 10th), 962 (March 28th), 35 (April 23rd), and 399 (April 8th), respectively. Estimates of redd survey life (Table 5.2) averaged 3.7 weeks across sites. The number of cells with redds represented 96-98% of the number of redds actually counted, indicating that there were very few cases when there was more than one redd located in the same grid cell on the same survey. We used an average survey life of 4 weeks in the spawn timing model. Estimates of the total number of redds created and peak spawn dates from the spawn timing model were 3,264 (March 20th), 2,310 (March 6th), 88 (March 27th), and 1,215 (March 13th) respectively. The spawn timing model generally provided very good fits to the redd count data, explaining 81, 87, 68, and 91% of the variability in counts over the spawning season in 2003, 2004, 2006, and 2007, respectively (Fig. 5.3).

The distribution of redds across elevations (Fig. 5.4) was determined by the interaction between flow regime and spawn timing, as well as flow-independent factors. Spawning at elevations >340 $m^3 \cdot sec^{-1}$ only occurred between January and March during experimental years when flows were high. There was generally very little spawning above 227 $m^3 \cdot sec^{-1}$ in normal operating years (2006, 2007) when flows were lower during this period. During experimental years, high maximum flows (Fig. 5.1b) coincided with periods of considerable spawning activity (Fig. 5.3), resulting in a relatively large proportion of redds being created at elevations > 227 $m^3 \cdot sec^{-1}$. In experimental years, spawners were able to construct redds and deposit eggs in high elevation habitats despite

the fact that they were dewatered for at least 9 (227 m^3·sec^{-1}) to 11 (340 m^3·sec^{-1}) hours per day (Table 5.1). The percentage of fish spawning at lower elevations increased between January and March in all years despite relatively high flows over this period. As flows over these months were relatively consistent within years, the seasonal pattern in redd hypsometry was driven by factors other than flow. High flows are necessary to allow fish to spawn at higher elevations, but they do not appear to completely inhibit spawning at lower elevations.

Predictions and Observations of Flow-Dependent Incubation Mortality

The incubation mortality model predicted that 24%, 50%, 5%, and 11% of the total number of redds created in 2003, 2004, 2006, and 2007 did not produce viable larvae due to fluctuations in flow, respectively (Table 5.3). The model predicted negligible mortality due to fluctuating flows in control years 2006 and 2007, because almost all spawning was restricted to elevations below 227 m^3·sec^{-1} where intergravel temperatures rarely exceeded lethal limits (Fig. 5.4). In experimental years 2003 and 2004, there was little predicted mortality for the progeny of the few fish that spawned before mid-January, as they were predicted to emerge by approximately mid-March before intergravel temperatures exceeded the lethal limit (Fig. 5.5). As there was little spawning at elevations > 227 m^3·sec^{-1} after March 31st, flow-dependent mortality predominantly affected cohorts that were fertilized between mid-January and March 31st. All predicted mortality in 2003 occurred at elevations greater than 227 m^3·sec^{-1}. Predicted mortality was higher in 2004 (Fig. 5.5) because a slightly larger proportion of spawning occurred during the experimental period when flows were higher (Fig. 5.3), resulting in a greater number of redds being created at higher elevations where mortality was predicted to occur. In addition, the model predicted that there was almost total mortality in the 142-227 m^3·sec^{-1} elevation band in 2004, because of a delay in the time of the morning discharge increase on Sunday, March 21st, which resulted in intergravel temperatures exceeding the lethal threshold.

Flow-dependent incubation mortality predictions were relatively insensitive to assumptions about maximum lethal temperature limits. Mortality rates did not change as the lethal limit for eggs and alevins was increased from 16 to 20 ^{o}C in 2007, decreased by less than 3% in 2003 and 2006, and by 8% in 2004 (Table 5.3). The model was relatively

insensitive to changes in lethal limits because the increase in intergravel temperatures due to flow fluctuations was very rapid as ambient air temperatures rose in March. Intergravel temperatures exceeded 20 ^{o}C only about two weeks later than the date when 16 ^{o}C was first exceeded (Fig. 5.2). Given a minimum incubation time predicted by the model of approximately 60-70 days, the delay associated with the higher lethal limit would only have eliminated flow-dependent incubation mortality for cohorts fertilized in the last two weeks of January. As only a small proportion of the total number of redds were created over this time period (Fig. 5.3), and approximately 50% of these were at lower elevations not vulnerable to flow-dependent mortality (Fig. 5.4a), there was little effect of increases in the lethal limit on the overall mortality rate. Reducing the lethal limit for alevins from 16 to 14 ^{o}C resulted in no change in predicted mortality rates in all years. Eliminating the effects of flow on incubation mortality to simulate the case where alevins are mobile and can avoid unsuitable conditions reduced incubation mortality rates by 6% in 2003, and by only 2% or less in other years. The model was insensitive to changes in the alevin lethal temperature threshold because it predicted that most embryos die before they hatch.

General trends in predicted incubation mortality agreed with trends in mortality determined by directly examining the viability of embryos in a subsample of redds in 2004. Out of a total of 125 randomly selected redds that were excavated, 80 contained eggs (Table 5.4). Inferences from redds without eggs are difficult to make as they could indicate that fry had already emerged, that complete mortality and decomposition of eggs or alevins had already occurred, failure to find the egg pocket, or the presence of a test pit. When egg pockets were found, they almost always consisted entirely of either healthy looking eggs that were clear with a visible embryo, or dead eggs, which were easy to identify because they were opaque. Limiting the analysis to the 80 redds that contained eggs from which more defensible inferences can be made, 30% were classified as non-viable. The percentage of non-viable redds increased progressively with elevation and was four-fold higher in April and May than in February and March. We suspect that the actual egg and alevin mortality rate in April and May was higher than the data suggests as many of the redds without eggs had a strong ammonia odor indicative of recent decomposition. These results were consistent with general trends predicted from the incubation mortality model in 2003 and 2004, with showed much greater mortality

127

after March 31st (Fig. 5.5) and total mortality at higher elevations (100% mortality at elevations >227 m^3·sec^{-1}).

Comparison of Predicted and Backcalculated Hatch Date Distributions and Effects of Flow-Dependent Incubation Mortality on Age-0 Abundance

The hatch date distributions predicted by the flow-dependent incubation mortality model generally had similar shapes to those predicted by flow-independent model (Fig. 5.5). In experimental years, flow-dependent incubation mortality tended to flatten the peak in the hatch date distribution relative to the flow–independent prediction. However, even in these years, 98% (2003) and 88% (2004) of the variation in the flow-dependent model of hatch timing could be explained by the flow-independent model based on predictions from all 52 weeks, and 92% (2003) and 72% (2004) based on predictions from only 17 weeks between March and June when the majority of hatching occurred (Table 5.5). There was a lower correlation between predicted flow-independent and – dependent models in 2004 when the overall flow-dependent mortality rate was higher. Because predictions of flow-dependent mortality were negligible in control years, the correspondence in predicted hatch timing between flow-dependent and –independent models was almost perfect.

Effects of flow-dependent incubation mortality were not readily apparent in backcalculated hatch date distributions (Fig. 5.5). Both flow-dependent and –independent models explained substantial and almost identical amounts of variation in backcalculated hatch date distributions (Table 5.5). In 2004, when the total flow-dependent mortality was highest, the flow-dependent model did better at predicting the backcalculated distribution between March and April when flow-dependent mortality was highest (Fig. 5.5). However, this resulted in an overprediction in the proportion of fish hatching in May. Both models underpredicted the strength of the hatch in January and February in 2004. The shape of the predicted and backcalculated distributions were very similar in 2003 and 2006. The backcalculated hatch date distributions lagged the predicted ones by about 3 weeks in 2007. This discrepancy was due to higher mortality of early life stages for cohorts spawned before April 1st (see results from Chapter 6). Backcalculated hatch date distributions were relatively insensitive to the assumed instantaneous mortality rate (Fig. 5.6). For example, the date at which 50% of the fish had hatched declined by only

128

one week when the mortality rate was increased from 0 to 0.01 in 2004 and in other years (not shown for brevity).

The abundance of age-0 rainbow trout in the Lee's Ferry reach was resilient to changes in spawning stock size, as indexed by either the estimated total number of redds created, or the number of viable redds (Fig. 5.7). The fit of the Beverton-Holt models to these data suggests that survival rates from egg deposition to approximately two months from hatch (as indexed by abundance of age-0 trout in July) were strongly density dependent. However, this prediction is uncertain due to limited sample size. Flow-dependent incubation mortality in 2003 and 2004 was predicted to result in the loss of 769 and 1067 redds. While these losses were substantial, the preliminary stock-recruitment relationship suggests they were not sufficient to reduce the number of viable redds to the point where the age-0 population would decline. The estimate of the Goodyear compensation ratio for the Lee's Ferry reach rainbow trout population was 25.

5.4   Discussion

Increased hourly fluctuations in flow from Glen Canyon dam in 2003 and 2004 resulted in substantial incubation mortality for rainbow trout, but effects were not apparent in the age-0 population due to potentially strong compensation in mortality rates between fertilization and approximately two months from hatch. Model predictions were consistent with general trends in the frequency of incubation mortality from redd excavations, which showed greater morality at higher elevations and later in the incubation period when intergravel temperatures were higher. Patterns of flow-dependent incubation losses were also consistent with mortality rates measured in laboratory studies at equivalent dewatering rates, but only under some circumstances. Reiser and White (1983) found that periods of exposure of 15 hours resulted in complete mortality of Chinook salmon eggs, but that mortality was negligible when the dewatering period was 12 hours per day. The former result is consistent with our observation of 100% mortality for eggs located above elevations inundated by 227 $m^3 \cdot sec^{-1}$ in April 2004, after they had been dewatered for 20 hours per day each Sunday in March. However, 100% of the redds excavated in May were not viable even though they had been dewatered for only 7 hours

per day during their egg incubation period in April. This highlights that substantial incubation mortality can occur at dewatering periods lower than those shown to be lethal in laboratory studies due to elevated intergravel temperatures in the field. Given the consistency of flow-dependent incubation mortality predictions with the results from the redd excavation study and the literature where appropriate, there is strong support for our first hypothesis that incubation mortality rates will depend on flow fluctuations that in turn determine where and when intergravel temperatures exceed lethal limits.

Results from the stock-recruitment analysis did not support our second hypothesis that the extent of a compensatory post-emergent survival response is weak and not sufficient to mitigate for flow-dependent incubation losses. The number of redds created in 2006, almost all of which were predicted to be unaffected by flow fluctuations, was at least an order of magnitude lower than the number of viable redds produced in other years. Yet in spite of this large decline in viable egg deposition, the age-0 population declined to only about ½ of the abundance estimated in other years. Such compensation appears to have been more than sufficient to mitigate for incubation losses resulting from flow fluctuations in experimental years, and explains the poor correlation between the number of viable redds and age-0 abundance. Strong density dependence in early survival rates is also supported by differences in predicted and backcalculated hatch date distributions. In 2006, when the viable number of redds was very low, predicted and backcalculated hatch date distributions were virtually identical. In other years, there were substantive differences in the distributions, which may have been caused by density dependent differences in early survival rates among weekly spawning cohorts.

We are uncertain as to whether the strength of compensation estimated in this study, which is based on a sample size of only four years and a single observation at low stock size, is representative of the true productivity of the Lee's Ferry population. Additional observations at low stock size are required to reduce this uncertainty. Very strong compensation early in the life history of salmonids is certainly plausible, and both the strength and timing of compensatory survival responses that were observed in this study are consistent with what has been documented for other salmonid populations. The preliminary estimate for the Goodyear compensation ratio for the Lee's Ferry reach rainbow trout population of 25, while admittedly highly uncertain because of the limited

130

sample size and uncertainty about the equilibrium spawning stock size, is virtually the same as the expected value for salmonids from Myers et al. (1999) meta-analysis of 25.1 (106 populations) and within the range they reported for freshwater salmonids (six populations) of 24.1-27.1. The strong compensation observed in this study occurred within a few months from emergence. This is consistent with Elliot's (1986, 1994) work, that conclusively demonstrated that the majority of density dependent mortality in a small brown trout (Salmo trutta) population occurred when fry first emerge from their incubation environments and compete for limited feeding territories. Other studies have also documented strong density dependent survival in the first few months from emergence, but like Elliot's, all have been conducted in very small and unregulated streams (e.g., Nislow et al. 2004, Einum and Nislow 2005). More stock-recruitment observations from the rainbow trout population in the Lee's Ferry reach are required to determine if the strength and timing of compensation observed in smaller systems apply in a large regulated river setting as suggested here.

There was little information in the hatch date analysis about the effects of flow-dependent incubation mortality. The shapes of the predicted hatch date distributions from flow-dependent and –independent models were generally very similar, even in years with substantive flow-dependent incubation mortality (Fig. 5.5, Table 5.5). The similarity in predictions among alternate models was not anticipated, and occurred because the proportion of spawning at lower elevations, that are relatively invulnerable to effects of flow fluctuations, increased as the spawning season progressed (Fig. 5.4a). This dynamic mitigated the effects of increasing impacts in dewatered areas resulting from higher air temperature. In 2004, when differences in predicted distributions were greatest (Fig. 5.5), the flow-dependent hatch date prediction was flatter than the flow-independent one due to the timing of mortality, but the amount of variation in the backcalculated distribution explained by both models was similar. The flow-dependent model provided a better fit to the backcalculated distribution in March and April, but substantially overpredicted the proportion of fish hatching in May. Discrepancies between predicted and backcalculated hatch date distributions could have been caused by differences in the magnitude of compensatory survival rates among daily or weekly cohorts of fish, as well as by biases in the backcalculated distributions that are discussed below.

Conclusions from the hatch date analysis depend in large part on the validity of assumptions of the flow-independent and –dependent incubation mortality models. The spawn-timing model, which is common to both incubation mortality models, assumes that seasonal variation in spawning activity can be well approximated by a beta distribution, and does not include effects of process error in spawn timing predictions. Uncertainties in predictions of relative mortality from the flow-dependent incubation model, which would be caused by errors in the hypsometry and intergravel temperature data and the dynamics of temperature-dependent mortality, were also not included. Redd hypsometry and intergravel water temperatures were well determined from extensive data collection although minor interpolation and measurement errors are likely. While lethal temperature limits for egg and alevin stages of rainbow trout have been well determined through multiple studies, few have explicitly tried to describe the effects of both duration and magnitude of exposure to warm temperatures. However, in-situ studies in the Lee's Ferry reach (Montgomery and Tinning 1993) showed that an exposure period of only 6 hours reduced alevin survival rates by 50% and that morality rates from exposure periods as low as 3 hours could be as high as 60% if temperatures exceeded 11 $^{\circ}$C. We have assumed that there is total mortality if the average temperature over 15 minutes exceeds 16 $^{\circ}$C. It is possible that periods of moderately high temperatures shorter than 3 hours result in little mortality. We examined the hourly intergravel temperature histories and found that by late March, lethal temperatures were typically exceeded for 5-10 consecutive hours, and by April, such events generally occurred on a daily basis. As incubation time is approximately 60-70 days, errors associated with overestimating the impacts of brief high temperature events would at most only affect the small proportion of larvae that were fertilized before February (Fig. 5.3) and therefore have only a minor impact on our estimates. In addition, the model was not sensitive to the assumed lethal temperature limit within reasonable ranges (Table 5.3) due to the rapid rise in intergravel temperatures over the period when the majority of incubation occurs.

The hatch date analysis depends on the assumption that the backcalculated hatch date distributions are unbiased or stable. Instability in hatch date distributions is likely when all samples are collected over a short period relative to the duration of the hatch period and there is a large difference in the cumulative mortality for fish of different ages

132

in the sample. Campana and Jones (1992) proposed two sampling solutions to this problem: 1) take a single sample after mortality rates among ages have stabilized; or 2) take multiple samples through time over a period that is at least as long as the time over which the hatch occurs. The first alternative was not feasible in our study because we do not know the age at which mortality rates stabilize, and even if we did, it may well be greater than the age at which reliable age determinations can be made from counts of daily otolith increments. We adopted approach 2), sampling age-0 fish multiple times over a 6 to 9 month period that was considerably longer than the 4 month period when the vast majority of spawning occurred. Given this strategy, it is not surprising that the hatch date distributions were relatively stable under a range of instantaneous mortality rates (Fig. 5.6). However, relative to backcalculated distributions, predicted hatch date distributions substantially underestimated the proportion of fish hatching in January-February in 2004, and overestimated and underestimated the proportion hatching in March and May-June in 2007, respectively (Fig. 5.5). We feel it is unlikely that this occurred because of errors in redd counts, because our surveys were thorough, conditions for counting redds in the Lee's Ferry reach are ideal, and there was very good correspondence between predicted and backcalculated hatch date distributions in 2003 and 2006. When backcalculating the hatch date distributions, we assumed that survival and growth of weekly cohorts that emerged from the gravel were independent of hatch date. The latter assumption is supported by the otolith data (Chapter 4). Thus, we conclude that discrepancies between predicted and observed hatch date distributions in 2004 and 2007 were likely driven by seasonal variation in age-0 mortality rates, such as those documented for age-0 Atlantic salmon from experimental manipulations (Letcher et al. 2004, Einum and Nislow 2005). We evaluate evidence for this hypothesis by applying a stock synthesis model to the same data used in this analysis in Chapter 6.

In the process of developing models to predict spawn timing and flow-dependent mortality, we made some unique observations of the spawning biology of rainbow trout in a large regulated river. Substantial spawning was observed over a 3-month period from mid-February to mid-May, and some spawning was observed in every month between November and June. This is a highly protracted spawning period for rainbow trout, perhaps one of the longest ever documented for a single population. We speculate this

unusual timing is caused by both environmental and genetic factors. Emergence timing is controlled by stabilizing selective processes (Einum and Fleming 2000, Letcher et al. 2004). In natural systems, salmonids that emerge too early face unfavorable conditions associated with the freshet, while late emerging fish will be less competitive with larger cohorts that emerged earlier, and will have a shorter growing period prior to winter. Flow regulation, which has removed spring freshets, and stabilized temperature and food availability in the Lee's Ferry reach, has likely reduced the strength of these selective pressures, leading to expression of phenotypes that would not normally survive under natural conditions. The Lee's Ferry reach was stocked with rainbow trout from the late 1960's through the 1990's with spring-spawning Kamloops trout and the Bel-Aire hatchery strain whose spawn timing has been altered through selective breeding to occur in the fall. It is probable that the current population is a mixture of at least these two strains, thereby providing the broad genetic basis to support its highly protracted spawn timing.

Our results point to the need to rigorously assess instream flow decisions using both biological- and habitat-based methods. Redd dewatering is an obvious thing to casually observe, and in some cases, can appear to be quite extensive (e.g. Fig. 5.4b). However, these observations can be misleading if the system-wide hypsometry of spawning habitat use is not considered. In the Lee's Ferry reach, many redds were dewatered in experimental years. However, the majority of redds were below the minimum daily flow elevation (Fig. 5.4a) and therefore not vulnerable to dewatering. We commonly observed spawning at depths of 2 m at minimum daily flows, and at a few sites, observed redds and fish exhibiting spawning behaviours at depths averaging 4 m in the center of the channel. To our knowledge, extensive deep-water spawning in riverine salmonid populations has only been reported for Chinook salmon (Chapman et al. 1986, McMichael et al. 2005) and would be considered unusual for rainbow trout, especially for spawners that range from 30-45 cm in length. In large regulated rivers, where the freshet is much reduced, we suspect that redd surveys will underestimate the extent of deep water spawning if they are designed based on the paradigm that fish only spawn in shallow habitats. This bias will result in an overestimate of the proportion of redds vulnerable to the effects of flow fluctuations. More importantly, even if representative

spawning surveys are conducted, assessments need to measure the net effects of flow fluctuations by sampling the juvenile population. Strong density dependent compensation in post-emergent survival rates has considerable potential to mitigate for losses incurred during the incubation period due to flow fluctuations and other anthropogenic or naturally-occurring disturbances.

Table 5.1. Average dewatering duration (hours per day) for elevations that would be inundated at flows of 227 and 340 $m^3 \cdot sec^{-1}$, by year and month. Note that experimental flows were implemented in February and March in 2003 and 2004.

	Feb	Mar	Apr	May	Jun
227 $m^3 \cdot sec^{-1}$			Weekday		
2003	9	9	5	4	0
2004	7	7	5	6	0
2006	0	6	5	6	0
2007	0	5	5	6	0
			Sunday		
2003	9	9	18	12	0
2004	13	20	7	9	0
2006	0	6	6	7	0
2007	0	6	6	7	0
340 $m^3 \cdot sec^{-1}$			Weekday		
2003	11	11	13	11	7
2004	9	9	11	18	8
2006	6	19	17	22	8
2007	15	21	16	17	7
			Sunday		
2003	11	11	24	24	24
2004	21	24	24	24	10
2006	9	22	22	24	12
2007	20	23	23	24	12

Table 5.2. Statistics used to compute redd survey life at intensively monitored sites (FM, PL, and PH = Four Mile, Pumphouse, and Powerline Bars, respectively) in 2004. Survey life (weeks) is calculated based on the ratio of AUC (area under the curve) to the number of 1 m² cells with new redds (see equation 4). Numbers in parentheses are the actual number of redds counted (shown in parentheses). See text for more details of survey life computations.

Site	Old Redds	Faded Redds	New Redds	Redds Present	AUC (redd-wks)	Survey Life (wks)
FM	183	745	625	808 (835)	2180	3.5
PL	103	245	194	297 (311)	816	4.2
PH	19	78	70	89 (93)	233	3.3

Table 5.3. Predicted flow-dependent incubation mortality rates (non-viable redds/total redds in %) under different assumptions about the maximum lethal temperature limit for eggs and alevins by year. A lethal limit of 16 °C for both eggs and alevins was the default assumption used in most analyses.

	Lethal Temperature Limit (°C)				
Eggs	**16**	**18**	**20**	**16**	**16**
Alevins	**16**	**18**	**20**	**14**	**none**
2003	24	23	21	24	18
2004	50	45	42	50	48
2006	5	4	2	5	3
2007	11	11	11	11	11

Table 5.4. Statistics from the redd excavation study in 2004 showing the total number excavated, the number where eggs were found, and the percentage of redds with only dead eggs. Results are stratified by two-month periods and discharge levels that would inundate the redds that were excavated.

Inundation Discharge ($m^3 \cdot sec^{-1}$)	Feb - Mar	Apr - May	Total
Redds Excavated			
<227	27	8	35
227-340	46	12	58
340-566	32	0	32
Total	105	20	125
Redds with eggs			
<227	15	5	20
227-340	33	4	37
340-566	23		23
Total	71	9	80
% Redds with only dead eggs			
<227	13	60	25
227-340	24	100	32
340-566	30		30
Average	24	78	30

Table 5.5. Correlations (r^2) between predicted hatch date distributions based on flow-independent (H_0) and – dependent (H_1) models, and between predicted and backcalculated (B) hatch date distributions. Correlations were computed based on all 52 weeks of predictions for each year, as well as a subset of only 17 weeks between March and June when the majority of hatching occurs.

	H_o vs H_1	H_o vs B	H_1 vs B
All 52 weeks			
2003	0.98	0.94	0.93
2004	0.88	0.87	0.88
2006	1.00	0.95	0.96
2007	1.00	0.86	0.87
17 Weeks only (March-June)			
2003	0.92	0.85	0.83
2004	0.72	0.78	0.77
2006	0.98	0.87	0.91
2007	1.00	0.47	0.48
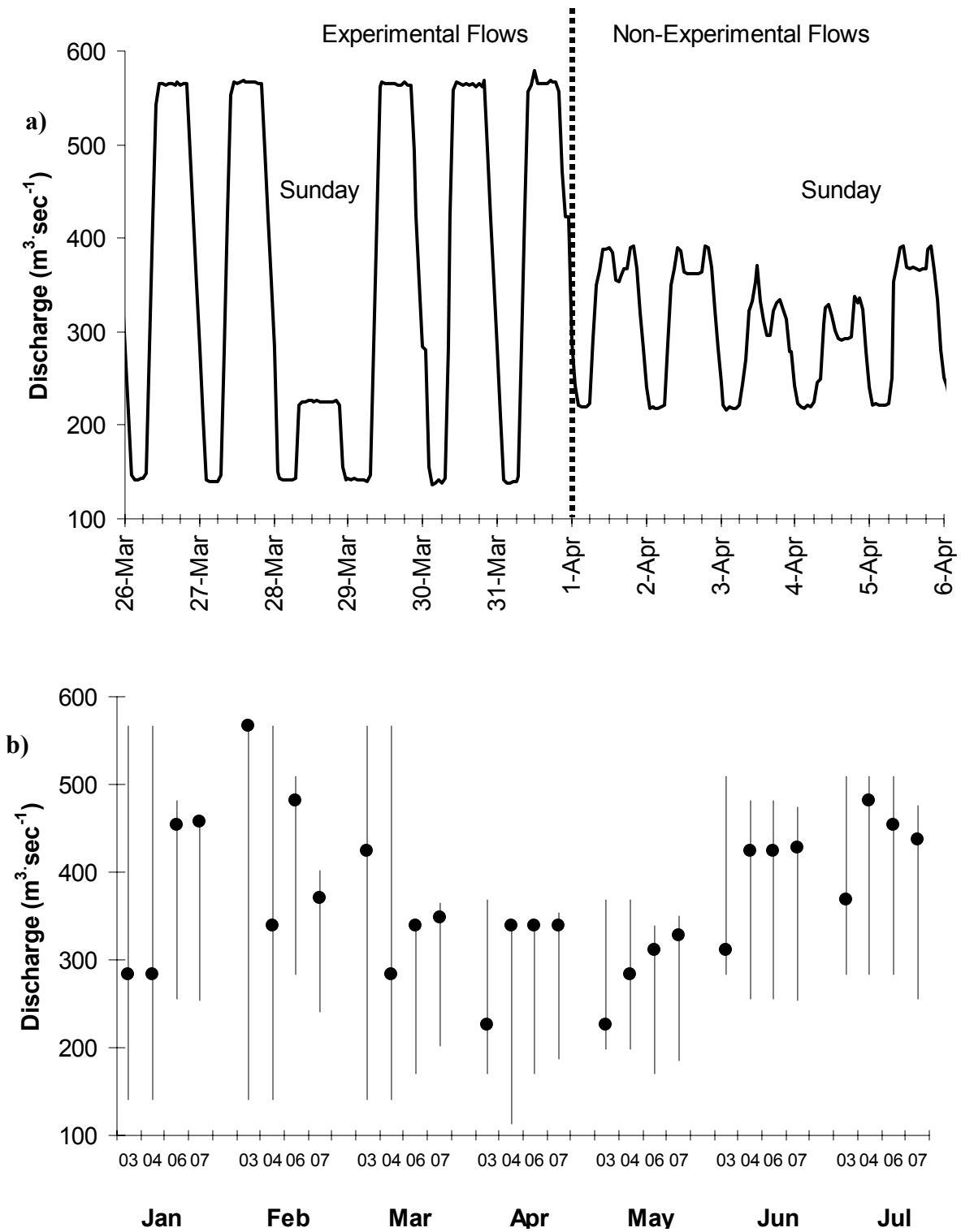
Figure 5.1. Discharge from Glen Canyon Dam over 11 days spanning the transition from experimental (January-March) to non-experimental flows in 2004 (a), and average daily minimum and maximum flows during weekdays (vertical lines) and the average daily maximum flow on Sunday (points) over the study period in experimental (2003, 2004) and control (2006, 2007) years (b).
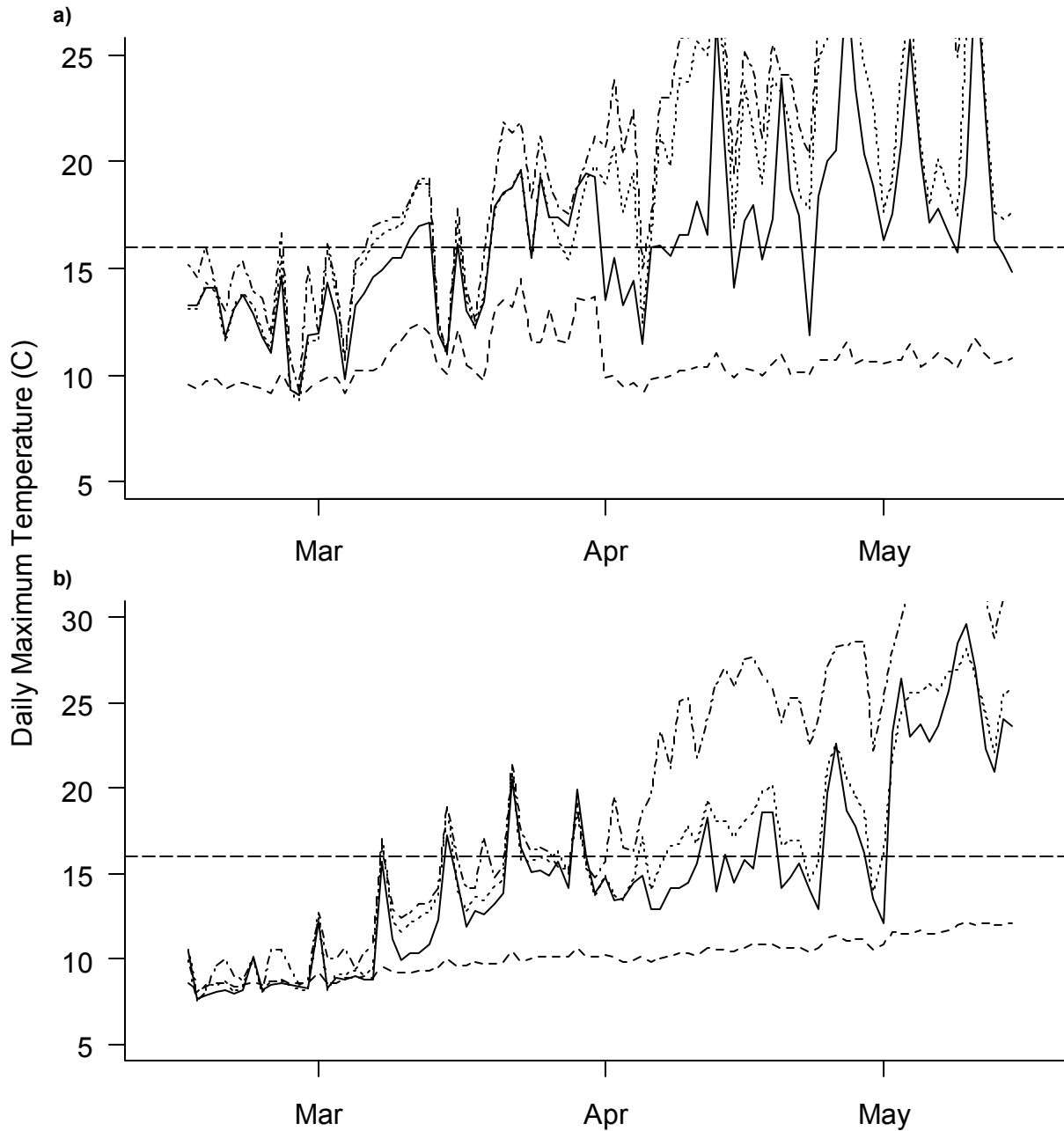
Figure 5.2. Daily maximum intergravel temperatures at Four Mile Bar in the Lee's Ferry reach over the majority of the spawning and incubation period in 2003 (a) and 2004 (b). Temperatures were recorded at elevations inundated by flows of 113, 227, 283, 368, and 481 $m^3 \cdot sec^{-1}$, and represent intergravel temperatures in the <142 (dashed line), 142-227 (solid line), 227-340 (dotted line), and 425-566 (dotted-dashed line) $m^3 \cdot sec^{-1}$ redd hypsometry classes, respectively. For clarity, temperatures at 368 $m^3 \cdot sec^{-1}$ (the 340-425 $m^3 \cdot sec^{-1}$ class) are not shown. The dashed horizontal line denotes a 16 °C lethal temperature limit.
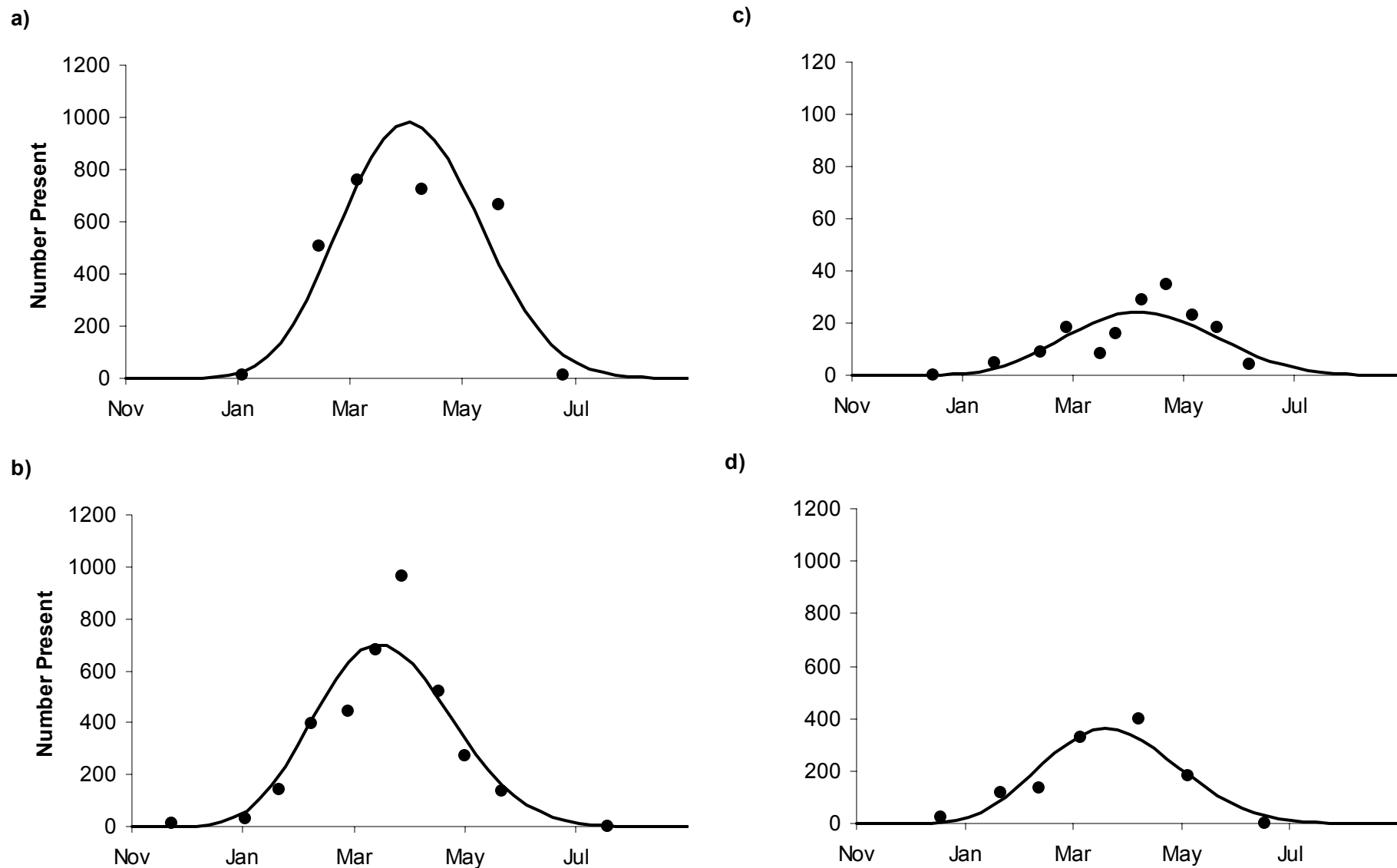
Figure 5.3. The total number of redds counted on each survey date (circles) and the number predicted to be present from the spawn-timing model (lines) assuming a redd survey life of 4 weeks in 2003 (a), 2004 (b), 2006 (c), and 2007 (d).

a)
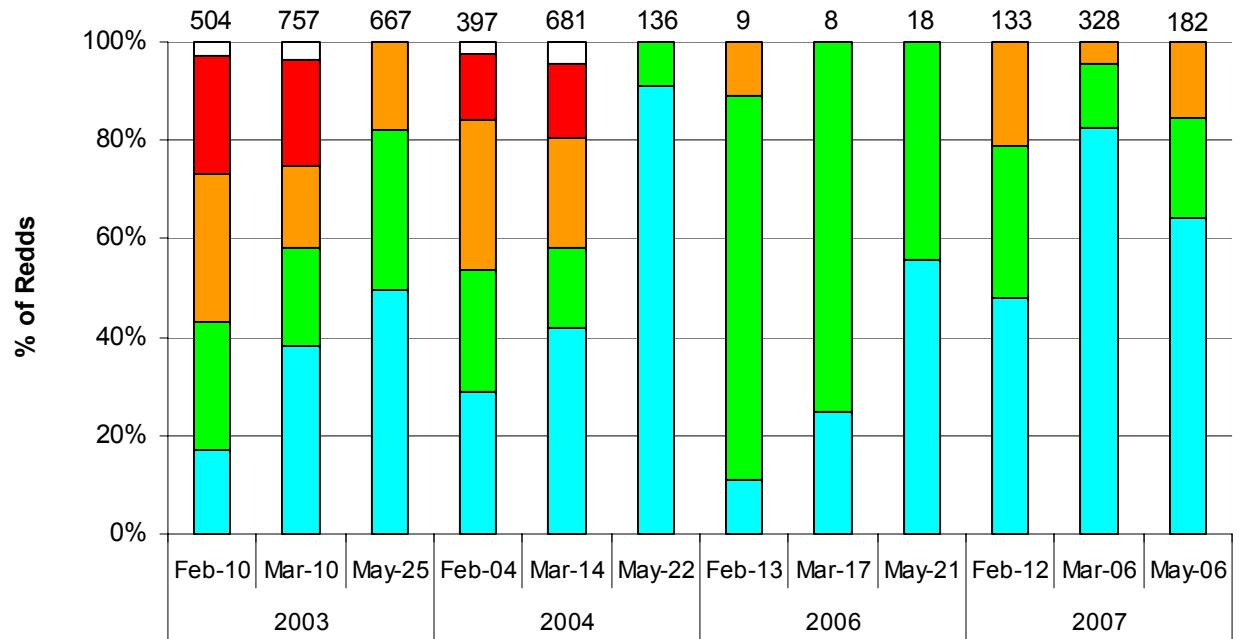
Figure 5.4. The distribution of redds across elevations inundated by flows <142 (blue), 142-227 (green), 227-340 (orange), 340-425 (red), and 425-566 (white) $m^3 \cdot sec^{-1}$ between February and April in the Lee's Ferry reach (a). The total number of redds counted on each survey are shown at the top of the bars. As an example of the data used to derive redd hypsometry, b) shows the elevations of redds inundated by the same discharges categories at Four Mile Bar over all survey periods in 2003.

b)

Figure 5.4. Con't.

144
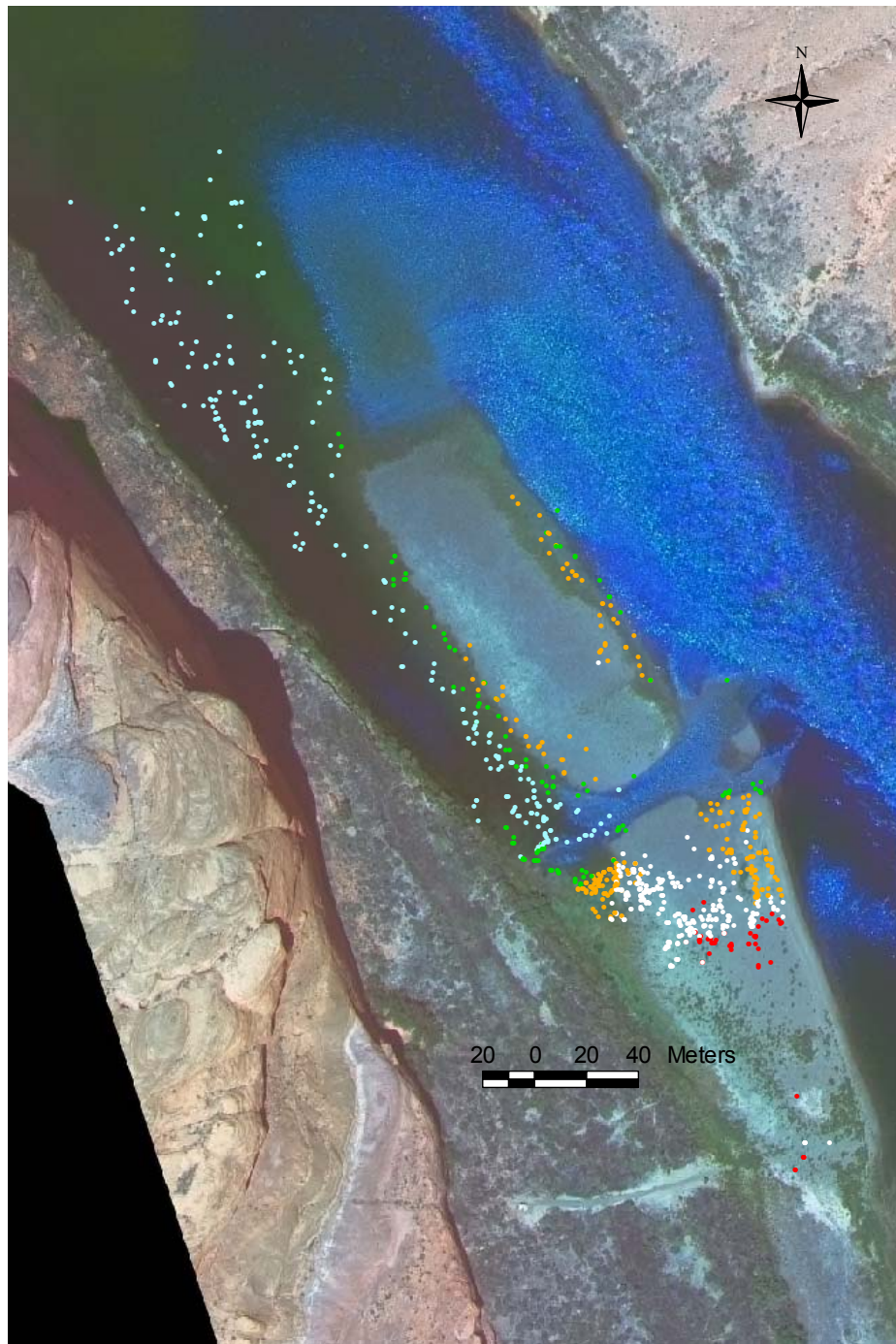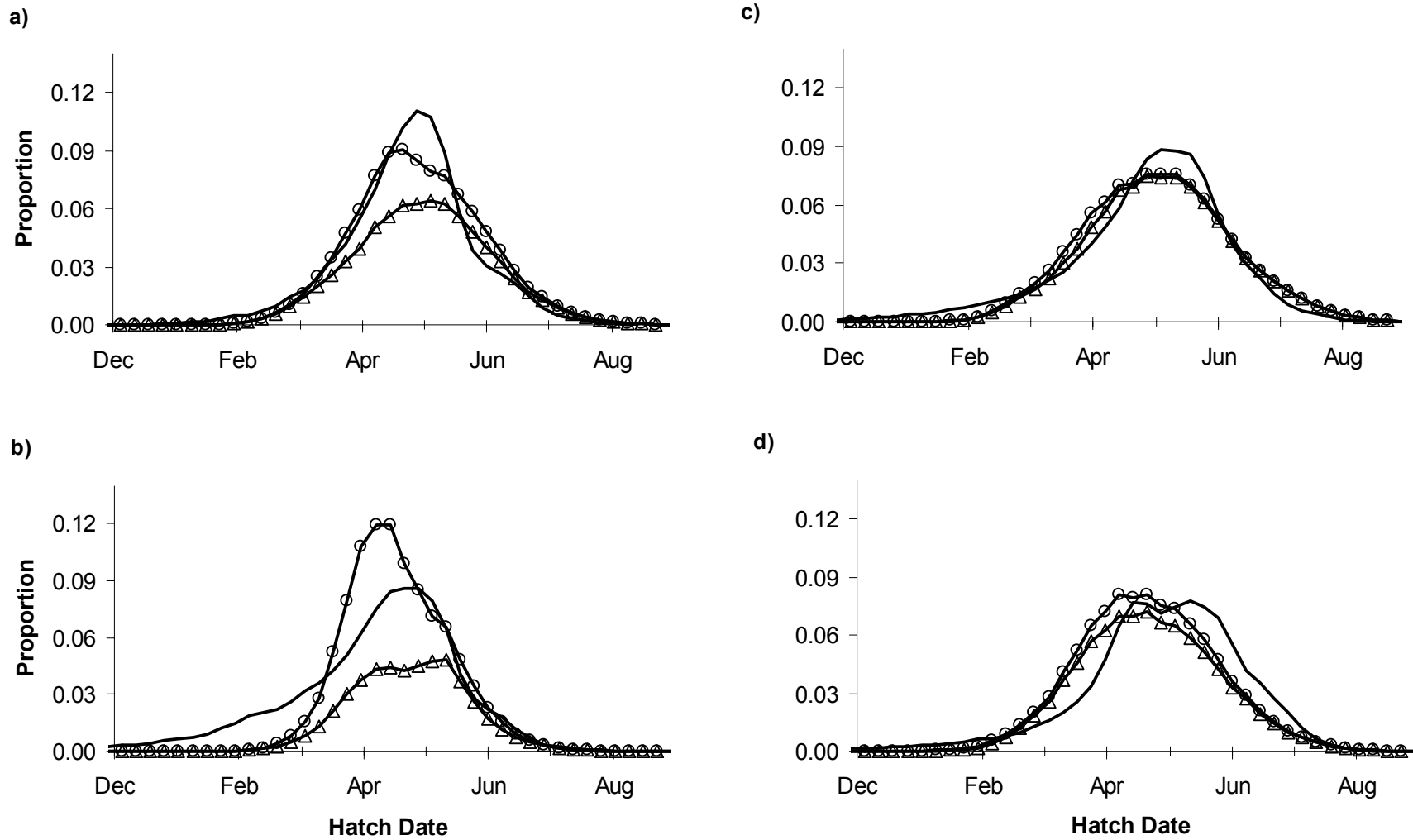
Figure 5.5. Predicted hatch date distributions based on the flow-independent (lines with circles) and flow-dependent (lines with triangles) incubation mortality models and backcalculated hatch date distributions (lines) assuming an instantaneous mortality rate of 0.005 for 2003 (a), 2004 (b), 2006 (c), and 2007 (d). The difference in the areas under the predicted hatch date distributions within years is proportional to the magnitude of flow-dependent incubation mortality (24%, 50%, 5%, and 11% in 2003, 2004, 2006, and 2007, respectively).

145
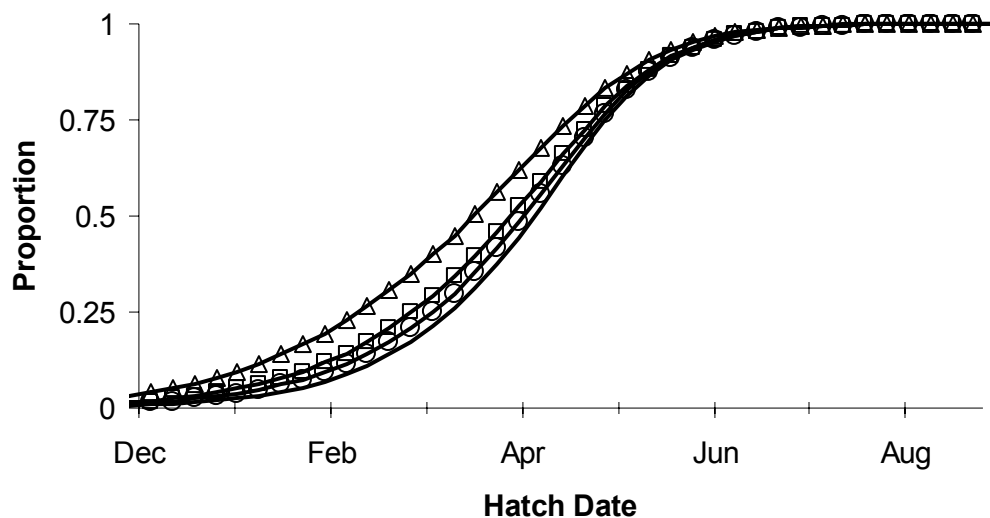
Figure 5.6. Backcalculated cumulative hatch date distributions in 2004 based on instantaneous mortality rates (M) of 0 (line only), 0.005 (circles), 0.01 (squares), and 0.02 (triangles). For brevity, distributions for other years are not shown but the distributions at M=0.005 are shown in Fig. 5.5.
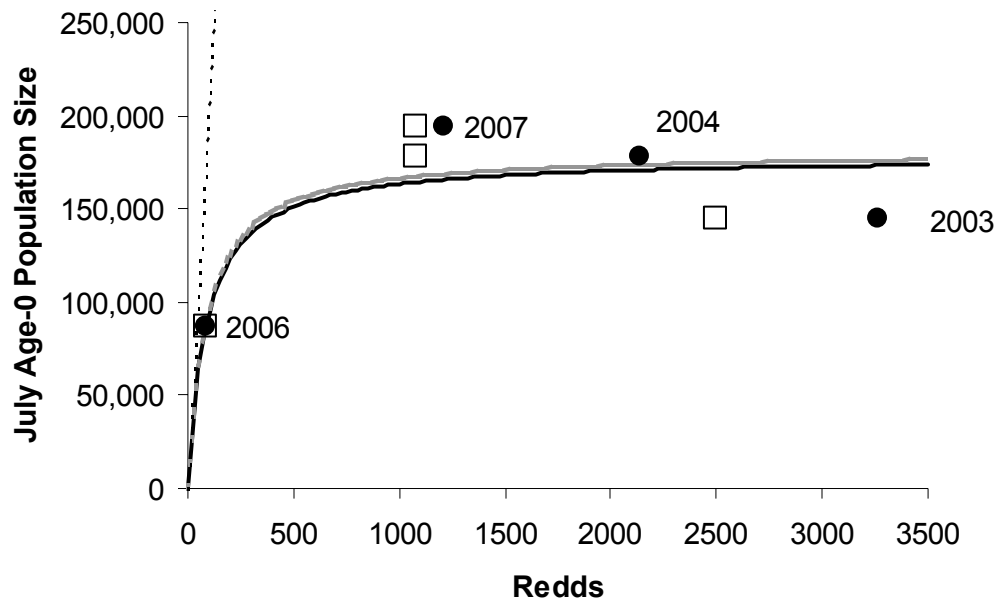
Figure 5.7. The relationship between the total number of redds in the Lee's Ferry reach each study year and the population size of age-0 trout in July (filled circles). The relationship between the number of viable redds predicted by the flow-dependent incubation mortality model and the age-0 population is also shown (open squares). The solid lines shows the fits of Beverton Holt models to total redds (black line) and viable redds (light gray line). The dashed line is the average Goodyear (1980) compensation ratio for freshwater salmonids (25) reported by Myers et al. (1999).

5.5 References

Barnthouse, L.W., Klauda, R.J., Vaughn, D.S. and R.L. Kendall (*Editors*). 1988. Science, law and Hudson River power plants. American Fisheries Society Monograph No. 4.

Becker, C.D., D.A. Neitzel, and D.H. Fickeisen. 1982. Effects of dewatering on Chinook salmon redds: Tolerance of four developmental phases to daily dewaterings. Trans. Am. Fish. Soc. **111**: 624-637.

Berg. S., and J. Jorgensen. 1991. Stocking experiments with 0+ and 1+ trout parr, Salmo trutta L., of wild and hatchery origin: 1. Post-stocking mortality and smolt yeid. J. Fish. Biol. **39:** 151-169.

Campana, S.E. 1992. Measurement and interpretation of the microstructure of fish otoliths. *In* Otolith microstructure examination and analysis. Edited by D.K. Stevenson and S.E. Campana. Can. Spec. Publ. Fish. Aquat. Sci. **117**. pp. 59-71.

Campana, S.E., and C.M. Jones 1992. Analysis of otoliths microstructure data. *In* Otolith microstructure examination and analysis. Edited by D.K. Stevenson and S.E. Campana. Can. Spec. Publ. Fish. Aquat. Sci. **117**. pp. 59-71.

Crecco, V., and T. Savoy. 1987. Effects of climactic and density-dependent factors on intra-annual mortality of larval American Shad. American Fisheries Society Symposium **2:** 69-81.

Chapman, D.W., Weitkamp, D. E., Welsh, T.L., Dell, M.B., and T.H. Schadt. 1986. Effects of river flow on the distribution of chinook salmon (*Onchoynhus-thawytscha*) redds. Trans. Am. Fish. Soc. **115**: 537-547.

Connor, E.J., and D.E. Pflug. 2004. Changes in the distribution and density of pink, chum, and Chinook salmon sapwing in the Upper Skagit River in response to flow management measures. Nor. Am. J. Fish. Mgmt. **24**: 835-852.

Elliott, J.M. 1986. Spatial distribution and behavioural movements of migratory trout Salmo Trutta in a Lake District stream. J. Anim. Ecol. **55**: 907-922.

Elliott, J.M. 1994. Quantitative ecology and the brown trout. Oxford University Press, Oxford.

Einum, S., and I.A. Fleming. 2000. Selection against late emergence and small offspring in Atlantic salmon (*Salmo salar*). Evolution, **54**: 628-639.

Einum, S. and K.H. Nislow. 2005. Local-scale density-dependent survival of mobile organisms in continuous habitats: an experimental test using Atlantic salmon. Oecologia **143**: 203-210.

Fletcher, R.I., and R.B. Deriso. 1988. Fishing in dangerous waters: remarks on a controversial appeal to spawner-recruit theory for long-term impact assessment. *In* Science, law and Hudson River power plants. Edited by L.W. Barnthouse, R.J. Klauda, D.S. Vaughn, and R.L. Kendall. American Fisheries Society Monograph No. 4. pp. 232-244.

Ford, B. S., P. S. Higgins, A. F. Lewis, K. L. Cooper, T. A. Watson, C. M. Gee, G. L. Ennis and R. L. Sweeting. 1995. Literature reviews of the life history, habitat requirements and mitigation/compensation strategies for thirteen sport fish species in the Peace, Liard and Columbia River drainages of British Columbia. Can. Manuscr. Rep. Fish. Aquat. Sci. **2321**.

Fournier, D.A., Hampton, J., and J.R. Sibert. 1998. MULTIFAN-CL: a length-based, age-structured model for fisheries stock assessment, with application to the South Pacific albacore, *Thunnus alalunga*. Can. J. Fish. Aquat. Sci. **55**: 2105-2116.

Goodyear, C.P. 1980. Compensation in fish populations. *In* Biological monitoring of fish. Edited by C. Hocutt and C.J. Stauffer. Lexington Books, D.C. Heath Co., Lexington, MA.

Hilborn, R., Bue, B.G., and S. Sharr. 1999. Estimating spawning escapements from periodic counts: a comparison of methods. Can J. Fish. Aquat. Sci. **56**: 888-896.

Hilborn, R., and Mangel, M. 1997. The ecological detective: confronting models with data. Mon. Pop. Bio. **28**. Princeton University Press, Princeton, New Jersey.

Houde, E.D. 1987. Fish early life dynamics and recruitment variability. American Fisheries Society Symposium **2**: 17-29.

Hume, J.M.B., and E.A. Parkinson. 1988. Effects of size at and time of release on the survival and growth of stealhead fry stocked in streams. N. Am. J. Fish. Mgmt. **8:** 50-57.

Jensen, J.O.T., McLean, W.E., Rombough, P.J., and T. Septav. 1992. Salmonid incubation and rearing programs for IBM-compatible computers. Can. Tech. Rep. Fish. Aquat. Sci. **1878**: 46 p.

Letcher, B.H., Dubreuil, T., O'Donnell, M.J., Obedzinski, M., Griswold, K., and K.H. Nislow. 2004. Long-term consequences of variation in timing and manner of fry introduction on juvenile Atlantic salmon (Salmo salar) growth, survival, and life-history expression. Can. J. Fish. Aquat. Sci. **61**: 2388-2301.

McKinney, T., Speas, D.W., Rogers, R.S., and W.R. Persons. 2001. Rainbow trout in a regulated river below Glen Canyon Dam, Arizona, following increased minimum flows and reduced discharge variability. Nor. Am. J. Fish. Mgmt. **21**: 216-222.

McMichael, G.A., Rakowski, C.L., James, B.B., and J.A. Lukas. 2005. Estimated fall Chinook salmon survival to emergence in dewatered redds in a shallow side channel of the Columbia River. Nor. Am. J. Fish. Manage. **25**: 876-884.

Mietz, S.W. 2003. Evaluating historical electrofishing distribution in the Colorado River, Arizona, based on shoreline substrate. M.Sc. thesis, Department of Biology, Northern Arizona University, Flagstaff, AZ.

Montgomery, W. L. and K. Tinning. 1993. Impact of fluctuating water levels on early life history of rainbow trout. Report prepared for Glen Canyon Environmental Studies. Available online at www.gcmrc.gov.

Nislow, K.H. Einum, S., and C.L. Folt. 2004. Testing predictions of the critical period for survival concept using experiments with stocked Atlantic salmon. J. Fish Biol. **65** (Supplement A): 188-200.

Methot, R.D. 1983. Seasonal variation in survival of larval northern anchovy, Engraulis Mordax, estimated from the age distribution of juveniles. Fish. Bull. **81**: 741-750.

Myers, R.A., Bowen, K.G., and N.J. Barrowman. 1999. Maximum reproductive rate of fish at low populations sizes. Can. J. Fish. Aquat. Sci. **56**: 2404-2419.

Oliver, G.G. and L.E. Fidler. 2001. Towards a water quality guideline for temperature in the province of British Columbia. Report prepared for BC Ministry of Environment, Lands, and Parks, Water Management Branch by Aspen Applied Sciences Ltd., Cranbrook, BC. Available from: http://wlapwww.gov.bc.ca/wat/wq/BCguidelines/temptech/index.html

Peterman, R.M., Bradford, M.J., Lo, N.C.H., and R.D. Method. 1988. Contribution of early life stages to interannual variability in recruitment of Northern Anchovy (Engraulis mordax). Can. J. Fish. Aquat. Sci. **45**: 8-16.

Piper, R.G., McElwain, I.B., Orme, L.E., McCraren, J.P., L.G. Fowler, and J.R. Leonard. 1986. Fish Hatchery Management. American Fisheries Society.

Randle, T.J., and E.L. Pemberton. 1987. Results and analysis of STARS modeling efforts of the Colorado River in Grand Canyon. U.S. Department of Interior, Bureau of Reclamation. NTIS No. PB88-183421/AS.

Reiser, D.W., and R.G. White. 1983. Effects of complete redd dewatering on salmonid egg-hatching success and development of juveniles. Trans. Am. Fish. Soc. **112:** 532-540.

Stevenson, D.K. and S.E. Campana [*Editors*]. 1992. Otolith microstructure examination and analysis. Can. Spec. Publ. Fish. Aquat. Sci. **117**. 130 p.

Travnichek, V.H., Bain, M.B. and M.J. Maceina. Recovery of a warmwater fish assemblage after the initiation of a minimum-flow release downstream from a hydroelectric dam. Trans. Am. Fish. Soc. **124**: 835-844.

Vernieu, W.S, Hueftle, S.J., and S.P. Gloss. Water quality in Lake Powell and the Colorado River. *In* The state of the Colorado River ecosystems in Grand Canyon. Edited by S.P. Gloss, J.E. Lovitch, and T.S. Melis. U.S. Geological Survey Circular 1282. Available from http://www.gcmrc.gov/products/score/2005/score.htm.

6.0 Joint Estimation of Spawn Timing and Magnitude, Incubation Mortality, and the Growth, Movement, and Mortality of Age-0 Rainbow Trout using a Stock Synthesis Model[5]

6.1 Introduction

Flow regulation is a widespread anthropogenic disturbance in stream environments that potentially influences both the abiotic conditions in egg, larval, and juvenile habitats, as well as the intensity of biotic interactions such as competition and predation (Heggenes and Dokk 2001, Shea and Peterson 2007). These dynamics are poorly understood in large rivers, where there is much concern over the effects of hydropower operations on fish populations. Early life stages experience high mortality rates, undergo major shifts in habitat use, and are difficult to sample in large rivers. These characteristics limit the application of existing methodologies, such as open-population mark-recapture models, to quantify key aspects of early life history dynamics. It will not be possible to understand how flow regulation impacts fish populations until methods that quantify vital rates, like incubation and age-0 mortality and growth, become available.

In a companion paper (Chapter 4), seasonal trends in length frequencies and population size for age-0 rainbow trout in the Lee's Ferry reach of the Colorado River, Arizona, were used to describe habitat use, movement, and potential differences in mortality among habitat types and with changes in flow. We speculated that unnatural aspects of the flow regime from Glen Canyon Dam, such as hourly hydropeaking operations (see Fig. 4.1 of Chapter 4), would result in greater mortality in low-angle shorelines (e.g., cobble and sand bars) than in high-angle shorelines (e.g., talus slopes) due to differences in the extent of temporal variation in the location of suitable habitat. Greater temporal instability in suitable habitat in low-angle shorelines due to hourly flow

---

[5] A version of this chapter may be submitted for publication. Korman, J., Martell, S.D., and C.J. Walters. Joint estimation of spawn timing and magnitude, incubation mortality, and the growth, movement, and mortality of age-0 rainbow trout using a stock synthesis model.

fluctuations could also stimulate movement of age-0 trout to high-angle shorelines with more stable habitat but higher predation risk. In addition, we were interested in whether sudden changes in the hydrograph, like experimental floods or reductions in the minimum flow (see Fig. 4.1 of Chapter 4), led to substantial mortality of age-0 trout. Based on examination of population trends, we were not able to separate the effects of movement on differential mortality among habitat types, or to separate effects of temporal variation in recruitment to the age-0 population from temporal variation in age-0 mortality rates. We were also interested in determining the significance of differences in mortality rates among years, and among months within years, but were unable to do so based on a simple examination of population trends. A more integrated analysis is needed to quantify these dynamics.

In an attempt to limit the population of adult rainbow trout in the Colorado River below Glen Canyon Dam as part of a native fish recovery effort, hourly fluctuations in flow from Glen Canyon Dam were experimentally increased between January 1st and March 31st from 2003-2005 to dewater incubating life stages (Coggins 2008). We evaluated the efficacy of this experimental regime using a hatch date analysis (Chapter 5). Predicted hatch date distributions based on flow-independent and –dependent models were compared to the realized distribution determined by backcalculating hatch dates of a large sample of age-0 trout. A key assumption used to backcalculate the hatch date distributions, and therefore in the comparison of flow-independent and -dependent models, was that mortality rates were similar for different weekly cohorts of age-0 trout that were captured. This assumption is common to almost all hatch date analyses (e.g., Methot 1983) and a more advanced analysis was recommended to determine if conclusions regarding flow effects on incubation success were sensitive to assumptions about seasonal variation in age-0 mortality rates.

Over the last decade there have been considerable advances in the development of stock synthesis models that integrate multiple sources of data into a single framework to jointly estimate parameters such as recruitment, growth, and mortality (e.g., Fournier et al. 1998, Eveson et al. 2004, Taylor et al. 2005, Deriso et al. 2007). These models are typically applied to annual data from commercially important populations to provide advice for fisheries management regarding sustainable harvest rates and quotas. In this

paper, we develop a stock synthesis model to estimate spawn timing and magnitude, and the mortality, growth, ontogenetic movement, and abundance of weekly cohorts of age-0 rainbow trout in low- and high-angle habitats in the Lee's Ferry reach. The model jointly estimates parameters describing these processes by maximizing the fit to redd count (Chapter 5), length-at-age (Chapter 4), and length-frequency (Chapter 4) data. The model also integrates information on habitat-specific capture probabilities and length-dependent vulnerability determined from mark-recapture experiments (Chapter 2), and seasonal trends in relative incubation success predicted from a flow-dependent incubation loss model (Chapter 5). The framework provides an objective means of addressing uncertainties related to alternate models of early life history dynamics that are of direct interest in the evaluation of the incubation, movement, and mortality hypotheses described above.

The modeling approach we describe in this paper has a number of unique aspects. To our knowledge, a stock synthesis model has never been used to estimate parameters describing the population dynamics of freshwater early life history stages. Unlike other applications of stock synthesis models to data from commercial fish populations, ours is based exclusively on scientific survey data, which includes independent estimates of recruitment and vulnerability to sampling. The integrated sampling and modeling approach that is described very likely has a wide range of applications in the investigation of population dynamics for early life stages of freshwater fishes and can provide a consistent means of evaluating the success of various habitat management actions.

6.2   Methods

Methods are described in five sections that represent the major components of the field program and modeling approach. We first briefly describe the study site and field methods. This is followed by a description of the stock synthesis model and how it is applied to the data to estimate model parameters. We then identify alternate model structures that will be used to evaluate recruitment, mortality, and movement hypotheses. Finally, we describe a simulation exercise used to evaluate potential bias in estimated parameters and the degree to which true underlying models can be correctly identified using an information theoretic approach.

Study Area and Field Methods

This study was conducted in the Lee's Ferry reach of the Colorado River, AZ. The reach begins at Glen Canyon Dam and extends 26 km downstream to the confluence of the Paria River (Lat:36.86638, Long:-111.58638). The fish fauna in the Lee's Ferry reach is almost exclusively comprised of nonnative rainbow trout that reproduces naturally (McKinney et al. 2001). Spawning occurs over an extended period from November through May, with a pronounced peak between mid-March and mid-April (Chapter 5). Data on spawning and early life history stages was collected in 2004, 2006, and 2007. Field investigations are logically divided into those focusing on spawning biology and incubation success (Chapter 5), age-0 growth, habitat use, abundance, and mortality (Chapter 4), and application of mark-recapture and depletion methods to estimate the capture probability of age-0 fish to electrofishing (Chapter 2). Details of field methods have been described elsewhere and are only briefly summarized here.

We conducted between seven and eleven system-wide redd surveys per year to estimate spawn-timing and magnitude. The elevation of redd locations was also recorded on each survey. In conjunction with measurements of intergravel temperature at a range of elevations over the entire spawning and incubation period, a physical model was developed to estimate the impact of fluctuating flows from Glen Canyon Dam on incubation success of weekly spawning cohorts. This model was partially validated by direct examination of egg mortality through redd excavations. Details of the spawning and incubation component of the study are provided in Chapter 5.

Age-0 catch data were collected from 40 randomly selected shoreline sites sampled on a near-monthly basis between April and December (2004), or between June and November (2006 and 2007). Sampling was conducted using backpack and boat electrofishing in low- (cobble bars, sand bars, and debris fans) and high-angle (talus) shoreline types, respectively. On each survey, a length- and habitat-stratified sample of fish was collected for later analysis of otolith microstructure to estimate daily age from hatch and emergence. Details of field and ageing methods, timing of sampling, and sample sizes, and general trends in growth and abundance of the age-0 population are provided in Chapter 4. Depletion and mark-recapture experiments were conducted in 2006 and 2007 to estimate capture probability, and determine how it was influenced by

fish density, fish size, flow, and other factors (Chapter 2). Data from the mark-recapture component of this study was used to estimate habitat- and gear-specific relationships between capture probability and fish size, which is a component of the stock synthesis model and will be described below.

Stock Synthesis Model

The model predicts the magnitude and timing of spawning and fry emergence, and the mortality, growth, ontogenetic movement, and abundance of age-0 rainbow trout cohorts in low- and high-angle habitats in the Lee's Ferry reach at a weekly time step for a one-year period beginning December 1st. Recruitment in this analysis represents the total number of fish emerging in the Lee's Ferry reach per week and is predicted based on estimates of the timing and magnitude of redd deposition, required time from fertilization to emergence, and predicted weekly changes in incubation success. Mortality rates of age-0 fish depend on fork length and can vary by habitat type and across sampling intervals. The proportion of fish migrating from low- to high-angle habitat (ontogenetic movement) can depend on fish size. Size-at-age is predicted from a von Bertallanfy growth model. The number of fish alive at each age and timestep is translated into a length frequency based on an age-length key and size-dependent vulnerability to sampling. Model parameters describing all these processes are jointly estimated in a maximum likelihood framework, by minimizing the sum of negative log likelihoods for redd count, length-at-age and age-0 catch data.

We used Hilborn et al.'s (1999) maximum likelihood application of the Area-under-the-Curve (AUC) method to predict the magnitude and timing of spawning. The number of redds created per weekly timestep is simulated using a beta distribution,

$$(1) \qquad\qquad R_t = \chi \theta_t^{(\alpha-1)} \left(1 - \theta_t\right)^{(\beta-1)},$$

where, R_t is the number of redds created in week t, χ is the total number of redds created over the spawning season, and α and β are parameters of the beta distribution that determines the proportion of the total redds created per week (i.e., the timing of spawning (Table 6.1). θ_t is a constant and represents the proportional date of spawning (t/T). The probabilities returned from the beta distribution are standardized so they sum to 1. We use a convenient reparameterization of the beta distribution where the week of peak

156

spawning (γ, i.e., the mode of the beta distribution) and the relative precision in spawn timing (α) are estimated and β is computed as $\beta = \dfrac{\alpha - 1}{\gamma} + 2 - \alpha.$

The number of fish that successfully emerge and recruit to the age-0 population each week (G_t) is predicted from,

(2) $$G_{t+W_t} = R_t e^{-\eta_t} \phi$$

where, W_t is the number of weeks between spawning and emergence for each weekly cohort, η_t is their relative incubation mortality rate, and ϕ is the maximum number of fish that can emerge per redd. W_t is a weekly constant that depends on measured intergravel temperatures and the accumulated thermal units as predicted by an incubation-timing model (Jensen et al. 1992). Note that fish emerging each week can originate from more than one cohort because W_t can vary among weeks. η_t can either be fixed at zero to simulate the null hypothesis that there is no temporal variation in incubation mortality, can be treated as an environmental forcing variable, or estimated for specific blocks of weeks. If treated as a forcing variable, η_t is based on the flow-dependent incubation loss model described in Chapter 5 which depends on: 1) the proportion of fish spawning at different elevations that determines redd dewatering frequency and duration; 2) intergravel temperatures within redds driven by dewatering statistics and seasonal variation in air temperature; and 3) the assumed lower and upper lethal temperature limits of incubating stages. Alternatively, η_t can be estimated to evaluate hypotheses about the effects of seasonal changes in the flow regime from Glen Canyon Dam on incubation success. ϕ represents the product of the number of eggs deposited per redd, fertilization and maximum survival rates, and a factor which accounts for any bias in the estimate of the total redds created.

The number of fish alive (N) that are one week old (a_1) each week in low- (h_L) and high- (h_h) angle habitats is predicted from,

(3) $$N_{h_L,a_1,t} = G_t \delta$$
$$N_{h_H,a_1,t} = G_t (1 - \delta)$$

where, δ is the proportion of recruits that migrate to low-angle habitat after emergence. The numbers alive for subsequent ages are predicted from,

$$(4) \qquad N_{h_L,a,t} = N_{h_L,a-1,t-1}(1-\varphi_a)e^{-\mu_{h_L,a,t}}$$

$$N_{h_H,a,t} = (N_{h_S,a-1,t-1} + N_{h_L,a-1,t-1}\varphi_a)e^{-\mu_{h_H,a,t}}$$

where, φ_a is the proportion of fish that move from low- to high-angle habitat (ontogenetic movement) and μ is the weekly instantaneous mortality rate. Mortality can vary by habitat type, over time, and by age based on,

$$\mu_{h,t} = \mu_h e^{\varepsilon_{h,i}}$$

$$(5) \qquad \mu_{h,a,t} = \mu_{h,t}(\frac{l_a}{l_r})^C$$

where, μ_h is the base mortality rate for each habitat type, i is an index for the block of weeks between each sampling period, $\varepsilon_{h,i}$ is the estimated temporal mortality deviation for each block of weeks ($\sum_i \varepsilon_{h,i} = 0$), l_a is the fork length for fish of age a, l_r is the reference fork length where the mortality rate is $\mu_{h,t}$, and C is the allometric exponent of the mortality-fork length relationship (Lorenzen 2000). Morality rates will decline with increase fish size if $C<0$ and will be constant with fish size if $C=0$. Mortality rates for fish of a given size will be constant over time if $\varepsilon_{h,i}=0$.

Ontogenetic movement is assumed to be unidirectional from low- to high-angle habitats and can depend on size-at-age based on the following logistic function,

$$(6) \qquad \varphi_a = \frac{\rho_0}{1+e^{-(\frac{l_a-\rho_\mu}{\rho_\sigma})}}$$

where, ρ_0 is the maximum proportion moving per timestep, ρ_μ is the fork length where movement is 50% of the maximum, and ρ_σ is the standard deviation of the fork length-movement relationship. Mean length-at-age is predicted based on the reparameterization of the von Bertalanffy growth model of Schnute and Fournier (1980),

$$(7) \qquad l_a = \lambda_1 + (\lambda_A - \lambda_1)\frac{1-e^{-\kappa(a-1)}}{1-e^{-\kappa(A-1)}}$$

where, λ_1 and λ_A are fork lengths at emergence (a_1) and at one year from emergence (A), respectively, and κ is the Brody growth parameter.

Remaining components of the model describe observation processes. The predicted number of redds present on each model week ($\hat{r}_t$) is calculated as the difference

between the cumulative number of redds created (Eqn. 1) and the cumulative number that have faded (F_t),

$$(8) \qquad \hat{r}_t = \sum_t R_t - \sum_t F_t$$

A redd is designated as faded when it exceeds its survey life (S in weeks) and is therefore no longer visible to an observer (i.e., $F_t = R_{t-S}$).

Assuming variation in length-at-age is normally distributed, the total probability of a fish being length x at age a is calculated as,

$$(9) \qquad P_{j,a} = \frac{1}{\sigma_a \sqrt{2\pi}} \int_{x-\frac{w}{2}}^{x+\frac{w}{2}} e^{-\frac{(x-l_a)^2}{2\sigma_a^2}} dx$$

where, w is the width of each length interval (5 mm), j is the index for the length interval x-w/2 to x+w/2, and σ_a^2 is the variance in size-at-age. Error in size-at-age is assumed to be normally distributed with mean l_a, with σ_a^2 computed as $(l_a v_l)^2$, where v_l is the coefficient of variation in length-at-age. $P_{j,a}$ values are normalized so they sum to one for each age.

The vulnerability of age-0 fish to capture by electrofishing varies by habitat type and with fork length according to the logistic function,

$$(10) \qquad V_{h,a} = \frac{\pi_h}{1 + e^{-(\frac{l_a - \psi_h}{\tau_h})}}$$

where, π_h is the proportion of the population captured within areas that are sampled for fish that are large enough to be fully vulnerable to sampling, and ψ_h and τ_h are the length at which vulnerability to sampling is 50% of the maximum, and the standard deviation of the fork length-vulnerability logistic function, respectively.

The predicted number of fish caught within length interval j in sample week t and in habitat type h ($\hat{C}_{h,t,j}$) is computed from,

$$(11) \qquad \hat{C}_{h,t,j} = E_{h,i} \sum_a V_{h,a} P_{j,a} N_{h,a,t}$$

where, $E_{h,t}$ is the sampling effort by habitat type and week. Effort is expressed as the proportion of shoreline length electrofished each sampling trip relative to the total amount of shoreline in the Lee's Ferry reach of that habitat type. Habitat-specific

vulnerabilities therefore represent the proportion of fish within sampled areas that are caught (i.e., the probability of capture).

Parameter Estimation

We use an integrated maximum likelihood approach to jointly estimate parameters that predict redd counts, length-at-age, and catch data by sampling trip, size class, and habitat type. An independent likelihood term is defined for each data type. Error in redd count, length-at-age, and catch data are assumed to follow Poisson, normal, and Poisson distributions, respectively. The negative log likelihood for the Poisson model for redd counts (NLL_r) omitting constants is,

$$(12) \qquad NLL_r = \sum_t \hat{r}_t - \tilde{r}_t \log(\hat{r}_t)$$

where, $\tilde{r}_t$ and $\hat{r}_t$ are the observed and predicted number of redds on sample week t. Note the likelihood is only computed for weeks when redd surveys were conducted. The negative log likelihood for the length-at-age data (NLL_{la}) omitting constants is,

$$(13) \qquad NLL_{la} = \sum_k \log(\sigma_{l,k}) + \frac{(\tilde{l}_k - \hat{l}_k)^2}{2\sigma_{l,k}^2}$$

where $\tilde{l}_k$ and $\hat{l}_k$ are the observed and predicted length for fish of known age, k is the index for each length-at-age observation, and $\sigma_{l,k}^2$ is the variance for each observation computed as $\sigma_{l,k} = \hat{l}_k v_l$. The negative log likelihood for catch data (NLL_C) omitting constants is,

$$(14) \qquad NLL_{c,h} = \sum_t \sum_j \hat{C}_{h,t,j} - \tilde{C}_{h,t,j} \log(\hat{C}_{h,t,j})$$

where, $\tilde{C}_{h,t,j}$ is the observed catch in habitat type h, sample week t, and size class j. Note the log-likelihood is only computed for weeks when age-0 surveys were conducted.

We used the nonlinear iterative search procedure in the AD model-builder (ADMB) software (Otter Research 2004) to minimize the sum of negative log-likelihoods. The total negative log-likelihood (NLL_T) that was minimized is,

$$(15) \qquad NLL_T = NLL_r + NLL_{la} + NLL_{c,L} + NLL_{c,H}$$

All parameters were estimated in an untransformed state except for ρ_0, which was logit-transformed to ensure values ranged from 0-1. To ensure that a global minimum was

found, a minimum of 10 different random initial conditions were used to estimate parameters. Initial values used in the estimation were randomly drawn from bias-corrected log-normal distributions centered around base initial values (Table 6.2) with a coefficient of variation of 0.5. This CV was selected so that 95% of the initial values were ± 50% of the base initial values with extreme values range from 30-250%. Asymptotic estimates of the standard error of parameter estimates and the covariance among parameters (Pearson correlation coefficient) at their maximum likelihood values were computed from the inverse of the Hessian matrix returned by ADMB.

We did not estimate parameters for the size-vulnerability relationship (Eqn. 10), but fixed them at their maximum likelihood estimates determined from two-day mark-recapture experiments (see Table 2.2 from Chapter 2). The most likely logistic vulnerability relationships explained 90% of the variation in size-stratified recapture rates. Estimates were based on the recapture of 908 marked fish out of a total release of 2946 fish over 42 mark-recapture experiments conducted between June and November, 2007. Depletion and mark-recapture experiments showed that the variation in flow experienced over this study did not effect capture probability. Thus it is reasonable to assume that the vulnerability relationships are stationary across sampling trips.

Alternate Model Structures

A nested series of models were used to evaluate alternate hypotheses concerning incubation success (recruitment), age-0 mortality and movement. Three models were used to evaluate the dynamics of incubation success (Table 6.3). The null recruitment model (R1) assumes that the numbers of age-0 trout emerging from the gravel each week depends on spawn-timing as estimated using a beta distribution (Eqn. 1) and time required for incubation (W_t) only, and that incubation mortality is identical for all weekly cohorts. The flow regime-based recruitment model (R2) estimates a single incubation mortality rate that is applied to all cohorts spawned before April 1st ($\eta_1=\eta_{2,...}=\eta_{18}$). This date was selected because it coincided with the end of the period when hourly variation in flow was experimentally increased between 2003 and 2005 to reduce incubation success (see Fig. 4.1 from Chapter 4). As η_{19-52} is fixed at 0, η_{1-18} represents the additional incubation mortality incurred during the experimental flow period. The flow-forcing recruitment model (R3) has the same number of parameters as R1, but uses fixed values

of η_t predicted by the flow-dependent incubation loss model, which integrates effects of spawn timing, spawning elevation, and spatial and temporal trends in intergravel temperature (Chapter 5). Values for η_t vary by year and were substantially higher in 2004 when flow fluctuations were increased (Fig.'s 5.1b and 6.1). The predicted reduction in the percent loss in redds which produced viable young as a result of fluctuating flows was 50%, 5%, and 11% in 2004, 2006, and 2007, respectively (see Table 5.3, Chapter 5). In 2004, when the predicted incubation mortality was substantial, the fit of model R3 should be better relative to R1, which assumes no temporal deviation in incubation mortality rates.

The number of fry that emerge per redd estimated by the model represents emergence success. It is computed as $e^{\eta_{1-18}}\phi$ and $e^{\eta_{19-52}}\phi$ for periods before and after April 1st, respectively (see Eqn. 2). It is important to note that estimates of emergence success and age-0 mortality (μ_h) are partially confounded because we captured very few age-0 trout that were less than one month old from emergence, due to their very low vulnerability to electrofishing (see Chapter 2). Because of this confounding, differences in estimates of 'emergence success' across years, or before and after April 1st within years, will be partially driven by variation in age-0 mortality between emergence and the time when fish are first captured.

We examine 4 nested age-0 mortality models and 3 nested models describing ontogenetic movement from low- to high-angle habitat. The null mortality model assumes that mortality rates in low- and high-angle habitat are equivalent and constant through time (M1, Table 6.3). The habitat-dependent model estimates habitat-specific mortality rates, which are assumed constant through time (M2). The next complex mortality model assumes mortality rates are constant among habitat types but can vary across sampling intervals (M3). The most complex model allows mortality to vary by habitat type and over time (M4). Three alternate ontogenetic movement models were examined: a null model which assumes no movement (O1); a size-independent model where the proportion moving per timestep is constant (O2); and a size-dependent model where the proportion moving increases with fork length (O3). We examined all combinations of recruitment, movement, and mortality models and identify model

combinations by concatenating codes. For example, R2-M3-O1 refers to a model based on recruitment model R2, mortality model M3, and ontogenetic movement model O1.

Alternate models were fit to the data and compared using the Akaike Information Criteria (AIC). AIC is an information theoretic approach that can be used to identify the most parsimonious model by formally recognizing the tradeoff between bias and variance (Burnham and Anderson 2002). A more complex model with more parameters will almost always fit the data better than a simpler model with fewer parameters (i.e., will have a larger log likelihood), however parameter estimates from the more complex model will be more uncertain. When comparing a range of candidate models, the model with the lowest AIC value looses the least amount of information, achieves the best balance between bias and variance, and will therefore have the best predictive performance when applied to replicate datasets. Models with similar AIC values relative to the best model (ΔAIC=0-2) are considered to have strong support, while those with larger AIC values are considered to have moderate (ΔAIC=4-7) or essentially no (ΔAIC>10) support.

Simulation Modelling

A simulation model was used to evaluate the extent of bias in maximum likelihood estimates (MLEs) of model parameters. The simulation model used the same model equations and assumptions already described to generate simulated data sets for redd counts, length-at-age, and numbers of fish caught by length interval, habitat type, and sampling trip. Parameters were then estimated from the simulated data and compared to the true values used to drive the simulation. Errors that were simulated were consistent with the error structure used in the estimation model and included Poisson variation in the number of redds created per week, normal variation in length-at-age, and Poisson variation in catch within sampling trip-fish size strata. Sampling and process error were simulated using the rejection method (Press et al. 1992).

Length-at-age samples were generated by simulating the stratified-sampling approach used in the field program, where a fixed number of samples were taken from each unique habitat type, sampling trip, and 10 mm length interval combination. The probabilities of sampling a fish of a particular age and length depended on the simulated length-at-age key, length-dependent vulnerability to capture, and Poisson sampling error in catch. Within strata, the number of age samples could not exceed the number of fish

163

caught and the maximum length of fish sampled for ageing was set at 90 mm which approximated the maximum size of fish that were aged (see Fig. 4.5 from Chapter 4). Two levels of redd- and age-0 sampling were simulated. A high-resolution simulation was based on 11 redd surveys and 8 age-0 surveys per year and reflected the sample timing and effort in 2004. A lower-resolution simulation was based on 7 redd surveys and 5 age-0 surveys per year and reflected the sample timing and effort in 2006 and 2007. The number of length-at-age samples typically generated from these scenarios was 350 and 175, respectively, which approximated the sample sizes obtained in 2004 and 2006/2007, respectively (see Table 4.1, Chapter 4).

Bias in maximum likelihood estimates was evaluated using Monte Carlo simulations where we compared average parameter estimates across 100 trials with their true simulated values (% bias = 100 * (estimate-true)/true). For each trial, initial values for parameters in the estimation procedure were randomly selected from a log-normal bias-corrected distribution centered around the true simulated values with a coefficient of variation (CV) of 0.5 (Table 6.2). Simulations were conducted based on recruitment model R1 for all six combinations of mortality models M1 and M2, and movement models O1, O2, and O3 (Table 6.3). We applied all 6 estimation models to data generated from each simulation scenario to compare bias when both correct and incorrect model structures were applied to the generated data. We also evaluated the ability of the AIC model selection procedure to identify the correct simulating model. AIC statistics were computed for each estimation model on each trial. We then compared AIC scores across estimation models within trials and computed the percentage of trials where the correct simulating model was identified. In cases where the correct model was identified, we computed the average difference between the lowest AIC score and the next lowest AIC score, to determine the typical degree of support for alternate models.

6.3   Results

Model Evaluation by Simulation

Examination of the covariance matrix from a single simulation-estimation trial for model R1-M2-O3 highlights partial confounding among some model parameters (Table 6.4). In this single case, maximum likelihood estimates for most model parameters were

unbiased and precise. The maximum movement rate (ρ_0) had lower precision, and ρ_σ was substantially overestimated (+ 124%) and had very low precision. There was high correlation among movement parameters (r=0.74-0.86) indicating that multiple combinations of alternate values provided similar fits to the data. Although estimates of individual movement parameters were uncertain, predicted movement rates for a wide range of fish sizes were very similar to those predicted by the relationship used to drive the simulation. For example, the simulated proportions of fish with fork lengths of 20, 40, 60, and 80 mm that moved from low- to high-angle habitat, were 0, 0, 0.15 and 0.15, while estimated values were 0, 0.02, 0.15, and 0.16, respectively. As is common in estimation of length-at-age relationships, growth parameters were confounded. The strong negative correlation between κ and λ_A indicates that the data are almost as equally well described by slower growth and a larger size at the terminal age or visa-versa. This confounding was caused in part by the simulated length-at-age sampling regime where samples were limited to fish < 90 mm, leading to uncertainty in the estimate of λ_A. This uncertainty remains even though spawn-timing and length-frequency data provide additional information about λ_A. The negative correlation between the total number of redds (χ) and the number of fry emerging per redd (ϕ) demonstrates alternate ways of producing similar recruitment to the age-0 population. Partial confounding was also evident in emergence per redd, the initial proportion colonizing low-angle habitat (δ), and age-0 mortality rates (μ_h). For example, as ϕ increases so does δ and μ_L, while μ_H decreases. In this case, increasing the number of emerging fry per redd requires an increase in the proportion initially colonizing low-angle habitat in conjunction with higher values mortality in low-angle habitat which in turn requires reduced mortality in high-angle habitat. There was correlation between growth parameters and mortality rates because length-at-age influences both size-dependent mortality (Eqn. 5) as well as the rate of migration to and from habitat types with different mortality rates (Eqn. 6).

There was little bias in estimated parameters when the same models were used for both simulation and estimation (Table 6.5). For brevity, we show results for the low-resolution sampling scenario only, which provides a worst-case scenario. Bias in most model parameters was generally less than 5%. The Brody growth coefficient (κ) had a slightly larger bias ranging from 4-10%, which was caused by an overrepresentation of

young fast-growing fish in the simulated sample due to size-dependent differences in vulnerability (as shown in Taylor et al. 2005). Movement parameters had little bias with the exception of ρ_σ, which was underestimated by approximately 20%. Although this bias was substantial, there were negligible differences in realized movement rates across a wide range of fish sizes (e.g., MV_22.5 to Mv_82.5 values in Table 6.5).

As expected, bias in model parameters increased when using different simulation and estimation models, but the extent of bias was very dependent on model complexity (Table 6.6). For brevity, we show a subset of cases that demonstrate the full range of potential biases. There was little bias in cases where we simulated a single constant mortality rate among habitat types (M1-O1) but estimated parameters using the more complex habitat-specific model (M2-O1). Mortality and length-dependent movement rates were also unbiased in cases where the estimated movement model was more complex than the simulated case (M1-O1/M2-03, M2-01/M2-03, M2-02/M2-03). However, substantial biases in mortality, movement, and some growth (κ) and recruitment (ϕ, δ) parameters occurred in cases where the estimated mortality (M2-O1/M1-O1) or movement (M2-O2/M2-O1, M2-O3/M2-O1, M2-O3/M2-O2) models were simpler than the models used to generate the data.

The AIC method reliably identified the model used to generate simulated data under a range of model structures and sampling regimes (Table 6.7). The generating model was identified correctly at a minimum rate of 82% (M1-O2) and a maximum rate of 99% (M2-O3). In four (low-resolution) or 5 (high-resolution) of the 6 scenarios, the correct generating models were identified at rate of 90% or higher. There was minimal loss of information in cases where more complex estimation models were applied to data generated from relatively simple simulation models. For example, when simulating M1-01, the average difference in AIC between this model and the next best model was 1.59 (low-resolution sampling) or 1.63 (high-resolution sampling, Table 6.7a). Under this scenario, model M2-01 was usually identified as the next best model (Table 6.7b). As M2-O1 has only one more parameter than M1-O1, the maximum AIC difference (i.e., the extent of information loss), should not exceed two. Applying Burnham and Anderson's (2002) criteria to this situation, we would conclude that there was substantive support for both models. However, as estimates for morality in low- and high-angle habitat types

166

under M2-01 were virtually identical to each other and to the mortality rate estimated from M1-01 (Tables 6.6 and 6.5), the analysis leads to the correct conclusion that there is little support for differences in mortality rates among habitat types. As model complexity increased, there were larger differences in AIC scores because the reduced fit associated with applying simpler models to data generated from a more complex process much outweighed the reduction in the number of parameters. As a result, AIC differences between the best and the next-best model were larger, indicating substantial information loss for simpler models. The AIC approach also provided a sensible ranking of models. For example, when simulating M1-01, M2-01 was identified as the next best model in 73% of the cases, followed by M1-02, and then M2-O2 (Table 6.7b). Similar logical rankings occurred for the other scenarios. There was little effect of the alternate sampling resolutions that were simulated on AIC model identification performance.

Evaluation of Hypotheses by Applying the Model to Field Data

Simple (e.g., R1-M2-O1) and complex (e.g. R2-M4-O3) models applied to data from 2004, 2006, and 2007 showed large differences in fit. In 2004, the simple model provided good fits to the redd count and length-at-age data (Fig. 6.2a i and ii), but the fit to the catch (Fig. 6.2a iii and iv) and length-frequency data (Fig. 6.2a v and vi) was poor. Allowing movement and temporal variation in mortality (model R2-M4-03) resulted in much-improved fits to both total catch (Fig. 6.2b iii and iv) and length-frequency data (Fig. 6.2b v and vi). Fits of simple and complex models to the 2006 (Fig. 6.3a and b) and 2007 (Fig. 6.4a and b) data showed similar patterns described for 2004. The simple model applied to the 2007 data underestimated length-at-age, indicating a potential conflict between growth as determined by direct ageing compared to what is implied based on estimated spawn-timing (as estimated by redd counts) and length-frequency data (Fig. 6.4a ii). This conflict was not evident under a range of more complex model structures, including R2-M4-03 (Fig. 6.4b ii) which allowed age-0 mortality rates to vary over time, thus altering the contribution of cohorts fertilized on different weeks to the length-frequency data. Thus, there is only a conflict between the length-at-age and length-frequency data under the assumption of no temporal variation in incubation or age-0 mortality.

Maximum likelihood estimates of model parameters indicated that there was both ontogenetic movement and differences in mortality rates among habitat types and over time (Table 6.8). As the complexity of movement models increased (i.e., O1 to O3) there was a decline in ϕ and an increase in δ. This occurred because a greater proportion of fish were required to colonize low-angle habitat to compensate for losses to high-angle habitat due to movement. In the absence of movement (O1), mortality rates under M2 were two- (2004, 2006) to four-fold (2007) higher in low-angle habitat than in high-angle habitat. In contrast, mortality rates under M2 with movement (O2 or O3) were much greater in high-angle habitat relative to low-angle habitat, and in a few cases (e.g. R1-M2-O2), the MLEs for the mortality rates in low-angle habitat were constrained by the lower bound (Fig. 6.5). This pattern occurred because mortality rates needed to compensate for losses of fish from low-angle habitat and gains in high-angle habitat resulting from unidirectional movement. Age-0 mortality rates under M1 were similar across years, as were habitat-dependent mortality rates (M2) in most cases (Fig. 6.5). There were substantial deviations in mortality rates for some intervals between sampling trips. Assuming equal mortality rates among habitat types (M3), higher mortality between August and September was evident in all years and between November and December in 2004 (Fig. 6.6a). This pattern was also evident in high-angle habitat (Fig. 6c) when mortality rates were allowed to vary by habitat type (M4). There was generally little scope for variation in mortality rates after the July-August interval in low-angle habitat (Fig. 6.6b) because mortality rates were very low to compensate for increasing losses due to movement as fish grew.

There were substantial differences in many parameters estimates for 2006 compared to other years (Table 6.8c). The total number of redds created in 2004 and 2007 were 25- and 14-fold higher than in 2006, respectively. As age-0 abundance in 2006 was approximately $1/3^{rd}$ of the abundance in other years (see Table 4.3a from Chapter 4), the estimate of the number of the maximum number of emergent fry per redd (ϕ) needed to be four- to seven-fold higher in 2006 to fit both the redd count and age-0 abundance data. There was less evidence for movement in 2006 compared to other years under models where mortality could vary by habitat type (M2 and M4). In the majority of models in 2006 where movement was low (e.g. M4-O2 and M4-O3), mortality rates in low-angle habitat were greater than in high-angle habitat, exactly the opposite of what

was predicted under the same models in 2004 and 2007, which showed substantial movement. Thus, the estimated extent of differences in mortality rates among habitats was determined in large part by the estimated extent of unidirectional movement.

Results from recruitment model R2 suggest that the relative weekly incubation mortality rate up to April 1st (η_{1-18}) was substantial in all study years, especially in 2004 (Table 6.8b) and 2007 (Table 6.8f). This mortality rate did not vary much across model structures within years and averaged 1.75, 0.88, and 2.38 in 2004, 2006, and 2007 translating to incubation survival rates of 0.18, 0.43, and 0.10, respectively (Tables 6.8b, d, and f). There was considerable variation in the maximum number of emergent fry per redd (ϕ) across years, and ϕ was always higher under model R2 compared to R1 to compensate for the additional incubation mortality (η_{1-18}) estimated under the former model. Across years, emergence success in the control period (i.e., ϕ) declined with increases in the estimated number of total redds, and was much higher in 2006 (Fig. 6.7). A negative relationship between estimated incubation success during the treatment period $e^{\eta_{1-18}}\phi$ and total redds was also apparent. If flows were the dominant factor determining incubation success during this period, emergence success would have been considerably lower in 2004 than in other years. This was certainly the case when compared to 2006, however because of potential compensatory survival in 2006 resulting from very low spawning activity, flow and density effects were confounded. Although there was considerably less flow variation up to April 1st in 2007 relative to 2004, emergence success was 1.4-fold higher in 2004. This occurred despite that fact that spawning activity and potential density dependent effects were greater in 2004.

The higher estimates of relative incubation mortality up to April 1st in 2007 was driven in part by the potential discrepancy between length-at-age and spawn-timing and length-frequency data discussed earlier. This discrepancy, which occurred under simpler R1 models (e.g. Fig. 6.4a ii), was not apparent under equivalent R2 models, as seen by differences in estimates of the CV for length-at-age relationships, which were considerably lower under model R2 (typically v_l=0.11-0.12, Table 6.8f) compared to R1 (typically v_l=0.15, Table 6.8e). Higher values of η_{1-18} reduced the abundance of cohorts produced during the first half of the spawning period, which in turn made the length-frequency data more consistent with redd count data. This conflict could also be reduced

169

under R1 models if the mortality and movement dynamics models were sufficiently complex (e.g., M4-03) to reduce the abundance of early cohorts (Table 6.8e). Assuming the length-at-age data from 2007 is not biased, we conclude that there was a greater reduction in emergence success for cohorts spawned before April 1st in 2007 than in 2004, even though there were considerably fluctuations in flow were greater in 2004.

The AIC comparison of 36 alternate models (Table 6.3) clearly identified that the most complex model (R2-M4-03) lost the least amount of information when applied to data from 2004 and 2007 (Table 6.9a and c). The most parsimonious model based on the 2006 data was R2-M4-O1, but there was also substantial and moderate support for R2-M4-O2 and R2-M4-O3, respectively (Table 6.9b). The smallest difference in AIC scores between the best model and others in 2004 and 2007 was 59 and 40, respectively, indicating essentially no support for any of the alternate models. Further, within any mortality model, there was essentially no support for O1 or O2, and within movement models, there was essentially no support for habitat-independent (M1 and M3) or time-independent (M1 and M2) mortality models. Differences in AIC scores in 2006 were smaller and indicate greater uncertainty about the extent of movement. Under the most parsimonious mortality model (M4), O1 was the best model but there was strong and moderate support for O2 and O3, respectively.

The AIC analysis indicated strong support for model R2 in all years, which implies higher incubation mortality for cohorts fertilized before April 1st (Table 6.9). Differences in AIC scores between models R1 and R2 were greatest in 2004 and 2007 relative to 2006, consistent with differences in MLEs for η_{1-18} (Table 6.8). Within years, differences in AIC scores between R1 and R2 were less for models that allowed temporal deviation in mortality rates compared to those that did not. In 2004, when flow fluctuations before April 1st were increased to reduce incubation success (Fig. 6.1), model R3 resulted in a substantial improvement in fit relative to R1, and there was essentially no support for R1 relative to R3 (Table 6.9a). In 2006, when predicted incubation success was high and similar over the entire spawning period (Fig. 6.1), there was essentially no difference in fit or AIC values between R1 and R3. In 2007, values of η_t used in R3 indicate slightly greater incubation survival for cohorts fertilized in January and early-February (Fig. 6.1). This in turn slightly exaggerated the conflict between length-at-age

and spawn-timing and length-frequency data, degrading the fit of R3 relative to R1. The net result was that R3 had essentially no support relative to R1 based on differences in AIC scores.

6.4   Discussion

A comparison of a wide range of candidate models indicated there were substantial differences in age-0 mortality rates between habitat types, across months, but not across years, and that emergence success for cohorts fertilized during the first half of the spawning period (before April 1st) was lower. There was strong evidence for length-dependent movement from low- to high-angle habitat types in 2004 and 2007 but not in 2006. The simulation analysis indicated that a stock synthesis modeling approach can provide a relatively accurate and precise characterization of mortality, growth, and ontogenetic movement for age-0 trout under the levels of sampling effort achieved in this study, and under a wide range of population dynamics. Substantial biases in parameter estimates can occur if the underlying model used in the estimation oversimplifies the true mortality or movement dynamics. However, the evaluation of model identification error indicated that we are unlikely to conclude that there is no evidence for movement or habitat-dependent mortality if it in fact exists.

We hypothesized that the carrying capacity of low-angle shorelines to support age-0 trout is compromised in regulated rivers with considerable hourly variation in flow or that experience erratic flow events. As a result, we would expect mortality rates to be greater in low-angle shorelines due to stranding (Bradford 1997, Saltveit et al. 2001, Halleraker et al. 2003) or indirect effects (Scrutton et al. 2003). Alternatively, age-0 trout may modify their behaviour in low-angle shorelines to limit such mortality (see Chapter 3) as well as actively migrate from low- to high-angle shorelines. Estimated movement rates from low- to high-angle habitat were substantial in 2004 and 2007 and mortality rates were greater in high-angle habitat. These results provide support for the latter hypothesis.

The patterns of movement among habitat types and relative differences in mortality rates that were estimated in this study are consistent with field observations and experimental studies in smaller streams and lakes. The timing and magnitude of

ontogenetic habitat shifts will depend on the relative differences in growth potential and predation risk among habitat types (Werner and Gillian, 1984). Deeper habitats, such as high-angle shorelines, are riskier environments for small fish like age-0 trout if piscivores are present (Schlosser 1987). Thus, it is perhaps not surprising that age-0 mortality rates were greater in high-angle shorelines. Habitats like low-angle cobble bars are normally highly utilized by age-0 trout in smaller unregulated streams (Chapman and Bjornn 1969, Everest and Chapman 1972). However, diurnal variation in stage in the Lee's Ferry reach reduces benthic invertebrate densities (Blinn et al. 1995) and limits the use of immediate nearshore by age-0 trout in low-angle habitats (Chapter 3). As habitat use can depend on relative differences in energetic profitability (Nislow et al. 2000, 2004b), and the fluctuating zones of low-angle shorelines in the Lee's Ferry reach appear to be relatively unprofitable, it is perhaps not surprising that the model indicates that age-0 trout actively migrate to higher-angle shorelines in spite of the greater predation risk and higher mortality in these environments.

There was strong support for length-dependent movement from low- to high-angle habitat across a wide range of likely candidate models in 2004 and 2007, but equivocal support for movement in 2006. We speculate that ontogenetic movement occurred earlier in the summer in 2006 than in other years, which in turn made it more difficult to estimate given the timing of sampling. Alternatively, there was little movement and patterns of abundance were determined based on relative differences in mortality rates and initial rates of colonization (δ). Our data are not sufficient to distinguish among these hypotheses. Note that 2006 was the only year when the maximum population estimate in high-angle habitat was obtained on the first sample period (see Fig. 4.2d of Chapter 4). It is also worth noting that the abundance of age-0 trout in 2006 was approximately 1/3rd the abundance in other study years due to very limited spawning activity. This was caused in part by a 2-fold reduction in the adult population (see Fig. 1.1 of Chapter 1) and low rates of maturation, which were likely caused by a sustained release of oxygen-depleted water from Glen Canyon Dam in 2005 (Ward and Rogers, 2006). It is possible that earlier movement to high-angle habitat in 2006 was driven by either reduced predation risk, or reduced competition with larger conspecifics, in high-angle habitat.

We hypothesized that some unnatural elements of the hydrograph from Glen Canyon Dam have the potential to cause temporal variation in mortality rates for age-0 trout (Chapter 4). In particular, we were interested in the effects of a sudden decrease in the minimum flow that occurs over a brief period between August and September, and the effects of an experimental flood in November 2004 (see Fig. 4.1, Chapter 4). Both of these hypotheses were supported across a range of models that allowed temporal variation in mortality rates. The mortality rate between the August and September sampling trips was generally at least two-fold higher than adjacent periods in all 3 years of study. Determining whether mortality increased over this period relative to adjacent months was not possible based on examination of habitat-specific population trends alone (see Fig. 4.2 of Chapter 4) because those trends are influenced by variable rates of movement among habitat types and variable recruitment to the age-0 population. The effect of the experimental flood in November 2004 was large and very apparent in the both population trends and in the estimated mortality deviations, but it is uncertain whether the flood caused mortality or movement. Both assessments inherently assume that the age-0 trout population is closed, that is, fish cannot move to deep-water habitat that is not sampled within the Lee's Ferry reach, and cannot migrate downstream into Grand Canyon. Given higher current velocities and predation risk in deep-water habitat, we consider it unlikely that it is utilized in any substantive way by age-0 trout, and even more unlikely that movement to deep water would be stimulated by a high flow event. However, it is certainly plausible that high flows resulted in a downstream movement of age-0 fish, and discuss this issue below.

We hypothesized that greater fluctuations in flow during the spawning and incubation period would reduce emergence success (Chapter 5). This hypothesis predicts reduced emergence success for cohorts fertilized before April 1st in 2004 when flow fluctuations were greater, but no difference in success for cohorts fertilized on or after April 1st (control period) because flows were similar (see Fig. 5.1b of Chapter 5). In support of the flow hypothesis, 2004 was the only year when the flow-dependent incubation loss model (R3) provided an improvement in fit and had lower AIC values relative to the null model of constant incubation mortality. However, even in 2004, there was essentially no support for R3 relative to R2. In addition, all other comparisons

showed little evidence of a flow effect. Emergence success during the control period (ϕ) was highly variable among years and was negatively correlated with the estimated total number of redds. During the experimental period, emergence success ($e^{-\eta_{1-18}}\phi$) in 2004 was 1.4-fold higher than in 2007 even though flow fluctuations in 2004 were greater as were negative density-dependent effects due to greater spawning activity. Emergence success before April 1st was much higher in 2006 under less fluctuating conditions, but since spawning activity was over an order of magnitude lower than in 2004, the effect of reduced fluctuations was confounded with potentially reduced density-dependent mortality. Emergence success during the control period was much higher in 2006 than in other years, clearly indicating strong density-dependent effects. Given the effect of spawning activity on emergence success during both control and treatment periods, and higher emergence success during the treatment period in 2004 compared to 2007 when flows were more stable, it seems reasonable to conclude that the extent of spawning activity, rather than flow, is the most important variable controlling emergence success in the Lee's Ferry reach over the range of flows that were investigated, and that the enhanced fluctuations in 2004 did not result in any measurable reduction in the abundance of the age-0 population. As described earlier, estimates of emergence success and age-0 mortality are partially confounded because we do not capture fish immediately after they emerge. Our data are therefore not adequate to determine whether the majority of density-dependence occurs at spawning, incubation, or in the month between emergence and first capture. Nevertheless, our conclusions about the effect of spawning activity and flow on survival between spawning and first capture based on the stock synthesis model are consistent with those from the stock-recruitment and hatch date analysis presented in Chapter 5. The benefit of the stock synthesis approach is that it showed that there was temporal variation in emergence success in both treatment and control years, and demonstrated that the extent of this variation was consistent across various assumptions about movement and mortality of age-0 trout.

The stock synthesis model provides a viable way for estimating age-0 mortality rates and is therefore a useful long-term monitoring tool. Estimated weekly instantaneous mortality rates typically ranged from 0.03–0.12 based on habitat-dependent mortality models (M2, M4), and from 0.04-0.1 based on habitat-independent models (M1, M3).

These values are consistent with age-0 summer mortality rates reported for smaller streams for Atlantic salmon (Nislow et al. 2004a: 0.07-0.14; Einum and Nislow 2005: 0.01-0.19), brown trout (Berg and Joregensen 1991: 0.05; Elliot 1994: 0.08), and rainbow trout (Hume and Parkinson 1988; 0.02-0.04). Mortality estimates from the habitat-independent stock synthesis models were in close agreement with estimates determined from the ratio of November to July age-0 abundance, which ranged from 0.03-0.10 (see Table 4.3a of Chapter 4). Mortality rates in low-angle habitat based on the ratio of abundances tended (see Table 4.3b of Chapter 4) to be higher than those from the stock synthesis model because the ratio method does not account for movement from low- to high-angle habitat.

This analysis assumes that the age-0 population in the Lee's Ferry reach is effectively closed with respect to emigration. If a substantial number of age-0 trout migrate downstream into Grand Canyon, estimates of mortality will be inflated. Densities of age-0 trout in the Lee's Ferry reach were 12- and 15-fold higher than densities in the first 60 miles downstream of the Lee's Ferry reach in June and August, 2004 (Korman et al. 2005). These differences indicate that downstream movement of age-0 trout during the summer of 2004 was negligible. A recent comparison of historical (1991-2004) length frequency distributions based on electrofishing at increasing distances from Glen Canyon Dam shows a distinct absence of age-0 fish downstream of the Lee's Ferry reach (Coggins 2008), further supporting our assumption that the Lee's Ferry reach can be treated as effectively closed for age-0 trout.

Improvements in experimental design would strengthen inferences concerning the main hypothesis addressed in this study. Additional replicates are needed to increase certainty in the relationship between early survival rates (fertilization to one- to two-months from fry emergence) and the number of redds, and to determine whether residuals from this relationship are related to flow. Additional replicates are also needed to better understand the effects of juvenile density, predation risk, and flow, on the timing and extent of ontogenetic habitat shifts and habitat-specific mortality rates. Most importantly, stronger inferences regarding effects of flow on age-0 mortality requires the implementation of a flow treatment that reduces the extent of hourly flow fluctuations during the summer and fall rearing period. Although this study has provided some

relatively rare estimates of mortality for juvenile fish in a large river, the extent to which these parameters depend on the flow regime is still uncertain.

The stock synthesis model described in this paper integrates multiple sources of information within a single framework to jointly estimate key early life history parameters under a wide range of alternate model structures. Although limitations in experimental design reduced the strength of inferences with respect to our primary recruitment, mortality, and movement hypotheses, this study has advanced our understanding of these dynamics in large regulated rivers. The model and sampling program can be used to quantify incubation success, and the growth, movement, and mortality rates of age-0 fish, and should be a useful tool for assessing responses of salmonid populations to various habitat improvement efforts in the Colorado River and in other systems.

Table 6.1. Model indices, constants, and parameters, Numbers in parentheses denote the value of constants.

Variable Name	Variable Description
Indices	
t, T	model week index (t=1-52) and terminal week (T=52)
i	Index for blocks of weeks between each age-0 sampling trip
j	Length interval index (1-31, representing 5 mm size classes from 20-175 mm)
k	Length-at-age sample index
a, A	Weekly age index (1-52) and terminal age (52)
h	Low- (h=L) or high- (h=H) angle habitat type
Constants	
S	Redd survey life (4 weeks)
W_t	Number of weeks between fertilization and emergence (8-10 wks.)
C	Allometric exponent of the mortality-fork length relationship (-1)
l_r	Reference fork length for allometric mortality-fork length relationship (50 mm)
$E_{h,i}$	Effort (proportion of shoreline length sampled by type and trip, ca.=0.025/0.045)
Parameters for Process Model	
χ	Total redds excavated per year
γ	Week of peak spawning
α	Relative precision in spawn timing
η_t	Relative weekly instantaneous incubation mortality rate
ϕ	Number of fish that emerge per redd assuming no incubation mortality (η_t=1)
δ	Proportion of fry that migrate to low-angle habitat after emergence
μ_h	Base weekly instantaneous mortality rate by habitat type
ρ_0	Maximum proportion moving from low- to high-angle habitat per week
ρ_μ	Fork length at which movement rate is reduced to 50% of the maximum (ρ_0)
ρ_σ	Standard deviation (inverse of slope) of movement-fork length relationship
κ	Brody growth coefficient
λ_1	Fork length one week from emergence (at age a_1)
λ_A	Fork length one year from emergence (at terminal age A)
$\varepsilon_{h,i}$	Mortality deviations by habitat type and block of weeks between sampling intervals
Parameters for Observation Model	
ν_l	Coefficient of variation (CV) in length-at-age
π_h	Probability of capture for fish large enough to be fully vulnerable
ψ_h	Fork length at which capture probability is reduced to 50% of the maximum (π_h)
τ_h	Standard deviation (inverse of slope) of capture probability-fork length relationship

Table 6.2. Summary of initial values and lower and upper bounds for parameters of the estimation model, and parameters used to generate data for the simulation analysis. 'L' and 'H' denote low- and high-angle habitat respectively. Parameters where the lower and upper bounds are denoted as fixed indicates that the parameters are fixed at the initial values and not estimated. See Table 6.1 for definition of parameters.

Parameter	Estimation		Simulation Scenario		
	Initial Values	**Lower and Upper Bounds**	**All Scenarios**		
χ	200	10 - 5000	2000		
γ	15	1 - 40	15		
α	10	1 - 500	10		
η_t	0	0 - 5	0		
ϕ	1000	100 - 1E6	1000		
δ	0.56	0.001 - 1	0.56		
κ	0.005	0.001 - 5	0.015		
λ_1	20	1 - 50	20		
λ_A	150	100 - 200	135		
$\varepsilon_{h,i}$	0	-1.5 - 1.5	0		
ν_l	0.1	0.01 - 0.3	0.1		
π_h	L=0.34, H=0.31	Fixed	L=0.34, H=0.31		
ψ_h	L=26.61, H=39.89	Fixed	L=26.61, 2.60 H=39.89, 4.57		
τ_h	L=2.60, H=4.57	Fixed			
			M1	**M2**	
μ_L	0.1	0.001 - 2	0.1	0.15	
μ_H	0.1	0.001 - 2	0.1	0.05	
			O1	**O2**	**O3**
ρ_0	0.27	0 - 1	0	0.15	0.15
ρ_μ	50	1 - 150	10	10	50
ρ_σ	5	0.1 - 1E6	.1	.5	2

Table 6.3. Parameterization for alternate models of incubation success (recruitment), and age-0 mortality and movement. For model R3, 'f(flow)' denotes that incubation mortality is predicted based on the flow-dependent incubation loss model (see Chapter 5). See Table 6.1 for definition of parameters.

Model Type	Model Description	Model Code	Estimated Parameters	Fixed Parameters
Recruitment	Null	R1		$\eta_t=0$
	Flow-Regime	R2	$\eta_1=\eta_{2,\dots}=\eta_{18}$	$\eta_{19\text{-}52}=0$
	Flow-Forcing	R3		$\eta_t=f(flow)$
Mortality	Null	M1	μ_L	$\mu_H=\mu_L,\ \varepsilon_{h,i}=0$
	Habitat	M2	$\mu_L,\ \mu_H$	$\varepsilon_{h,i}=0$
	Temporal Deviations	M3	$\mu_L,\ \varepsilon_{L,i}$	$\mu_H=\mu_L,\ \varepsilon_{H,i}=\varepsilon_{L,i}$
	Deviations by Habitat	M4	$\mu_L,\ \mu_H,\ \varepsilon_{h,i}$	
Movement	Null	O1		$\rho_0=0,\ \rho_\mu=10,\ \rho_\sigma=0.1$
	Constant	O2	ρ_0	$\rho_\mu=10,\ \rho_\sigma=0.1$
	Fork length	O3	$\rho_0,\ \rho_\mu,\ \rho_\sigma$	

Table 6.4. Maximum likelihood estimates (MLE), coefficient of variation (CV) in MLEs, and Pearson correlation coefficients describing covariance among parameters for a single simulation trial where model R1-M2-O3 was used for both simulation and estimation. Correlations greater than ± 0.4 are highlighted in bold. See Table 6.1 for definition of model parameters.

Parameter	Simulated Value	MLE	CV of MLE	χ	γ	α	ϕ	δ	κ	λ_1	λ_A	ν_l	ρ_0	ρ_μ	ρ_σ	μ_L
χ	2000	1930	0.02													
γ	15	15.3	0.01	0.23												
α	10	10.5	0.02	0.05	0.31											
ϕ	1000	942	0.06	**-0.46**	-0.33	-0.04										
δ	0.56	0.54	0.05	-0.03	-0.14	0.04	**0.53**									
κ	0.015	0.016	0.09	0.02	0.13	0.22	0.24	**0.52**								
λ_1	20	20	0.02	0.06	0.23	-0.13	**-0.50**	**-0.49**	**-0.72**							
λ_A	135	133	0.01	0.01	0.00	-0.18	-0.19	**-0.50**	**-0.95**	**0.58**						
ν_l	0.1	0.11	0.02	-0.04	-0.10	**0.48**	0.05	0.09	0.19	-0.14	-0.27					
ρ_0	0.15	0.16	0.21	0.00	0.01	0.00	-0.18	-0.01	-0.06	0.03	0.07	-0.01				
ρ_μ	50	48.3	0.11	-0.01	-0.02	0.00	0.08	0.31	0.11	-0.09	-0.12	0.01	**0.86**			
ρ_σ	2	4.49	0.85	0.00	0.01	-0.02	-0.25	0.07	-0.06	0.04	0.07	-0.03	**0.84**	**0.74**		
μ_L	0.15	0.14	0.08	-0.01	-0.05	0.03	**0.71**	**0.73**	0.38	-0.34	-0.36	0.04	-0.32	0.11	-0.41	
μ_H	0.05	0.05	0.07	0.01	0.04	-0.08	-0.19	**-0.75**	**-0.52**	0.28	**0.59**	-0.16	0.22	-0.14	0.23	**-0.66**

Table 6.5. Bias (%) in model parameters under alternate mortality (M) and movement (O) models based on low-resolution sampling regime and the same simulation and estimation model types. The last 4 rows show the difference between the estimated and true simulated proportion moving from low- to high-angle habitat types per week for fish with fork lengths of 22.5, 42.5, 62.5, and 82.5 mm. See Tables 6.1 and 6.3 for definition of model parameters and structures, respectively.

	Model Structure					
Simulated	M1	M2	M1	M2	M1	M2
	O1	O1	O2	O2	O3	O3
Estimated	M1	M2	M1	M2	M1	M2
	O1	O1	O2	O2	O3	O3
Parameter						
χ	1.2	2.2	2.4	0.4	0.4	0.4
γ	2.0	3.4	4.0	0.5	0.5	0.5
α	2.6	1.1	0.6	2.5	3.0	2.9
ϕ	-4.3	-4.2	-5.4	-4.8	-3.5	-2.9
δ	0.1	-0.1	-0.5	-1.6	0.3	0.4
κ	10.5	5.6	6.4	3.6	9.4	7.8
λ_1	0.6	1.0	1.4	1.1	0.2	0.1
λ_A	-1.9	-1.3	-1.4	-0.5	-1.3	-1.0
ν_1	6.4	4.4	4.0	3.2	4.9	3.8
ρ_0			-0.1	-1.8	-1.7	-5.7
ρ_μ					0.6	3.8
ρ_σ					-20.8	3.4
μ_L	-2.3	-1.3	-2.6	-4.4	-1.2	-0.6
μ_H		-5.0		-1.5		-2.5
Mv_22.5	0.00	0.00	0.00	0.01	0.00	0.00
Mv_42.5	0.00	0.00	0.00	0.01	0.00	0.00
Mv_62.5	0.00	0.00	0.00	0.01	0.00	0.00
Mv_82.5	0.00	0.00	0.00	0.01	0.00	0.01

Table 6.6. Bias (%) in model parameters under alternate mortality (M) and movement (O) models based on low-resolution sampling regime with different simulation and estimation model structures. The last 4 rows show the difference between the estimated and true simulated proportion moving from low- to high-angle habitat types per week for fish with fork lengths of 22.5, 42.5, 62.5, and 82.5 mm. See Tables 6.1 and 6.3 for definition of model parameters and structures, respectively.

	Model							
Simulated	M1	M1	M2	M2	M2	M2	M2	M2
	O1	O1	O1	O1	O2	O2	O3	O3
Estimated	M2	M2	M1	M2	M2	M2	M2	M2
	O1	O3	O1	O3	O1	O3	O1	O2
Parameter								
χ	1.2	0.3	0.8	0.3	1.2	1.5	2.1	3.3
γ	2.1	0.4	0.9	0.5	1.9	2.4	3.3	5.2
α	2.6	3.7	3.3	3.1	1.8	1.3	1.1	-0.6
ϕ	-4.3	-2.5	-11.1	-5.6	29.5	-1.7	14.3	-22.8
δ	0.5	-1.9	-60.1	-1.9	-6.4	-5.6	21.1	23.2
κ	10.6	10.9	-35.6	4.4	14.1	3.7	24.9	-2.5
λ_1	0.5	-0.1	6.4	1.0	-0.6	1.3	-2.6	2.1
λ_A	-1.9	-1.6	5.6	-0.6	-2.1	-0.8	-3.6	-0.2
ν_l	6.4	6.1	3.5	4.3	3.9	3.1	4.5	3.2
ρ_0		-54.3		-68.3		-76.9		26.2
ρ_μ		24.3		39.0		654.0		
ρ_σ		>1000		>1000		>1000		
μ_L	-2.1	-4.2	-48.2	-5.4	76.5	5.5	24.4	-38.1
μ_H	-2.7	2.7	55.3	1.7	-15.4	-4.1	-29.6	11.9
Mv_22.5	0.00	0.00	0.0	0.01	-0.15	-0.03	0.00	0.10
Mv_42.5	0.00	0.00	0.0	0.01	-0.15	-0.01	0.00	0.10
Mv_62.5	0.00	0.00	0.0	0.01	-0.15	0.00	-0.15	-0.05
Mv_82.5	0.00	0.00	0.0	0.01	-0.15	0.02	-0.15	-0.05

Table 6.7. Assessment of the Akaike Information Criteria (AIC) to identify the correct data-generating model. One hundred data sets were generated from each of six alternate simulation models. AIC statistics were then computed by estimating parameters for all models applied to each of the 100 trials for each set of simulations. The percentage of trials where the correct data-generating model was identified, and the average difference between the lowest AIC and the next lowest AIC for these cases, are shown for both low- and high-resolution sampling regimes (a). In cases where the data-generating model was identified correctly, b) shows the distribution of models that had the next lowest AIC (% of trials). See Table 6.3 for definition of alternate model structures.

a)

Simulation Type		Low-Resolution		High-Resolution	
Mortality	Movement	% Correct Identification	Avg. ΔAIC	% Correct Identification	Avg. ΔAIC
M1	O1	93	1.59	94	1.63
M2	O1	91	1.81	95	1.84
M1	O2	82	1.49	83	1.56
M2	O2	91	2.87	96	3.65
M1	O3	89	9.42	90	5.16
M2	O3	99	22.7	98	42.25

b)

Mortality	Mortality Movement	M1 O1	M2 O1	M1 O2	M2 O2	M1 O3	M2 O3
Low-resolution sampling regime							
M1	O1		73	22	5	0	0
M2	O1	0		2	90	0	8
M1	O2	0	0		88	6	5
M2	O2	0	1	49		1	49
M1	O3	0	0	4	8		89
M2	O3	0	0	2	5	93	
High-resolution sampling regime							
M1	O1		74	25	1	0	0
M2	O1	0		0	98	0	2
M1	O2	0	0		91	5	4
M2	O2	0	5	16		1	77
M1	O3	0	0	1	9		90
M2	O3	0	0	2	7	91	

Table 6.8. Maximum likelihood estimates of model parameters based on recruitment models R1 and R2 for 2004 (a, b), 2006 (c, d), and 2007 (d, e). See Tables 6.1 and 6.3 for definitions of model parameters and structures, respectively. Blank cells denote that the parameter was not estimated.

a) R1 2004

Parameter	M1			M2			M3			M4		
	O1	O2	O3	O1	O2	O3	O1	O2	O3	O1	O2	O3
χ	2250	2260	2260	2260	2260	2260	2223	2235	2239	2225	2228	2225
γ	14.7	14.7	14.7	14.7	14.7	14.6	13.9	14.0	14.0	13.8	13.9	13.9
α	6.9	6.8	6.7	6.8	6.8	6.8	6.7	6.4	6.3	6.6	6.5	6.6
ϕ	581	463	500	640	311	400	681	478	519	976	437	585
η_{1-18}												
δ	0.35	0.78	0.52	0.72	0.72	0.26	0.35	0.77	0.52	0.75	0.72	0.35
κ	0.015	0.022	0.020	0.026	0.014	0.010	0.023	0.026	0.023	0.035	0.024	0.018
λ_1	17	16	17	16	17	18	16	16	17	15	16	16
λ_A	146	137	141	133	149	156	144	137	142	131	144	153
ν_l	0.18	0.17	0.16	0.16	0.17	0.18	0.17	0.16	0.16	0.16	0.16	0.16
ρ_0		0.09	0.15		0.20	0.25		0.10	0.14		0.18	0.25
ρ_μ			38.50			32.40			36.35			36.43
ρ_σ			0.14			2.24			0.15			0.13
μ_L	0.12	0.11	0.12	0.18	0.00	0.00	0.13	0.12	0.12	0.28	0.02	0.03
μ_H				0.08	0.16	0.17				0.09	0.14	0.14

Table 6.8. Con't.

Parameter	M1			M2			M3			M4		
	O1	O2	O3	O1	O2	O3	O1	O2	O3	O1	O2	O3
χ	2210	2210	2220	2210	2210	2210	2220	2230	2230	2220	2220	2210
γ	13.8	13.9	13.9	13.9	13.9	13.9	13.7	13.8	13.8	13.8	13.8	13.7
α	7.2	7.0	6.9	7.0	7.0	7.0	6.7	6.5	6.4	6.7	6.7	6.7
ϕ	909	715	765	802	626	651	750	533	586	686	556	644
η_{1-18}	1.73	1.67	1.6	1.68	1.67	1.63	1.84	1.86	1.78	1.85	1.83	1.82
δ	0.34	0.62	0.48	0.57	0.60	0.42	0.35	0.66	0.51	0.64	0.73	0.50
κ	0.014	0.018	0.017	0.019	0.011	0.009	0.005	0.004	0.006	0.007	0.005	0.005
λ_1	23	23	23	23	23	23	23	25	24	25	24	23
λ_A	155	147	149	144	160	165	166	163	162	157	165	169
ν_l	0.17	0.16	0.16	0.17	0.17	0.16	0.17	0.17	0.16	0.17	0.16	0.16
ρ_0		0.05	0.07		0.11	0.14		0.09	0.13		0.14	0.23
ρ_μ			38.70			30.10			38.00			39.20
ρ_σ			0.10			5.21			0.10			0.13
μ_L	0.12	0.12	0.12	0.18	0.00	0.00	0.11	0.09	0.10	0.23	0.03	0.03
μ_H				0.09	0.17	0.17				0.06	0.11	0.12

Table 6.8. Con't.

c)   R1   2006

Parameter	M1			M2			M3			M4		
	O1	O2	O3	O1	O2	O3	O1	O2	O3	O1	O2	O3
χ	89	89	89	89	89	89	89	90	90	88	88	88
γ	17.7	17.7	17.7	17.7	17.8	17.8	16.7	16.8	16.7	16.7	16.7	16.7
α	8.2	8.2	8.2	8.2	8.2	8.2	7.3	6.8	6.8	7.4	7.4	7.4
ϕ	3780	3330	3630	3540	3140	3630	4392	2986	3433	4224	4224	4224
η_{1-18}												
δ	0.28	0.46	0.35	0.48	0.39	0.33	0.28	0.51	0.37	0.42	0.42	0.42
κ	0.027	0.033	0.030	0.035	0.028	0.029	0.029	0.033	0.031	0.034	0.034	0.034
λ_1	25	24	24	24	25	25	25	24	24	24	24	24
λ_A	136	129	131	126	135	133	133	127	129	127	127	127
ν_1	0.12	0.12	0.12	0.12	0.12	0.12	0.12	0.13	0.13	0.12	0.12	0.12
ρ_0		0.07	0.12		0.17	0.13		0.08	0.13		0.00	0.01
ρ_μ			47.10			45.40			47.05			113.75
ρ_σ			0.14			0.10			0.17			0.14
μ_L	0.11	0.11	0.11	0.17	0.00	0.10	0.07	0.06	0.07	0.11	0.11	0.11
μ_H				0.08	0.14	0.12				0.06	0.06	0.06

Table 6.8. Con't.

d)   R2   2006

Parameter	M1			M2			M3			M4		
	O1	O2	O3	O1	O2	O3	O1	O2	O3	O1	O2	O3
χ	89	89	89	89	89	89	88	89	89	88	88	88
γ	16.3	16.2	16.2	16.2	16.2	16.2	16.8	16.8	16.8	16.7	16.7	16.7
α	7.0	7.0	7.0	7.0	7.0	7.0	8.0	7.3	7.5	7.7	7.7	7.7
ϕ	4720	4240	4600	4510	3990	4634	4500	3180	3610	4290	4290	4290
η_{1-18}	0.65	0.69	0.69	0.68	0.69	0.69	1.24	1.13	1.20	0.95	0.95	0.95
δ	0.28	0.47	0.36	0.48	0.41	0.33	0.28	0.50	0.38	0.42	0.42	0.42
κ	0.029	0.036	0.034	0.038	0.031	0.032	0.030	0.034	0.033	0.034	0.034	0.034
λ_1	25	24	24	24	24	24	25	24	25	24	24	24
λ_A	133	126	128	123	131	130	131	125	127	126	126	126
ν_l	0.12	0.12	0.12	0.12	0.12	0.12	0.12	0.12	0.12	0.12	0.12	0.12
ρ_0		0.07	0.12		0.16	0.14		0.08	0.13		0.00	0.00
ρ_μ			47.30			45.60			47.10			117.00
ρ_σ			0.15			0.10			0.12			1.29
μ_L	0.11	0.10	0.11	0.16	0.00	0.09	0.04	0.04	0.04	0.09	0.09	0.09
μ_H				0.07	0.14	0.11				0.04	0.04	0.04

Table 6.8. Con't.

e)   R1   2007

Parameter	M1			M2			M3			M4		
	O1	O2	O3	O1	O2	O3	O1	O2	O3	O1	O2	O3
χ	1260	1270	1270	1270	1270	1270	1215	1230	1230	1212	1208	1208
γ	15.3	15.4	15.4	15.5	15.4	15.4	13.4	13.3	13.3	13.3	13.2	13.1
α	6.0	5.6	5.6	5.6	5.6	5.6	4.3	3.8	3.8	4.3	4.3	4.2
ϕ	879	694	694	907	494	540	1392	954	988	1411	956	1078
η_{1-18}												
δ	0.39	0.86	0.86	0.77	0.96	0.57	0.39	0.79	0.68	0.74	0.98	0.65
κ	0.017	0.021	0.021	0.027	0.013	0.012	0.021	0.017	0.018	0.020	0.009	0.007
λ_1	18	19	19	18	19	19	20	22	22	23	24	23
λ_A	132	127	127	121	139	141	139	140	140	135	156	163
ν_l	0.17	0.15	0.15	0.15	0.15	0.15	0.15	0.13	0.13	0.14	0.13	0.12
ρ_0		0.08	0.15		0.15	0.16		0.08	0.08		0.11	0.16
ρ_μ			11.90			27.00			26.78			39.12
ρ_σ			1000000			0.10			0.10			0.13
μ_L	0.08	0.07	0.07	0.13	0.00	0.00	0.10	0.09	0.09	0.16	0.04	0.04
μ_H				0.03	0.12	0.12				0.03	0.08	0.09

Table 6.8. Con't.

f)   R2   2007

Parameter	M1			M2			M3			M4		
	O1	O2	O3	O1	O2	O3	O1	O2	O3	O1	O2	O3
χ	1210	1210	1210	1210	1210	1210	1210	1220	1220	1200	1210	1200
γ	13.4	13.4	13.4	13.3	13.4	13.4	13.7	13.7	13.7	13.4	13.7	13.7
α	4.5	4.4	4.4	4.4	4.4	4.4	4.8	4.4	4.4	4.7	5.1	5.2
ϕ	1540	1300	1300	1470	1160	1160	1600	1130	1130	1590	1250	1400
η_{1-18}	2.16	2.05	2.05	2.1	2.01	2.01	2.96	2.58	2.58	2.32	2.84	2.93
δ	0.39	0.69	0.69	0.66	0.71	0.71	0.38	0.70	0.70	0.70	0.82	0.67
κ	0.013	0.017	0.017	0.023	0.012	0.012	0.016	0.013	0.013	0.019	0.011	0.010
λ_1	27	27	27	26	27	27	27	28	28	27	27	27
λ_A	150	144	144	134	152	152	145	145	145	137	152	155
ν_1	0.13	0.12	0.12	0.12	0.11	0.11	0.14	0.12	0.12	0.13	0.12	0.12
ρ_0		0.08	0.08		0.14	0.14		0.08	0.08		0.11	0.14
ρ_μ			24.30			23.50			20.50			39.50
ρ_σ			0.10			0.14			0.28			0.14
μ_L	0.09	0.09	0.09	0.16	0.03	0.03	0.05	0.05	0.05	0.14	0.02	0.02
μ_H				0.04	0.12	0.12				0.02	0.05	0.05

Table 6.9. Comparison of model fit, AIC, and differences in AIC for alternate recruitment, mortality and movement models applied to data from 2004 (a), 2006 (b), and 2007 (c). Bolded values denote models with the lowest AIC scores within recruitment models. ΔAIC is the difference between each models AIC and the lowest AIC across all models, within years. See Table 6.3 for definition of alternate model structures.

a) 2004

Mortality Model	Movement Model	# Parameters Recruitment Model			Log Likelihood Recruitment Model			AIC Recruitment Model			ΔAIC Recruitment Model		
		R1	R2	R3	R1	R2	R3	R1	R2	R3	R1	R2	R3
M1	O1	10	11	10	-2747	-2472	-2667	5514	4966	5354	1,270	723	1,110
	O2	11	12	11	-2557	-2309	-2482	5136	4642	4986	892	398	743
	O3	13	14	13	-2527	-2290	-2451	5080	4607	4929	837	364	685
M2	O1	11	12	11	-2596	-2343	-2519	5215	4710	5060	971	466	816
	O2	12	13	12	-2520	-2269	-2447	5064	4565	4918	821	321	675
	O3	14	15	14	-2498	-2258	-2427	5024	4546	4883	780	302	639
M3	O1	18	19	18	-2421	-2363	-2396	4878	4764	4828	635	521	585
	O2	19	20	19	-2234	-2168	-2207	4505	4377	4451	262	133	208
	O3	21	22	21	-2213	-2155	-2183	4468	4354	4409	225	110	165
M4	O1	27	28	27	-2232	-2165	-2205	4518	4386	4465	275	143	221
	O2	28	29	28	-2197	-2134	-2166	4450	4325	4388	206	82	145
	O3	**30**	**31**	**30**	**-2148**	**-2091**	**-2121**	**4356**	**4244**	**4303**	**113**	**0**	**59**

Table 6.9. Con't.

b) 2006

Mortality Model	Movement Model	# Parameters Recruitment Model			Log Likelihood Recruitment Model			AIC Recruitment Model			ΔAIC Recruitment Model		
		R1	R2	R3	R1	R2	R3	R1	R2	R3	R1	R2	R3
M1	O1	10	11	10	-818	-807	-818	1657	1636	1656	247	226	246
	O2	11	12	11	-787	-774	-787	1596	1573	1596	186	163	186
	O3	13	14	13	-781	-768	-781	1588	1564	1587	178	154	177
M2	O1	11	12	11	-790	-778	-790	1603	1580	1602	193	170	192
	O2	12	13	12	-785	-772	-785	1595	1571	1594	185	161	184
	O3	14	15	14	-781	-768	-780	1590	1566	1589	180	156	179
M3	O1	15	16	15	-763	-752	-763	1555	1536	1556	146	126	146
	O2	16	17	16	-726	-716	-727	1485	1465	1485	75	55	75
	O3	18	19	18	-721	-709	-721	1477	1457	1478	67	47	68
M4	**O1**	**21**	**22**	**21**	**-690**	**-683**	**-690**	**1423**	**1410**	**1423**	**13**	**0**	**13**
	O2	22	23	22	-690	-683	-690	1425	1412	1425	15	2	15
	O3	24	25	24	-690	-683	-690	1429	1416	1429	19	6	19

Table 6.9. Con't.

c) 2007

Mortality Model	Movement Model	# Parameters Recruitment Model			Log Likelihood Recruitment Model			AIC Recruitment Model			ΔAIC Recruitment Model		
		R1	R2	R3	R1	R2	R3	R1	R2	R3	R1	R2	R3
M1	O1	10	11	10	-1889	-1566	-1907	3799	3153	3833	1,528	883	1,562
	O2	11	12	11	-1695	-1364	-1714	3411	2751	3450	1,140	481	1,180
	O3	13	14	13	-1695	-1364	-1711	3415	2755	3448	1,144	485	1,177
M2	O1	11	12	11	-1717	-1373	-1736	3456	2770	3494	1,185	499	1,223
	O2	12	13	12	-1679	-1361	-1699	3382	2748	3423	1,111	478	1,152
	O3	14	15	14	-1675	-1361	-1696	3378	2752	3419	1,107	482	1,149
M3	O1	15	16	15	-1637	-1515	-1645	3305	3062	3321	1,034	792	1,050
	O2	16	17	16	-1438	-1318	-1451	2907	2670	2935	636	399	664
	O3	18	19	18	-1436	-1318	-1451	2908	2674	2939	637	403	668
M4	O1	21	22	21	-1324	-1179	-1335	2691	2403	2712	420	132	441
	O2	22	23	22	-1279	-1133	-1291	2603	2311	2627	332	40	356
	O3	**24**	**25**	**24**	**-1264**	**-1110**	**-1277**	**2577**	**2271**	**2602**	**306**	**0**	**332**
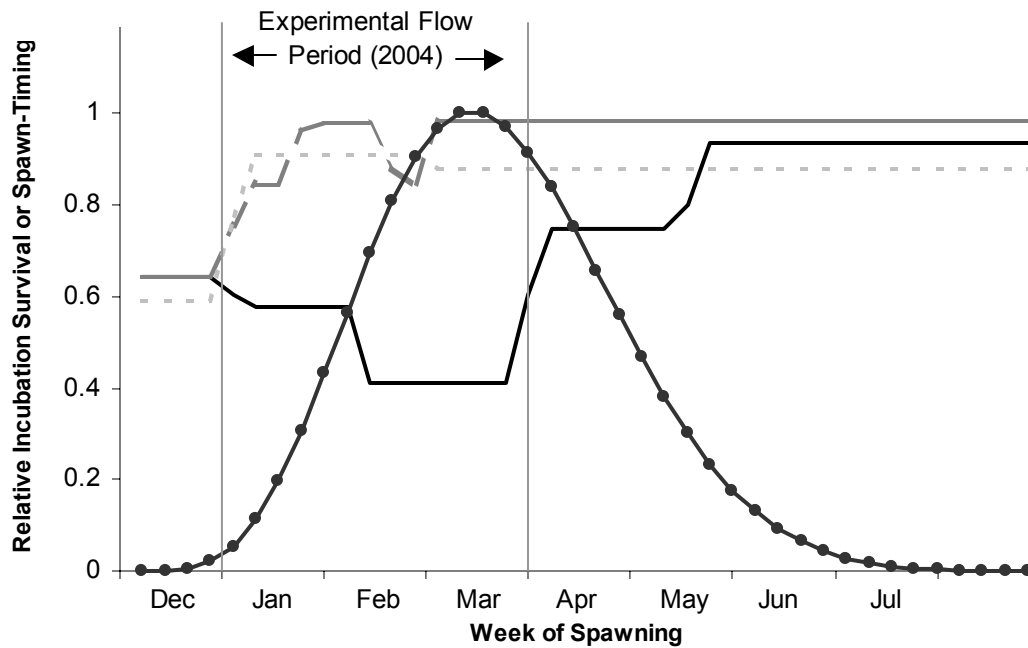
Figure 6.1. Predictions of temporal variation in incubation survival for weekly cohorts (by spawning date) determined based on measured redd hypsometry, intergravel temperatures, estimated incubation time, and assumed lethal temperature limits for incubating stages (see Flow-dependent incubation loss model from Chapter 5). Predictions for 2004, 2006, and 2007 are denoted by the solid black line, dashed dark gray line, and dotted light gray line, respectively. For reference, typical spawn-timing (α=15, β=6 from Eqn. 1) is shown by the black solid line with circles. The vertical solid gray lines denote the period in 2004 when daily fluctuations in flow were increased to reduce incubation success.

a)
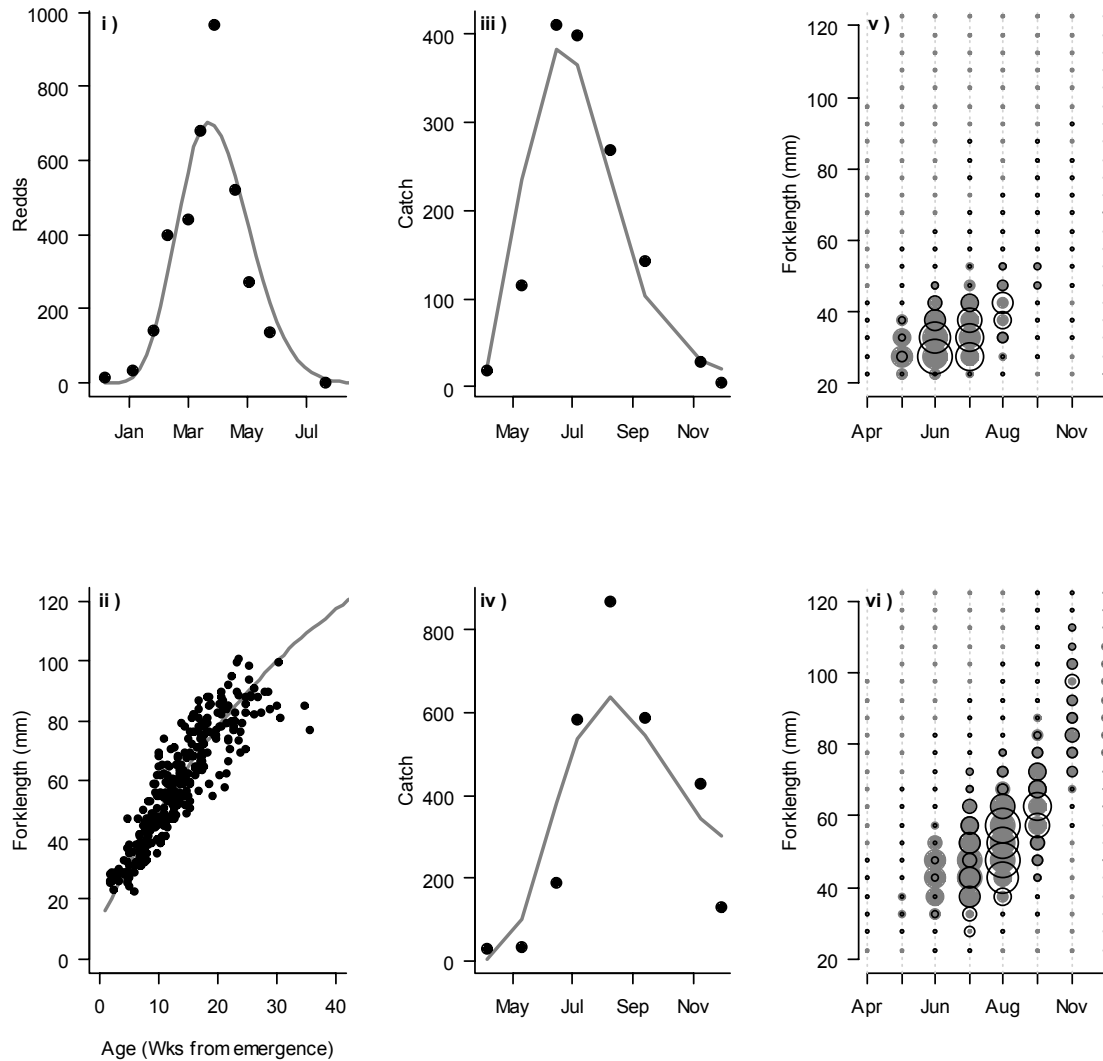
Figure 6.2. Comparison of most likely fits to data from 2004 based on models R1-M2-O1 (a) and R2-M4-O3 (b). Graphs i-iv show predicted (gray lines) and observed (solid black circles) redd counts by survey (i), length-at-age (ii), and catch in low- (iii) and high- (iv) angle habitats by survey. Graphs v and vi show predicted (solid gray circles) and observed (open black circles) catch by 5 mm length categories and sampling trip in low- and high-angle habitat, respectively. For v) and vi), the size of the circles is proportional to the ratio of catch per sampling trip and length category relative to the maximum catch over all the strata. Open black circles that are larger than solid gray circles represent over predictions while the converse represent under predictions. See Table 6.3 for definition of model structures.

194

b)

Figure 6.2. Con't.

195
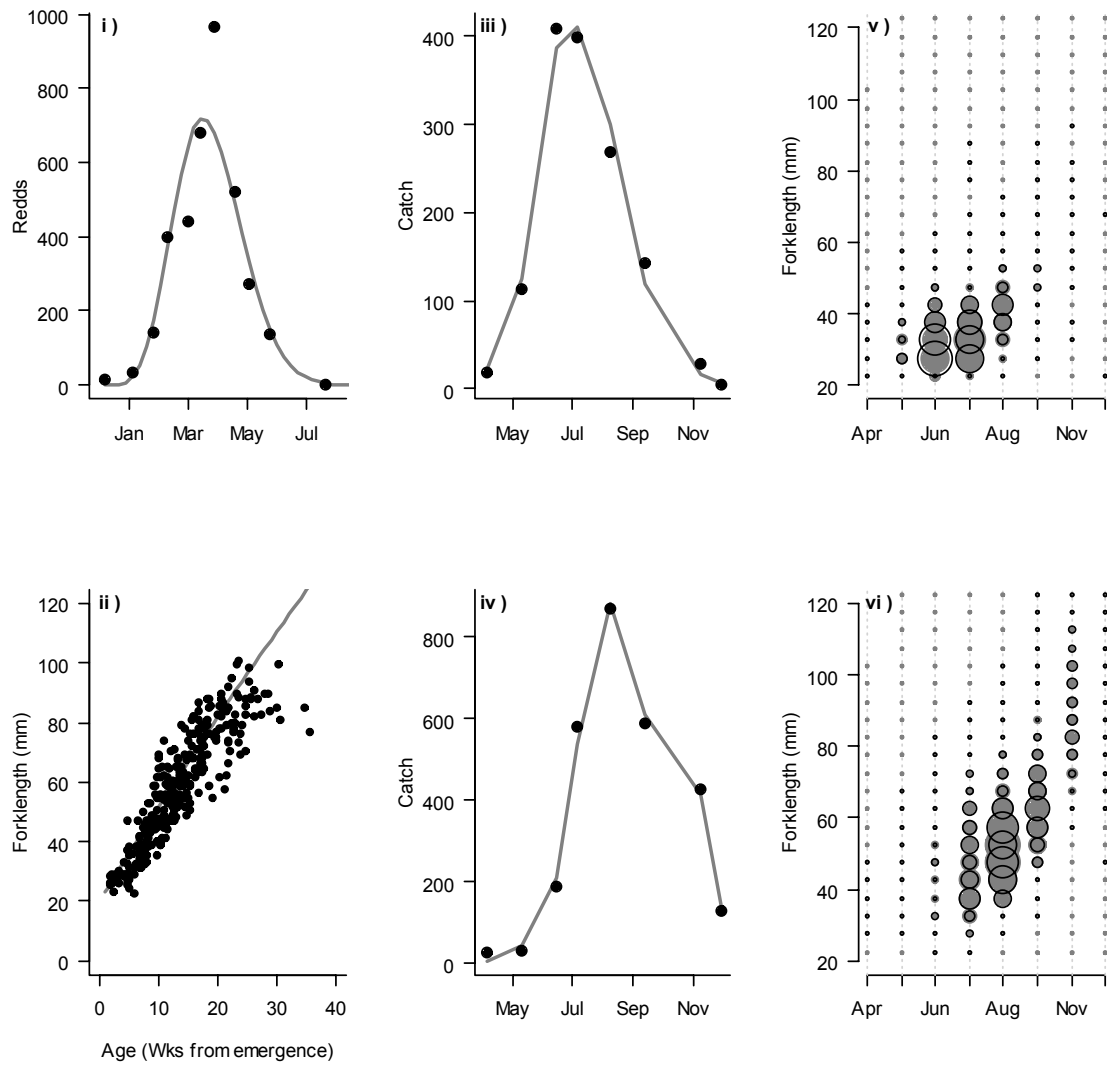
a)
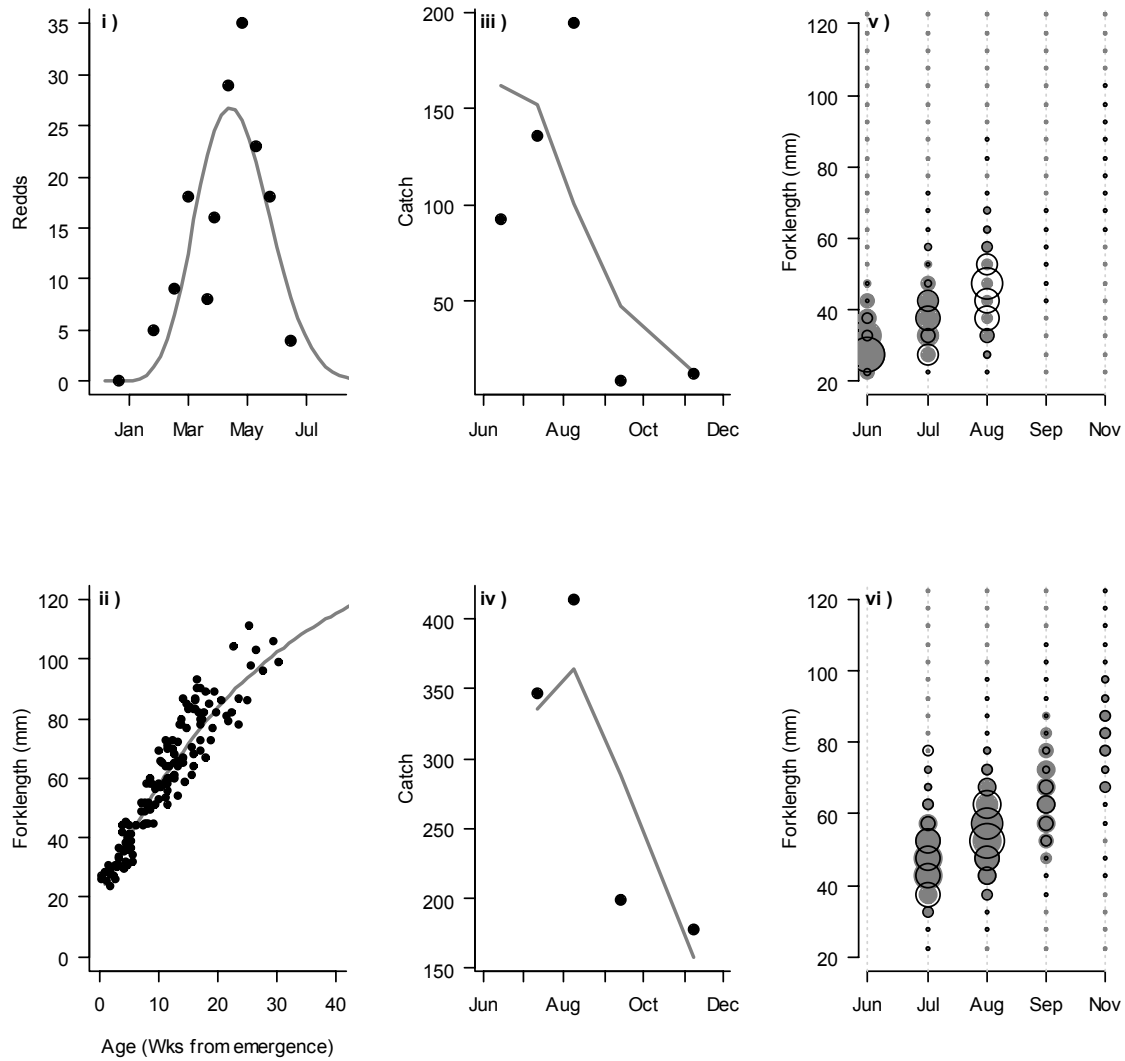
Figure 6.3. Comparison of most likely fits to data from 2006 based on models R1-M2-O1 (a) and R2-M4-O3 (b). See caption for Fig. 6.2 for details.
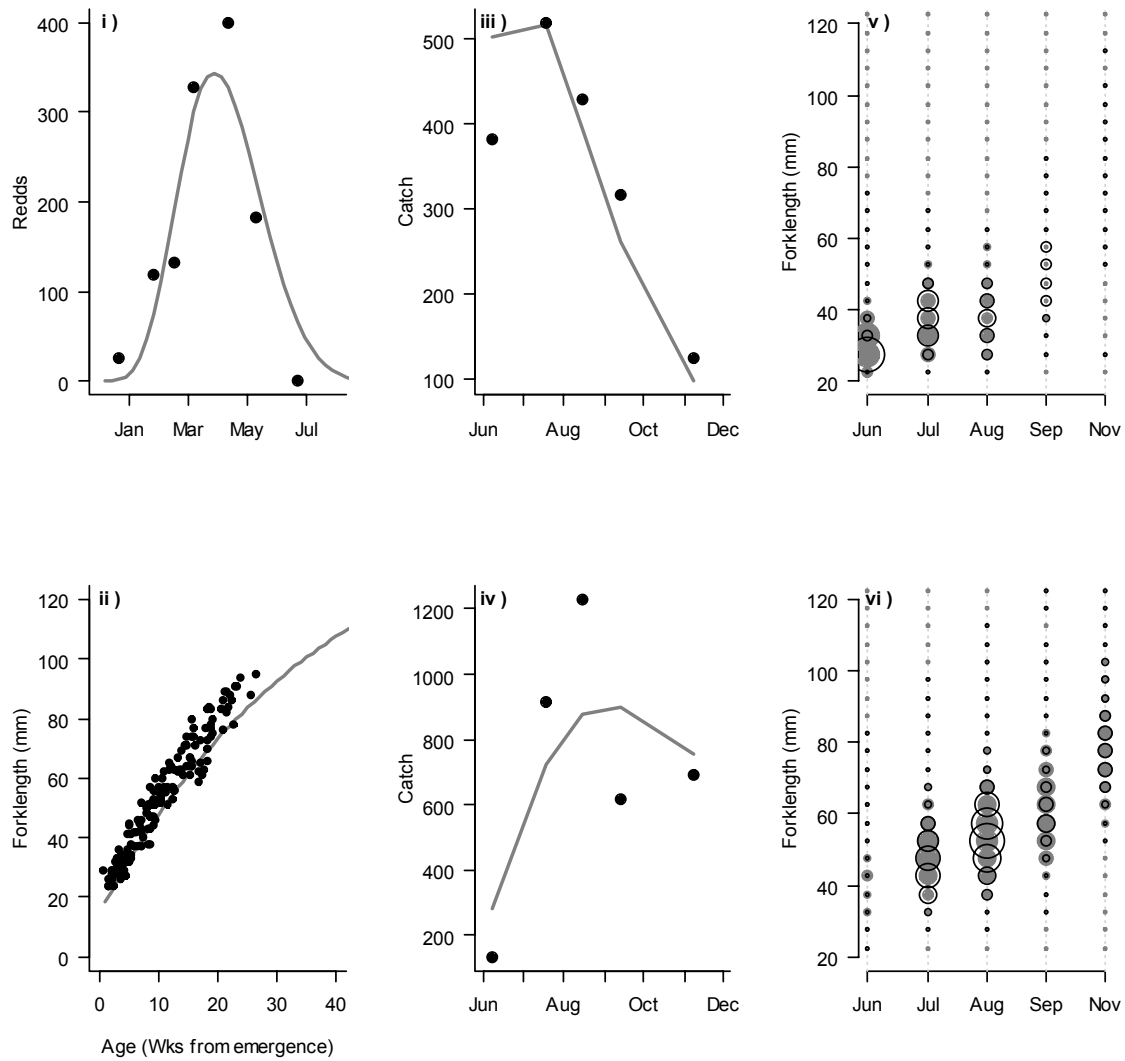
b)
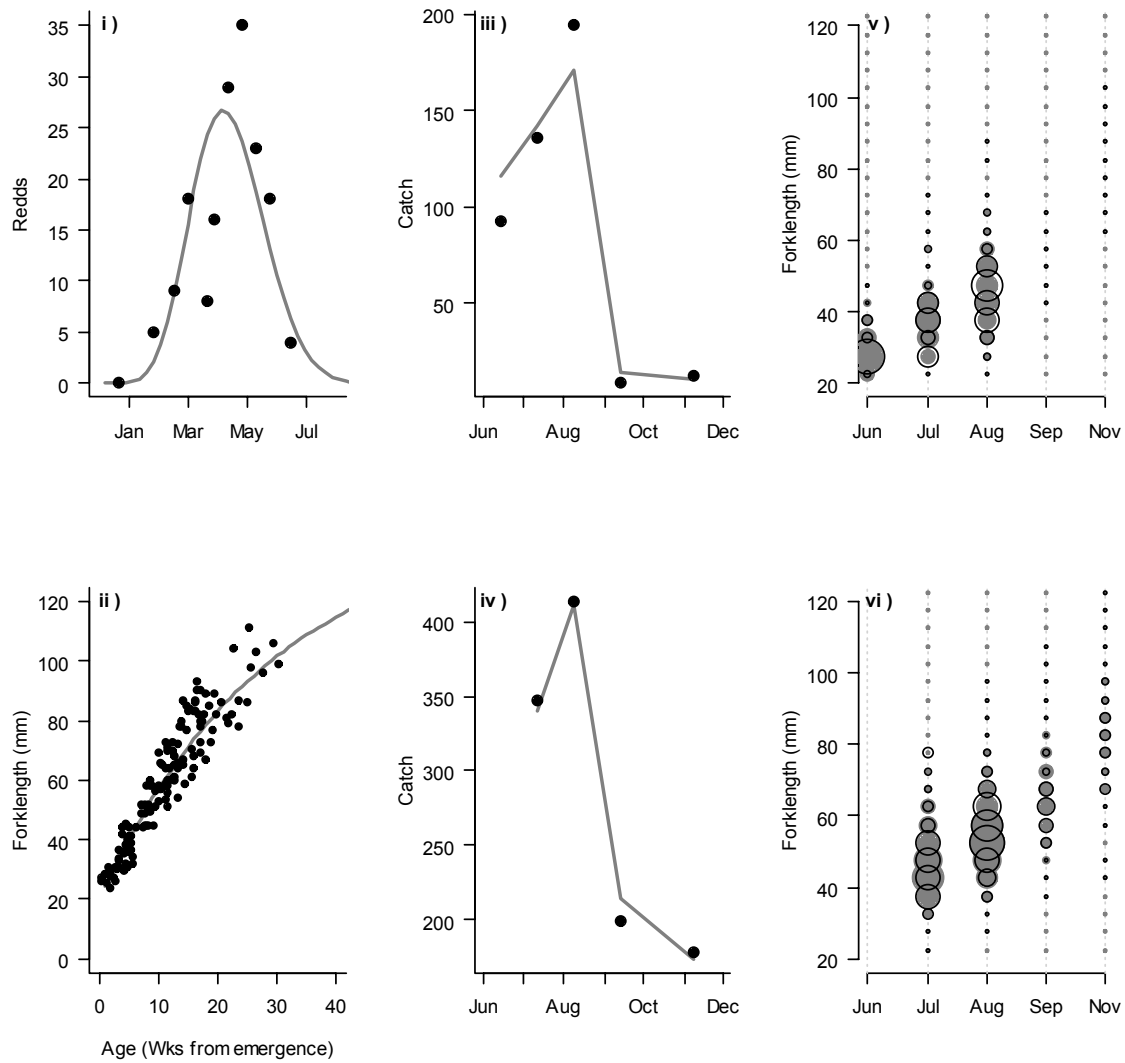
Figure 6.3. Con't.

a)

Figure 6.4. Comparison of most likely fits to data from 2007 based on models R1-M2-O1 (a) and R2-M4-O3 (b). See caption for Fig. 6.2 for details.
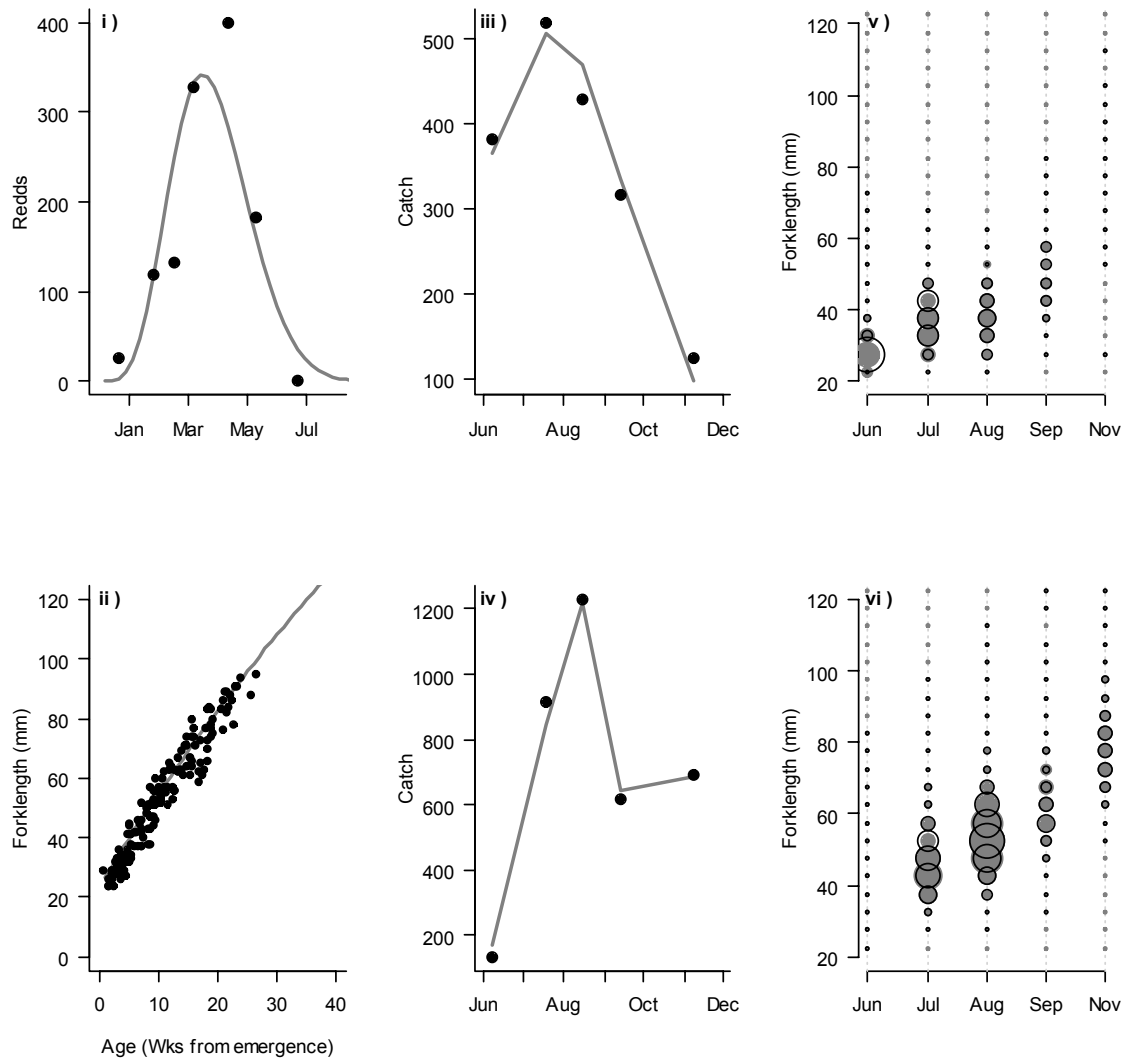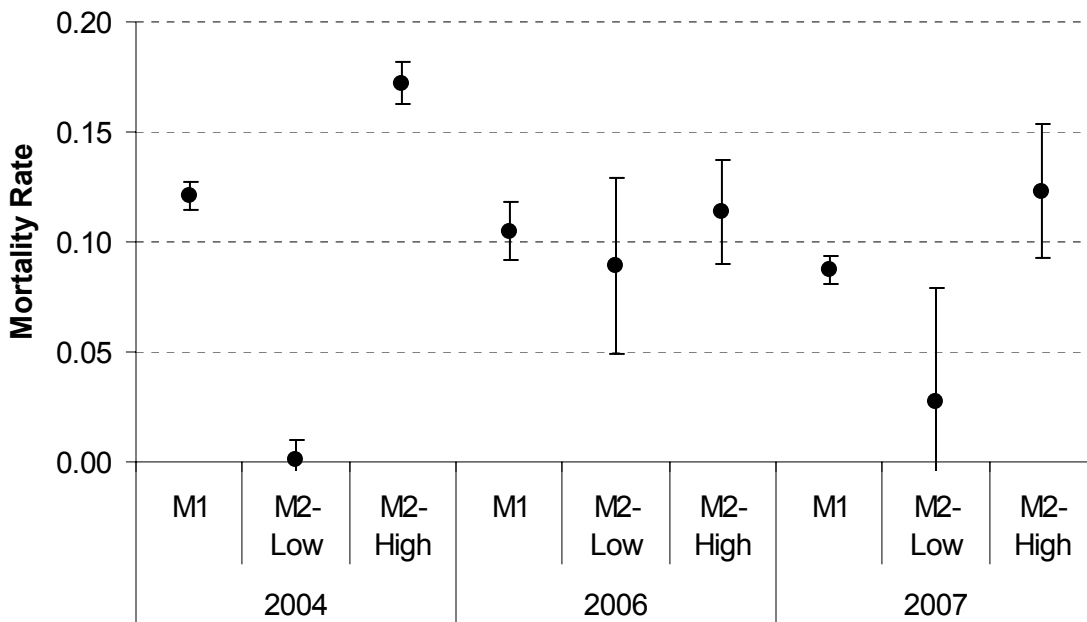
b)

Figure 6.4. Con't.

Figure 6.5. Comparison of most likely estimates of instantaneous mortality rates assuming mortality is equal among habitat types (M1) or based on independent estimates in low- and high-angle habitat (M2), by year. All estimates are based on recruitment model R2 and ontogenetic movement model O3. Error bars denote 95% confidence limits.
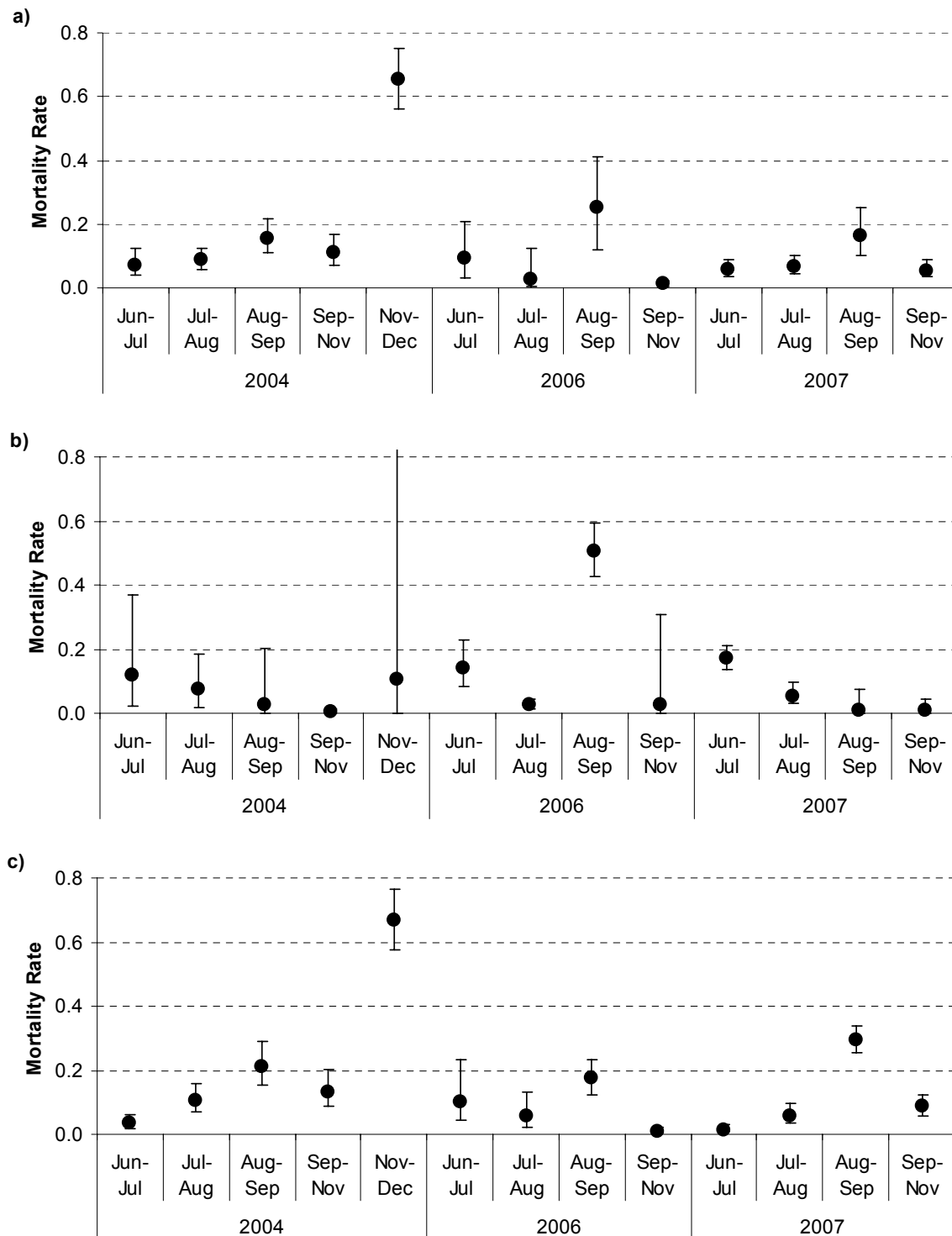
Figure 6.6. Comparison of most likely instantaneous mortality rates between sampling trips assuming mortality is equal among habitat types (a) and based on independent estimates in low-(b) and high-angle (c) habitat, by year. Estimates in a) are based on model R2-M3-03. Estimates in b) and c) are based on most parsimonious model for each year (Table 6.9), which was R2-M4-03 for 2004 and 2007, and R2-M4-O1 for 2006. Error bars denote 95% confidence limits.
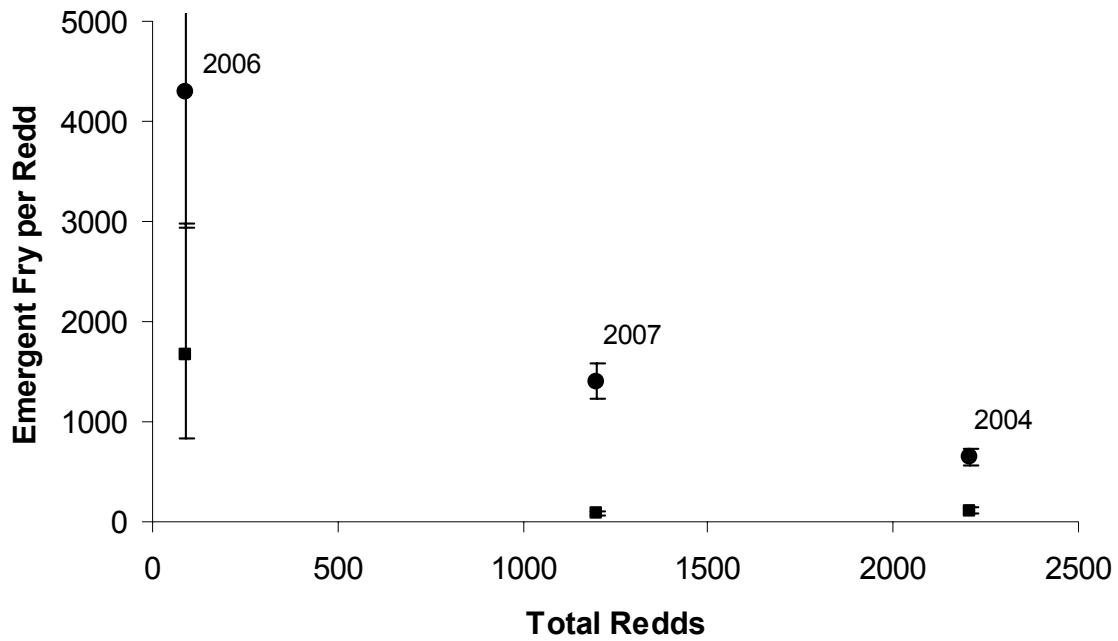
201

Figure 6.7. Relationship between estimates of the total redds (χ) excavated per year and number of emergent fry per redd before ($e^{-\eta_{1-18}\phi}$, squares) and after (ϕ, circles) April 1$^{\text{st}}$ based on model R2-M4-03. Error bars denote 95% confidence limits.

6.5   References

Berg. S., and J. Jorgensen. 1991. Stocking experiments with 0+ and 1+ trout parr, Salmo trutta L., of wild and hatchery origin: 1. Post-stocking mortality and smolt yeid. J. Fish. Biol. **39:** 151-169.

Biro, P.A., Post, J.R., and Parkinson, E.A. 2003. Population consequences of a predator-induced habitat shift by trout in whole-lake experiments. Ecology **84:** 691-700.

Blinn, D.W., Shannon, J.P., Stevens, L.E., and J.P. Carder. 1995. Consequences of fluctuating discharge for lotic communities. J. Am. Ben. Soc. **108:** 215-228.

Bradford, M.J. 1997. An experimental study of stranding of juvenile salmonids on gravel bars and in sidechannels during rapid flow decreases. Reg. Rivers: Res. Mgmt. **13**: 395-401.

Chapman, D.W., and T.C. Bjornn. 1969. Distribution of salmonids in streams, with special reference to effects of food and feeding, p. 153-156. *In* Symposium on salmon and trout in streams. H.R. MacMillan Lectures in Fisheries. British Columbia. Vancouver, BC.

Coggins, L.G. Jr. 2008. Active Adaptive Management for native fish conservation in the Grand Canyon: Implementation and Evaluation. Ph.D. thesis, Department of Fisheries and Aquatic Sciences, University of Florida. 170 pp.

Burnham, K.P., and D.R. Anderson. 2002. Model Selection and Multimodel Inference, 2nd edition. Springer-Verlag, NY.

Deriso, R.B., Maunder, M.N., and J.R. Skalski. 2007. Variance estimation in integrated assessment models and its importance for hypothesis testing. Can. J. Fish. Aquat. Sci. **64:** 187-197.

Elliott, J.M. 1994. Quantitative ecology and the brown trout. Oxford University Press, Oxford.

Einum, S. and K.H. Nislow. 2005. Local-scale density-dependent survival of mobile organisms in continuous habitats: an experimental test using Atlantic salmon. Oecologia **143**: 203-210.

Everest, F.H., and D.W. Chapman. 1972. Habitat select and spatial interaction by juvenile Chinook salmon and steelhead strout in two Idaho streams. F. Fish. Res. Bd. Canada **29:** 91-100.

Eveson, J.P., Laslett, M., and T. Polacheck. 2004. An integrated model for growth incorporating tag-recapture, length-frequency, and direct ageing data. Can. J. Fish. Aquat. Sci. **61:** 292-306.

Fournier, D.A., Hampton, J., and J.R. Sibert. 1998. MULTIFAN-CL: a length-based, age-structured model for fisheries stock assessment, with application to the South Pacific albacore, *Thunnus alalunga*. Can. J. Fish. Aquat. Sci. **55**: 2105-2116.

Halleraker, J.H., Saltveit, J.J., Harby, A., Arnekleiv, J.V., Fjesdstad, H.P., and B. Kohler. 2003. Factors influencing stranding of wild juvenile brown trout (*Salmo trutta*) during rapid and frequent flow decreases in artificial stream. River Research and Applications **19**: 589-603.

Hilborn, R., Bue, B.G., and S. Sharr. 1999. Estimating spawning escapements from periodic counts: a comparison of methods. Can J. Fish. Aquat. Sci. **56:** 888-896.

Heggenes, J., and J.G. Dokk. 2001. Contrasting temperatures, waterflows, and light: Seasonal habitat selection by young Atlantic salmon and brown trout in a boreonemoral river. Regul. Rivers: Res. Mgmt. **17**: 623-635.

Hume, J.M.B., and E.A. Parkinson. 1988. Effects of size at and time of release on the survival and growth of stealhead fry stocked in streams. N. Am. J. Fish. Mgmt. **8:** 50-57.

Jensen, J.O.T., McLean, W.E., Rombough, P.J., and T. Septav. 1992. Salmonid incubation and rearing programs for IBM-compatible computers. Can. Tech. Rep. Fish. Aquat. Sci. **1878**: 46 p.

Korman, J., Kaplinski, M. Hazel, J., Melis, T., Sneep, J. and S. Hall. 2005. Effects of 2003-2004 fluctuating flows from Glen Canyon Dam on the early life history stages of rainbow trout in the Colorado River. Report prepared for Grand Canyon Monitoring and Research Center, Flagstaff, AZ.

McKinney, T., Speas, D.W., Rogers, R.S., and W.R. Persons. 1999. Rainbow trout in a regulated river below Glen Canyon Dam, Arizona, following increased minimum flows and reduced discharge variability. Nor. Am. J. Fish. Mgmt. **21**: 216-222.

Lorenzen, K. 2000. Allometry of natural mortality as a basis for assessing optimal release size in fish stocking programmes. Can. J. Fish. Aquat. Sci. **57:** 2374-2381.

Methot, R.D. 1983. Seasonal variation in survival of larval northern anchovy, Engraulis Mordax, estimated from the age distribution of juveniles. Fish. Bull. **81**: 741-750.

Nislow, K.H., Folt, C.L., and D.L. Parrish. 2000. Spatially explicit bioenergetic analysis of habitat quality for age-0 Atlantic salmon. Trans. Am. Fish. Soc. **129:** 1067-1081.

Nislow, K.H. Einum, S., and C.L. Folt. 2004a. Testing predictions of the critical period for survival concept using experiments with stocked Atlantic salmon. J. Fish Biol. **65** (Supplement A): 188-200.

Nislow, K.H., Sepulveda, A.J., and C.L. Folt. 2004b. Mechanistic linkage of hydrologic regime to summer growth of age-0 Atlantic salmon. Trans. Am. Fish. Soc. **133:** 79-88.

Otter Research Ltd. 2004. An introduction to AD Model Builder version 7.1.1. for use in nonlinear modeling and statistics. 194 pp. Report available from otter-rsch.com.

Press, W.H., Teukolsky, S.A., Vetterling, W.T., and Flannery, B.P. 1992. Numerical recipes in Fortran: The art of scientific computing, 2nd Edition. Cambridge University Press, Cambridge UK.

Rosenfeld, J.S., and S. Boss. 2001. Fitness consequences of habitat use for juvenile cutthroat trout: energetic costs and benefits in pools and riffles. Can. J. Fish. Aquat. Sci. **58:** 585-593.

Saltveit, S.J., Halleraker, J.H., Arnekleiv, J.V., and A. Harby. 2001. Field experiments on stranding in juvenile Atlantic Salmon (*Salmo Salar*) and Brown Trout (*Salmo Trutta*) during rapid flow decreases caused by hydropeaking. Reg. Rivers: Res. Mgmt. **17:** 609-622.

Schlosser, I.J. 1987. The role of predation in age- and size-related habitat use by stream fishes. Ecology **68:** 651-659.

Schnute, J.T. and D.A. Fournier 1980. A new approach to length frequency analysis: growth structure. Can. J. Fish. Aquat. Sci. **37:** 1337-1351.

Scruton, D.A., Pennell, C.J., Robertson, M.J., Ollerhead, L.M.N., Clarke, K.D., Alfredsen, K., Harby, A., and McKinley, R.S. 2005. Seasonal response of juvenile

atlantic salmon to experimental hydropeaking power generation in Newfoundland, Canada. Nor. Am. J. Fish. Mgmt. **25:** 964-974.

Shea, C.P., and J. T. Peterson. 2007. An evaluation of the relative influence of habitat complexity and habitat stability on fish assemblage structure in unregulated and regulated reaches of a large Southeastern warmwater stream. Trans. Am. Fish. Soc. **136:** 943-958.

Taylor, N.G., Walters, C.J., and S.J.D. Martell. 2005. A new likelihood for simultaneously estimating von Bertalanffy growth parameters, gear selectivity, and natural and fishing mortality. Can. J. Fish. Aquat. Sci**. 62:** 215-223.

Ward, D., and S. Rogers. 2006. Lee's Ferry, Long-term rainbow trout monitoring. Report submitted to Grand Canyon Monitoring and Research Center, Flagstaff, AZ.

7.0 General Conclusions, Uncertainties, and Future Research

In this concluding chapter, I provide a brief summary of Chapters 2-6, discuss the wider implications of the work, and identify major uncertainties and areas of further research.

7.1 Summary of Research

In Chapter 2, I estimated capture probability of age-0 rainbow trout in the Lee's Ferry Reach of the Colorado River by backpack and boat electrofishing at discrete shoreline sites using both depletion and mark-recapture experiments. My objectives were to evaluate the feasibility of estimating capture probability for juvenile salmonids in larger rivers, to determine how it is influenced by fish size, habitat, flow, and density, and to test population closure assumptions. Eighty percent of capture probability estimates from 66 depletion experiments and 42 mark-recapture experiments ranged from 0.28-0.75 and 0.17-0.45, and the average CV of estimates was 0.26 and 0.25, respectively. There was strong support for a fish size-capture probability relationship that accounted for differences in vulnerability across habitat types. Smaller fish were less vulnerable in high-angle shorelines that were sampled by boat electrofishing. There was little support for capture probability models that accounted for within-day variation in flow, but the effects of across-month variation in flow were confounded with the effects of fish size. The effects of fish density on capture probability were challenging to discern, variable among habitat types and estimation methodologies, and confounded with the effect of fish size. I concluded that mark-recapture experiments are an effective way to estimate capture probabilities for juvenile salmonids in large rivers.

In Chapter 3, I evaluated the effects of hourly variation in flow caused by power load following at Glen Canyon Dam on the nearshore habitat use and growth of age-0 rainbow trout downstream in the Colorado River. Reducing the extent of hydropeaking is a common element of restoration efforts in regulated rivers. Empirical support for such recommendations is limited, and this study fills an important gap by documenting how juvenile fish respond to short-term variation in stage and velocity, and the consequence of this response to growth. Catch rates of age-0 rainbow trout in nearshore areas were 2- to

4-fold higher at the daily minimum flow compared to the daily maximum, indicating that most age-0 trout do not maintain their position within immediate shoreline areas during the day when flows are high. A striping pattern, identified by the presence of atypical daily increments formed every 7 days, was evident in over 50% of 259 otoliths examined in 2003, but in only 6% of 334 examined in 2004. The weekly pattern was caused by a reduction in the extent of hourly flow fluctuations on Sundays during the growing season, which occurred in 2003, but not in 2004. Atypical increments were 25% wider than adjacent increments and were indicative of significant short-term increases in otolith growth. The somatic growth rate determined from fish with otoliths where striping was present (11.2 mm·month^{-1}) was slightly greater than the rate from otoliths without striping (10.8 mm·month^{-1}), but the difference was not significant. I suggest that otolith growth improved on Sundays in 2003, because it was the only day of the week when most age-0 fish were found in immediate shoreline areas where higher water temperatures, lower velocities, and increased food availability provided better growing conditions.

In Chapter 4, I evaluated the effects of flow, density, and fish size on habitat use, growth, and survival of age-0 rainbow trout in the Lee's Ferry reach. High-angle shorelines contained greater densities and much higher biomass of age-0 trout than low-angle shorelines. Trends in length-frequencies and population size by habitat type over the summer and fall suggested an ontogenetic habitat shift from low- to high-angle habitat that appeared to depend on fish size and density. There was preliminary evidence of strong density-dependence in survival rates between spawning and one to two months from emergence. The apparent survival rate over this period, determined from the ratio of reach-wide age-0 abundance in July to the total egg deposition, increased over 6-fold in 2006 when egg deposition was less than 1/10th the level estimated in other years. Apparent survival rates of age-0 fish from July to November were relatively consistent among years, ranging from 0.18-0.32, and there was no indication that these survival rates were density-dependent. Daily age, determined by otolith microstructure, explained 82-93% of variation in fork length among individuals. Growth was highest in 2006 when age-0 abundance was lowest, but was almost as high in 2007 when abundance was greatest. Given this pattern and only four years of data, it is uncertain whether age-0

growth is density dependent. There were very small differences in growth among habitat types in most study years except 2004, where growth was greater in high-angle habitat.

In Chapter 5, data on spawn timing, spawn location, and intergravel temperatures were integrated in a model to predict seasonal trends in incubation mortality resulting from fluctuations in flow from Glen Canyon Dam. Fluctuations increased dewatering frequency and intergravel temperatures at higher spawning elevations and were predicted to result in flow-dependent incubation mortality rates of 24% in 2003 and 50% in 2004, when flow was experimentally manipulated to reduce trout abundance, compared to 5% in 2006 and 11% in 2007 under normal operations. Predictions were consistent with direct observations of the frequency of egg mortality determined from redd excavations; redds containing only dead eggs were encountered twice as frequently at elevations inundated by flows of 340 $m^3 \cdot sec^{-1}$ compared to 227 $m^3 \cdot sec^{-1}$ in February and March, and four times as frequently in April and May. Survival from egg deposition to one or two months from emergence was over 6-fold higher when spawning stock was very low. Because of this potentially strong compensation, flow-dependent incubation mortality in experimental years was likely not large enough to reduce the abundance of age-0 trout. Predicted hatch date distributions from flow-independent and –dependent models were similar and explained high and equal amounts of variation in backcalculated hatch date distributions. There was no evidence from the hatch date and stock-recruitment analysis that flow-dependent incubation losses effected the age-0 population. The strength of the inference from the stock-recruitment analysis is limited due to the low sample size, and additional years of data collection are required to reduce this uncertainty.

In Chapter 6, I developed a stock synthesis model that integrated data on spawning, incubation conditions, and age-0 growth and abundance to evaluate alternate hypotheses concerning effects of flow regime and habitat on early life history dynamics that were initially examined in Chapters 4 and 5 using more traditional methods. Specifically, I evaluated whether increased hourly flow fluctuations during the incubation period reduced the survival rate from egg deposition to a few months from emergence (early survival), whether an ontogenetic habitat shift of age-0 trout from low- to high-angle habitat occurred, and whether mortality varied among habitats or over time in response to flow changes. Similar to results from Chapter 5, there was little indication

from the stock synthesis model that greater fluctuations in flow during incubation reduced early survival rates. The benefit of the model was that is showed there was seasonal variation in early survival rates in both treatment and control years, and that conclusions regarding flow effects were consistent across various assumptions about movement and mortality. The stock synthesis model indicated that the extent of movement from low- to high-angle habitat was greater for larger fish, and was very limited in 2006 when juvenile and adult abundance was low. Age-0 mortality rates were over two-fold higher between August and September sampling trips when the minimum flow was suddenly reduced by 50%, relative to mortality rates estimated for adjacent periods. Age-0 mortality rates in high-angle habitat were two-fold greater than in low-angle habitat in 2004 and 2007, with the opposite pattern occurring in 2006 when densities were lower and when there was little evidence of an ontogenetic habitat shift. Our understanding of the recruitment dynamics of juvenile fishes can be substantially improved by using a stock synthesis modeling approach to interpret monitoring data on early life history stages.

7.2   Major Uncertainties and Future Research

Capture probability for juvenile fish needs to be determined to reliably index or estimate juvenile population size. These estimates are in turn fundamental to answer a number of important questions about early life history dynamics, such as the strength of compensatory survival responses for different life stages. To my knowledge there are no published studies of capture probability for juvenile fish in large rivers. Methodologies and results from Chapter 2 therefore fill an important knowledge gap, and are broadly applicable to the study of juvenile population dynamics in other large river systems. However, there are two fundamental mark-recapture assumptions that require further investigation. I assumed that fish captured by electrofishing and marked have the same capture probability as ummarked fish. The validity of this assumption potentially varies with fish size, which likely influences their response to capture and handling. I also assumed that mark-recapture sites could be treated as effectively closed over the 24-hour period between marking and recapture. The data suggest that this assumption may be valid for small fish, but could become increasingly tenuous as fish become larger,

resulting in potential changes in swimming capabilities, habitat preferences, and responses to capture and handling. I am currently evaluating both of these assumptions in the Lee's Ferry reach and in the Cheakmaus River, B.C., and hope to report on these results in a future paper.

In Chapters 4-6, I suggest that there is potentially very strong density dependence in survival rates sometime between fertilization and about one month from emergence, and that survival of age-0 trout after this period is not density dependent. If these preliminary conclusions about the strength and timing of density dependence are correct, the ideal period to adjust flows to regulate the abundance of trout in the Lee's Ferry reach is early summer. By this time, the majority of density dependence in survival would have already occurred, yet age-0 trout would still be very small and thus highly dependent on immediate nearshore environments that are destabilized by fluctuating flows. More years of data are required to build confidence in the stock-recruitment relationships that form the basis of this prediction. There are only a handful of long-term datasets that adequately describe stock-recruitment dynamics for non-anadromous salmonids across multiple early life stages (Elliot 1994, Lobon-Cervia 2007). Both of these datasets are from very small streams. Continued monitoring of the spawning and juvenile life stages of the rainbow trout population in the Lee's Ferry reach would yield a highly informative dataset for a large river.

McKinney et al. (1999) showed that the Lee's Ferry trout population increased by 3-fold following stabilization in flows in the early 1990's, and speculated that the more stable flow regime increased the survival rates of eggs, alevins, and juveniles, which in turn increased the recruitment rate of juveniles to the adult population. Although this thesis has provided a substantive gain in our understanding about the early life history dynamics of the Lee's Ferry trout population, the underlying mechanism behind the population increase over the 1990's remains uncertain. The preliminary stock-recruitment relationships developed in this study indicates that the majority of density dependence occurs shortly after emergence, which suggests that the population increase was driven largely by an increase in juvenile survival rate, rather than by an increase in survival for incubating life stages. However, flow-dependent incubation losses, estimated using the model presented in Chapter 5, but driven by the flow regime between 1988 and 1991,

were likely over 75% (Korman et al. 2005). These high incubation mortality rates, in conjunction with the smaller population size of adults at that time, would likely have been sufficient to limit the abundance of the adult population. In the absence of early life history data prior to the stabilization of flows during the 1990's, the mechanism behind the increase in adult abundance remains uncertain.

This thesis contributes to the current understanding of the effects of flow on the early life history dynamics of fish in larger rivers. I showed that otolith growth and nearshore habitat use of age-0 trout were affected by hourly fluctuations in flow, and speculated that these responses could lead to reduced growth and survival of young fish. I presented results that showed substantial use of high-angle shorelines by very small age-0 trout, considerable movement from low- to high-angle shorelines, and differences in mortality rates among habitat types. I speculated that hourly fluctuations in flow could be driving these dynamics, and that the carrying capacity of the Lee's Ferry reach to produce young trout would increase if flow fluctuations were reduced during the summer. Ultimately, these predictions need to be tested by comparing observations collected to date with those obtained under a future stead-flow regime. The U.S. Fish and Wildlife Service's Biological Opinion for the ESA-listed humpback chub population in Grand Canyon calls for elimination of hourly flow fluctuations in some years to increase nearshore warming and stability (USFWS 1994). Lost power revenues associated with this action could exceed $20 M per year (Palmer and Burbidge 2001). Based on the results from this thesis, I suggest that juvenile rainbow trout in the Lee's Ferry research could serve as a model for understanding potential flow-responses of native fish living further downstream. At a minimum, the Lee's Ferry population could be used to develop and test sampling and assessment methods to apply to native fish. This concept requires further investigation and critical review, but is worth pursuing as there are a number of scientific and logistic advantages to working with the abundant juvenile trout population in the Lee's Ferry reach relative to the sparse and endangered native fish populations in Grand Canyon.

In the introduction to this thesis, I argued that poor understanding of critical mechanisms regulating fish populations makes it very difficult to provide reasonably substantiated arguments in support of informative flow experimentation. Implementation

of a long-term steady flow experiment, along the lines of what has been identified in the USFWS biological opinion for humpback chub in Grand Canyon, has been the most contentious environmental issue in the history of Glen Canyon Dam. Considering the substantial losses in hydropower revenues associated with this flow regime, the poor status of endangered and endemic species, and the limited understanding of factors governing recruitment dynamics in larger rivers, it is not surprising that this debate has occurred for over two-decades and has been the motivation for numerous lawsuits. This thesis has provided a clearer articulation of the mechanisms through which fluctuations in flow from Glen Canyon Dam potentially alter habitat use and reduce growth and survival of juvenile rainbow trout in the Colorado River. It has also provided baseline data, as well as more sensitive monitoring and assessment methods, to evaluate responses of juvenile trout populations to future changes in the flow regime. Some of the methodologies, hypotheses, and results presented here are potentially transferable to native fish downstream, and to other large regulated rivers. All these components should help strengthen the scientific case for implementing more informative flow experiments in the future.

7.3 References

Elliott, J.M. 1994. Quantitative ecology and the brown trout. Oxford University Press, Oxford.

Korman, J., Kaplinski, M. Hazel, J., Melis, T., Sneep, J. and S. Hall. 2005. Effects of 2003-2004 fluctuating flows from Glen Canyon Dam on the early life history stages of rainbow trout in the Colorado River. Report prepared for Grand Canyon Monitoring and Research Center, Flagstaff, AZ.

Lobon-Cervia, J. 2007. Numerical changes in stream-resident brown-trout (Salmo trutta): uncovering the roles of density-dependent and density-independent factors across space and time. Can. J. Fish. Aquat. Sci. **64:** 1429-1447.

Palmer C.S., and C. Burbidge. 2001. The financial impacts of the low summer steady flow experiment at Glen Canyon Dam. Report prepared by Western Area Power Administration for the Grand Canyon Monitoring and Research Center, Flagstaff, AZ.

U.S. Fish and Wildlife Service (USFWS). 1994. Final Biological Opinion, Operation of Glen Canyon Dam as the modified low fluctuation flow alternative of the Final Environmental Impact Statement, Operation of Glen Canyon Dam (2-21-93-F-167). Ecological Services, Arizona State Office, U.S. Fish and Wildlife Service: Phoenix, Arizona.